



San Francisco

Pacific Ocean

San Francisco Bay



GEOLOGY OF SAN FRANCISCO, CALIFORNIA

United States of America

Geology of the Cities of the World Series

**Association Engineering Geologists
Geology of Cities of the World Series
Geology of San Francisco, California, United States of America**

Issued to registrants at the 61st Annual Meeting of the Association of Environmental & Engineering Geologists and 13th International Association of Environmental & Engineering Geologists Congress in San Francisco, CA – September 16 through 22, 2018.

Editors:

Kenneth A. Johnson, PhD, CEG, PE
WSP USA, San Francisco, CA

Greg W. Bartow, CHg, CEG
California State Parks, Sacramento, CA

Contributing Authors: John Baldwin, Greg W. Bartow, Peter Dartnell, George Ford, Jeffrey A. Gilman, Robert Givler, Sally Goodin, Russell W. Graymer, H. Gary Greene, Kenneth A. Johnson, Samuel Y. Johnson, Darrell Klingman, Keith L. Knudsen, William Lettis, William E. Motzer, Dorinda Shipman, Lori A. Simpson, Philip J. Stuecheli, and Raymond Sullivan.

It is hard to be unaware of the earth in San Francisco (Wahrhaftig, 1984).

A generous grant from the AEG Foundation, Robert F. Legget Fund, helped make this publication possible. Founded in 1993, the Robert F. Legget Fund of the AEG foundation supports publications and public outreach in engineering geology and environmental geology that serve as information resources for the professional practitioner, students, faculty, and the public. The fund also supports education about the interactions between the works of mankind and the geologic environment.

Cover Plate: European Space Agency

Table of Contents

| | |
|--|----|
| PREFACE | v |
| ABSTRACT | 1 |
| INTRODUCTION | 1 |
| Geographic Setting | 1 |
| Climate | 6 |
| History and Founding | 6 |
| Native Americans | 6 |
| European Founding of San Francisco | 7 |
| Gold Rush and Its Impact to San Francisco | 11 |
| Between the Gold Rush and the 1906 Earthquake | 13 |
| Quarries in San Francisco | 16 |
| 1906 Earthquake | 19 |
| Rebuilding after the 1906 Earthquake and Fire | 23 |
| Panama-Pacific International Exposition | 24 |
| World War II: Military Base Expansion | 24 |
| Post-WWII High-Rise Building Boom: The Manhattanization of San Francisco | 25 |
| San Francisco in the Future: Major New Transit Projects on the Horizon | 25 |
| GEOLOGY AND GEOLOGIC HISTORY | 30 |
| Overview of the Geology of the San Francisco Bay Region | 30 |
| Introduction: The Road to Accretion | 30 |
| Geologic Overview of the San Francisco Bay Region | 33 |
| Geology of San Francisco | 41 |
| San Francisco Basement Complex Rocks | 41 |
| Geologic Structures in San Francisco | 51 |
| Tertiary Overlap Sequences | 51 |
| Quaternary Deposits in San Francisco | 52 |
| San Francisco's Offshore Geology | 58 |
| Geologic History of San Francisco | 61 |
| Rocks Passing Through | 61 |
| Rocks From Somewhere Else | 62 |
| Neogene Paleogeography | 64 |
| GEOTECHNICAL AND ENGINEERING GEOLOGY CHARACTERISTICS OF GEOLOGIC UNITS | 67 |
| Artificial Fill | 67 |
| Eolian Deposits and Dune Sands | 67 |
| Young Bay Mud | 68 |
| Colma Foundation | 68 |
| Index Properties | 68 |
| Hydraulic Conductivity | 68 |
| General Engineering Practice | 69 |
| Yerba Buena Mud (Old Bay Deposits) | 69 |
| Index Properties | 69 |
| Relative Density and Consistency | 69 |
| Hydraulic Conductivity | 69 |
| Franciscan Complex Rocks | 69 |
| Quarries | 70 |

| | |
|---|-----|
| Rock Falls and Slope Stability | 70 |
| GEOLOGIC ASPECTS OF NATURAL HAZARDS | 70 |
| Earthquake Hazards | 70 |
| San Andreas Fault | 71 |
| Hayward–Rodgers Creek Fault | 78 |
| San Gregorio Fault | 79 |
| Calaveras Fault | 80 |
| Faults of San Francisco | 81 |
| Liquefaction and Lateral Spreading | 82 |
| WATER RESOURCES | 84 |
| San Francisco’s Water Supply | 84 |
| Early Years | 84 |
| Post Gold Rush | 84 |
| Search for a Sierra Source | 84 |
| Sunset Well Field | 86 |
| Hetch Hetchy Regional Water System | 87 |
| Water System Improvement Program | 87 |
| Auxiliary Water Supply System | 90 |
| Diversification of Water Supplies | 92 |
| Local Groundwater | 92 |
| Non-Potable Water | 92 |
| Recycled Water | 92 |
| San Francisco Creeks and Lakes | 93 |
| Lobos Creek | 93 |
| Mountain Lake | 93 |
| Lake Merced | 93 |
| Vista Grande Drainage Basin Improvement Project | 95 |
| Groundwater | 95 |
| Westside Groundwater Basin | 95 |
| Lobos Groundwater Basin | 102 |
| Marina Groundwater Basin | 102 |
| Visitacion Valley Groundwater Basin | 103 |
| Downtown Groundwater Basin | 103 |
| Islais Valley Groundwater Basin | 105 |
| South San Francisco Groundwater Basin | 105 |
| ENVIRONMENTAL CONCERNS | 106 |
| Regulatory Setting | 106 |
| GeoTracker | 106 |
| Maher Ordinance | 106 |
| Hunters Point Naval Shipyard | 108 |
| Cleanup Program at the Shipyard | 108 |
| Treasure Island Naval Shipyard | 108 |
| Presidio of San Francisco | 109 |
| Environmental Issues | 111 |
| Mission Bay | 113 |
| Geologic Hazards | 116 |
| Environmental Hazards and Regulatory Framework | 116 |

| | |
|--|------------|
| Manufactured Gas Plants | 117 |
| MAJOR ENGINEERING PROJECTS | 120 |
| Golden Gate Bridge | 120 |
| Major Structural Foundation Elements | 120 |
| North Anchorage Structure and Tower | 120 |
| South Tower | 122 |
| South Approach and Anchorage Structure | 122 |
| San Francisco–Oakland Bay Bridge | 123 |
| Western Span | 123 |
| Yerba Buena Tunnel | 125 |
| Eastern Span | 125 |
| Port of San Francisco—San Francisco Seawall at Embarcadero | 127 |
| Treasure Island | 132 |
| Hydraulic Fill | 132 |
| Shoal Deposits (Estuarine Sands) | 134 |
| Young Bay Mud (Estuarine Clays) | 134 |
| Older Bay Deposits (Undifferentiated) | 136 |
| Geotechnical Mitigation Measures for Treasure Island Redevelopment | 136 |
| Transportation Tunnels in San Francisco | 136 |
| Southern Pacific Tunnels to the Peninsula | 136 |
| Fort Mason Tunnel | 137 |
| Stockton Street Tunnel | 137 |
| Twin Peaks Tunnel | 138 |
| Sunset Tunnel | 138 |
| Broadway Tunnel | 138 |
| Bay Area Rapid Transit | 138 |
| San Francisco Municipal Railroad (Muni) | 139 |
| Muni Metro—Market Street Subway | 139 |
| T-Third Street Line/Central Subway | 139 |
| SFPUC Sewer System | 143 |
| Wastewater Tunnels | 144 |
| PROFESSIONAL PRACTICES | 145 |
| Seismic Building Codes: Early Motivations and First Seismic Provisions | 145 |
| Mandatory Soft Story Retrofit Program | 146 |
| City of San Francisco Unreinforced Masonry Program | 147 |
| Sea Level Rise: Forecasts, Adaptation Plans, and Policy | 147 |
| Naturally Occurring Asbestos (NOA) | 150 |
| SUMMARY | 150 |
| ACKNOWLEDGMENTS | 150 |
| CONTRIBUTING AUTHORS | 152 |
| REFERENCES | 153 |
| Plate 1. Geologic Map of the City and County of San Francisco. | 182 |
| Plate 2. Treasure Island Geology and Stratigraphy. | 183 |

PREFACE

Over the course of the last 38 years the Association of Environmental and Engineering Geologists *Geology of the Cities of the World* Committee has sponsored peer-reviewed technical papers following a uniform format. That format has now been changed to allow flexibility to address issues related to each city. As such different parts of a city may have been elaborated on more than others. Generally, the papers share a discussion focusing on the environmental and geologic circumstances that brought people to settle in the cities making up the series to date. In addition to the natural resources that brought original inhabitants to settle these regions, the series highlights the geologic conditions that have essentially controlled the development and expansion of each city. Geologists and engineers will continue to address these same geologic and environmental conditions while meeting the challenges of supporting sustainability and/or growth in cities.

The geology of San Francisco has been dominated by plate tectonics, faulting and fault related products as well as sea level changes. Historically, the San Francisco area was initially populated by Native Americans, followed by the Spanish Missionaries, and then Forty-Niners seeking gold; it became a major west coast port supporting California goldfields. Later the city became a home to several military bases, and a financial center. Today, San Francisco is one of America's most popular tourist destinations and is a major cultural, financial, trade and high-tech center. It is with great pleasure that we add *The Geology of San Francisco, California, United States of America*, to the Association of Environmental and Engineering Geologists' *Geology of the Cities of the World* Series.

Sincerely,

Robert Anderson, PG, CEG
Series Editor, *Geology of the Cities of the World* Series
Loomis California
Bobanderson86@gmail.com

Listing of published papers in the series:

| | |
|---|---|
| Albuquerque, New Mexico – 1984 | Long Beach, California – 1983 |
| Boston, Massachusetts – 1991 | Los Angeles, California – 2007 |
| Boulder, Colorado – 1987 | Memphis, Tennessee – 2012 |
| Cairo, Egypt – 1988 | Montreal, Québec, Canada – 1985 |
| Christchurch, New Zealand – 1995 | Pittsburgh, Pennsylvania – 2015 |
| Dallas, Texas – 1986 | Port Elizabeth, Republic of South Africa – 1987 |
| Denver, Colorado – 1982 | Plymouth, England – 2001 |
| Granada, Spain – 2012 | Reno, Nevada – 1992 |
| Hong Kong, China – 1989 | Rome, Italy – 1989 |
| Indianapolis, Indiana – 1983 | Sacramento, California – 2018 |
| Johannesburg, Republic of South Africa – 1986 | Salt Lake City, Utah – 1990 |
| Kansas City, Missouri and Kansas – 1988 | San Francisco, California – 2018 |
| Las Vegas, Nevada – 1993 | Seattle, Washington – 1991 |
| Lima, Perú – 1997 | |

Key Terms: San Francisco geology, 1906 earthquake, Loma Prieta earthquake, Franciscan Complex, accretionary Wedge, subduction zone, transportation, water supply, tunnels, bridges, groundwater, San Francisco history, faulting, seismicity, dams, Gold Rush, liquefaction, subsidence, environmental contamination, military bases

ABSTRACT

The City of San Francisco is located at the northern tip of the San Francisco Peninsula on the western edge of the North American plate. Its location at the mouth of one of the premier natural anchorages on the west coast of North America was crucial in the city's development since the city's inception. San Francisco's strategic location led to the growth of San Francisco during the Gold Rush. The riches of the goldfields caused an explosion in the population of San Francisco and made it the key trading hub between the goldfields and the world. The location served as the western terminus of a water way from San Francisco to Sacramento via the Sacramento River where goods and men were disembarked from ships and traveled to the goldfields. Without the goldfields to the east, San Francisco's early history may have been very different from what it was. This shows that geology directly affected the development of San Francisco in its early days.

The city and the peninsula are within the San Andreas transform margin that forms the tectonic boundary between the North American plate and the adjacent Pacific plate. The geologic and tectonic setting of San Francisco are inextricably linked to this active transform boundary and its evolution from its previous life as a convergent subduction margin. The basement geology of San Francisco consists nearly entirely of the world-famous Cretaceous Franciscan Complex, which represents an accretionary wedge complex related to the prior subduction zone. Franciscan Complex rocks crop out atop the many hills of San Francisco. Quaternary and Neogene sedimentary deposits are draped over the Franciscan Complex rocks and comprise the surficial geology between these outcrops and along the shoreline.

San Francisco's colorful history and patterns of growth have been strongly influenced by the local and regional geology, including several significant earthquakes and the discovery of gold and other mineral resources, which led to periods of economic boom and bust. Today, the geology of San Francisco continues to present challenges for the city and its citizens. Hazards related to the tectonic setting include earthquakes, slope instability, coastal erosion, and climate change. This paper summarizes the geologic history of the San Francisco Bay Area and the engineering characteristics of geologic units, geologic hazards, water resources, infrastructure development, environmental issues, and ge-

ologic issues associated with major engineering structures built in San Francisco.

INTRODUCTION

by Greg W. Bartow, Raymond Sullivan, William E. Motzer, and Kenneth A. Johnson

Geographic Setting

The City and County of San Francisco encompasses 124 km² (48 square miles) of the northernmost portion of the San Francisco Peninsula, and has a population of approximately 805,000 (US Census Bureau, 2010). It is the only joint city and county in California. The Greater San Francisco Bay Area is normally considered to include San Francisco and the eight other counties that border the Bay Area: Alameda, Contra Costa, Marin, Napa, San Mateo, Santa Clara, Solano, and Sonoma (Figure 1). These counties comprise 17,900 km² (6,900 square miles) and have a population of more than 6.7 million people (U.S. Census Bureau, 2010). This paper includes a general overview of the geology and tectonic setting of the San Francisco Bay Area, but the more detailed discussions that follow focus on the City and County of San Francisco in particular. Limiting the scope of the paper in this way allows us to address the geology of San Francisco without overwhelming the reader with the many other geologically interesting parts of the greater Bay Area.

San Francisco is bounded by water on three sides. The Pacific Ocean forms the western boundary and San Francisco Bay forms the northern and eastern boundary (Figure 2). San Francisco Bay is largely fed by the Sacramento and San Joaquin Rivers which drain over 40% of the surface area of California. The waters from San Francisco Bay exit to the Pacific Ocean under the Golden Gate Bridge. The central portion of the bay has an average depth of 13 m (42.7 ft), but the depth below the Golden Gate Bridge is 110 m (360.9 ft) (Dartnell, et al., 2006).

Geographically, San Francisco is located in the Coast Ranges Province, one of the 11 geomorphic provinces into which California is divided (Figure 3). Each province has its distinct geologic characteristics. The Coast Ranges Province occupies a band along the Pacific Ocean 644 km (400 miles) long by 80–121 km (50–75 miles) wide. The Coast Ranges are a series of more or less parallel ranges, all running generally

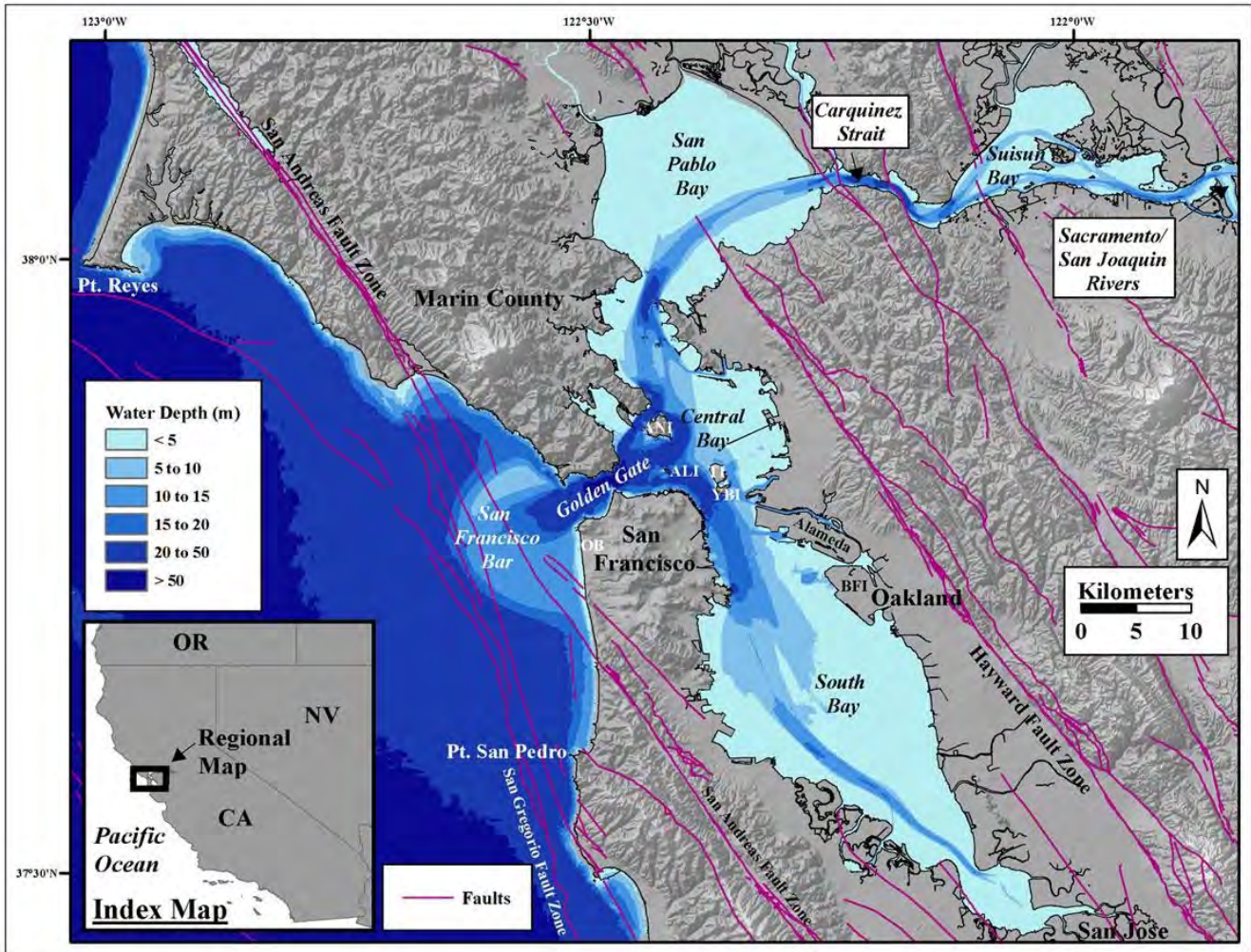


Figure 2. Bay Area map with shaded relief and faults (Barnard et al., 2013).



Figure 3. California geomorphic provinces (CGS, 2002).

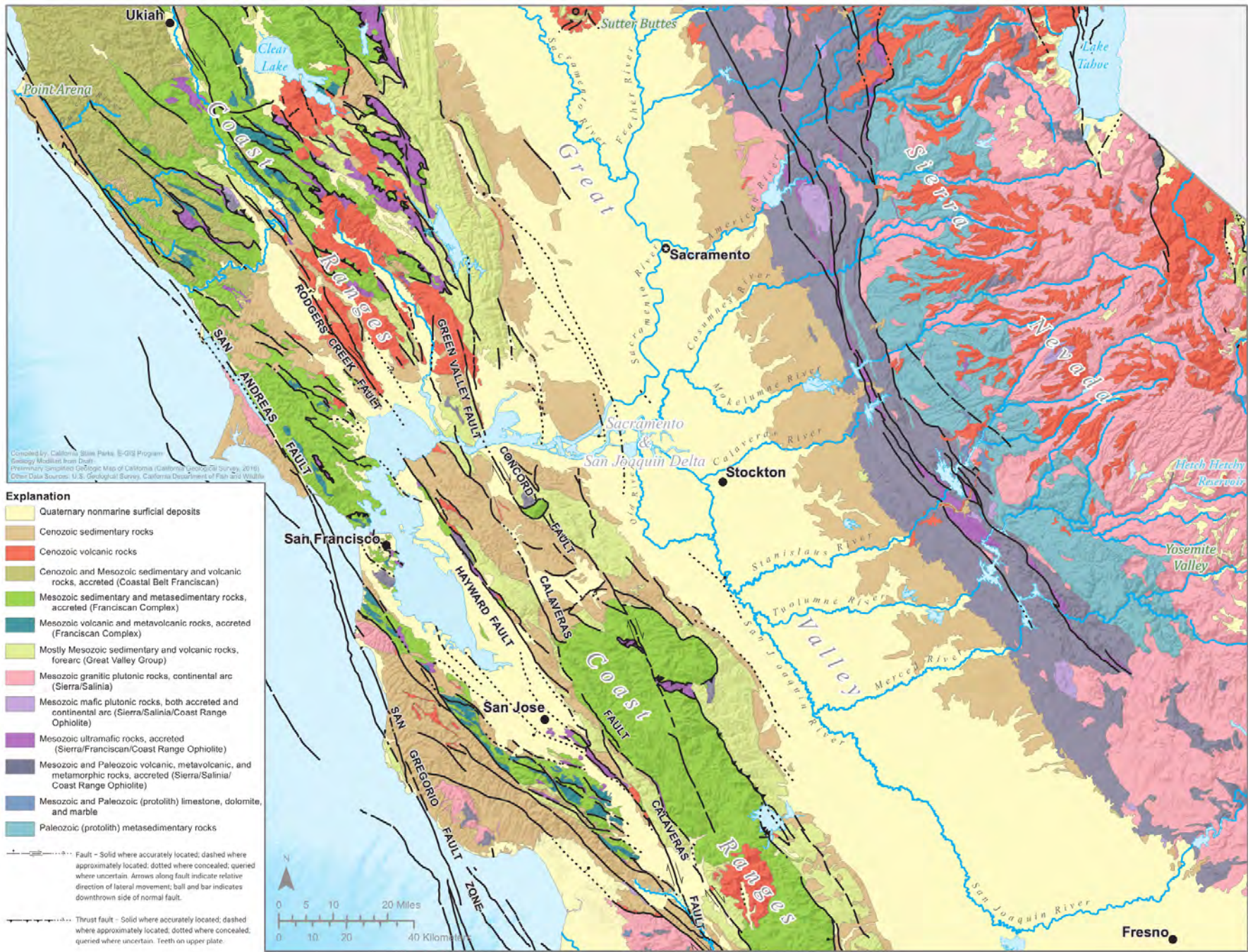


Figure 4. Generalized geologic map of part of northern California. Geology Modified from Draft–Preliminary Simplified Geologic Map of California (California Geological Survey, 2018).

Climate

San Francisco has a Mediterranean climate characterized by wet mild winters and dry summers. San Francisco’s weather is strongly influenced by the cool currents of the Pacific Ocean, which moderates temperature swings and produces a remarkably mild year-round climate with little seasonal temperature variation. Fog is a regular feature of San Francisco summers. Because of the varied topography and maritime influences, San Francisco has a multitude of distinct microclimates. Neighborhoods on the western side of the city tend to be cooler and wetter than neighborhoods on the eastern side.

Based upon 30-year averages (NOAA, 2018), the mean monthly temperatures are warmest in September (17 °C, 63 °F) and coldest in January (11 °C, 51 °F). The highest recorded temperature at the official National Weather Service downtown observation station (currently at the United States Mint building) was 41 °C (106 °F) on September 1, 2017. The lowest recorded temperature was -3 °C (27 °F) on December 11, 1932. Average precipitation is 602 mm (23.7 in) with the bulk of the rain occurring from October to April, with the driest month (August) averaging 2.5 mm (0.1 in) of precipitation, and the wettest month (January) averaging 114 mm (4.5 in) of precipitation.

Variation in precipitation from year to year is high. In 1983, a record high of 974 mm (38 in) of rainfall was recorded in San Francisco. In 2013, San Francisco received a record low 86 mm (3.4 in) of rainfall (NOAA, 2018).

History and Founding

The following section covers San Francisco’s colorful history and patterns of growth, which have been strongly influenced by the local and regional geology, including several significant earthquakes and the discovery of gold and other mineral resources, which led to periods of economic boom and bust. The reader is directed to later sections of this report that dive deeper into the geologic setting, engineering geology, natural hazards, water resources, environmental concerns, major engineering projects, and professional practices.

Native Americans

The earliest evidence of human occupation of California occurred near the end of the Pleistocene epoch

around 13,000 calendar years ago (13,000 years BP) on the Channel Islands off of the Southern California coast (Reeder-Myers, et al., 2015). The Channel Islands have never been connected to the mainland, even when Ice Age sea levels were much lower. Artifacts of tools, stem points and human remains dating from 13,000 to 10,000 years BP have been found indicating that the inhabitants most likely arrived by boat. This sea-based culture traveled on what has been called the “Kelp Highway.”

If the first peoples did indeed arrive in the San Francisco Bay Area around 13,000 years BP the sea level would have been 90 m (295 ft) shallower and San Francisco Bay would not yet have existed (Figure 5) (Sloan, 2006). Because these Native Americans were primarily a coastal people, deriving their subsistence from the sea and adjacent onshore environments, there is scarce or little evidence left of these original arrivals. Indeed, little is known about the Native American cultures of the San Francisco Bay Area in the period of 13,000–5,500 years BP (Milliken, et al., 2009). In addition, any Native American establishments west of the present shoreline, dating to before about 8,000 years BP, would be underwater (Figure 5).

One of the most important and frequently cited archeology discoveries in San Francisco was the 1970 identification of a Native American skeleton, dated at 5,630 years BP, during excavation of the Bay Area Rapid Transit (BART) tunnel near the present location of San Francisco’s Civic Center (Moratto, 1984). In 2014, the discovery of a well-preserved Native American burial 17 m (55 ft) below ground surface, during excavation for the Transbay Transit Center in downtown San Francisco, yielded a radiocarbon date of 7,570 years BP (Meyer, 2014). Radiocarbon dates associated with major strata and Transbay Man are shown in Figure 6.

In San Francisco, subsurface and buried Ohlone artifacts have been discovered at approximately 50 sites, including one of the largest village remains near Candlestick Point. Other sites include those at Islais Creek, Bayview–Hunters Point, Visitacion Valley (adjacent to the Cow Palace), Mission Creek near AT&T Park, and at a site near Mission Dolores. On the northern waterfront, several smaller sites were discovered, including three at Fort Mason, and others in the South of Market, Civic Center BART, and Lake Merced. However, most if not all remains have been reburied or interred at the request of and agreements with Native Americans

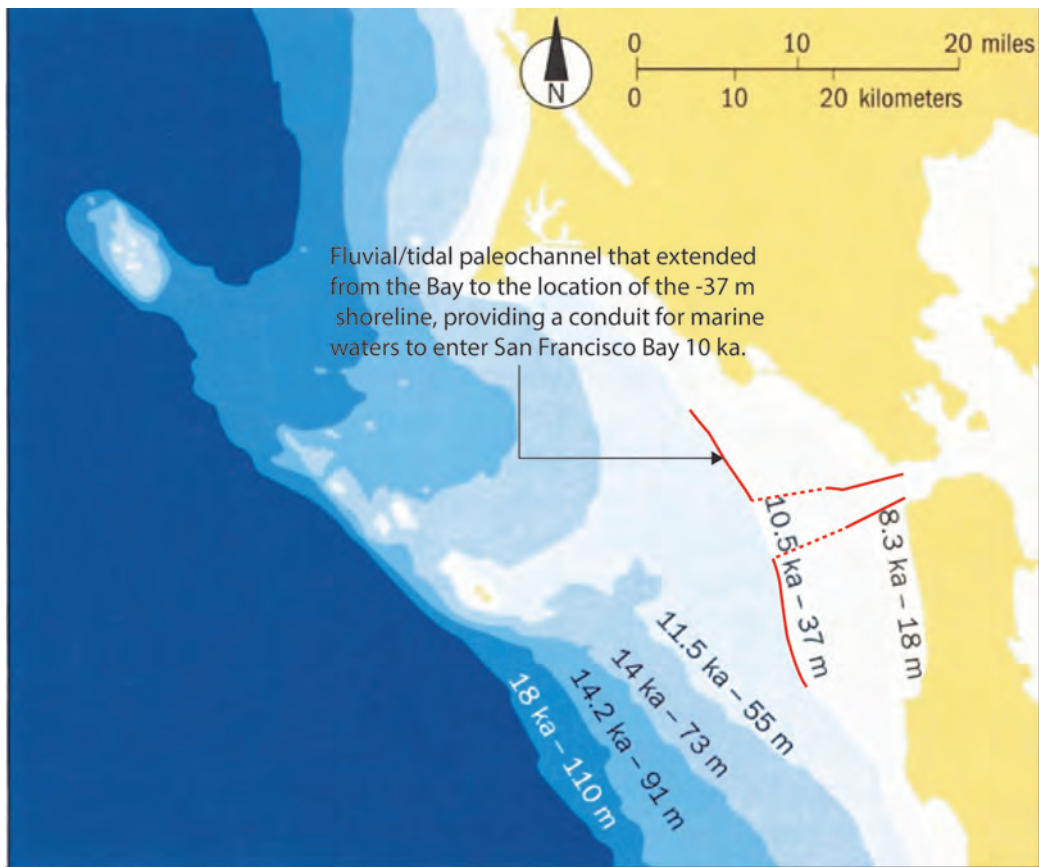


Figure 5. Pacific coast depth intervals at different time periods after the last Ice Age (from Sloan, 2006) modified to show fluvial/tidal paleochannel providing a conduit for marine waters to enter the San Francisco Bay 10,000 years ago (10 ka) (Johnson et al., 2015a). This paleochannel is now filled with sediment.

under several antiquity act requirements.

On the surface, little if any artifacts (such as mortar holes and petroglyphs) of the Native Americans are present in San Francisco, for at least two reasons:

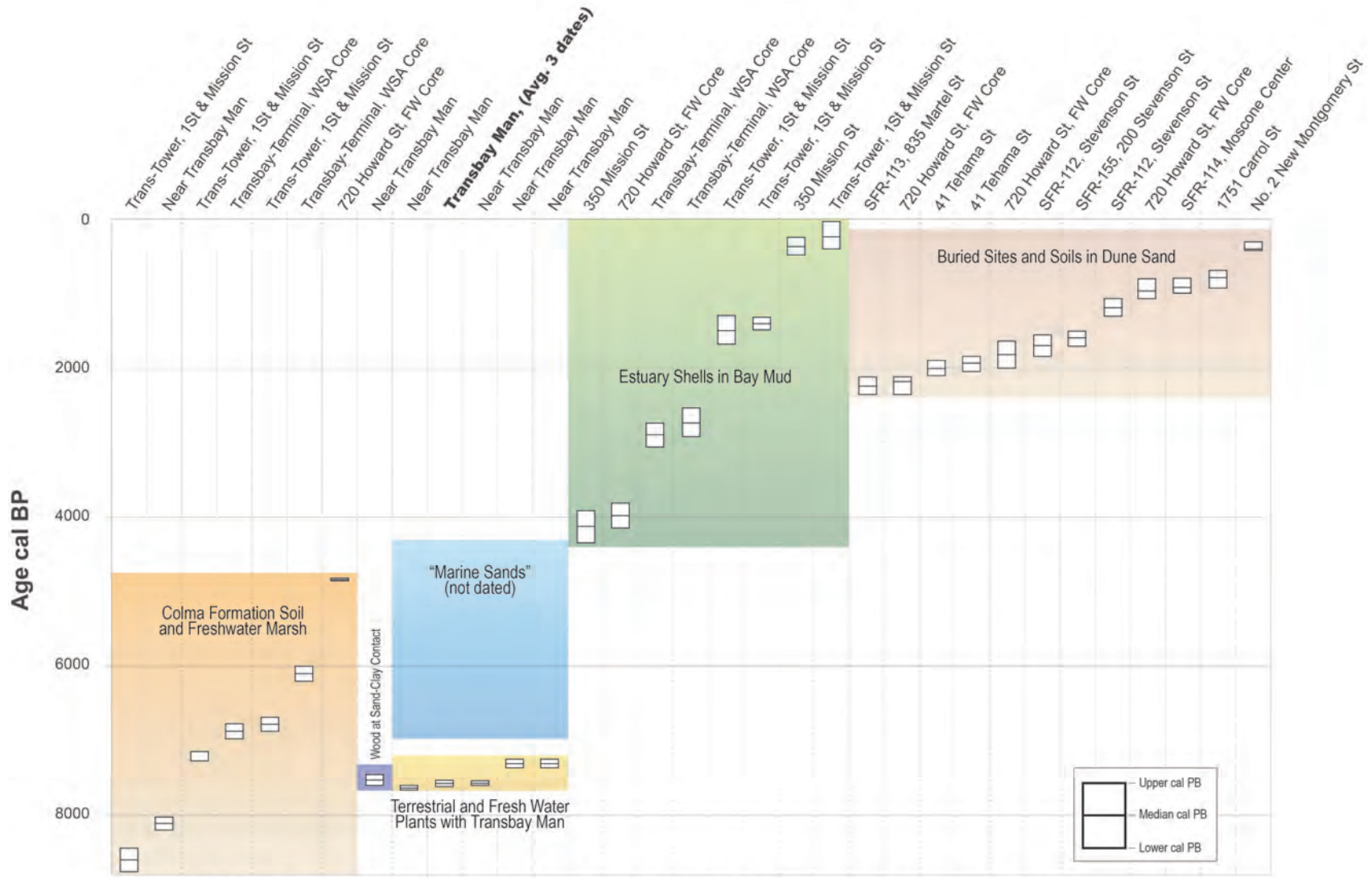
(1) **Geology:** About one third of San Francisco was originally covered with dune sand (See “Quaternary Deposits of San Francisco” section). These dunes were largely barren of vegetation, containing only a few scrub trees (Smith, 2005). Being a fishing-based society, San Francisco’s Ohlone generally kept to the shore with villages adjacent to marshes and creeks draining into the bay. Outcrops of chert and serpentine do not readily allow for either the establishment and/or preservation of such artifacts because chert is hard and brittle and serpentine, particularly in San Francisco, is sheared and rather fissile. Additionally, original shoreline areas along San Francisco Bay have been filled in, burying and effectively erasing the original village sites.

(2) **Infrastructure:** During the Gold Rush (1848–1862),

with the rapid increase of European settlers, much of downtown San Francisco was rapidly built over and many of the original hills (e.g., Rincon Hill) were either modified (leveled) or cut through. By the late 1870s much of San Francisco’s downtown infrastructure was completed (Smith, 2005).

European Founding of San Francisco

When first discovered by the Spanish explorers in 1769, the Bay Area was inhabited by two Indian tribes: the Ohlone on the San Francisco Peninsula, and the Coast Miwok on the Marin and Tiburon Peninsulas (Heizer, 1951). The Native Americans used a variety of natural materials, such as seashells, rocks, and plants, for making tools and ornaments. They subsisted on plants and especially on marine life, as is shown by the contents of their refuse mounds (“kitchen middens”) which are numerous on the shores of the bay and somewhat less common on the ocean shore (Kroeber, 1911). Some of the mounds are thought to have been started 3,500 years ago (Schlocker, 1974).



Note: "FW" is Far Western; "WSA" is William Self and Associates; "Avg. 3 dates" is average of all three bone dates at the 2-sigma range; "TBM" is Transbay Man.

Figure 6. Radiocarbon dates associated with major strata and Transbay Man in Yerba Buena Cove (Meyer, 2014).

Before the Spanish arrived on the San Francisco Peninsula, the Ohlone were organized into perhaps more than 50 societal tribelets occupying small villages along the coast and marshlands. In what is now San Francisco, villages were located at today’s Fort Mason, Crissy Field, and the Sutro Baths, totaling perhaps several hundred persons. The overall Ohlone population from San Francisco south to Monterey is estimated to have been approximately 17,000 (Milliken et al., 2009). Figure 7 from Byrd et al., 2017, shows ethnographic groups and regions, and Spanish missions at the time of the Spanish entry.

The first Europeans known to have visited San Francisco Bay arrived in 1769 as part of an exploration party led by Don Gaspar de Portolá, an agent of the Visitador General of Spain. Spanish explorers made several additional forays to the region prior to establishing a permanent settlement. The first European settlement was started in 1776 when 193 Spanish military and civilian settlers arrived by ship at San Francisco Bay’s entrance establishing a military garrison known as El Presidio de San Francisco as part of Spain’s desire to establish their empire in “Alta California.” They also established, along with civilian settlements, the Fran-



Figure 7. Ethnographic groups and regions, and Spanish missions (after Milliken 2010, in Byrd et al. 2017).

ciscan Mission San Francisco de Assisi, now known as Mission Dolores, located several kilometers inland (Figure 8).

In 1810, Mexico rebelled against three centuries of Spanish colonial rule and eventually won its independence in 1821. Among the territories the new nation inherited from Spain was the remote northern colony of Alta California. Mexico liberalized customs regulations to encourage foreign traders to drop anchor in Yerba Buena Cove, a protected cove within San Francisco Bay.

For the Ohlone, life dramatically changed. By 1810, disease, forced labor, and religious and cultural indoctrination led to significant cultural and population declines (NPS, 2015b). Under the Spanish missionization, the following Mexican period, and the subsequent arrival of Europeans, the Ohlone were removed from their remaining lands, essentially becoming serfs and even slaves (although slavery was outlawed by the Mexican government). They were denied legal status by state and federal governments, and early in the 20th century were declared “extinct” by an influential anthropologist (Leventhal, et al., 1994).

In 1834, the Mexican government secularized the Fran-

ciscan missions of Alta California, including Mission Dolores, and granted vast tracts of former mission lands to favored individuals. As a result of this, William Richardson, an Englishman, became the first white person to settle in Yerba Buena (later renamed San Francisco in 1847). In 1835, he obtained a deed to land located along Yerba Buena Cove and the following year he began building and planning a settlement (Sonoma State University Library, 2018). In the same year, Yerba Buena was formally designated as a pueblo, or civil settlement, by the Mexican government for use as a trading post and place where ships could resupply.

As early as 1835, the American government began attempting to acquire the San Francisco Bay from Mexico. American political and business leaders coveted the bay, seeing it as an ideal base for the nation’s growing trade with Asia. The American government was also anxious to prevent the strategic but weakly held harbor from falling into the hands of Britain or Russia.

In 1846, American troops entered disputed territory in the Rio Grande Valley of Texas, provoking a war between the United States and Mexico. After a year and a half of fighting, the Mexican government capitulated. On February 2, 1848, the two nations signed the Treaty of Guadalupe–Hidalgo. By its terms, Mexico ceded 1.3

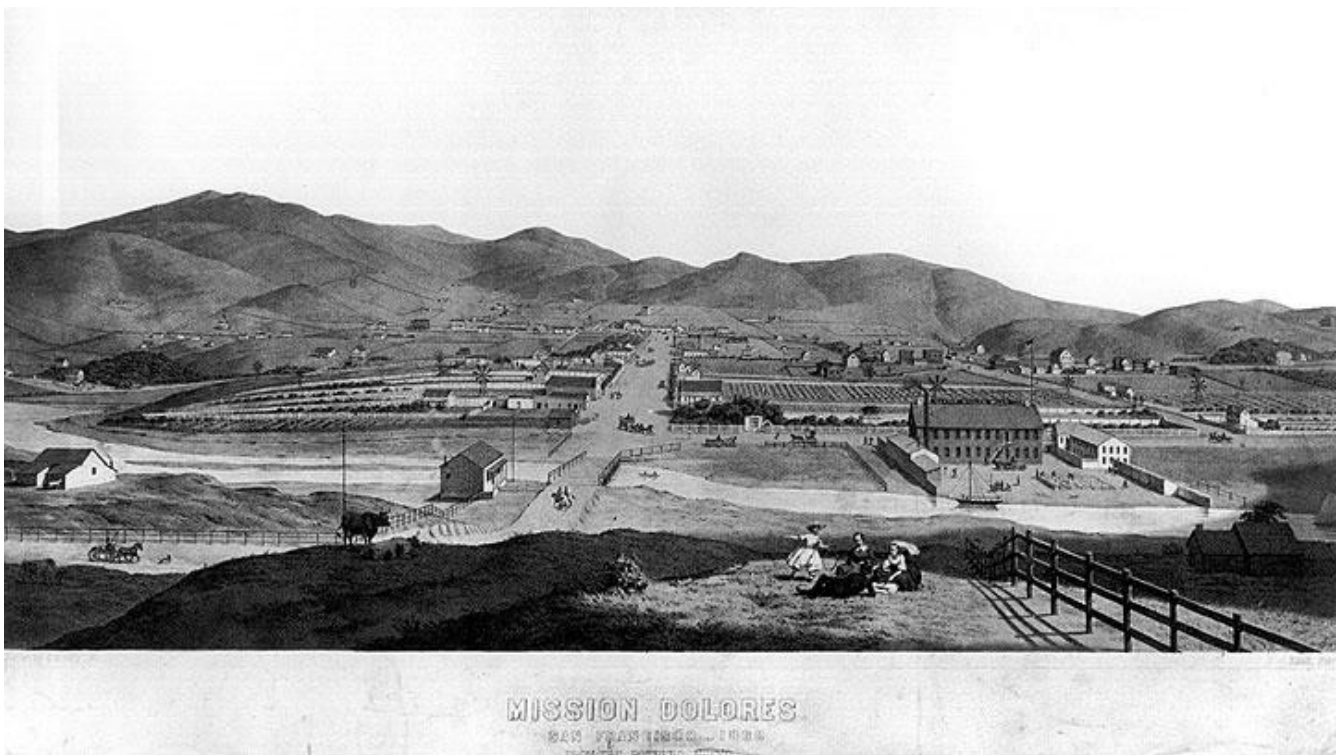


Figure 8. Early etching of Mission Dolores (ca. 1860) with view toward the west along 16th Street (FoundSF.org, 2017).

million km² (525,000 square miles) of territory to the United States in exchange for a lump sum payment of \$15 million and the assumption of \$3.5 million of debt owed by Mexico to American citizens.

On July 9, 1846, Captain John B. Montgomery landed in Yerba Buena and raised the American flag above the Custom House. Mexican rule came to an end in the pueblo without a shot being fired. On the eve of the American conquest, the population of Yerba Buena numbered around 850. Lieutenant Washington Bartlett was appointed to be the first American mayor of Yerba Buena. One of Bartlett's first actions was to rename the settlement "San Francisco," which he did on January 30, 1847. Another of Bartlett's priorities was to extend

the boundaries of the fast-growing community. In 1847, he hired an Irish immigrant named Jasper O'Farrell to complete the city's first survey under American rule. Anticipating the need for a direct route from Yerba Buena Cove to Mission Dolores, O'Farrell laid out Market Street, a 30-meter (100-foot) wide thoroughfare oriented parallel to the old Mission Wagon Road. Market Street followed a southwesterly diagonal alignment to skirt the marshlands ringing Mission Bay (Figure 9).

Gold Rush and Its Impact to San Francisco

The discovery of gold in January 1848, at Sutter's Mill, on the South Fork of the American River unleashed an unprecedented population explosion 210 km (130 miles) away in San Francisco. News of the discovery

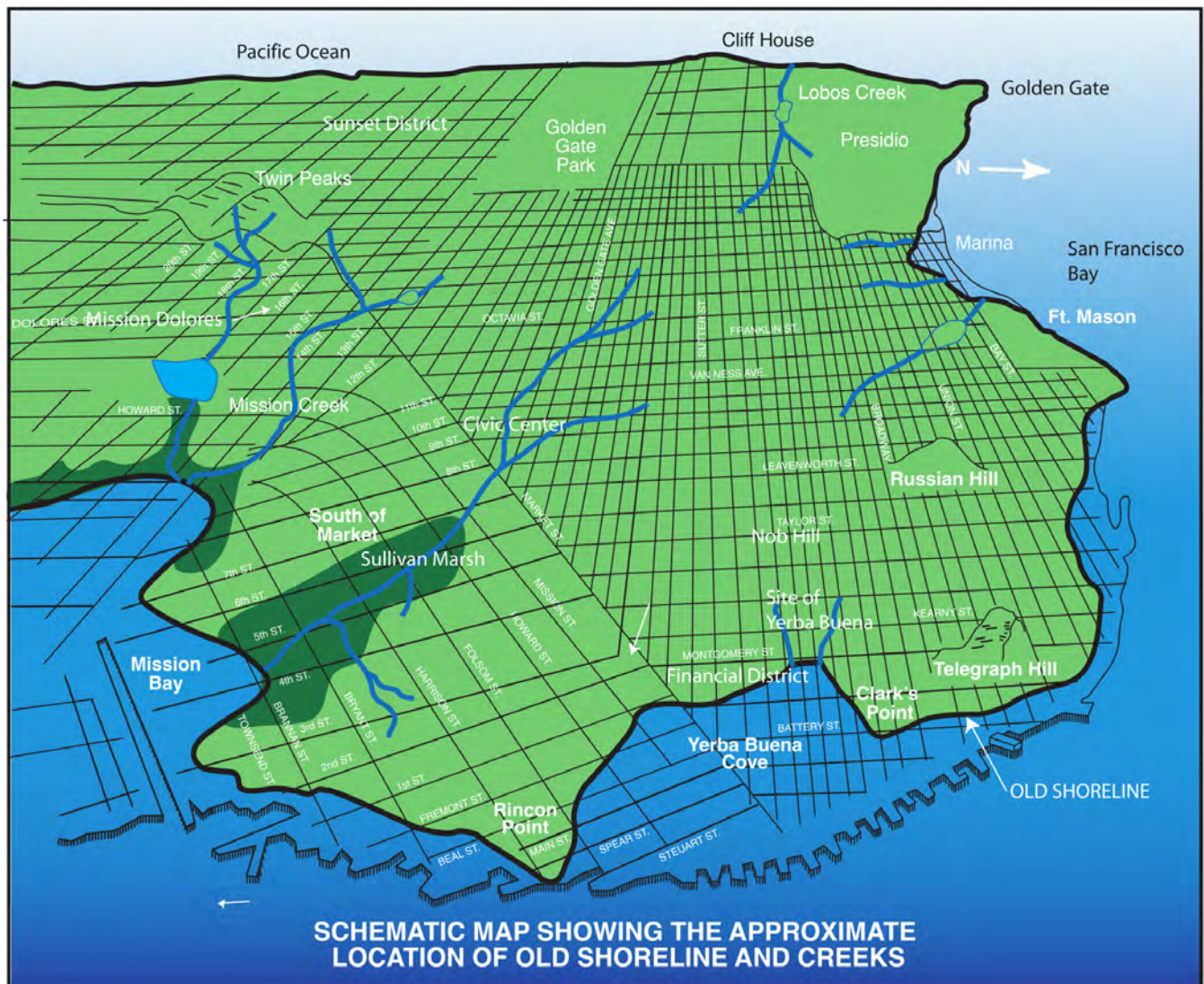


Figure 9. Schematic diagram of San Francisco street grid pattern and the location of the former shoreline and creeks prior to urbanization (Sullivan, 2006).

moved slowly at first, but by the end of 1848, thousands of gold-seekers from around the world, dubbed “Forty-Niners,” made their way to San Francisco. Between 1848 and 1852, the population of San Francisco grew from fewer than 1,000 to almost 35,000 people. The discovery of gold impacted the entire nation but more importantly shaped society in San Francisco and California, particularly in demographics, transportation, and economics.

Four thousand miners descended on the region by the end of 1848, escalating to about 100,000 by 1852 (Tuolumne County Historical Society, 2013). By August 1848, news of the discovery had reached the east coast, subsequently setting off the Great California Gold Rush with thousands of additional itinerant miners descending on the rich surface and near surface placer deposits of the western Sierra Nevada in 1849.

In 1849, the continental railroad was still a generation in the future, with construction beginning in 1863 and completion in 1869. But a rail route from Sacramento eastward across the Sierra Nevada was actually being considered in 1849 and 1850 (Ambrose, 2000). The

best way to get to the gold fields was through San Francisco and it became the hub of the west and the focus for all those with gold fever. They came by sea on sailing and steam ships (Figure 10), overland by walking, horseback, mule pack and oxen pulling wagon train, and finally by stage coach.

Sacramento acted as a bridgehead into the Sierra foothills where adventures were flocking from all over the world to look for gold starting in 1848. This was in part due to the ease of navigation of the Sacramento River from the San Francisco Bay Area, through the Sacramento–San Joaquin Delta to the riverside docks in Sacramento. Sacramento also served as a transfer point between deeper draft river boats (steam and sail) serving San Francisco and shallower draft boats serving towns up river.

Sacramento was also a logical transfer point for gold seekers and supplies coming from San Francisco headed for the Northern Mines. The first stagecoach lines in California started in 1849, running out of Sacramento to the goldfields.



Figure 10. Sailing card for the clipper ship California, depicting scenes from the California Gold Rush, ca. 1850 (Wikimedia Commons: https://commons.wikimedia.org/wiki/File:California_Clipper_500.jpg).

These Forty-Niners also followed the placer deposits back to their quartz vein origins or to the “Mother Lode,” where underground mining began in 1849 at the Mariposa mine in Mariposa County. The discovery announcement eventually resulted in one of the largest historical human migrations with at least 300,000 and perhaps 500,000 people world-wide eventually descending on California with the desire to reap instant wealth (Goldcalifornia.net, 2011b; Matthews, 2012).

The Gold Rush made significant changes to California’s inhabitants and these changes also profoundly impacted residents of the newly named San Francisco. In 1846, both California and what is now San Francisco were virtually unknown to ordinary citizens inhabiting states east of the Mississippi River, and California was still relatively unpopulated. However, this changed quickly because of the lure of potential instant wealth to inhabitants of the eastern overpopulated cities.

In 1848 and 1849, San Francisco was rapidly being transformed into a boomtown. With creation of new businesses, corporations, and banks, there was a severe shortage of legal tender to facilitate financial transactions. The answer was to produce readily available coinage.

In 1852, Congress voted and authorized construction of the San Francisco Mint, which began in 1853 on a Commercial and Montgomery Street lot. The three-story brick building did not last long because it was too small, hot and poorly ventilated, and noisy. To expand operations, in 1867, Mint officials purchased land at the corner of Fifth and Mission Streets (GovMint.com, 2016).

The San Francisco Mint was more than just a coin-producing facility. Raw or native gold (as placer dust and ore) was also brought to the Mint where it was refined (smelted) into coins and ingots (GovMint.com, 2016).

Between the Gold Rush and the 1906 Earthquake

In 1853, after the city had burned a number of times, an ordinance was passed that required wooden buildings in the commercial/financial district to be replaced by brick ones. Initially, most buildings were two or three stories (Figure 11). In the late 1850s and 1860s newly available structural cast iron was used to open up the facades of buildings and to utilize less brick. A wide variety of ornamented buildings emerged and heights increased to four and five stories.

Table 1. Some gold exports from San Francisco: 1848–1855.

| Report Date | Newspaper and Other Report Comment | Dollar Amount Value for that Year | Value in 2016 Dollars* |
|--------------------|--|--|-------------------------------|
| November 28, 1848 | <i>“U.S.S. Lexington” departed San Francisco with...gold destined for the U.S. Mint in the East.</i> | \$500,000 | \$14,773,840 |
| January 1, 1852 | <i>Gold exports for the year 1851...</i> | \$34,492,000 | \$1,043,424,390 |
| September 1, 1852 | <i>Gold dust...has been shipped East so far this year</i> | \$29,195,965 | \$862,673,323 |
| January 1, 1853 | <i>Gold exports for the year 1852 amounted to...</i> | \$45,587,803 | \$1,347,014,271 |
| January 1, 1855 | <i>Gold exports for the year 1854 amounted to...</i> | \$51,429,101 | \$1,390,285,697 |
| January 1, 1856 | <i>Gold exports for the year 1855...</i> | \$44,640,090 | \$1,181,623,182 |

Notes: *2016 dollars calculated from inflation values provided by Friedman (2017).
Sources: The Virtual Museum of the City of San Francisco, 2017a, 2017b, 2017c.



Figure 11. Original Russ building at Montgomery and Pine streets ca. 1860 (Fireman's Fund).

It took a few years for the street grid plan that had been adopted by the city to be extended beyond the downtown and as it grew the streets were extended up steep hills without regard for the topography (Figure 12 and Figure 13). The marshland along the bay margin was prime property for the rapidly growing city and new land was created utilizing the vast amount of sand from the nearby sand dune belt. In the meantime, the original commercial and financial center around Portsmouth Square spread to include Jackson Square and Montgomery Street. The city of this period was Victorian in design with very ornate buildings with decorative facades giving an overall impression of a

city uncoordinated and untidy in architectural design (Figure 13).

In 1865 and 1868, earthquakes on nearby faults damaged many buildings in downtown San Francisco. These events led to City Hall being moved away from Portsmouth Square to Buena Vista Park on the east side of Market Street, an open space that had previously been the city's cemetery. Construction of the new City Hall began in 1872 and was finally completed in 1899. The South of Market area became the site of working class boarding houses, warehouses, and small businesses (Figure 14). Market Street became the main boulevard of the city. Hotels and upscale

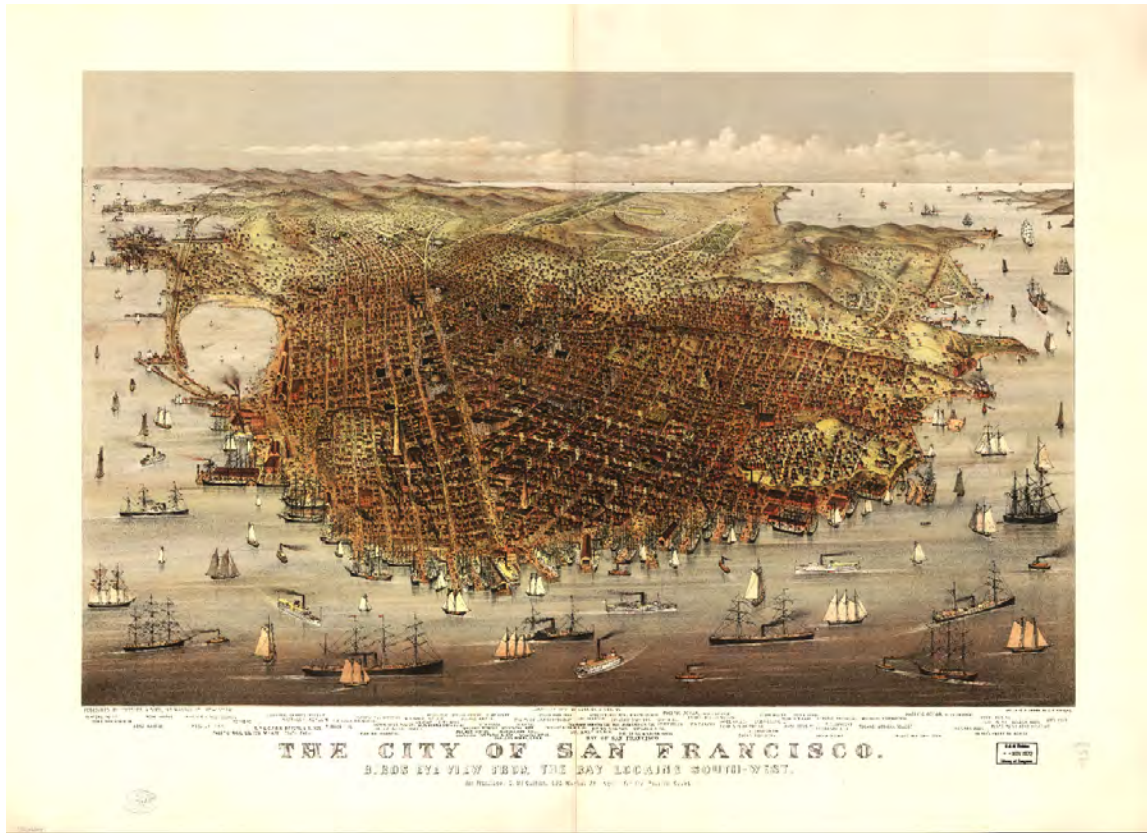


Figure 12. San Francisco in 1878. Bird's-eye view from the bay looking southwest (Parsons, 1878).



Figure 13. Market Street before the 1906 earthquake and below the Grand and Palace Hotels at Market and New Montgomery (Fireman's Fund).



Figure 14. South of Market from Second and Howard streets in 1880 (San Francisco Library).

commercial businesses were constructed along the avenue including the seven-story Palace Hotel (1875), Grand Hotel (1875), and the Baldwin Hotel (1877). The Palace Hotel was a major advancement in technology since it was a reinforced iron structure, which utilized very advanced mechanical systems including elevators. Banks and government buildings followed including the U.S. Mint (1874) on Fifth Street, and the Main Post Office (1905) on Seventh Street.

The 1890s saw the introduction of new steel framed construction built under the supervision of trained structural engineers. The architectural design of these buildings were influenced by the *École Beaux-Arts*, or the *City Beautiful*, movement that was spawned by the 1893 Chicago Columbian Exposition (Woodbridge and Woodbridge 1982). The new earthquake-resistant high-rises included the Chronicle Building (1889), Mills Building (1891), Hibernia Bank (1892), Call Building (1898), Kohl Building (1901) and St. Francis Hotel (1904). There were a total of 42 of these “fireproof” buildings in downtown San Francisco and several others under construction in 1906. They formed the tallest buildings together with the church spires, a few smoke stacks, and the Selby Shot tower in the South of Market (Figure 14). They were scattered among a city skyline dominated by the wood-and-iron framed Victorians and a few brick buildings.

The residents of San Francisco were alerted to the imminent danger of earthquakes by several small to moderate tremors that occurred towards the end of the century. A moderate earthquake occurred on March 26, 1884, the most violent since 1868. Others followed in 1888, 1890, 1892, and 1898. The new steel frame buildings performed well in these tremors although buildings on fill were often badly shaken, particularly in the 1898 quake (Tobriner, 2006). Little concern existed about the likelihood of a major earthquake. The city was prospering at the end of the century and growing more affluent. The 1900 census indicated that San Francisco had 450,000 residents.

Quarries in San Francisco

The hills of San Francisco offered an excellent source of rock used for a wide variety of construction purposes in the late 19th and early 20th centuries. These hills were present due to the generally good quality, erosion-resistant rock that comprised the hills. As San Francisco was growing in the 1860s, the hills closest to the center of the city, Telegraph Hill and Rincon Hill, were candidates for excavation for building materials. Other quarries sprang up in progressively more distant parts of the city including Corona Heights (Figure 15), Diamond Heights, Noe Valley, and others.



Figure 15. The Gray Brothers Quarry and Brick Factory in Corona Heights, 1888 (FoundSF.org).

Among a number of quarry operators that included the Gray Brothers, the Wetmore Brothers, and John Kelso, the Gray Brothers became infamous due to their utter disregard of properties adjacent to the quarry operations and their ambition to level Telegraph Hill entirely. George and Harry Gray dominated the quarry business in San Francisco in the late 1880s through the turn of the century. They operated quarries throughout San Francisco and had offices in Los Angeles, Oakland, and Alameda, but the core of their business revolved around Telegraph Hill. By this time, Telegraph Hill had developed into a residential community topped with houses occupied by some of San Francisco's elite citizens. As the Gray Brother's quarry advanced from the east and north sides of Telegraph Hill, houses and structures on top of the hill would rather routinely be undermined and destroyed, in some cases with inhabitants inside! The trials and tribulations of the Gray Brothers are described in some detail in David Myrick's colorful book entitled *San Francisco's Telegraph Hill* (Myrick, 1972).

Harry and George Gray had complementary skills and predilections, at least during the prime time of their lives. George Gray was the operator of the quarry operations and possessed a rough character to suit his business. Harry, on the other hand, was cut from a different cloth and circulated in the high society of San Francisco, including associations with such well known figures as A.B. Spreckels of the sugar family. Harry was elected secretary of the exclusive San Francisco Club in January 1898. The distinct social circles inhabited by the brothers allowed Harry to smooth over numerous instances of reckless behavior in the quarry business. Harry was able to make amends with City Hall officials even when the quarry operator ignored new laws restricting blasting within the city limits, such that penalties were not levied and operations continued for a time. The callous quarry operations drew neighborhood protests that escalated into pelting the quarry crews with rocks until they ceased blasting. San Francisco police were brought in to protect the quarrymen and prevent blasting.

As described later in the “Major Engineering Projects” section of this publication, the Gray brothers were tremendously successful during the beginning era of the San Francisco construction due to their proximity to construction sites. Their fortunes changed after the 1906 earthquake and operations gradually declined to the point that they began to pay creditors with stone rather than cash. Another unforeseen and difficult element of the Gray Brothers activities was that much of the stone excavated from the quarries in Corona Heights was unsuitable for concrete production because it had an unacceptably high opal content, and the opal was deleterious when mixed with cement to produce concrete. From these operational difficulties and cash flow challenges, George Gray was eventually murdered by one of his employees, Joe Lococo (Figure 16), a poor and destitute Italian immigrant who repeatedly tried to get paid for his work, only to be brushed back

by George time after time. Eventually Lococo was so despondent that on his last unsuccessful visit to get paid, he shot George twice, killing him. Interestingly, at that point, the Gray brothers were so despised by many San Franciscans that upon publication of the story in the newspapers, Lococo found himself the recipient of cash support for living expenses and legal fees for his defense. He was ultimately was acquitted on April 6, 1915, to a cheering courtroom.

Blasting on Telegraph Hill ended in 1914 as a result of the mounting neighborhood, legal, and other public pressures. The quarry activity was important to San Francisco’s growth; however, the blasting and quarrying activity had loosened the rock and steepened the slopes such that rock falls and associated damages are still occurring to this day. Of all the locations where quarry operations had occurred, Telegraph Hill was the most heavily populated and built upon, and the clash between

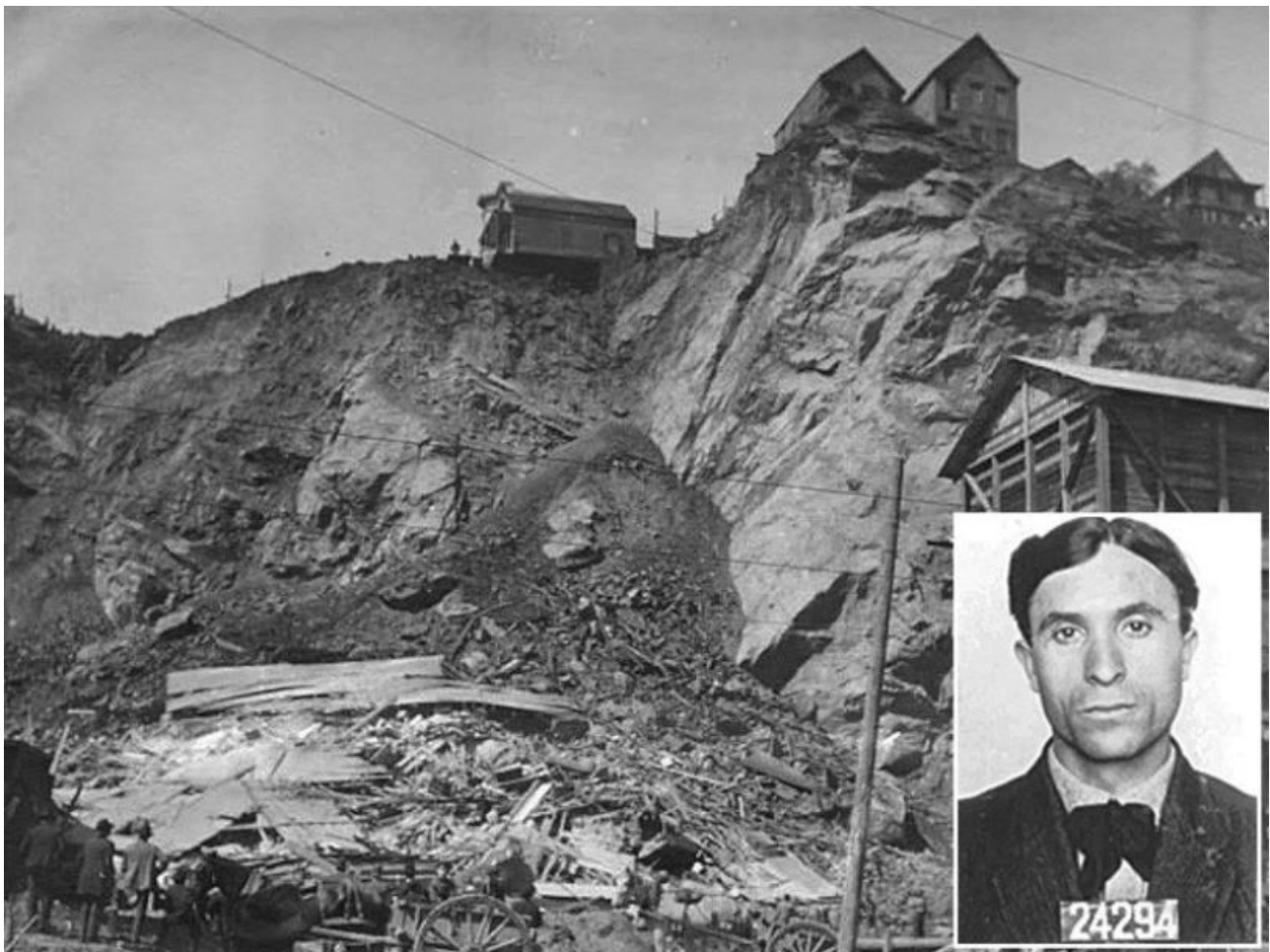


Figure 16. Face of Gray Brothers Telegraph Hill Quarry showing a house destroyed at the foot of the hill and another leaning over the edge at the top of the hill, with an inset of Joe Lococo, who killed George Gray (San Francisco Examiner).

slope stability and quarry operations continues to be played out.

1906 Earthquake

A major earthquake on the San Andreas Fault, with a magnitude (M) of 7.9 struck the city at 5:12 a.m. on Wednesday, April 18, 1906, with an epicenter a few kilometers west of San Francisco off the entrance to the Golden Gate. (For more details on the San Andreas Fault, see later sections on the “Geologic Overview of the San Francisco Bay Region,” “Offshore Geology,” and “Geologic Aspects of Natural Hazards”). The tremor was felt strongly throughout the region. In the city, the damage and death toll were greatest on the artificially filled land in the South of Market. Filled areas on the north side of Market Street were also badly damaged, including the Produce District on Washington Street and the Fish Market located on Merchant Street. On review, buildings generally throughout the city were severely shaken but often only lightly damaged, although cornices and walls of some of the structures cracked or collapsed into the street (Figure 17). No steel reinforced buildings were severely damaged in the downtown and, for the most part, the buildings of wood frame construction, mainly located in the hills and outer part of the city, had little damage.

Liquefaction, however, was widespread on filled ground in the South of Market and Marina District. It resulted in lateral spreading and ground ruptures (Pease and O’Rourke 1998). Buildings on artificial fill were shifted off their foundations, many tilted at odd angles. Others collapsed, trapping residents in the lower floors of the wreckage. Debris on the streets made it difficult for vehicles to move around freely, and roads and sidewalks were buckled and fissured. Water mains and sewer lines were ruptured and spilled their contents over the streets. Electric lines were down, and broken gas lines also posed a major hazard as did fires that erupted in numerous locations. People gathered into the streets as the aftershocks continued to rattle the buildings. Three aftershocks occurred within the first hour at 5:18, 5:25 and 5:42 am. The largest aftershock of the day occurred at 8:14 a.m. Small tremors continued into the evening and kept the residents in a constant state of alert.

It became apparent to the authorities immediately after the earthquake that a major disaster was at hand in the city. A key person who played an important role in the events associated with the earthquake and fire was General Frederick Funston, acting commander of

the Army’s Pacific Division. His dawn inspection of the downtown area indicated the likelihood of a major disaster, and the need for the authorities to maintain law and order. The destruction of City Hall by the earthquake left Mayor Eugene Schmitz, and other municipal leaders, without a command center. The mayor, early that morning, relocated his administration to the Hall of Justice in Portsmouth Square. One crucial member of his staff, however, was absent. Fire Chief Dennis Sullivan had been fatally injured in his apartment on the third floor of Engine House No. 3 located on Bush Street near Kearney. His leadership was sorely missed as operations designed to control the spread of fire failed, and the city was doomed to destruction (D. Smith, 2005). All public transport ceased to operate, and downed telephone lines made it difficult for the public and authorities to assess the extent of the destruction.

The downtown was doomed by mid-morning when a new fire threat arose immediately west of the Civic Center (Figure 18). This blaze has been named the “Ham and Eggs” fire by historians. It originated at 395 Hayes Street, near the intersection with Gough, about three blocks from the Civic Center (Hansen and Condon 1989). Residents in the building attempted to cook breakfast on a damaged stove. Firemen arrived quickly at the scene and normally would have contained the blaze. However, there was no water supply in the area, and the fire soon spread fanned by the westerly breezes. It swept eastward through the Civic Center, crossed Market Street around Ninth Street, and joined up with the South of Market fires. When it became clear later that morning that the fires were gaining in intensity, a valiant attempt was made to contain the fire to the South of Market Street (Figure 17). Mayor Schmitz ordered the dynamiting of buildings in the immediate path of the fire. His other choice was to clear a wide perimeter to serve as a fire break some distance away from the fire zone (D. Smith, 2005). He hoped that his decision to fight the fire building by building would cause less damage to the city and contain the fires along the existing broad avenues such as Van Ness Avenue and Market Street. Dynamiting began on Eighth Street and then moved down Market to Third Street in order to protect the Palace Hotel and the Mint. Unfortunately, these efforts failed to save the Palace Hotel and other buildings along Market Street because of the lack of water and the poor use of explosives by inexperienced hands (Fradkin, 2006). By the afternoon,



Figure 17. The Call Building on fire, late morning April 18, 1906 (Fireman's Fund).

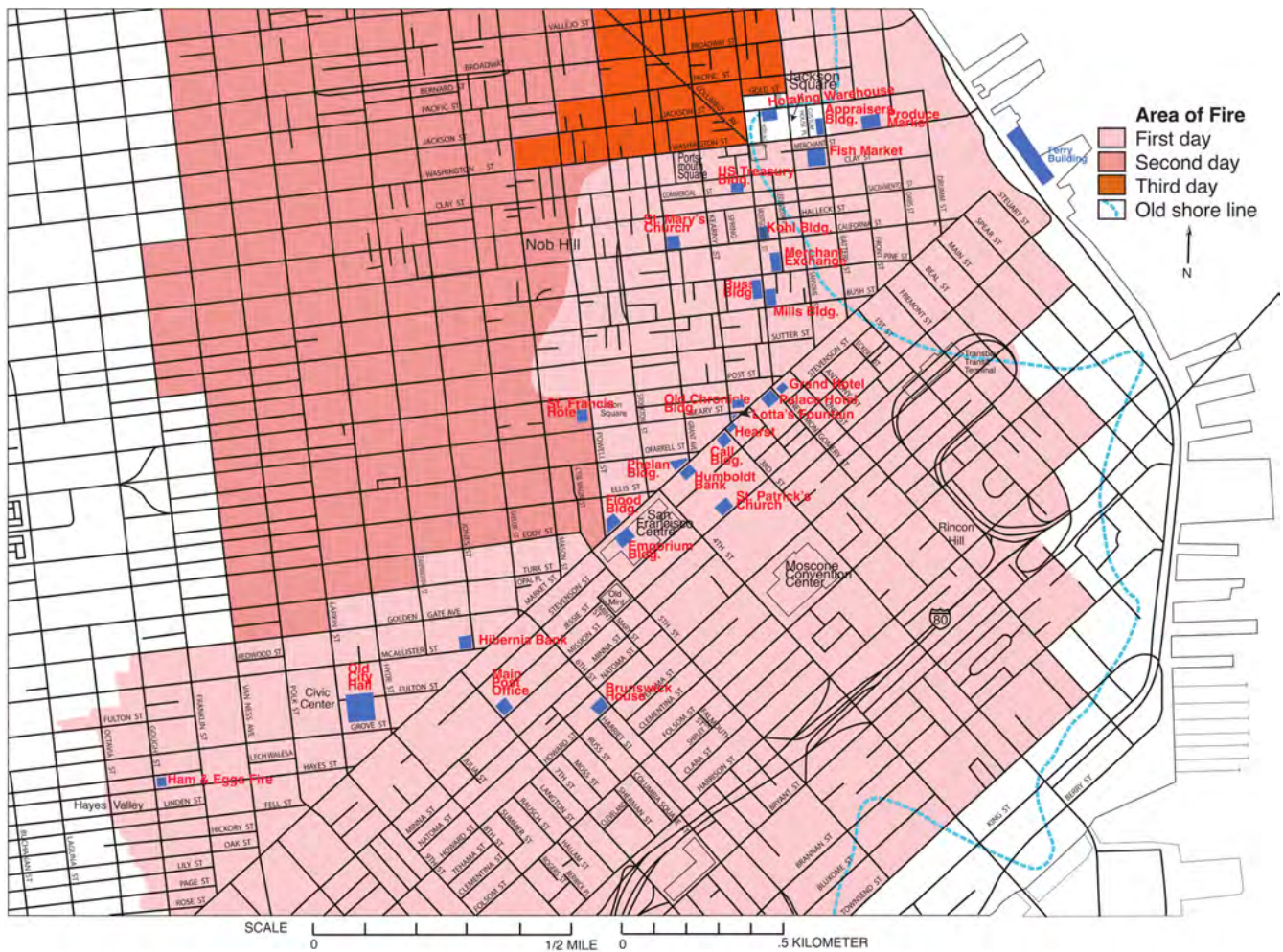


Figure 18. Map of downtown San Francisco showing the areas that burned during the three days of fire storm that followed the 1906 earthquake. The “Ham and Eggs” fire is shown in the lower left (Sullivan, 2006).

the fire crossed Market Street into the Financial District (Figure 18).

As darkness fell that first day, the low-lying area around the old bay margin had been destroyed with the exception of Jackson Square (Figure 18). It was now the turn of the residents living close to bedrock on the slopes of Nob Hill, Russian Hill, and Telegraph Hill to witness the next stage in the destruction of the city. Those residents living in these areas had believed, at first, that they had survived the worse of the disaster. They felt fortunate to have their homes still standing after the earthquake, and their residences were well beyond the fire zone. However, conditions deteriorated rapidly in the evening and in the morning of the second day fire swept through the hills of the city (Figure 18). In the meantime, martial law had been imposed throughout the city. No one entered or left the perimeter without permission. Fires were eventually brought under control

by dawn on Saturday, April 21, 1906.

The 1906 earthquake resulted in the greatest fire loss in U.S. history (Figure 19). Immediately after the earthquake and fire, the city set about the process of burying the dead, feeding and housing the homeless, and repairing its infrastructure as aid poured in from many parts of the world. As a result of the fires, over 250,000 people—more than half the city’s population—became homeless, and many fled by ferry across the bay, or camped in parks, or other open spaces. The exact death toll from the earthquake will most likely never be known particularly because large numbers of the dead were unaccounted for in the path of the fire. It is clear that the official number given in 1907 of 478 persons is grossly incorrect. Gladys Hansen, a former city librarian, estimated the number at more than 3,000 dead, and recently the Board of Supervisors has agreed

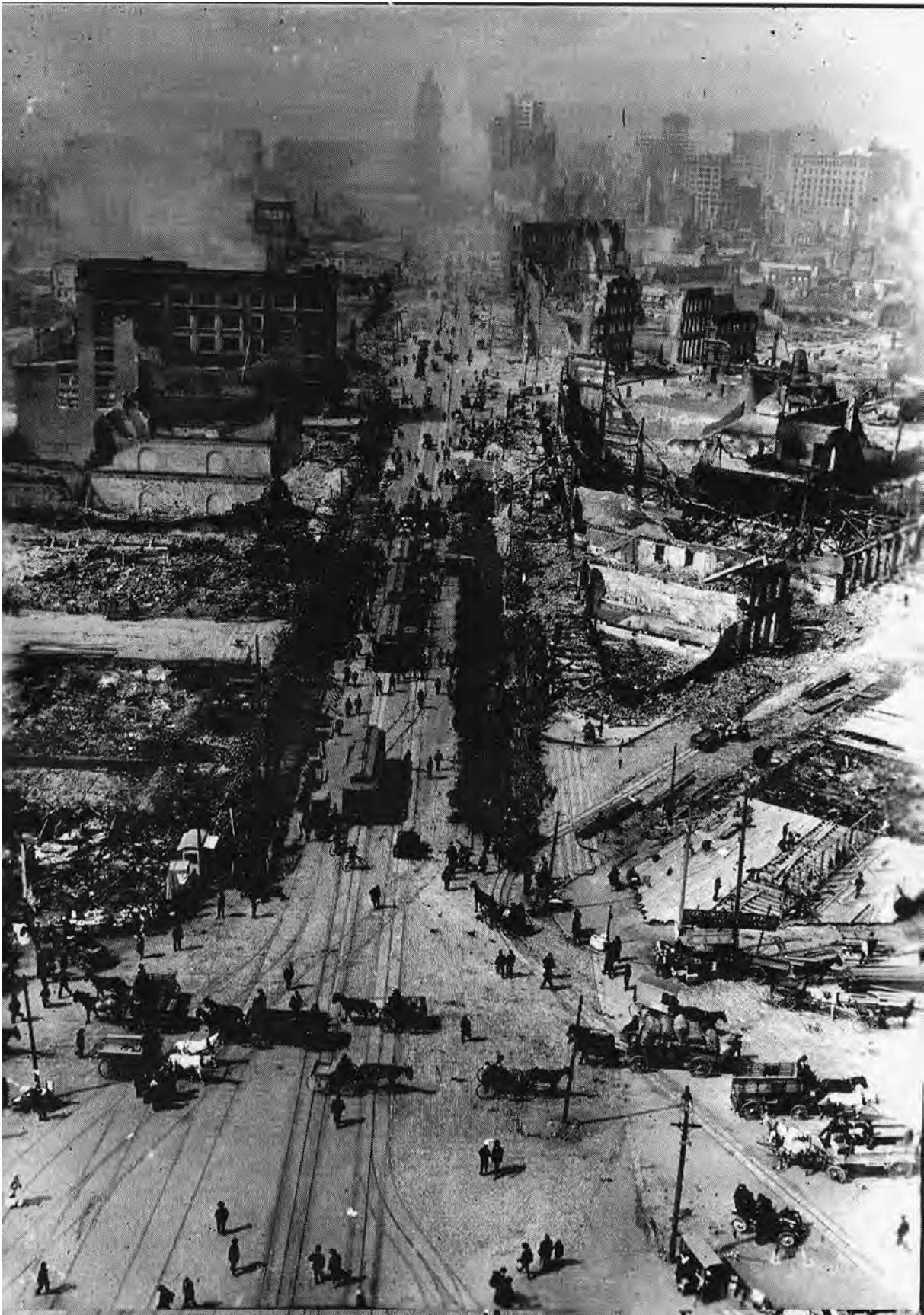


Figure 19. Scene showing the destruction along Market Street after the earthquake and fire (Fireman's Fund).

to do a recount in order to obtain a more accurate number.

It has been estimated that about 12.2 km² (4.7 square miles) or 508 blocks of the city were destroyed, containing some 28,188 buildings (Figure 19). The San Francisco Chamber of Commerce, in its 1927 report, estimated the property damage from the earthquake and fire combined to be between \$300 million to \$1 billion (Tobriner 2006). There is little doubt that the filled land, recovered from the bay, was the site of greatest damage to structures from ground shaking, and was the origin of most of the fires. The fire razed all wooden structures in its path, and only the facade of steel-framed and masonry buildings stood amid the ruins.



Figure 20. Scene on California Street showing the equipment used to fight the fire storm that engulfed the downtown following the 1906 tremor (Fireman's Fund).

The fire department was unprepared to fight such a fire storm particularly without the effective leadership of their Fire Chief. The department in 1906 was composed of 575 firemen and about an additional 100 relief in reserve. There were 38 engines, 12 ladder companies with nine men and an officer assigned to each fire engine (Figure 20). Most units were horse drawn. There were a total of 63 underground cisterns in the city, with a capacity of 37,900 to 132,000 liters (10,000 to 35,000 gallons), many dating back to the Gold Rush days. Most contained water but some were filled with trash and garbage or utility companies had run pipes through them. The water supply was located in three large reservoirs located on the peninsula south of the city and piped into San Francisco. However, two of the three of these distribution systems were damaged by liquefaction and ground shaking in the quake (Pease and O'Rourke 1998). There was little or no water in the downtown and other parts of the city to fight the inferno, and crews had to stand by and watch as fire engulfed the nearby buildings and the city burned for the next three days.

Rebuilding after the 1906 Earthquake and Fire

The city rapidly rose out of the debris after the disaster. The major federal buildings, the U.S. Mint, the Appraiser's Building, and the Post Office had survived in the downtown area. City Hall and most churches and banks were in ruins. The infrastructure such as power plants, water and sewage, and transportation centers were destroyed. Fortunately, the docks and warehouses along the bay were untouched by fire. The spirit of the citizens, however, was unbroken and a new city arose from the ashes.

Six thousand buildings had been completed by the summer of 1907, and three thousand others were under construction. The decision was made to rebuild as quickly as possible and not take advantage of a plan that had been recently drawn up by well-known city planner Daniel Burnham. It was ironic, therefore, that nature had presented the city with a unique opportunity to undertake a complete redesign of the downtown area. The opportunity was passed over as the city moved forward, as quickly as possible, with reconstruction. The decision was made to rebuild on the same lots using the former street grid. There was great concern about a financial panic and uncertainty if insurance companies would reimburse property owners. Insurance companies, however, largely honored their commitment

and provided the needed resources.

By 1909 most of the downtown was rebuilt. For the second time, San Francisco was an “instant city.” There were many new larger buildings although vacant lots still existed. The character of the downtown area had changed since all the Victorians were gone. Only the Chronicle and Mills buildings remained with their outmoded Romanesque architecture. A few stone facades remained but most buildings were clad in terra cotta. Ground level on commercial buildings was commonly glass to provide storefront displays. Most buildings had steel frames and fireproofing; a few still were built with load-bearing brick walls. The conservative architecture gave the city a modern and uncluttered look. Buildings were built of lower height because of the fear of earthquakes, and this gave the city a compact appearance.

The task of rebuilding was completed by 1914 in time for the Panama–Pacific International Exposition that was designed to show the new San Francisco to the world. The new City Hall unfortunately was not completed until a month after the Exposition closed. New building and fire codes had been adopted in the construction. Many new designs were introduced including the use of reinforced concrete as a substitute for brick in tall steel structures. Another innovation was brought in 1918 by architect Willis Polk who constructed the Hallidie Building at 130 Sutter, reported as the “first glass curtain walled structure in the World” (Corbett, 1979) whereby the glass is hung beyond the structural elements creating a structure of extraordinary precision and lightness.

See the “Professional Practices” section for more information on the evolution of seismic building codes.

Panama-Pacific International Exposition

For nine months in 1915, the Presidio’s bayfront and much of today’s Marina District was the site of a grand celebration of human spirit and ingenuity. Hosted to celebrate the completion of the Panama Canal, the Panama–Pacific International Exposition reflected the ascendancy of the United States to the world stage and was a milestone in San Francisco history. The vast fair, which covered over 2.43 km² (600 acres) and stretched along 4 km (2.5 miles) of waterfront property, highlighted San Francisco’s grandeur and celebrated a great American achievement: the successful completion of the Panama Canal. Nine years earlier, San Francisco

experienced a terrible earthquake and fire, declared one of America’s worst national disasters. The city overcame great challenges to rebuild and by the time the Exposition opened in 1915, San Francisco was ready to welcome the world. Ironically, the Exposition was partially constructed on land that was created by placing artificial fill on former wetlands. Indeed, some of the artificial fill was even debris from the 1906 earthquake. Later, a number of homes that were built on the former Exposition fill areas were structurally damaged during the 1989 Loma Prieta Earthquake. See additional discussion in later sections on “Artificial Fill” and the “1989 Loma Prieta Earthquake.”

Between February and December 1915, over 18 million people visited the fair, which promoted technological and motor advancements including wireless telegraphy and use of the automobile.

One hundred years later, the Exposition’s legacy is still evident in San Francisco. A few of the city’s buildings were either rebuilt or designed in the style of the Exposition, like the Marina’s Palace of Fine Arts or Lands Ends Legion of Honor. The fair’s location and design also required significant landscape changes, including the filling-in of acres of waterfront marshland. Today, the Marina Green and Crissy Field, two of the city’s most popular recreational open spaces, are products of these landscape changes (National Park Service, 2018a).

World War II: Military Base Expansion

World War II touched all of California very heavily, but nowhere more than San Francisco Bay. Preparations were massive, swiftly arming San Francisco. Following the 1941 Japanese attack on Pearl Harbor, when many felt a mainland invasion of California was imminent, Presidio soldiers dug foxholes along nearby beaches. Soon after, the Presidio conducted the internment of thousands of Japanese-Americans. As World War II progressed, the Presidio became headquarters of the Western Defense Command and the nearby Fort Mason Port of Embarkation shipped 1,750,000 American servicemen to fight in the Pacific theater.

Forts Baker, Barry, and Cronkite ringed the tip of Marin County; Fort Funston stood at the ocean base of San Francisco, with gun emplacements in between. Fort Point mounted guard on the Golden Gate Straits. Inside the bay, bases abounded. Fort Mason rested aside Aquatic Park in San Francisco; Moffett Naval Air Field

stood at Sunnyvale; Alameda Naval Air Station and the Army supply depot in Oakland faced San Francisco across the bay; Hamilton Air Field stood to the north in Marin County. In the middle, Treasure Island housed the Naval Training Station. During World War II, the population in the Bay Area grew through an influx of people from other parts of the United States, such as those who came to work in the shipyards at Hunters Point and Richmond (National Park Service, 2018b).

Post-WWII High-Rise Building Boom: The Manhattanization of San Francisco

The Great Depression and World War II slowed down construction. However, the completion of the Golden Gate and San Francisco–Oakland Bay bridges across the bay in 1936 and 1937 greatly improved traffic flow in and out of the downtown area. Only a few high-rises were constructed in the years following the 1906 earthquake but all this changed starting in the 1960s when skyscrapers began to spring up all over the downtown area (Figure 21). In more recent years, the high-rise construction has been extended from the Financial District to the fill land of the South of Market. These structures became feasible with the use of deep

foundations consisting generally of pile founded on shallow bedrock or a dense sand strata termed the Colma Formation as discussed in later sections regarding the geologic units of San Francisco and the engineering properties of these geologic units.

The San Francisco Transit Center plan adopted in 1985 envisioned South of Market to be the new heartland of the downtown. Key to the development of this plan was the removal of the Embarcadero Freeway following its damage in the Loma Prieta earthquake of 1989. The Freeway had created a sharp southern edge to the downtown. The project was funded by the sale of property of the Transit Center in the South of Market and increased tax assessments. Recent construction in this area includes the two-towered One Rincon Hill, Salesforce Tower (61 stories), the Millennium Tower (58 stories), as well as other residential/hotels and commercial buildings.

San Francisco in the Future: Major New Transit Projects on the Horizon

The Golden Gate and San Francisco–Oakland Bay bridges were both completed in 1937. BART's Transbay Tube opened in 1974. Since 1974, the Bay Area

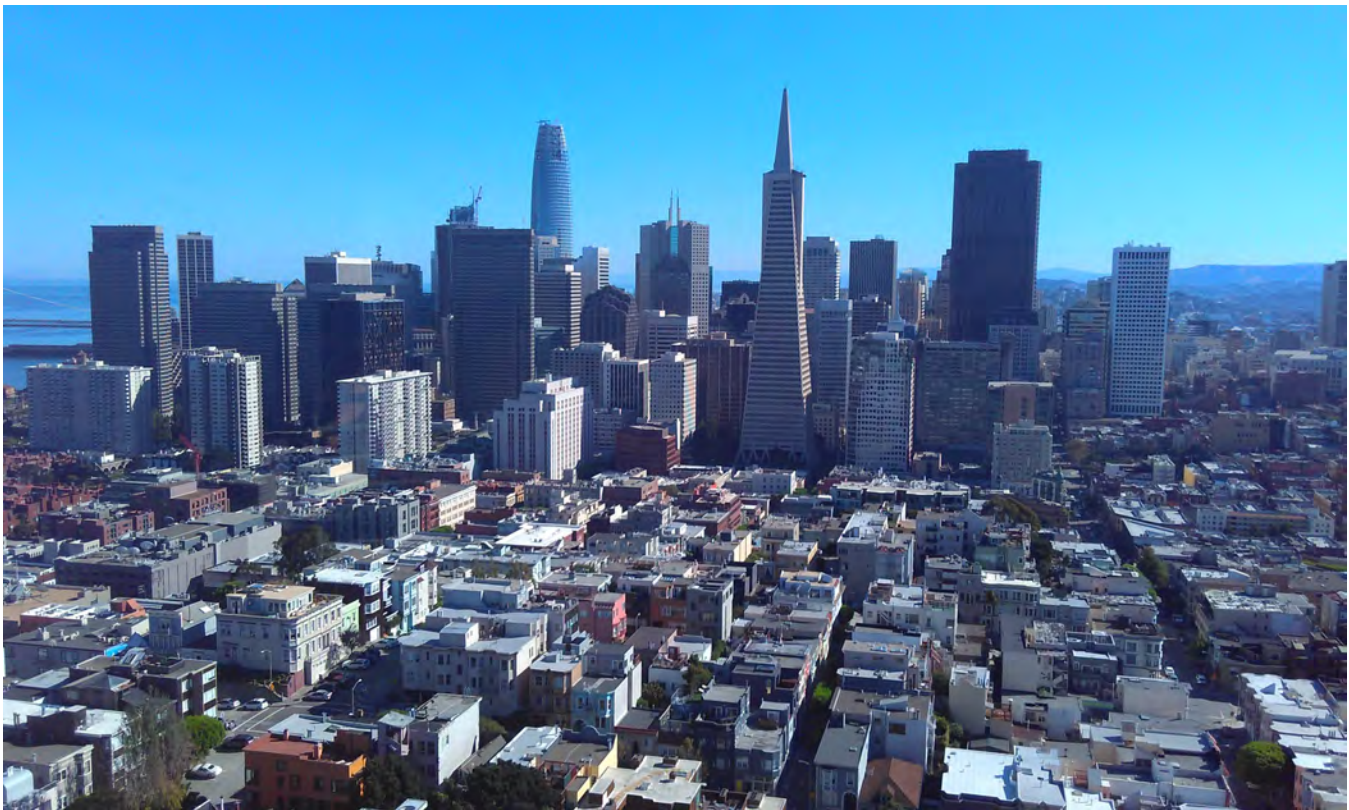


Figure 21. San Francisco skyline taken in 2017 from Coit Tower (photo by Andrés Gómez García).

has grown from 4.3 million to 7.6 million people. Thus, commutes into and out of San Francisco have become longer and slower. Since the 1940s, there have been several proposals to build a new bridge south of the San Francisco–Oakland Bay Bridge but none have been undertaken (Figure 22). More recently, new proposals have been made to reexamine such a new bridge and add a second transbay BART tube. In 2018 BART announced the launch of a \$200 million study to seriously look at a second transbay crossing with results expected by the end of 2018. In addition, the Central Subway, Central Corridor Planning Project, and High Speed Rail Projects will reshape transportation into and within San Francisco.

Central Subway and Central Corridor Project

The Central Subway railway project will extend the T-Third Line through South of Market, Union Square, and Chinatown. When the Central Subway is completed, T-Third Line trains will travel mostly underground from the 4th Street Caltrain Station to Chinatown, bypassing heavy traffic on congested 4th Street and Stockton Street (Figure 23). Four new stations will be built along the 2.7-kilometer (1.7-mile) alignment (San Francisco Municipal Transportation Agency, 2018). The \$1.5 billion project is expected to be completed in 2019.

Additional details about the Central Subway project are provided in the “Major Engineering Projects” section. A summary of the geologic and geotechnical conditions along the Central Subway corridor is presented in Yang and Johnson (2011a and 2011b).

The Central Corridor Planning Project aims to take advantage of the new transit infrastructure, while still maintaining a diverse neighborhood. The Planning Project is focused on the South of Market area of the Central Subway Railway where growth in the area is estimated to create 11,715 new housing units and 46,960 new jobs (Figure 24). It guides additional public services, ranging from public safety to library services to complement and capitalize on the new transit infrastructure. Its goal is to provide an integrated community vision that builds on this synergy of transportation and land use opportunity to promote new development, improve the public realm, and provide other community benefits (San Francisco Planning Department, 2011).

High Speed Rail to San Francisco

In 2008, California voters passed a \$10 billion bond issue to help fund the first high-speed rail system in the country, which broke ground soon after. Phase I of the Project is projected to open in 2029, and will connect Anaheim with San Francisco through the San



Figure 22. An architect’s 1950s rendering of a proposed Southern Crossing at Hunters Point in San Francisco. It was one of several versions of the bridge proposed between the 1940s and 1970s but never undertaken (Amin and Stokle, 2016).



Figure 23. Central Subway railway alignment and new stations (San Francisco Municipal Transportation Agency, 2018).

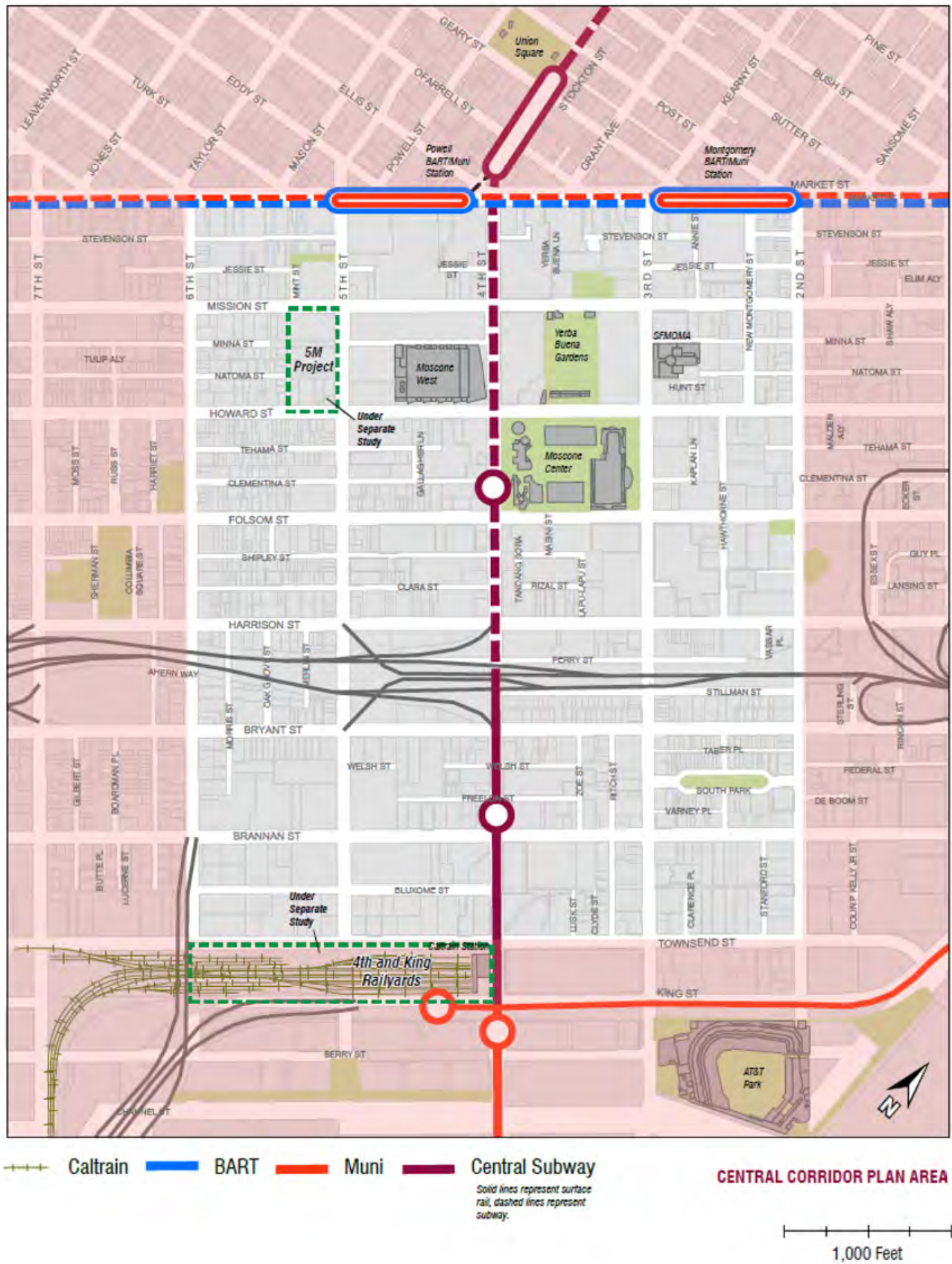


Figure 24. San Francisco Central Corridor Plan Area (San Francisco Planning Department, 2011).

Joaquin Valley (Figure 25). Phase II will extend south from Los Angeles to San Diego and north from Merced to Sacramento. Current plans call for a rail system that could operate at speeds of over 322 km/hr (200 mph). Thus, a trip from San Francisco to the Los Angeles basin could be completed in under three hours.

The current plan is to use the existing rail station at 4th Street and King Street as an interim station until the Downtown Extension to the new Transbay Transit Center is completed (California High Speed Rail Authority, 2017, SPUR 2017).



Figure 25. Planned California High Speed Rail System (California High Speed Rail Authority, 2017).

GEOLOGY AND GEOLOGIC HISTORY

Overview of the Geology of the San Francisco Bay Region

by Russell W. Graymer

Introduction: The Road to Accretion

The geology of San Francisco and the surrounding northern and central California area has played a pivotal role in the development of our understanding of Earth processes, especially the process of tectonic accretion at a continental margin and the development of transform plate margins. The Franciscan Complex, which underlies most (or perhaps all) of the city and county of San Francisco, is widely considered the “type” accretionary complex. More regionally, the Sierra Nevada, Great Valley, and Coast Ranges are often used as an illustration of the arc-forearc-accretionary prism geometry of a continental convergent margin, and the San Andreas fault, just offshore to the west of San Francisco, serves as the prototype transform plate margin, although as illustrated below the actual geometry and geologic history is more complicated.

Geologic studies in and around San Francisco date back to the years following the discovery of gold in the Sierra Nevada foothills in 1848. The first partial geologic map of the city and region was part of a report to the United States War Department focused on practical routes for developing an intercontinental railroad (Blake, 1853). Lawson (1895) provided the first detailed description of the geology of San Francisco, including a revised and expanded geologic map. Following geologic maps (e.g., Crandall, 1907; Lawson, 1914; Bowen and Crippen, 1951; Schlocker et al., 1958) and other studies culminated in the maps of Schlocker (1974) and Bonilla (1971) that serve as the primary basis for the geologic map presented here (Plate 1). Important among the other studies, Bailey et al. (1964) provided an important overview of the Franciscan Complex as well as its relation to the unmetamorphosed latest Jurassic and Cretaceous Great Valley (forearc) strata to the east, and Hsu (1968) developed the idea of *mélange* that so well explains the chaotic nature of so much of the Franciscan.

As the revolutionary theory of plate tectonics came to the fore through the 1960s and 70s, the geology in and around San Francisco played an important role. The theory of plate tectonics demonstrates the mechanism

whereby rocks can be transported far from their place of origin and brought into proximity with rocks of greatly different provenance. Hamilton (1969) and Ernst (1970) suggested that Franciscan rocks were juxtaposed with Great Valley strata at a subduction zone. Jones et al. (1978; 1982) refined that theory to incorporate the concept of “accretion,” or the addition of smaller masses to the larger continental masses at convergent margins. The rocks in and around San Francisco (especially the Marin Headlands terrane, described below) provided a model for how that works, as laid out in detail in various papers within Blake (1984) and in the much more accessible pages of Wahrhaftig (1984a), the well-known *Streetcar to Subduction*.

Since then, much work has been done refining and expanding the concepts of the origin, transport, accretion, and post-accretion geologic history of San Francisco. It is beyond the scope of this introduction to list, or even highlight, those contributions, although many of them are cited below.

The geologic units and structures of San Francisco were carefully described by Schlocker (1974) and Bonilla (1971), and more recently summarized and illustrated in Sloan (2006). Furthermore, the best places to view the geology are described in *Streetcar to Subduction* (Wahrhaftig, 1984a), along with several other excellent field guides. As such, this work is not intended to describe the geology of the city in great detail, or to point out good exposures. Instead, what follows is a summary of a modern view of the regional geologic framework that encompasses San Francisco, a discussion of how the rocks in the city fit into that framework, and a description of the dynamic processes that brought the rocks of San Francisco to their present location while taking others away.

Overview of Plate Tectonics and Tectonic Accretion

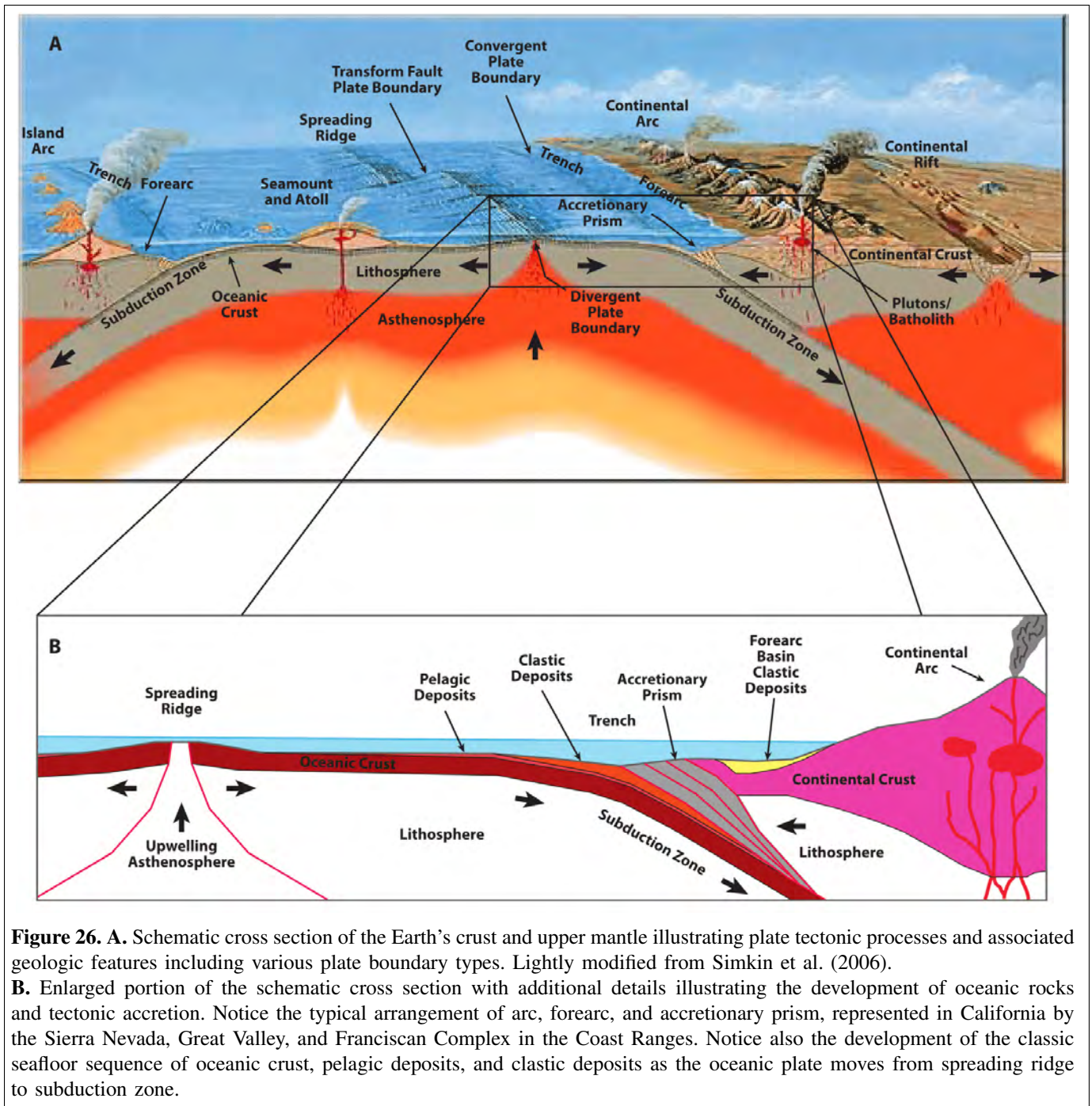
Plate tectonics is the scientific theory that explains many observations about the dynamic nature of the Earth's crust. As illustrated in Figure 26A, the Earth has a relatively thin outer shell called the lithosphere, which is <280 km (<174 miles) or <4.4% of the Earth's radius. The lithosphere is made up of the even thinner crust and the uppermost part of the mantle. The lithosphere is not a solid shell, but instead is broken into many plates. Some plates are made of oceanic lithosphere, which is relatively dense (~2.9 g/cc) and about 50-140 km (31-87 miles) thick, including about 5-10 km (3-6 miles) of mafic oceanic crust. Other plates are made of continental lithosphere, which is relatively buoyant (~2.7 g/cc) and about 40-280 km (25-174 miles) thick, including 30-50 km (19-31 miles) of more silicic continental crust.

Where heat from the Earth's interior causes an upwelling of hot mantle material, the plates move apart, and new oceanic crust is formed from partially melted mantle material at long chains of submarine volcanoes called spreading ridges. Similar mantle upwelling beneath continental lithosphere leads to continental rifts, which can eventually evolve into spreading ridges in oceanic lithosphere as the split pieces of continental lithosphere move apart. These kinds of boundaries—where plates are moving away from each other and new crust is being formed—are called divergent plate boundaries.

At convergent plate boundaries one plate slides under another in a process called subduction. Denser oceanic lithosphere always slides under the more buoyant continental lithosphere. The down-going material is incorporated back into the mantle, balancing the upwelling mantle material at divergent plate boundaries.

There is a third kind of plate margin, neither convergent nor divergent, where plates slide past each other along transform faults. These plate boundaries form connecting offset segments of spreading ridge. They form also where spreading ridges have moved into subduction zones, the convergent and divergent plate motion tending to cancel each other, leaving lateral motion along a transform fault. The San Andreas Fault just west of San Francisco is part of just such a transform plate boundary.

Tectonic accretion is the process by which continental crust grows along convergent plate margins by addition of material transferred from the down-going oceanic plate at the subduction zone. As illustrated in Figure 26B, oceanic crust formed at a spreading ridge cools and sinks as it moves away. In the deep ocean, the crust accumulates a covering of pelagic deposits, mostly planktic material mixed with very fine windblown clay particles, which grows thicker with time as the oceanic crust continues to move away from the spreading ridge. In most places, deep ocean water is cold, and carbonate material dissolves, so that pelagic deposits are a siliceous ooze that separates into layers of nearly pure silica separated by very thin layers of clayey mud, and then hardens into ribbon chert like that seen in Golden Gate Park and elsewhere in San Francisco. In places with shallow ocean floor or in the tropics, with warmer ocean water and more abundant plankton, the pelagic deposits are carbonate rich, and form limestone. As the oceanic crust approaches the continental margin subduction zone, pelagic deposits are overwhelmed and replaced by clastic deposits, fining-upward sequences of sand, silt, and clay swept into the ocean off the continental slope by submarine sediment flows called turbidity currents. The clastic deposits form stacks of sandstone and shale (turbidites) that can be thousands of meters thick. As the down-going oceanic plate moves into and through the subduction zone on its way back into the mantle, some of the slab may be scraped off and transferred (accreted) to the overhanging continental crust. Often only the clastic sedimentary rocks are accreted, but sometimes the pelagic sedimentary rocks and the upper part of the oceanic crust are accreted as well. Shearing and cyclic flow in the subduction zone also provides the mechanism for upward transport of some high-grade metamorphic rocks and some mixing of rocks into the chaotic unit called *mélange* (which is described and discussed more below). Repetition of these processes leads to stacked packages of accreted material called an accretionary prism. Most of the rocks in California have been added to the continental crust by this process operating over hundreds of millions of years.



Geologic Overview of the San Francisco Bay Region

The San Francisco Bay region is composed of three Mesozoic to Paleogene basement complexes, each of which generally represents one of the main parts of a convergent continental plate margin: arc-forearc-accretionary prism. The basement complexes are overlain by Late Cretaceous, Tertiary, and Quaternary deposits (Figure 27), all of which have been cut and offset by the several faults of the Neogene San Andreas fault system (Figure 28).

These geologic units and structures, and their regional relations, are described briefly below to set the stage for the more detailed discussion of the geology and geologic history specific to the city and county of San Francisco that follows.

Basement Complexes

Salinian Complex

The Salinian Complex represents the continental arc of the classic convergent continental plate margin. In the San Francisco Bay region it lies entirely west of the San Andreas and the northern part of the Pilarcitos faults (Figure 28). The present position west of the forearc and accretionary prism basements is one of the complications to the simple model mentioned above.

The Salinian Complex is here composed mostly of granitic rocks, with a very small component of gabbro and metamorphic rocks (including marble, gneiss, schist, and quartzite). Granitic rocks have yielded radiometric ages of various types ranging from about 71 to 93 Ma (million years ago), with most between 84 and 87 Ma (Curtis et al., 1958; California Division of Mines and Geology, 1965; Leo, 1967; Naeser and Ryan, 1976; Kistler and Champion, 1997), while the gabbro has yielded a much older age of 161–165 Ma (James et al., 1994), and the metamorphic rock has detrital zircons suggesting a Paleozoic protolith: Youngest Zircon Population (YZP) ~280–360 Ma (Barbeau et al., 2005).

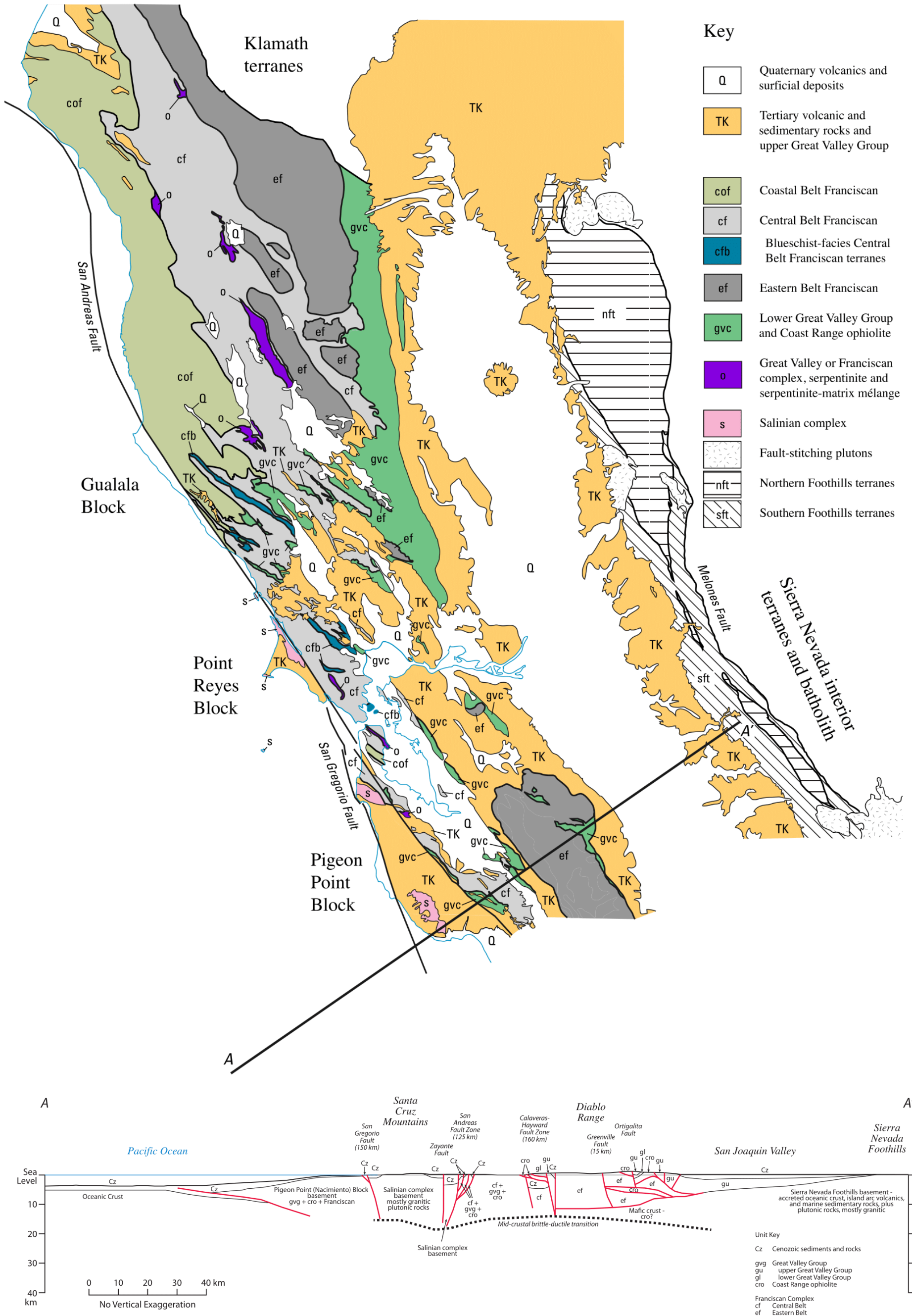
Salinian gabbro in the region has been correlated with coeval and lithologically similar gabbro in the San Emigdio Mountains, about 300 km (186 miles) to the south (Ross, 1970). This offset is attributed to (and along with other evidence constrains) Neogene long-term slip on the San Andreas fault. Restoration of San Andreas offset places the Salinian Complex rocks

adjacent to the Mojave block, southwest of the Sierra Nevada (Figure 29). This paleogeography suggests that the complex is derived from the Cretaceous batholith and wallrock associated with the continental arc at the western margin of North America, underthrust by Late Cretaceous forearc or trench strata (Ducea et al., 2009). The age and isotopic composition suggest that the granitic and older metamorphic rocks originated in the eastern part of the batholith (Gastil, 1975; Kistler and Peterman, 1978). During the Late Cretaceous thrusting and later extensional deformation the Salinian Complex rocks were transported westward (Saleeby, 2003) and subsequently cut and transported to their present position by the San Andreas fault. For more details and recent thinking about the Salinian Complex, the interested reader is referred to the work of Chapman et al. (2011; 2012; 2014), Hall and Saleeby (2013), and Jacobson et al. (2011).

Coast Range Ophiolite and Great Valley Group

This basement complex represents the forearc in the classic continental convergent margin. It is found in scattered fault-bounded bodies throughout the region east of the San Andreas fault and in long belts along the eastern margin of the Coast Ranges (see also “Outboard Blocks” section, below). It is composed of ophiolite at the base, overlain by latest Jurassic (Tithonian) and Early Cretaceous strata, which is in turn overlain by a Cretaceous and Paleocene sandstone and shale overlap sequence (Figure 27 and Figure 30).

The ophiolite at the base of the basement complex is called the Coast Range Ophiolite. It was first recognized by Bailey et al. (1970) and studied in detail by Hopson et al. (1981). It is not well expressed as a classic ophiolite sequence in the San Francisco Bay region. Instead, it crops out as tectonically thinned bodies of ophiolite components (basalt, diabase, gabbro, serpentinized peridotite) plus serpentinite-matrix *mélange* (see discussion of the Hunters Point Shear Zone below) and intermediate to silicic volcanics locally. The ophiolite was formed between about 164 and 173 Ma (Blake et al., 1992; Hagstrum, 1997; Hopson et al., 1997). The nature of its origin is somewhat controversial; see Dickinson et al. (1996) for three proposed origins. One origin (as described in Blake et al., 2002) is forearc spreading in an ocean-island arc system above an east-dipping subduction zone. In that model, the ophiolite and island-arc rocks were accreted to North



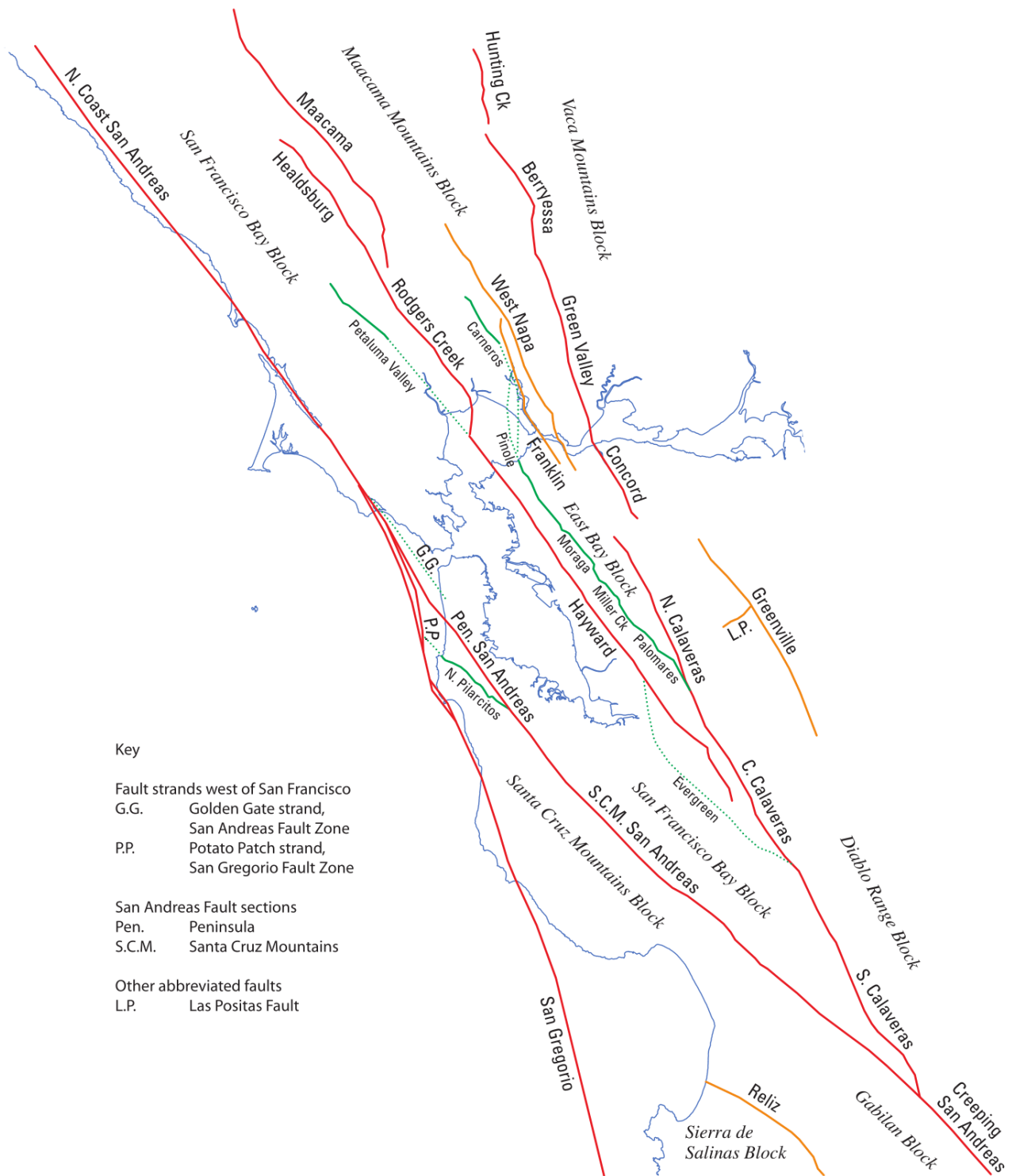


Figure 28. Simplified map of faults and structural blocks in the San Francisco Bay region. Primary seismicogenic strands of the San Andreas fault system are shown in red, secondary seismicogenic strands are shown in orange, and formerly important but now abandoned strands are shown in green, dotted where concealed by water or surficial deposits. (Modified from Graymer et al., 2006a; Bruns et al., 2002).

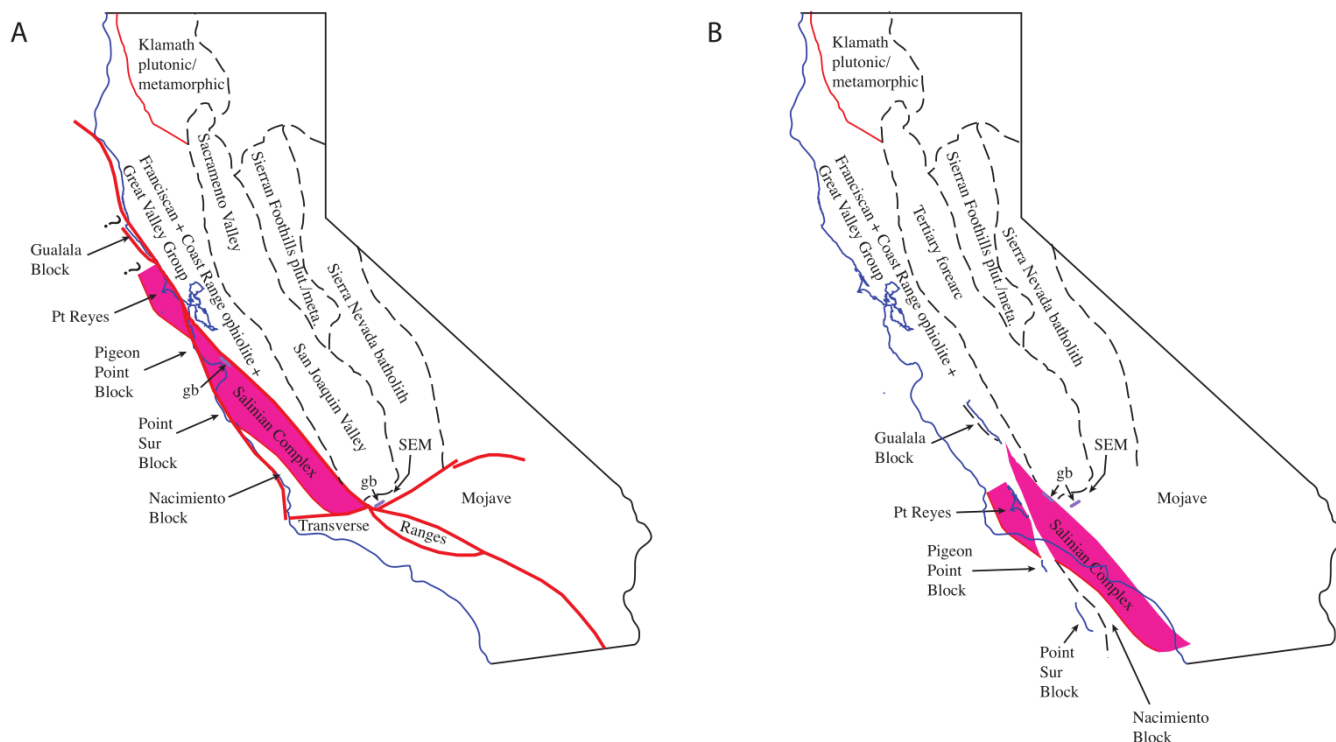


Figure 29. A. Simple map of California showing the present-day distribution of various basement provinces, structural blocks, and the Sacramento and San Joaquin Valley, with the Salinian Complex highlighted (pink). The general location of gabbro is shown as purple (labeled gb), both in the San Emigdio Mountains (SEM) and the Salinian gabbro south of the San Francisco Bay. Faults in the San Andreas system are shown as thick red lines. Other basement province bounding faults are shown as thin red lines. (Derived from Jennings, 1977).

B. Generalized palinspastic reconstruction of the Salinian Complex and outboard blocks to their location prior to offset along the San Andreas fault system. Present-day outline of California is shown for reference. Note that the gabbro bodies are restored to close proximity, and the Salinian Complex is restored to a position southwest of the Sierra Nevada batholith and west of the Mojave basement province. (Modified from Graymer et al., 2006b; and Chapman et al., 2012).

America during the Nevadan orogeny¹ (Blackwelder, 1914; Hinds, 1934), about 150 Ma (Graymer, 2005). For more about the Coast Range Ophiolite, including

¹As summarized by Edelman and Sharp (1989), the term Nevadan orogeny has been used to include all Late Jurassic deformation in the Sierra Nevada Foothills, but there are multiple stages of Late Jurassic deformation, and deformation termed “Nevadan” extends into the Cretaceous, so some workers reject the concept of a Nevadan orogeny. However, as defined by Hinds (1934), the Nevadan orogeny is limited to the regional low-grade metamorphism, isoclinal folding, and development of slaty cleavage in Middle to Late Jurassic marine andesitic volcanic (island arc) and associated clastic sedimentary rocks of the western foothills. This tectonic event is closely constrained in age to ~150 Ma by the Kimmeridgian age of the protolith strata and the U/Pb age of cross-cutting unfoliated plutonic rocks, as summarized in Graymer (2005). Because that is the precise event discussed here, the term is retained as originally defined, and the problematic expansion to encompass other events is rejected.

some different ideas, the interested reader is directed to the recent work of Shervais et al. (2005; 2004).

In many places in the region the only ophiolitic rocks present are serpentinite. Some workers (e.g., Blake et al., 2000; Graymer, 2000) have assigned these isolated serpentinites to the Coast Range Ophiolite, but other workers (e.g., Coleman, 2000; Wakabayashi, 2004) have suggested that some of the isolated serpentinites should be considered Franciscan, originating as serpentinite diapirs near spreading ridges, serpentinite flows extruded from transform faults, or transform-ridge junction core complexes. Spinel geochemistry in some isolated serpentinite bodies (Barnes et al., 2013) yielded ocean crust chemical signatures for some, not the arc-related signatures expected for the Coast Range Ophiolite. However, there is serpentinite in the Coast

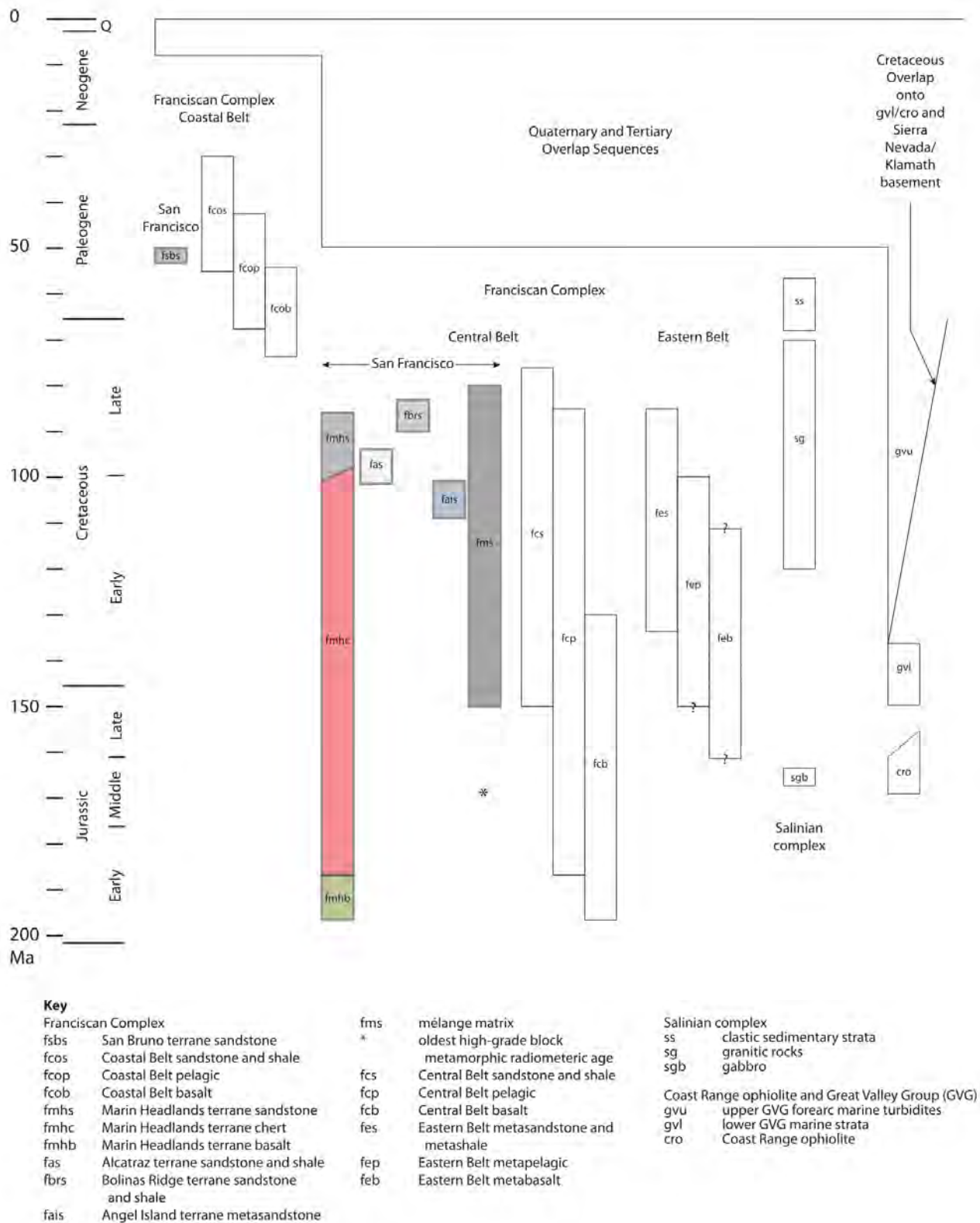


Figure 30. Tectonostratigraphic columns for the California Coast Ranges. Age range queried where poorly constrained. Protolith ages are shown for metamorphic rocks, except for the oldest metamorphic radiometric age of a high-grade block in mélangé, shown as an asterisk. Columns for Franciscan Complex terranes that crop out in San Francisco are shown individually and colored to match the geologic map (Plate 1), other columns for the Franciscan Complex are generalized into belts.

Range Ophiolite that is characterized by an ocean crust chemical signature (Choi et al., 2008), presumably related to subduction of a spreading ridge during the late part of ophiolite formation (Shervais et al., 2004). Therefore, herein most isolated serpentinites are designated as “Franciscan or Coast Range Ophiolite.”

The Coast Range Ophiolite is depositionally overlain by the basal strata of the latest Jurassic, Cretaceous, and Paleocene² Great Valley Group. The depositional contact is almost everywhere overprinted by faults, but is preserved locally, including at least two locations in the San Francisco Bay region (Graymer et al., 1996; Graymer, 2000). The Great Valley Group is made up of thousands of meters of interbedded sandstone and shale, with minor conglomerate. It has long been recognized as being largely sourced from the ancestral Klamath and Sierra Nevada arc-volcanic mountains (e.g., Ojakangas, 1968) and deposited as marine turbidites in the arc-trench gap (Dickinson and Rich, 1972).

The lower part of the Great Valley Group is more complicated, however, as it locally includes strata derived from the underlying ophiolite as well as the Klamath/Sierran arc (e.g., Phipps, 1984). In addition, it was recognized early on (e.g., Safonov, 1962) that the lower part of the Great Valley Group is limited to the western part of the basin. Different models have been proposed to explain the asymmetry of the Great Valley Group, including large lateral transport of the lower part (Wright and Wyld, 2007). Therefore, herein the Great Valley Group is divided into two parts, a lower part which is deposited only on the Coast Range Ophiolite, and an upper part which is deposited both on the lower part and on Klamath/Sierra Nevada Foothills basement (Figure 27). Because the upper part is deposited over multiple basement types, it represents the oldest overlap sequence in the region, discussed more below (Figure 30). For more about the Great Valley Group, the interested reader is directed to the references cited above as well as the recent work of Surpless (2015), Ingersoll (2012), and Williams and Graham (2008).

²The top of the Great Valley Group was originally considered Cretaceous, but fossil and isotopic studies within the uppermost members, such as the Moreno Formation and the Mokelumne River Sandstone, have shown that it includes strata as young as early Paleocene (e.g., McGuire, 1988)

Franciscan Complex³

The famous (at least among geologists) Franciscan Complex represents the accretionary prism of the classic convergent continental plate margin. Like the Coast Range Ophiolite and Great Valley Group, it is also found throughout the region east of the San Andreas fault, as well as in the fault sliver between the San Andreas and northern part of the Pilarcitos faults (Figure 28; see discussion of faulting below in “The San Andreas Fault System” section). It is composed of oceanic crust and overlying pelagic and terrigenous sedimentary rocks, accreted with varying amounts of subduction at the convergent western margin of North America (but see below for complications to the simple model).

The Franciscan Complex is known for blueschist (or glaucophane schist facies) metamorphic rocks. Coleman and Lee (1962) and Ernst (1965) used Franciscan rocks to establish that blueschist represents low temperature, high pressure metamorphism, and Blake et al. (1969) used relations in the Franciscan to suggest those conditions are related to regional thrust faulting. Hamilton (1969) and Ernst (1970) recognized the regional thrust as an ancient subduction zone, so blueschist in the Franciscan Complex has become a type example of subduction zone metamorphism.

The Franciscan Complex is also known for sedimentary-matrix *mélange*. The chaotic nature of much of the Franciscan Complex and the presence of large tectonic blocks, including high-grade metamorphic blocks surrounded by unmetamorphosed rocks, was recognized early on (e.g., Bailey et al., 1964), but not well explained. Hsu (1968) compared these disrupted Franciscan rocks with similar rocks around the world to develop the *mélange* concept, that tectonic mixing can form a unit composed of disparate blocks in a disrupted sedimentary matrix. He described evidence for both extensional and compressional dismemberment of coherent rocks.

³The description and interpretation of the Franciscan Complex is necessarily that of the author. Alternative narratives have been published that differ in nomenclature, structural style, and tectonic history (recent examples include Wakabayashi, 2015, 2017; Raymond, 2017; Ernst, 2017). To the extent that those alternatives bear directly on the geology of San Francisco, they are discussed in the text, but it is beyond the scope of this effort to describe all the differences across the California Coast Ranges or to discuss all the evidence and reasoning that causes preference of one alternative over others.

Cloos (1982) described a well-known model whereby such mixing, as well as uplift of blueschist to the surface, could take place by forced convection in the subduction zone, but the Franciscan also has a long history of post-accretion deformation which could contribute to tectonic mixing as well. Many workers (e.g., Page, 1978; Wakabayashi, 2011) have suggested that some or all Franciscan mélangé began as an olistostrome (massive marine landslide deposit) that was subsequently deformed, but observations in some parts of the mélangé (blocks apparently younger than matrix, blocks apparently torn from nearby coherent terranes) preclude olistostromal origin (Blake et al., 2002).

In northern California, the Franciscan has been divided into three large north-northwest trending belts (Irwin, 1960): Coastal, Central, and Eastern (Figure 27). The belts are distinguished by age, structural character and(or) metamorphic grade. The Eastern Belt is generally composed of folded subhorizontal slabs of rock metamorphosed at levels up to glaucophane schist facies, whereas the Central Belt is composed of generally steep-dipping slabs of various metamorphic grades generally surrounded by mélangé, and the Coastal Belt is made up of extensive folded fault-bounded slabs generally little metamorphosed and younger than other belts.

Each belt has been further divided into terranes, one or more large fault-bounded slabs of relatively coherent rock sequences and, locally, broken formation (bodies of stratigraphically related but structurally disrupted beds), with an internally consistent tectonostratigraphy that is different from that of other terranes. Each belt also contains sedimentary-matrix mélangé. Mélangé is most common in the Central Belt, and is rare in the Coastal Belt.

The Central Belt overlies the Coastal Belt on a gently east dipping thrust, locally modified by younger steeply dipping faults (Jones et al., 1978; McLaughlin et al., 2000; Blake et al., 2002, Langenheim et al., 2013). The contact between the Central and Eastern belts in the San Francisco Bay region is everywhere cut by steeply dipping younger faults, or concealed by overlap strata (Figure 27), so interpretation of the exact nature of the original contact here is speculative. Farther north the contact has been mapped as a northeast-dipping thrust (e.g., McLaughlin et al., 2000).

The terranes of the Coastal Belt and Central Belt, as

they appear in San Francisco, are described in more detail in “San Francisco Basement Complex Rocks” section of “Geology of San Francisco” below.

Overlap Sequences

Overlap sequences are sedimentary sequences originally deposited across two or more basement complexes. The overlap requires that the disparate basements were in proximity at the time of deposition, so the oldest overlap on basement complexes limits the time when those basements were amalgamated (tectonically juxtaposed) and exposed at the surface.

The stratigraphic relations of the various basement complexes and overlap sequences in the San Francisco Bay region are shown in Figure 30. The oldest overlap sequence in the San Francisco Bay region is the Cretaceous base of the upper Great Valley Group, which was deposited both on the lower Great Valley Group and Coast Range Ophiolite and on the plutonic and metamorphic rocks of the Klamath/Sierra Nevada (Blake et al., 1999).

The oldest stratigraphic link between Franciscan and Great Valley Group/Coast Range Ophiolite basement is Franciscan detritus in Paleocene strata overlying Great Valley Group (Berkland, 1973; Dickinson et al., 1979). The oldest strata mapped over both the Great Valley and Franciscan Complex is the Eocene Point of Rocks Sandstone (Dibblee, 1974) hundreds of kilometers to the southeast in Kern County, but that relation is limited to a very small outcrop, and the oldest unit deposited more widely across Franciscan and Great Valley basement is Oligocene to early Miocene Temblor Formation (e.g., Dibblee, 1974; Sims, 1988). The Coastal Belt of the Franciscan Complex includes sandstones as young as Miocene, however, so accretion of those terranes continued much later and that belt has a different overlap history. The oldest strata tying Coastal Belt to other Franciscan belts, as well as Great Valley Group and Coast Range Ophiolite, is the late Miocene Wilson Grove Formation (Blake et al., 2002; Powell et al., 2004).

Earlier workers described Eocene strata south of San Francisco deposited over both Salinian and Franciscan basement as Butano Sandstone (e.g., Dibblee, 1966), but later workers recognized the rocks east of the San Andreas fault as a different unit called the Whiskey Hill Formation (Pampeyan, 1993). The Butano Sandstone was then correlated with Eocene

Point of Rocks Sandstone over the Great Valley Group hundreds of kilometers south of the San Francisco Bay region (Clarke, 1973), but that correlation has also been called into question (Sharman et al., 2013). The oldest unquestioned Salinian overlap, then, is the late Oligocene to early Miocene Vaqueros Formation (Seiders, 1982) which overlies the Nacimiento fault between the Salinian and Franciscan complexes in the southern Coast Ranges (see “Outboard Blocks” section below). The oldest Salinian to Franciscan overlap in the San Francisco Bay region is latest Miocene to early Pliocene, the ~5.4–7.0 Ma Purisima Formation (McLaughlin et al., 2007), reflecting the large Neogene offset along the San Andreas fault system—even the Purisima is offset by about 74 km (46 miles).

Outboard Blocks

Three structural blocks lie west of the San Andreas fault system in the San Francisco Bay region (Figure 27), mostly obscured by the waters of the Pacific Ocean: the Gualala block (to the north), the Point Reyes block (central), and the Pigeon Point block (to the south).

The central Point Reyes block, which includes Point Reyes, Bodega Head, and the Farallon Islands, is composed of granitic basement overlain by Eocene and younger strata (Clark and Brabb, 1997). Basement and overlying rocks at Point Reyes have been correlated with rocks 150 km (93 miles) south at Point Lobo (just south of Monterey; Clark et al., 1984), so the Point Reyes–Farallon block is an offset piece of Salinian Complex basement and overlap (Figure 29).

The southern Pigeon Point block, exposed along the San Mateo County coast near Pigeon Point, is composed of Late Cretaceous (Campanian) strata over highly altered about 88 Ma silicic volcanics (Ernst et al., 2011). The strata and the underlying volcanics are too old to overlie Salinian basement, which was not brought to the surface until latest Cretaceous (Maastriichtian) time (Ducea, 2009), so the block is known to be offset from the Nacimiento Block, 150 km (93 miles) to the south. The Nacimiento Block is similar to the San Francisco Bay region east of the San Andreas fault, composed of amalgamated Franciscan, Coast Range Ophiolite, and Great Valley Group basements with Tertiary overlap strata.

The northern Gualala block, exposed along the Sonoma and Mendocino county coast near Gualala, is composed of altered basalt of unknown age, structurally overlain

by Late Cretaceous (Campanian) and younger strata. The identity and restoration of this block is controversial, although the Campanian age of the strata and the presence of the underlying altered but unmetamorphosed basalt does not fit correlation with the Salinian Complex. For more details on this block, the interested reader is referred to Elder (1998).

San Andreas Fault System

The San Francisco Bay region is cut by the faults of the San Andreas fault system (Figure 28), which forms the North American–Pacific plate boundary. Although it is fun to think of having one foot on the Pacific plate and another on the North American plate while standing astride a strand of the San Andreas fault, the plate-bounding fault system here is actually composed of multiple faults spanning a zone many tens of kilometers wide. In the San Francisco Bay region, these faults include four main active dominantly strike-slip faults, from west to east the San Gregorio, San Andreas, Hayward–Rodgers Creek–Maacama, and Calaveras–Concord–Green Valley–Berryessa. There are also lower slip-rate but still seismogenic faults, such as the West Napa and Greenville faults, and previously active but now abandoned faults such as the northern Pilarcitos and Petaluma Valley faults. Finally, there are faults that accommodate tectonic strain perpendicular to the main faults. This results from a small component of compression due to relative plate motion, plus variable compression or extension due to bends and steps in the main faults (e.g., Page, 1982; Graymer, 2000; Sawyer, 2015). Many faults in this last category root into the main faults, and so are likely not important independent seismic sources, but instead move with secondary or triggered slip during events on the main faults (e.g., slip on the Santa Cruz Mountains thrust zone during and/or immediately following the 1989 Loma Prieta earthquake; Schmidt et al., 1995).

The San Andreas fault system has accumulated a total of about 475–490 km of right-lateral offset in the Neogene (Hill and Dibblee, 1953; Matthews, 1976; Clark et al., 1984; Jachens et al., 1998). That long-term slip can be subdivided into three main fault zones or systems: about 175 km (109 miles) of offset along the San Gregorio fault; about 175 km (109 miles) on the East Bay fault system (Hayward–Rodgers Creek–Maacama, Calaveras–Concord–Green Valley–Berryessa, and others; McLaughlin et al., 1996; Graymer et al., 2002); and about 125 km (78 miles) on the Santa Cruz

Mountains–Peninsula segments of the San Andreas fault and the northern Pilarcitos fault. Where the San Andreas fault passes west of San Francisco, it only has about 22 km (14 miles) of offset, all since about 3.3 Ma (McLaughlin et al., 2007). The San Andreas–Pilarcitos fault system merges northward with the San Gregorio fault just northwest of San Francisco, so offset along the northern segment of the San Andreas, north of the Golden Gate, is a combined 300 km (186 miles). Likewise, the San Andreas merges southward with the East Bay fault system near Hollister, so San Andreas offset south of the San Francisco Bay region is about 300 km (186 miles). When discussing San Andreas fault offset, it is important to be clear what part of the San Andreas fault you mean.

The main faults of the San Andreas system divide the region into large structural blocks as shown in Figure 28. These blocks have undergone significant differential offset, both horizontal and vertical, in Neogene time, so that quite different Tertiary stratigraphies are juxtaposed in adjacent blocks, and the Salinian Complex is adjacent to the Great Valley Group, Coast Range Ophiolite, and Franciscan Complex across the San Andreas–northern Pilarcitos faults. For more details on the San Andreas Fault, see sections on the “1906 Earthquake,” “Offshore Geology,” and “Geologic Aspects of Natural Hazards.”

Geology of San Francisco

by Russell W. Graymer, Robert Givler, John Baldwin, William Lettis, Samuel Y. Johnson, H. Gary Greene, Peter Dartnell

San Francisco lies in the west-central part of the San Francisco Bay block (see Figure 28). The San Andreas fault zone runs just offshore to the west. A geologic map of San Francisco is shown in Plate 1. The geology of San Francisco itself is comparatively simple: several fault-bounded northwest trending bands of Mesozoic and Paleogene basement overlain by Quaternary surficial deposits (and artificial fill), and lacking any of the Late Cretaceous and Tertiary overlap sequences found elsewhere in the region, with the exception of a narrow band of Plio–Quaternary Merced Formation outcrops in the far southwest corner of the city. Mesozoic rocks are exposed in sea cliffs and as resistant knobs and hills throughout the city. Merced Formation is only seen in sea cliffs near Fort Funston. Quaternary surficial deposits are poorly exposed, filling the low-lying areas

between hills. Much of the land in the north and east side of the city is artificial fill overlying bay mud deposits.

The contrast in magnetic potential between the various basement units (Figure 31) allows for projection of basement unit boundaries beneath the extensive Quaternary surficial deposits. The resulting map of terranes is shown in Figure 32. Each band of basement is the upper surface of a steeply dipping slab of a coherent Franciscan Complex terrane, Franciscan *mélange*, or serpentinite-matrix *mélange* (Figure 33). Each of these units is described in detail below.

San Francisco Basement Complex Rocks

For an overview of the Franciscan Complex in the context of the larger San Francisco Bay region, see “Franciscan Complex” above.

Franciscan, Coastal Belt

San Bruno Mountain Terrane

This terrane is limited in outcrop to a single body in San Francisco and northernmost San Mateo counties (Figure 32). It forms a prominent northwest trending ridge, mostly in San Mateo County (San Bruno Mountain), and a lower east–west trending ridge in southern San Francisco (Lakeview Avenue). The fault-bounded body is surrounded on most sides by *mélange*. To the northwest the terrane probably extends under cover, as suggested by the aeromagnetic map, to the Golden Gate fault strand of the San Andreas fault zone offshore, where it is juxtaposed against unknown Franciscan rocks overlain by Tertiary strata (Bruns et al., 2002). To the north-northwest the terrane is adjacent to a covered southward projection of the Bolinas Ridge terrane outcrops at Lands End.

Rocks of this terrane were originally considered part of the Franciscan Group (Lawson, 1895; Schlocker et al., 1958), but were later considered probably part of the Great Valley Group (Schlocker, 1974). These rocks were eventually assigned to the San Bruno Mountain terrane of the Franciscan Complex by Blake et al. (1984). Later detrital zircon analyses by Snow et al. (2010) yielded a Youngest Zircon Population (YZP) of about 52 Ma, younger than any Coastal Belt terrane but equivalent to the age of some Coastal Belt graywackes. This, along with lithologic similarities, leads to reassignment of this terrane to the Coastal Belt. Rocks of the Bolinas Ridge terrane were originally included

in the San Bruno Mountain terrane, but those rocks have yielded older detrital zircon YZPs (84–90 Ma) and different overall zircon populations (Dumitru et al., 2016; W. Elder, NPS, written communication) so those rocks are now assigned to a separate terrane.

The San Bruno Mountain terrane is comprised entirely of potassium feldspar-bearing feldspathic graywacke and shale, lacking basalt or pelagic sediments. Sandstone bedding ranges from massive to thin, with sedimentary structures such as flute casts and graded bedding preserved locally (Blake et al., 1984). Bedding

has in places been pulled apart to form zones of broken formation, but the rocks are unfoliated. They locally contain metamorphic pumpellyite indicative of prehnite-pumpellyite facies metamorphism.

Franciscan, Central Belt

Bolinas Ridge Terrane

This terrane is found mostly to the north in Marin County. In San Francisco, Bolinas Ridge terrane is restricted to very limited outcrop near Point Lobos and the ruins of Sutro Baths in the northwest part of

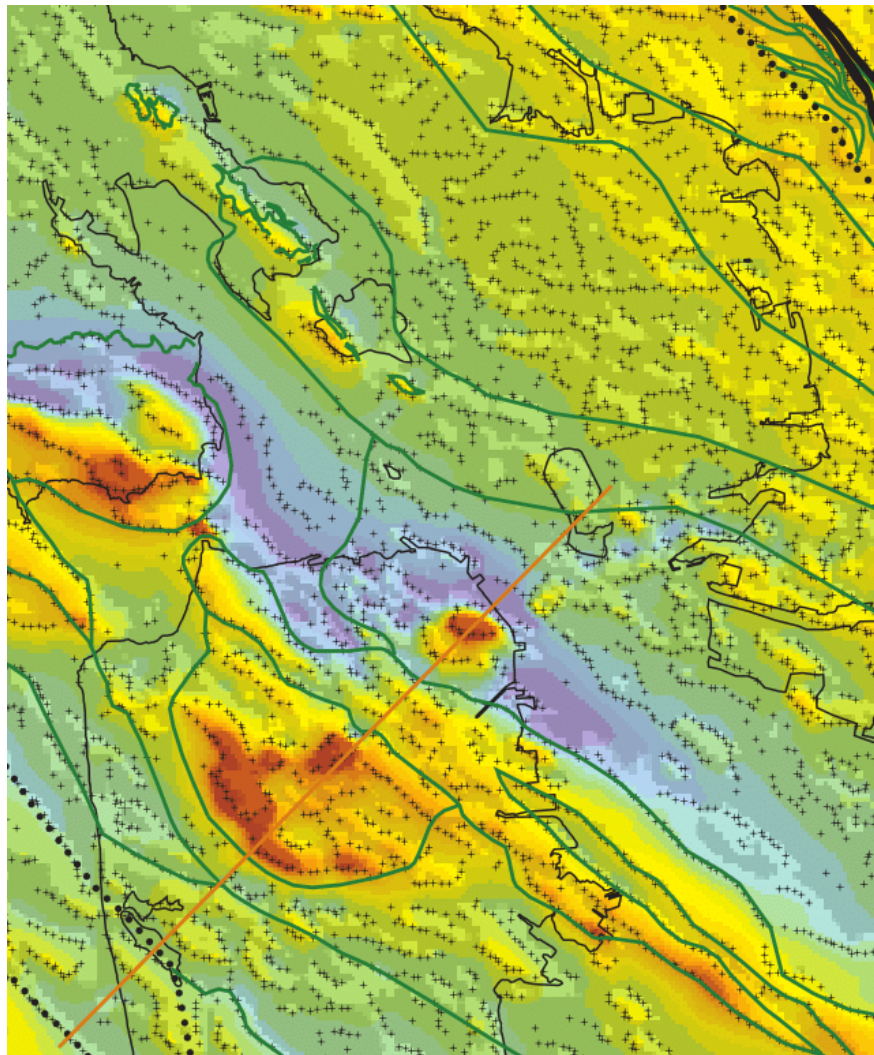


Figure 31. Aeromagnetic map of the City and County of San Francisco and surrounding areas overlain with San Andreas fault system strands (thick black lines, dotted where concealed by water or surficial deposits), and terrane bounding faults (medium-weight green lines). Shorelines shown as thin black line. Warm colors indicate areas of high magnetic susceptibility, cool colors indicate areas of low magnetic susceptibility. Black + symbols mark the location of maximum gradient inflections in the data. Section line for Figure 33 shown in orange. Aeromagnetic data processed to remove shift in magnetic anomalies related to inclination of Earth's magnetic field. (Aeromagnetic map modified from Jachens et al., 2002. Faults and contacts modified from Plate 1, Blake et al., 2000; Graymer, 2000; and Bonilla, 1998).

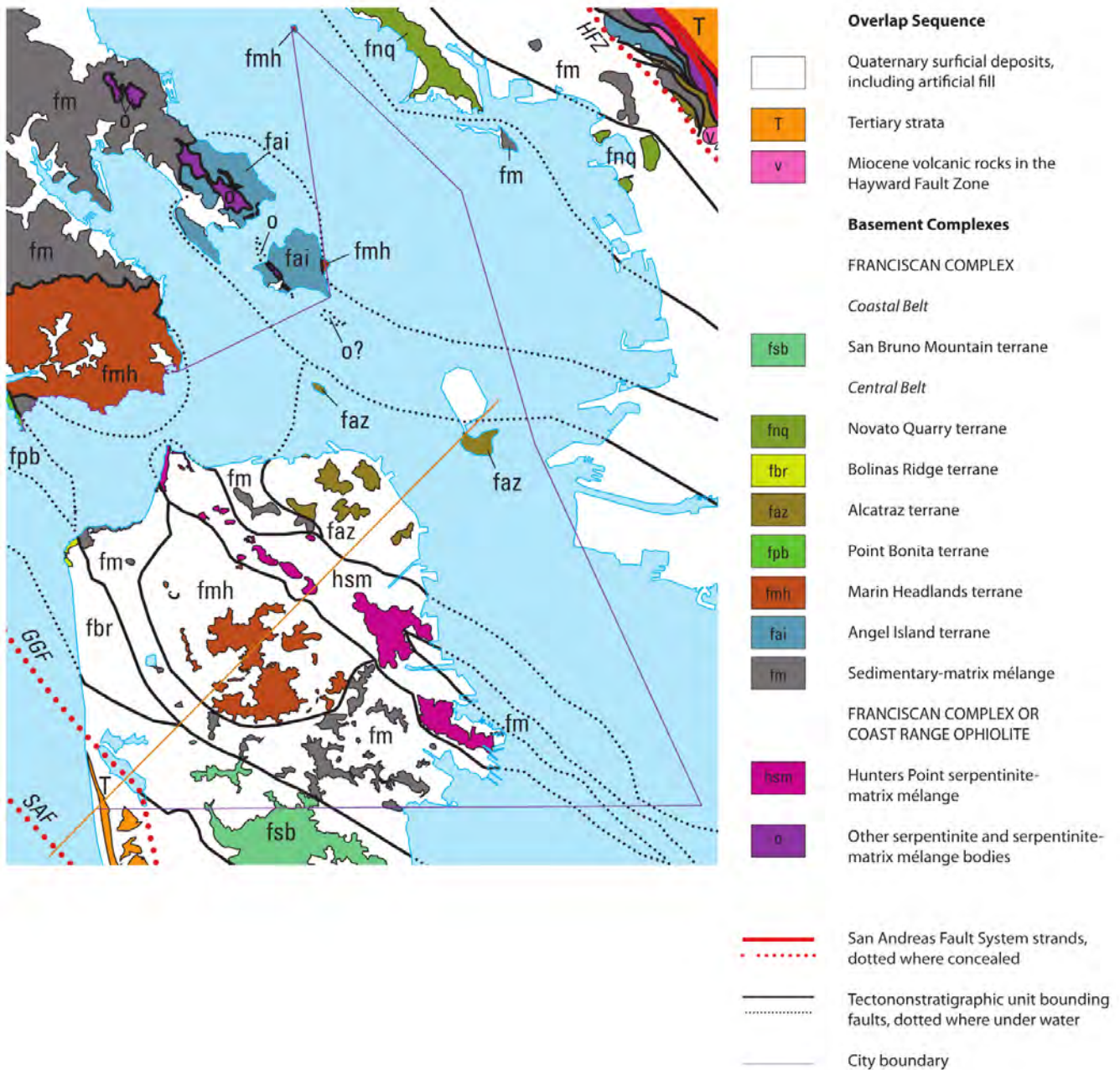


Figure 32. Tectonostratigraphic map of San Francisco and surrounding areas, the same area as Figure 31. Water bodies shown as blue. San Andreas Fault System strands: GGF, Golden Gate Fault; SAF, San Andreas Fault; HFZ, Hayward Fault Zone. Section line for Figure 33 shown in orange. Note that the Hayward Fault Zone includes many thin slices of different units too small to label, including Alcatraz and Angel Island terranes, sedimentary-matrix mélange, serpentinite and serpentinite-matrix mélange.

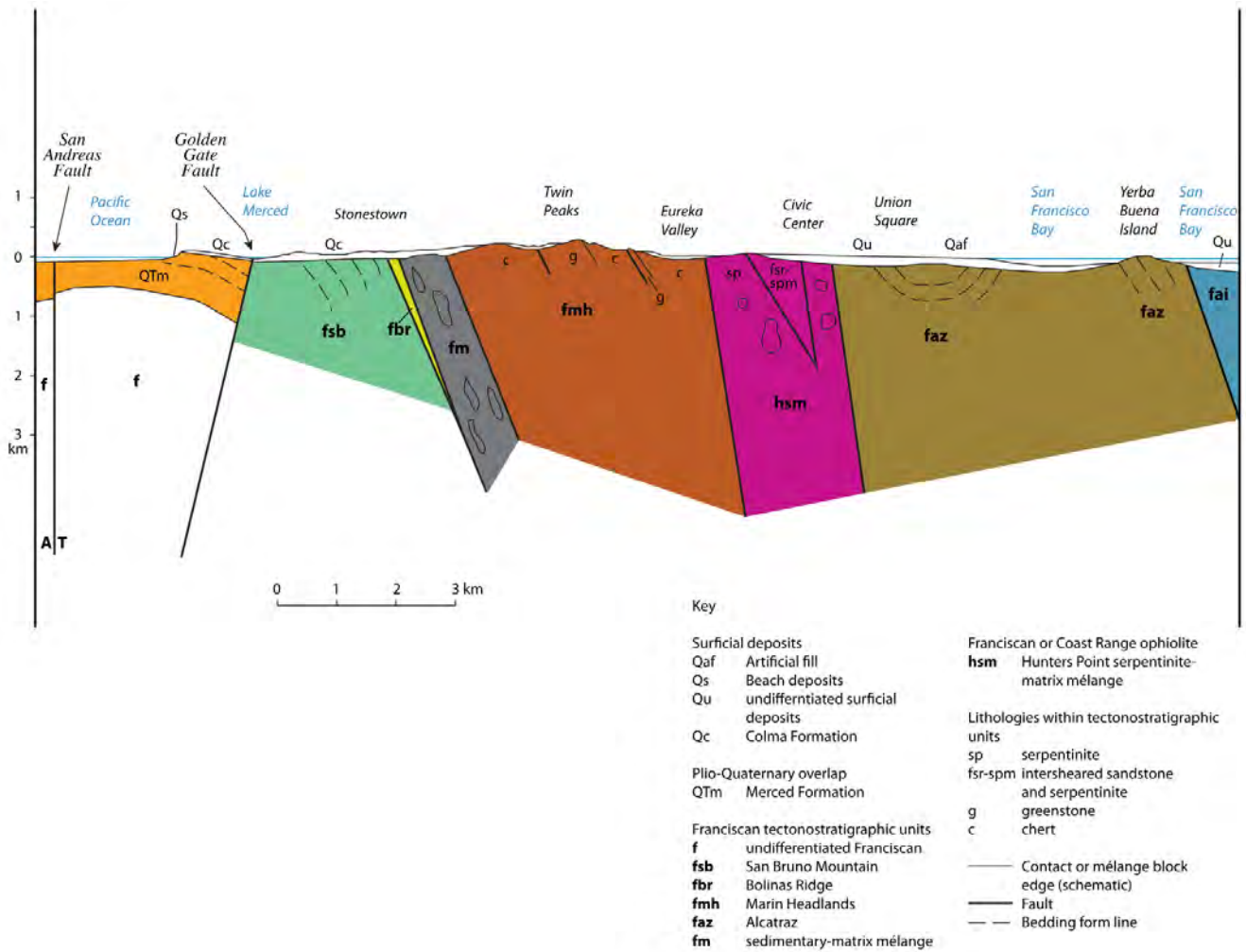


Figure 33. Geologic cross section of San Francisco from Yerba Buena Island to the Pacific Ocean through Twin Peaks and Lake Merced, showing terranes from Figure 32 (bold) and other units from Plate 1. Depiction of mélange blocks is schematic. No vertical exaggeration. Section line shown on Figure 31 and Figure 32.

the city (Figure 34), though the full body probably extends southward under Quaternary cover (Figure 31 and Figure 32). It is bounded on the east by the City College mélange, on the west and south by San Bruno Mountain terrane, and on the north under the waters of the Golden Gate by Point Bonita terrane (which does not crop out in San Francisco).

Although Schlocker (1958) suggested that the Point Lobos outcrops are part of the Great Valley sequence, the Bolinas Ridge slab in Marin County was correlated by Gluskoter (1964) with the Franciscan Complex Coastal Belt, and Blake et al. (1984) included all these rocks in the San Bruno Mountain terrane based on lithology and graywacke composition. As mentioned in the section above, Snow et al. (2010) found a YZP from graywacke collected at San Bruno Mountain of

~52 Ma, but more recently, detrital zircon dating of graywacke from Bolinas Ridge and Point Lobos gave YZP ages of 84–90 Ma (Dumitru et al., 2016; W. Elder, NPS, written communication), much older than the one from San Bruno Mountain, along with a significantly different overall zircon population. This, along with similarities in zircon population, led Wakabayashi (2015) to include Bolinas Ridge rocks in the Novato Quarry terrane. However, there are differences in YZP and overall zircon population (see the Data Repository for Dumitru et al., 2016, especially the plot on page 38) between Bolinas Ridge and Novato Quarry sandstones. Furthermore, Bolinas Ridge sandstones are somewhat more lithic than those of Novato Quarry terrane, so Bolinas Ridge is retained as a separate terrane.

Bolinas Ridge terrane is composed entirely of



Figure 34. Graywacke sandstone of the Bolinas Ridge terrane. Sutro Bath Ruins, San Francisco (photo by John Karachewski).

graywacke, lacking pelagic sediments and mafic volcanics. The sandstone is mostly fine- to medium-grained. Shale, coarse-grained sandstone, and conglomerate are present but not abundant. Sandstone is generally indistinctly bedded. The limited exposure of the Point Lobos slab suggests a syncline–anticline pair folded around a moderately southeast plunging axis (Schlocker, 1958). The sandstone of this terrane is pervasively sheared, and the shale interbeds have developed a platy cleavage. It is otherwise entirely unfoliated and original sedimentary textures (e.g., graded bedding) are preserved. Metamorphic pumpellyite has been observed. The Bolinas Ridge terrane sandstones have no known fossils.

Marin Headlands Terrane

The central part of San Francisco is underlain by Marin Headlands terrane, making up the hills of Mount Sutro and Twin Peaks, as well as scattered outcrops in Golden Gate Park and elsewhere. Rocks of the Marin

Headlands terrane also crop out on the eastern edge of Angel Island and Goat Island at the northernmost tip of the city limits, and form blocks in the City College *mélange* (see section titled “*Mélange*” below).

This terrane is the heart of the classic Franciscan “Series,” first named by Lawson (1895). These rocks were later named Marin Headlands terrane by Blake et al. (1982), and studied in detail by Wahrhaftig (1984b). The Marin Headlands terrane rocks on Angel Island were originally included with the metamorphic rocks of Angel Island by Schlocker (1974) and Blake et al. (1984), but were assigned to the Alcatraz “nappe” by Wakabayashi (1992) based on their metamorphic grade which is much lower than the rest of the rocks on Angel Island. However, these sandstones are too lithic (see figure 13, sample 10 of Schlocker, 1974) to be Alcatraz terrane, and were reassigned by Blake to Marin Headlands terrane (M.C. Blake, USGS, personal communication).

Marin Headlands terrane is composed of a basal unit of basalt and diabase, including pillow basalt (Figure

35), overlain by tightly folded thinly layered (ribbon) radiolarian chert (Figure 36), which is in turn overlain by lithic graywacke. In the Marin Headlands, just north of San Francisco, the depositional sequence is locally preserved, but repeated several times. Study of the chert (see below) showed that the repetition was due to imbricate thrusting, not repeated cyclical episodes. As mentioned in the Introduction, Wahrhaftig (1984a and 1984b) connected the basalt–chert–graywacke sequence to the tectonic history of oceanic plates and subduction, a seminal moment in plate tectonic research.

In San Francisco, the stacked relation is not as clearly expressed, with lenses of chert mapped within graywacke and graywacke mapped over greenstone without intervening chert in places. Nevertheless, the broad pattern of thrust repeated basalt/chert/graywacke stacks is present (Figure 33 shows a three-fold repetition of greenstone and chert at Twin Peaks). The rocks are low-grade, prehnite-pumpellyite facies, and not foliated.

The basal basalt geochemistry indicates that it origi-

nated at a mid-ocean ridge, although rocks originally included in Marin Headlands terrane at Point Bonita have geochemistry suggesting seamount or ocean island origin, leading to their assignment to a separate terrane (Wahrhaftig and Wakabayashi, 1989; Shervais, 1989; Blake et al., 2000). Paleomagnetic studies of Marin Headlands basalt (Curry et al., 1984) “do not provide conclusive evidence about changes with time of the latitude of Marin Headlands terrane,” but “may reflect their having been remagnetized long after extrusion.”

The radiolarians of the chert have been carefully studied (Murchey, 1980; Murchey and Jones, 1984), and range in age from Early Jurassic (Toarcian to Pleinsbachian) to middle Cretaceous (Cenomanian to late Albian), a span of almost 100 million years. The faunal affinities suggest that the chert was deposited at low latitudes (Murchey, 1984), and this is supported by paleomagnetic data from the chert (Hagstrum and Murchey, 1993).

Chert geochemistry (Karl, 1984; Murray et al., 1991) documents the tectonic movement of the terrane, with



Figure 35. Pillow basalts of the Point Bonita terrane, Point Bonita, San Francisco (photo by John Karachewski).



Figure 36. Tightly folded, thinly layered (ribbon) radiolarian chert, of the Marin Headlands terrane. O’Shaughnessy Blvd., near Glen Park, San Francisco (photo by Kenneth A. Johnson).

lower chert reflecting spreading ridge geochemistry, middle chert reflecting open-ocean environments, and upper chert reflecting continental margin influence. The geochemistry also shows that the ribbon layering in chert is a result of diagenetic processes, not primary depositional bedding (Murray et al., 1992), as had long been suspected (e.g., Wahrhaftig, 1984a).

The chert geochemistry, paleomagnetism, and faunal affinities, taken together describe a tectonic trajectory for the seafloor rocks that started at near equatorial latitude and stayed within tropical waters (<20° latitude) throughout a nearly 100-million-year tectonic traverse from a spreading ridge to the continental margin.

The overlying graywacke is very lithic, mostly thick-bedded with common thin-bedded intervals, and with sedimentary structures preserved locally. It has yielded ammonites of middle Cretaceous age (Albian in San Francisco; Schlocker et al., 1954; and Cenomanian in

Marin Headlands; Hertlein, 1956). More recently, detrital zircon studies have yielded YZPs ranging from 86 to 108 Ma (W. Elder, written communication; McPeak, 2015), suggesting that graywacke deposition continued well into the Late Cretaceous.

Large blocks of chert in *mélange* in Marin County have been correlated with the Marin Headlands terrane (Murchev and Jones, 1984), and graywacke, chert, and greenstone of the Marin Headlands terrane between Lands End and Baker Beach, as well as in southeast San Francisco, are herein interpreted as *mélange* blocks. It is also possible that the Angel Island and Goat Rock outcrops of Marin Headlands terrane are actually large blocks in *mélange*, like those in the City College *mélange*, as the intervening area, obscured by the bay, lacks the characteristic aeromagnetic highs associated with large slabs of Marin Headlands greenstone (Figure 31).

Alcatraz Terrane

Alcatraz terrane crops out in northeast San Francisco, including Alcatraz and Yerba Buena Island, where the Alcatraz terrane forms scattered hills that rise above the bay floor and flat-lying areas of the city. The hills probably represent erosion-resistant parts of a larger, but mostly hidden, northwest–southeast trending slab of the terrane, although it is possible that septa of mélangé are present, though eroded and covered, between them. The Alcatraz terrane in San Francisco is bounded on the southwest by Hunters Point serpentinite-matrix mélangé, and on the northeast by a parallel slab of Angel Island terrane.

The Alcatraz terrane is composed entirely of unfoliated sandstone, lacking the ocean crust and pelagic sediments present in some other terranes. The sandstone is biotite-bearing moderately lithic graywacke that includes minor potassium feldspar (Schlocker, 1974; Blake et al., 1984; Jayko and Blake, 1984). Bedding ranges from thin to thick. The orientation of thick beds is still distinct because of thin shale partings. Locally the beds are tightly folded or disrupted into broken formation. Fine-grained metamorphic prehnite and pumpellyite are commonly seen in thin sections of the unfoliated graywackes of this terrane. In fact, pumpellyite was first recognized as a metamorphic mineral in Franciscan graywacke from Alcatraz Island (Schlocker, 1974).

Fossils found in Alcatraz terrane graywackes have been the subject of considerable controversy. The first fossil ever found in the Franciscan was in a boatload of rock from Alcatraz Island. This was identified as *Inoceramus ellioti* of Cretaceous age (see Bailey et al., 1964, p. 115, for details of this occurrence). A subsequent discovery in 1976, near the west end of the island, was thought to consist of Early Cretaceous (Valanginian) *Buchias* (Armstrong and Gallagher, 1977). A third fossil was found near the east end of the island in 1992 and was identified as *Inoceramus pictus* of Late Cretaceous (late Cenomanian) age (Elder and Miller, 1993). These fossils and their conflicting ages were further described and discussed by Elder (1998), who pointed out that there was not enough stratigraphic distance between the ca. 134 Ma *Buchias* and the ca. 94 Ma inoceramids, and suggested that maybe the inoceramids were older than the Cenomanian age he had earlier provided. However, subsequent studies have documented detrital zircons from this terrane, including one sample collected near

the *Buchia* locality, with a YZP ranging from 95 to 101 Ma (Snow et al., 2010; W. Elder, NPS, written communication), showing that the older fossils must be reworked, and that the Cenomanian fossil probably best reflects the depositional age of the sandstone.

Angel Island Terrane

Angel Island terrane is widely distributed throughout Sonoma and Marin counties, but only has a tiny presence in San Francisco where the southeast tip of Angel Island at Blunt Point is inside the city limits.

On Angel Island and Tiburon Peninsula, serpentinite outcrop trends north-northwest, bisecting the extent of Angel Island terrane (Figure 31 and Figure 32). Previous workers (e.g., Bero, 2014) have mapped the serpentinite (and serpentinite matrix mélangé) as locally faulted flat-lying thrust klippe structurally over continuous Angel Island terrane. However, the aeromagnetic signature of the serpentinite suggests instead more extensive steeply southwest dipping bodies, probably dividing separate bodies of Angel Island terrane.

The rocks of the Angel Island terrane were originally included in the Yolla Bolly terrane (Blake et al., 1984). Wakabayashi (1992) reassigned them to his Angel Island “nappe,” which was later called Angel Island terrane (Konigsmark, 1998). The rocks of the Angel Island terrane differ from those of the Yolla Bolly terrane in age, chemical composition, and topographic expression, so that name is used herein.

The rocks of the Angel Island terrane are mostly metagraywacke, metachert, and metabasalt. There is also minor metaconglomerate, metamorphosed intrusive rocks, and metaserpentinite.

In San Francisco, the only lithology present is metagraywacke, which crops out as thick bedded gray sandstone, foliated parallel to bedding where bedding is preserved. The metagraywacke protolith is arkosic (Schlocker, 1974). The layers appear to be broadly folded. Bero (2014) maps a continuous section of metabasalt–chert–graywacke on the Tiburon Peninsula that is entirely overturned so that metabasalt is the structurally highest unit.

The most striking characteristic of the Angel Island terrane is the metamorphism: foliated metagraywacke, metabasalt, and metachert that contain blueschist-facies minerals including jadeitic pyroxene, glaucophane, and

lawsonite. Many of the early studies of Franciscan metamorphism were done on Angel Island, Tiburon Peninsula, and in the Berkeley Hills, where lawsonite- and jadeite-bearing metagraywackes were first recognized and described (Ransome, 1895; Bloxam, 1956; 1960).

YZP ages of detrital zircons from metagraywackes in this terrane are 102–109 Ma (Snow et al., 2010; Apen et al., 2016). There are no known fossils, either from graywacke or chert.

Mélange

The classic Franciscan mélange is sedimentary-matrix mélange, completely sheared and disrupted fine-grained sandstone and shale encompassing coherent blocks ranging in size up to hundreds of meters, including “exotic” blocks (i.e., blocks other than graywacke; Hsu, 1968). In San Francisco, these exotic blocks include chert, greenstone, blueschist, and serpentinite.

In San Francisco, Franciscan mélange crops out in a band that spans the western part of the city from southeast to northwest, which has been called the City College mélange, as well as a roughly triangular body in the northern part of the city (Figure 31 and Figure 32). As noted above, there may also be mélange beneath the bay or beneath Quaternary cover within areas shown as coherent terranes on Figure 31 and Figure 32, as well as small bodies of mélange interleaved within the coherent terranes.

The City College mélange was originally mapped as a broad shear zone around central fault called the City College fault (Schlocker, 1958). However, this work was prior to the introduction of the mélange concept (Hsu, 1968), and the band of pervasively sheared sedimentary rocks with blocks of coherent sandstone and other lithologies is now recognized as part of a body of mélange. The western boundary of the City College mélange is basically the same as the previously mapped western boundary of the “fault zone,” but the eastern boundary has been changed in this work, both at the north and south end to capture rocks previously included in the Marin Headlands terrane. This change reflects both the contrast in magnetic signature (these areas lack the strong magnetic high associated with Marin Headlands greenstone, in spite of the presence of mapped greenstone bodies, suggesting the greenstone bodies lack depth, as might be expected for a

mélange block) and the presence of rock types not found in Marin Headlands terrane, such as serpentinite and blueschist (Plate 1).

Many of the blocks in the Franciscan mélange have been correlated with nearby coherent terranes, for example the Marin Headlands rocks mapped along the northwest margin of San Francisco east of Lands End. The presence of blocks derived from nearby terranes supports the idea that mélange, at least in part, formed by deformation during and after subduction-accretion that allowed for tectonic mixing with adjacent rocks.

Franciscan Complex or Coast Range Ophiolite

Hunters Point Serpentinite-Matrix Mélange

The origin of the serpentinite-matrix mélange is not clear, which is why it’s listed under the heading “Franciscan Complex or Coast Range Ophiolite.” Wakabayashi (2004) has interpreted it as an accreted fragment of exhumed oceanic mantle (i.e., Franciscan) because of the inclusion of blocks of high-temperature metamorphic rocks (amphibolites) and because of his (erroneous, see below) interpretation of the unit as a folded subhorizontal slab interleaved in other Franciscan subhorizontal slabs. However, serpentinite with spinel geochemistry suggestive of forearc origin (and therefore Coast Range Ophiolite affinity) is known from a serpentinite body similarly structurally interleaved in the Franciscan to the south in San Mateo County (Barnes et al., 2013). Furthermore, high-temperature amphibolite blocks have been documented within serpentinite-matrix mélange at the base of the Coast Range Ophiolite along the west margin of the Sacramento Valley (Shervais et al., 2011). As such, a definitive assignment of the Hunters Point unit to either Coast Range Ophiolite or Franciscan is at present impossible.

The Hunters Point serpentinite-matrix mélange runs from the northwest corner of the city at Fort Point to the southeast corner at Hunters Point (Figure 31 and Figure 32). Aeromagnetic data (Figure 31) suggests that it extends to the southeast beyond the city limits, but to the northwest is abruptly truncated just offshore at the Golden Gate, separated from the Marin Headlands terrane to the north by a narrow zone of low magnetic-susceptibility rock interpreted herein as sedimentary-matrix mélange.

The serpentinite-matrix mélange is made up of perva-

sively sheared serpentinite encasing blocks and lenses of hard serpentinite, gabbro, pyroxenite, graywacke, chert, greenstone, and high-grade metamorphic rocks (Figure 37). There are also zones of sedimentary-matrix *mélange* intermixed with serpentinite, mapped as unit “fsr-spm” on Plate 1. Schlocker (1974) suggests that these rocks are mostly sandstone, an interpretation generally supported by the relative magnetic lows associated with them, but the presence of interleaved serpentinite at a scale too small to map separately suggests inclusion in the Hunters Point unit. A prominent elongate magnetic low that extends southeast from the large sandstone block near Potrero Point suggests a several-kilometer-long concealed lens of sandstone or sedimentary-matrix *mélange* between two serpentinite-matrix *mélange* bodies. A smaller lens-shaped magnetic low is associated with the blocks of Marin Headlands terrane sandstone, chert, and greenstone mapped at Hunters Point. Wakabayashi (2004) interprets the sandstone blocks at Potrero Hill as klippe of Alcatraz terrane sitting on top of serpentinite, but Schlocker (1974) interprets them as “tectonic inclusions

completely within serpentinite,” and shows a measured dip direction on one bounding fault placing sandstone under serpentinite (see Plate 1).

Wakabayashi (2004) includes the triangular area of sedimentary-matrix *mélange* in the north part of the city in the Hunters Point unit, but aeromagnetic data (Figure 31) shows an elongate low extends from mapped Franciscan *mélange* in Marin County down to the sedimentary-matrix *mélange* outcrops in San Francisco, so the San Francisco outcrops are herein considered part of that unit.

Wakabayashi (most recently in Wakabayashi, 2015) has interpreted the Hunters Point serpentinite as a nearly flat folded slab that extends northeastward from its surface contacts under the bay at a shallow level. However, the aeromagnetic map (Figure 31) shows this to be incorrect, as the bay east of the serpentinite-matrix *mélange* is marked by a magnetic low, not the broad magnetic high that would be expected from a shallow slab of serpentinite. This magnetic low is obscured in downtown San Francisco by an extreme



Figure 37. Serpentinite-matrix *mélange*, Presidio southwest of Fort Point, San Francisco (photo by John Karachewski).

magnetic high attributed to the many large steel buildings there, but is clearly evident to the southeast off China Basin. The aeromagnetic data show that the Hunters Point serpentinite-matrix *mélange* instead forms a steeply east dipping slab, with equally steeply east dipping lenses on non-magnetic rock (probably sedimentary-matrix *mélange* or sandstone) enclosed within it (Zoback et al., 1995).

Geologic Structures in San Francisco

The geologic structures in San Francisco are dominated by the terrane-bounding faults (Figure 31 and Figure 32). The aeromagnetic signature of the serpentinite in the Hunters Point serpentinite *mélange* suggest a steep northeast dip for these faults (Figure 33, see also cross section B of Schlocker, 1974), and the map pattern suggests that the coherent terranes form slabs, pods, and lenses, either juxtaposed or embedded in *mélange*.

Within the coherent terranes there is significant compressive deformation. The limited exposure of the Bolinas Ridge terrane suggests a syncline-anticline pair folded around a moderately southeast plunging axis; San Bruno Mountain terrane strata form an anticline around a shallowly southeast plunging axis; Alcatraz terrane strata appear broadly folded around a moderately northwest plunging axis; and the Marin Headlands terrane appears to be thrust repeated (Figure 32).

The basement structures are cut in San Francisco by a single San Andreas fault system strand, the onshore extension of the Golden Gate fault through Merced Lake. As described below in the discussion of the Merced Formation, this fault was probably a right-lateral oblique normal fault in Pliocene to early Pleistocene time, related to a releasing right step in the San Andreas fault zone, that was abandoned and then reactivated as a reverse fault some time prior to Colma Formation deposition, with potential for modest ongoing slip (Hengesh and Wakabayashi, 1995; Jachens et al., 2002). The main trace of the San Andreas fault runs offshore to the west, along with two main strands of the San Gregorio fault zone just west of that (Figure 28).

As noted above in the “*Mélange*” subsection of “Franciscan, Central Belt,” the zone of sheared rock previously mapped as the City College fault zone (Schlocker, 1974; Bonilla, 1971) is actually part of a band of Franciscan *mélange*. Likewise, the zone of sheared serpentinite and other rocks previously mapped as the

Hunters Point shear zone is now seen to be serpentinite-matrix *mélange*.

Tertiary Overlap Sequences

Merced Formation

The Merced Formation unconformably overlies or is in fault contact with Mesozoic Franciscan Complex rocks along a linear belt that is 2.4 km (1.5 mile) wide and 19 km (12 miles) long, located directly east of the San Andreas fault (Bonilla, 1965, Clifton et al., 1988; Pampeyan, 1994; Brabb, Graymer and Jones, 1998; Andersen et al., 2001). The deposits roughly span from Fort Funston in the north to Burlingame in the south. Outcrops of the Merced Formation occur in the southwestern part of San Francisco along the sea cliffs at Fort Funston and Thornton State Beach (Figure 39).

The Merced Formation principally consists of weakly lithified to well cemented thinly bedded to massive sandstone and siltstone with minor claystone and conglomerate beds and shell hash that were deposited in shallow marine to estuarine and non-marine, coastal environments (Hall, 1965; Clifton et al., 1988; Andersen et al., 2001). Hunter et al. (1984) describe a number of facies within the unit representing marine (shelf and near shore) and coastal nonmarine depositional environments. The deposit is about 1,525 m (5,000 ft) thick near the coastal bluffs of Mussel Rock.

The age of the Merced Formation is uncertain, but likely is between about 400,000 and 2 million years old based on volcanic ash beds (Clifton et al., 1988; Brabb and Pampeyan, 1998; Brabb, Graymer and Jones, 1998), with the uppermost beds found along the coast being younger than ~400,000 years (Kennedy, 2002). The tuff beds in the Merced have been correlated with the Bishop ash (~774,000 years old; Sarna-Wojcicki et al., 2000) and the Rockland ash (~575,000 years old; Maier et al., 2013). Hall (1966) describes the fossils found at various stratigraphic levels within the unit, including echinoids, mollusks, and mammals, ranging from Pliocene to early Pleistocene in age. The base of the unit is to the south, so that the part in San Francisco is in the upper, early Pleistocene part of the unit.

The Merced Formation is divided into upper and lower sections based on a mineral source change from the local coastal area to the volcanic and plutonic rocks of the Sierra Nevada (Hall, 1965). Clean to silty, fine-grained, poorly consolidated micaceous sands are characteristic of the upper Merced deposits, whereas non-micaceous

shallow marine sands and silts are characteristic of the lower Merced. Hall (1966) also points out a change in detrital heavy mineral content of the Merced strata near the Pliocene–Pleistocene transition. The minerals below reflect local, Franciscan and Salinian sources whereas the minerals above reflect Sierra Nevada and southern Klamath sources, indicating the initiation of Sacramento–San Joaquin River drainage through the San Francisco Bay region at this time as these rivers drained to the Pacific through the Lake Merced embayment prior to shifting through the Golden Gate. (Sarna-Wojcicki et al., 1985). An earlier estimate of 600 ka (thousand years ago) for the time of this transition was flawed by an inaccurate age for the Rockland ash, but using the more recently measured age and the average rate of deposition (0.55 m/ka, Hunter and others, 1984) to estimate the time between the transition and ash deposition gives an estimated time of about 800 ka for the transition. The current distribution of the Merced Formation results from tectonic deformation and uplift related to the San Andreas and Serra fault system (Bruns et al., 2002; Wakabayashi et al., 2004).

Implications of the Tertiary Overlap Sequences

As mentioned earlier, the only pre-Quaternary overlap unit in San Francisco is the Pliocene and Pleistocene Merced Formation, which is only exposed in sea cliffs west of Fort Funston in the southwest corner of the city (and extending south into San Mateo County). There, moderately (12–45°) east to northeast dipping beds are overlain by nearly horizontal (3–5° dip) beds of the Colma Formation. The angular unconformity demonstrates a period of east to northeast tilting in the Pleistocene, perhaps related to offset along the fault just to the east.

The Merced Formation is associated with a triangular gravity low northeast of the San Andreas fault (Jachens et al., 2002), suggesting deposition in a transtensional basin associated with a releasing right step between the San Andreas fault (main strand) and the Golden Gate fault. This unit interfingers to the southeast in San Mateo County with roughly coeval fluvial and alluvial nonmarine deposits of the Santa Clara Formation.

All this suggests that in Pliocene and early Pleistocene time, a right step in the San Andreas fault zone generated a narrow trough that connected the Pacific Ocean to the west through the San Francisco Peninsula to the fluvial and alluvial systems to the southeast. Around the end of the Pliocene, the local system became connected

to the Sacramento–San Joaquin River drainage, which then drained out through the Lake Merced embayment. However, the unconformable overlap of the Colma Formation suggests that the right step was abandoned, and sedimentary basin formation ceased, prior to Colma deposition. As mentioned above, the east and northeast tilting of Lake Merced strata unconformably below the relatively flat Colma Formation suggests further that the old northeastern basin bounding fault was reactivated as a reverse fault, lifting and exposing the basin-fill Merced Formation. Today, the extension of the Golden Gate fault through Lake Merced is marked by a topographic high to the southwest, suggesting that the reverse offset may be ongoing.

Marine sandstone, siltstone, and conglomerate near Bolinas, about 30 km (19 miles) to the northwest between the San Andreas and San Gregorio faults, has been correlated with the Pliocene part of the Merced Formation (Galloway, 1977; Clark et al., 1984). This outcrop presumably reflects a sliver of the Merced transtensional basin or oceanward overflow brought to its present position by northward offset on the San Andreas fault.

Quaternary Deposits in San Francisco

Mesozoic basement complex rocks that occasionally crop out in the steep hills of San Francisco are unconformably overlain by a variety of Quaternary terrestrial, submarine, and estuarine deposits that collectively reflect multiple origins ranging from major sea-level and climatic fluctuations as well as tectonic uplift (Schlocker et al., 1954; Schlocker, 1974; Atwater et al., 1977; Atwater, 1980; Helley and Lajoie, 1979). Three major depositional phases are recorded in the Quaternary stratigraphy in the San Francisco Bay Area: (1) Pleistocene shallow marine and near shore deposition, (2) accumulation of Pleistocene alluvium during sea-level low stands, and (3) estuarine and eolian deposition during Pleistocene and Holocene sea-level high stands (Figure 38). These climatic and tectonic forces created a complex stratigraphic package of intercalated Pleistocene alluvial and estuarine deposits overlain by Holocene estuarine and dune deposits (Figure 39) (Graymer et al., 2006).

The Quaternary stratigraphy of the San Francisco Bay Area has been greatly influenced by climatic changes related to glacial–interglacial cycles (Figure 38). Nearly all the major Quaternary stratigraphic packages in the Bay Area owe their origin to a rising or lowering of the

sea over these glacial–interglacial cycles. For example, late Quaternary sea levels fluctuated in elevation by over 100 m (328 ft) globally between glacial (sea-level low stand) and intervening interglacial (sea-level high stand) periods (Figure 38) resulting in different deposits within the city limits of San Francisco. At least three prior episodes of deposition occurred during sea-level high stands (interglacial) approximately 410,000, 330,000, and 120,000 years ago, when the sea reached inland at sufficient elevation to flood the ancestral Sacramento–San Joaquin Delta and Santa Clara valley, and thus forming ancient estuaries (i.e., slack water and marsh deposits) much like the present-day San

Francisco Bay (Atwater, 1979). During glacial periods, sea levels were up to 120 m (394 ft) lower than present-day, producing a shoreline as far west as the Farallon Islands (Helley and Lajoie, 1979). During these sea level low stands, fluvial, alluvial and eolian deposition predominated in the valleys and on hillslopes of the San Francisco Peninsula. In some cases, these non-marine Pleistocene deposits overlie earlier marine sediments deposited during earlier sea-level high stands (Helley and Lajoie, 1979) and in other cases the non-marine deposits are buried by marine deposits related to more recent sea-level high stands. During the early Holocene between 9,500 and 8,000 years ago, the Pacific Ocean

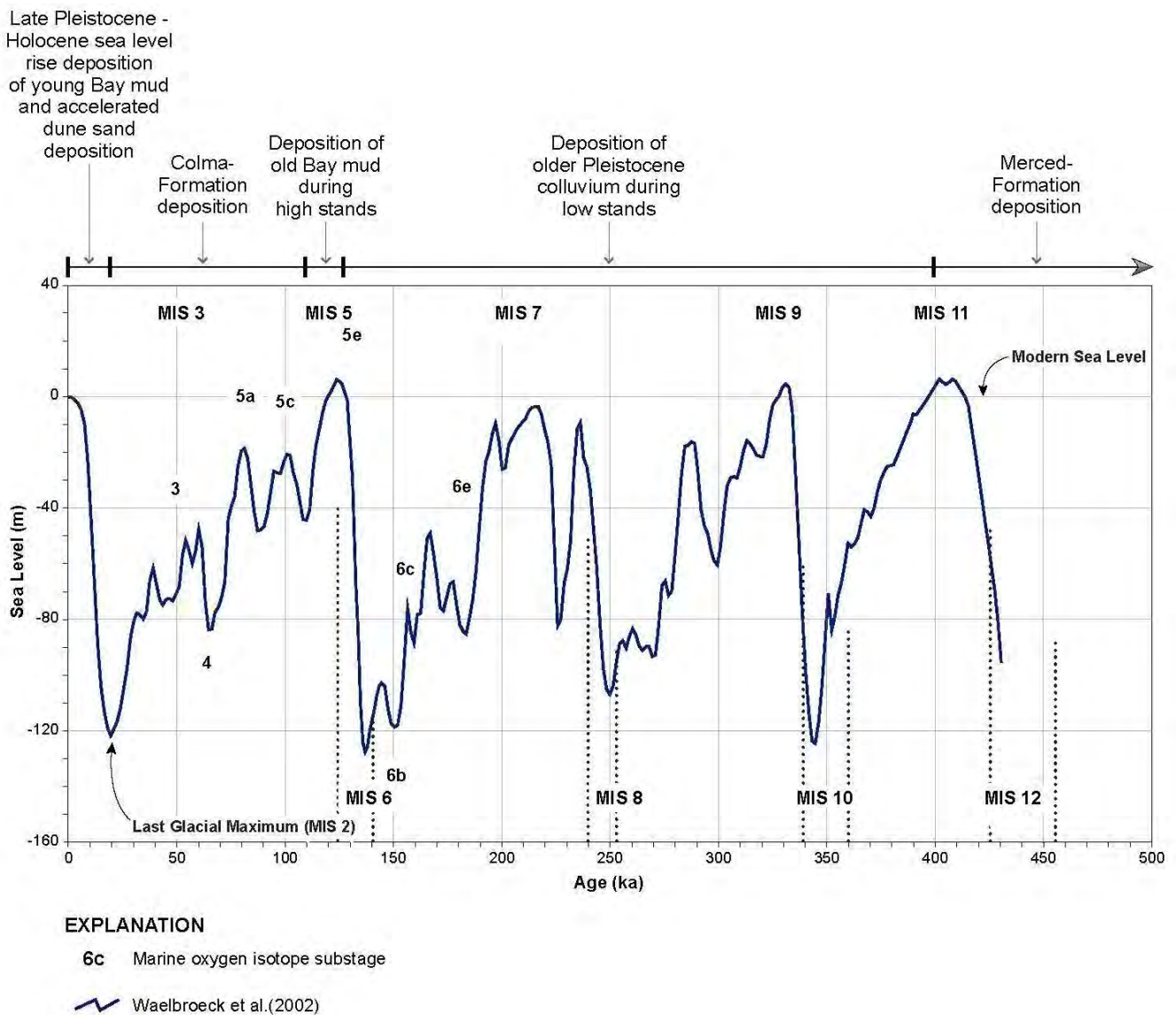


Figure 38. Global sea level fluctuation in the last 500,000 years correlated to depositional processes in San Francisco (Waelbroeck et al. 2002).



Figure 39. Geologic map of San Francisco illustrating Quaternary units (Graymer et al., 2006). Franciscan Complex Bedrock is not shown. Units include: Gray= Artificial Fill (AF), Pink= Landslide and hillslope deposits (Qsl), Yellow = Sand dunes (Qd), Orange = Colma Formation (Qc), green = older Quaternary Alluvium (Qpa); Merced Formation = light blue. Also shown is location of the shoreline in 1850 (blue dashed line) and the extent of historic marshes from 1898 (blue cross hatch pattern) (Sowers et al., 2007). Note: Young Bay mud is covered by artificial fill in San Francisco. C–C’ cross section is from Schlocker (1974) and is shown in Figure 40.

flooded the Golden Gate and sea level rose rapidly, about 2 cm/yr (0.8 in/yr) (Atwater et al., 1977). The rate of sea-level rise then declined by an order of magnitude between 8,000 and 6,000 years ago. Since 6,000 years ago, sea level has risen more slowly at a rate of 0.1 to 0.2 cm/yr (0.04 to 0.08 in/yr). Expansive tidal marshes in San Francisco Bay became established in the last 2,000 years as sea level stabilized at a slow enough rate to allow formation of persistent and widespread tidal marshes (Atwater et al., 1979).

The following provides a summary from oldest to youngest of the key geologic units on the San Francisco Peninsula and their association with glacial cycles.

Yerba Buena Mud (“Old Bay Deposits”)

The Yerba Buena Mud (referred to informally as the Old Bay Deposits or Old Bay Clay) was deposited approximately 120,000 years ago during an earlier sea-level high stand that was the most recent predecessor to today’s San Francisco Bay (Sloan, 1992) (Figure 38). This deposit overlies or interfingers with the Colma Formation (or undifferentiated Pleistocene alluvium) and consists of a sequence as much as 30 m (100 ft) thick of relatively homogenous gray, marine silty clay, and occasional thin laterally discontinuous lenses of fine sand and shell-rich horizons. It is generally highly plastic and commonly very stiff to hard (Atwater, 1977). Evidence for this prehistoric estuary comes from deposits of estuarine mud, 5 to 32 m (16 to 105 ft) thick, collected from exploratory boreholes drilled for critical infrastructure studies in San Francisco (Schlocker et al., 1958; Atwater et al., 1977; Sloan, 1992; Trask and Rolston, 1951; GHD-GTC, 2016). The criteria used to distinguish the Yerba Buena Mud from alluvial deposits typically found between the Yerba Buena Mud and the Young Bay Mud (see below) include stratigraphic position, color, grain size, bulk density, primary and secondary mineral constituents, and microfossils (Sloan, 1992; GHD-GTC, 2016).

Colma Foundation

The Pleistocene Colma Formation represents a broad grouping of geologic deposits including primarily beach sand, colluvium, and alluvium that overly the Merced Formation and Franciscan Complex bedrock. The Colma Formation is widely extensive in the southwestern part of San Francisco from Lake Merced to the Excelsior neighborhood (Figure 39). This formation was first named by Schlocker et al. (1958) and is

named after the type locality in the City of Colma, where the formation includes friable, well-sorted, fine to medium sand incised by the modern Colma Creek (Bonilla, 1998). In San Francisco, the Colma Formation is mapped in the subsurface along the margins of San Francisco Bay and along the southwestern portion of the city (Figure 39 and Figure 40) (Schlocker, 1974; Graymer et al., 2006). The Colma Formation described near the coast consists of poorly consolidated to unconsolidated fine-grained sand and silt, and represents a variety of non-marine environments, as well as nearshore, foreshore, and backshore beach deposits.

The total thickness of the Colma Formation is unknown, but may be as great as 60 m (197 ft) (Brabb and Pampeyan, 1998). The age of the deposit is estimated as latest Pleistocene, between about 130,000 and 11,000 years old (Bonilla, 1998; Kennedy, 2002). Inland from the coast and along the margins of topographic highs, the Colma Formation likely consists of discontinuous alluvial fan deposits and/or colluvium capping older alluvial surfaces (i.e., non-coastal and non-marine). During the last glacial period, 20,000 to 12,000 years ago, when sea levels were significantly lower, about 130 m (425 ft) in elevation below the current sea level, Colma Formation blanketed valleys of paleo-San Francisco Bay.

It is important to note that undifferentiated Quaternary alluvium (Pleistocene alluvium) is mapped between bedrock knobs in the Mission District (Figure 39) (Graymer et al., 2006). These undifferentiated deposits are poorly understood because of the urban development of the area. However, these deposits are likely Colma Formation equivalents (Figure 39 and Figure 40) (Schlocker, 1974).

Young Bay Mud

The poorly consolidated Holocene (younger than about 11,000 years) marine deposits commonly known as Young Bay Mud were deposited during the most recent sea-level intrusion coincident with present-day San Francisco Bay. They are generally less than 50 m (165 ft) thick and are actively being deposited (Helley and Lajoie, 1977; McDonald, 1978; Knudsen et al., 1997). Within the San Francisco city limits, Young Bay Mud is located along the margins of the bay, between the modern shoreline and historical limit of the tidal marsh (Figure 39), and generally buried by artificial fill (Nichols and Wright, 1971; Schlocker, 1974; McDonald, 1978; Holzer, 1998; GHD-GTC, 2016). The

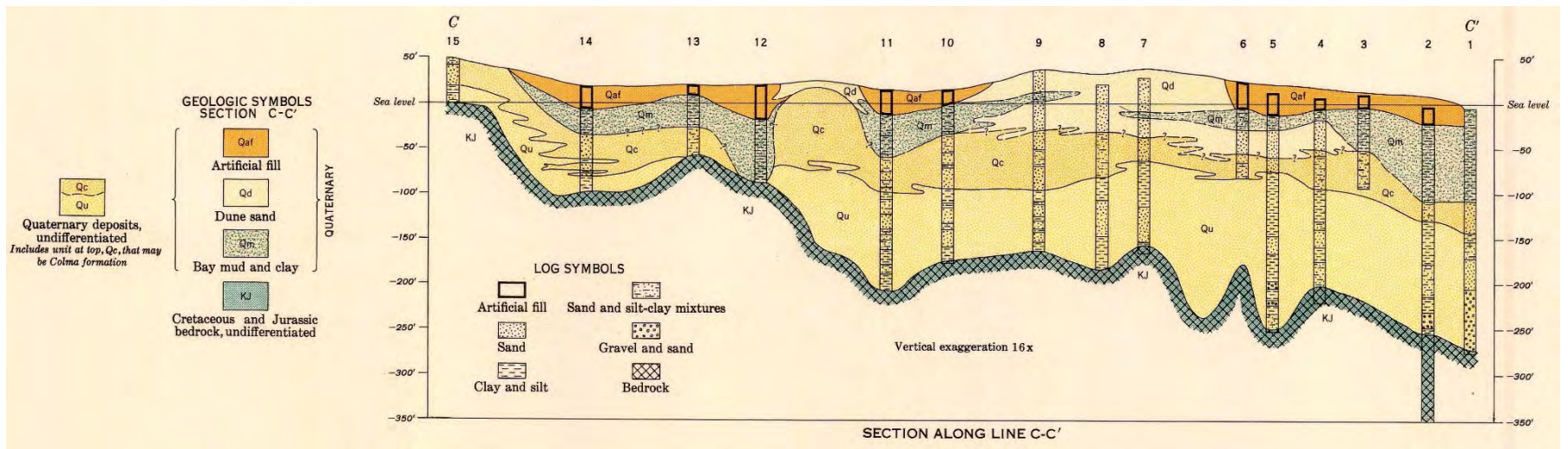


Figure 40. See Figure 39 for the section location. Cross section in the South of Market area of San Francisco (Schlocker, 1974). Qc—Colma Formation, Qm—Bay Mud, Qu—Undifferentiated Pleistocene deposits (pre-Colma Formation alluvial deposits?), Qd—Dune deposits.

Young Bay Mud is typically a moderate to high-plasticity silty clay that is highly compressible. It also can contain interbeds of alluvial silty sand and clayey sand lenses originating from nearshore streams and creeks along the margins of the bay (GHD-GTC, 2016). The Young Bay Mud typically rests unconformably on undifferentiated late Pleistocene–Holocene alluvial and eolian deposits (Schlocker, 1974; Holzer, 1998; GHD-GTC, 2016).

Eolian Deposits

Dune sand mantles much of western and central San Francisco (Figure 39) (Schlocker, 1974; Graymer et al., 2006). The dune deposits are formed by a prevailing westerly wind that sweeps sand from beaches along the Pacific Ocean eastward where it buries Pleistocene ravines and gullies formed by coastal erosion during previous Pleistocene low stands. Although some late Pleistocene eolian deposition occurred, deposition of the dune deposits accelerated in the Holocene coincident with rising sea-level and easterly migrating shoreline. The deposits are mapped across the high topography of the central part of San Francisco, up to 150 m (500 ft) above sea level, and attain a thickness of up to 45 m (150 ft) (Schlocker, 1974). The deposits typically consist of well-sorted, fine- to medium-grained sand. Because of urban development in the city, active dune transport and deposition is now restricted to a narrow zone at Ocean Beach (Schlocker, 1974; Elder, 2001) (Figure 39).

Landslide and Hillslope Deposits

Landslide and hillslope materials within the San Francisco area include a combination of colluvium and earthflow, debris flow, debris slide, and rotational slump deposits (Figure 39). Multiple maps prepared by the U.S. Geological Survey and California Geological Survey (Schlocker, 1974; Nilsen et al., 1979; Pike, 1997; Wentworth, 1997; Hillhouse and Godt, 1999; Wilson et al., 2000) have identified historical slope failures within the city concentrated near Mount Sutro, Twin Peaks, Mount Davidson, Diamond Heights, Potrero Hill and the Sea Cliff area (Figure 39). These deposits are found in several key areas: (1) steep slopes veneered with colluvium overlying Franciscan Complex bedrock, (2) coastal bluffs where high cliffs expose sheared Franciscan bedrock prone to debris slides and rock falls, and (3) steep slopes and sea cliffs in the southwestern part of San Francisco where the Merced Formation is prone to rotational and translational sliding. Sheared

Franciscan rock and serpentine are particularly prone to landsliding, especially in the area of Lands End (Schlocker, 1974). For instance, in this region, the sea cliffs are continuously ravaged by wave action and seeps that undercut the base of the slope promoting landslides and rockfalls. Landsliding in the San Francisco area can be caused by heavy rainfall (e.g., 1998 El Niño) (Hillhouse and Godt, 1999) or by earthquake-related strong ground shaking (e.g., Loma Prieta) (Keefer and Manson, 1998).

Artificial Fill

Since the 1800s the northeastern and eastern margins of the city of San Francisco have undergone significant landscape modification through multiple episodes of fill placement (Trask and Rolston, 1951; Schlocker, 1958; Goldman, 1969; Holzer, 1998; Hitchcock et al., 2008) (Figure 39). Areas receiving the most extensive artificial fill include inlets and coves, and saltwater marshes. Filling of the bay margins included a variety of fill placement methods ranging from dumping to hydraulic filling, as well as the intentional sinking of abandoned wooden sailing vessels. Artificial fill in the city includes a combination of local native sediments (i.e., hydraulically placed dune sand and bay sediments) and miscellaneous anthropogenic debris, such as brick, concrete, and timber all of which are typically placed on weak Young Bay Mud. In Yerba Buena Cove, artificial fill includes debris from Gold Rush-era ships that were sunk and used as fill (Dow, 1973; Hitchcock et al., 2008). Following the 1906 earthquake and fire, significant anthropogenic debris was disposed as fill along the bay margin north and east of Market Street (Figure 39). Because of the different source materials and methods used for placement, the artificial fill is highly variable and depends heavily on the source of the fill material. For instance, material sourced from the sand dunes and dredged bay sediments typically consists of loose, poorly graded sand to clayey sand and soft clay and often may be mixed or overlie rubble such as brick, asphalt, concrete, wood, broken rock, and scattered gravel (Holzer, 1998; Hitchcock et al., 2008; Sowers and O'Rourke, 1998. Refer to Goldman (1969), Holzer (1998), and Hitchcock et al., (2008) on the variation in fill types and depths along the margin of San Francisco Bay.

Artificial fill in the San Francisco Bay region is highly vulnerable to liquefaction and settlement during earthquake-related strong ground shaking (Goldman,

1969; Seed, 1969; Helley and Lajoie, 1977; Holzer, 1998; Knudsen et al., 1997 and 2000). Liquefaction susceptibility of the fill is based on (1) the nature and thickness of fill material, (2) whether the fill is engineered or non-engineered, and (3) its depth of saturation (Knudsen et al., 1997).

San Francisco's Offshore Geology

Marine geology and geomorphology were mapped offshore of San Francisco by the U.S. Geological Survey for the California Seafloor Mapping Program (Johnson et al., 2017), then merged with onshore geologic data compiled by the California Geological Survey to create seamless onshore–offshore geology maps (Figure 41) at the 1:24,000 scale (Greene et al., 2014, 2015). Offshore geologic units were delineated on the basis of integrated analyses of adjacent onshore geology with multibeam bathymetry and backscatter imagery (Dartnell et al., 2014a, b; 2015a, b), seafloor-sediment and rock samples (Reid et al., 2006; Barnard et al., 2007), digital camera and video imagery (Golden and Cochrane, 2015; Golden et al., 2014), and high-resolution seismic-reflection profiles (Sliter et al., 2014; Johnson et al., 2015).

The Figure 41 map area and Figure 42 shaded-relief bathymetric image include the Golden Gate channel, which connects the Pacific Ocean and San Francisco Bay. San Francisco Bay, the largest estuary on the U.S. west coast, is located at the mouth of the Sacramento and San Joaquin rivers and drains over 40% of the state of California. The large surface area of the bay and diurnal tidal range of 1.78 m (5.84 ft) creates an enormous tidal prism of about 2 billion m³ (70.6 billion ft³), and strong tidal currents, commonly exceeding 2.5 m/s (8.2 ft/s) (Barnard et al., 2006a, b; 2007). Acceleration of these currents through the constricted inlet has led to scouring of a bedrock channel that has a maximum depth of 113 m (370.7 ft) (Figure 41 and Figure 42). Large fields of sand waves (Figure 42; Barnard et al., 2007) have formed both west and east of this channel as flow expands and tidal currents decelerate. Sand wave fields resulting from tidal flow are also present in the nearshore along the Pacific Coast south of the Golden Gate channel (Figure 41).

The sand-wave fields appear to be variably mobilized by both ebb and flood tides, but the presence of an ebb-tidal delta that is about 150 km² (58 square miles) at the mouth of the bay west of the inlet indicates that net sediment transport has been to the west. The inner part

of the delta comprises a semicircular, inward-sloping (toward the Golden Gate channel), sandy seafloor at water depths of about 12 to 24 m (39 to 79 ft). This inner delta has a notably smooth surface, indicating sediment transport and deposition under different flow regimes (defined by tidal current strength and depth) than those in which the sand waves formed and are maintained. Further deceleration of tidal currents beyond the inner delta has led to sediment deposition and development of a large, shoaling, horseshoe shaped, delta-mouth bar, at a water depth of about 8 to 12 m (26 to 39 ft).

This feature (the “San Francisco Bar”) surrounds the inner delta, and its central crest is cut by a dredged shipping channel that separates its northern and southern parts. The shallow portion of the northern part of the bar is commonly referred to as the “Potato Patch,” notorious for hazardous navigation. The San Francisco Bar is shaped by both tidal currents and waves, which regularly exceed 6 m (20 ft) in height on the continental shelf during major winter storms (Barnard et al., 2007). Dallas and Barnard (2011) have documented significant shrinkage of the ebb-tidal delta since 1873 when the first bathymetric survey of the area was undertaken. They show an approximate 1 km (0.6 mile) landward migration of the crest of the San Francisco Bar, which they attribute to a reduction in the tidal prism of San Francisco Bay and a decrease in coastal sediment supply.

From outside the San Francisco Bar to the limits of the map area and beyond to the shelfbreak (about 45 km (28 miles) offshore), the notably flat shelf (gradient less than 0.2°) is subjected to the full, and sometimes severe, wave energy and strong currents of the Pacific Ocean (Storlazzi and Wingfield, 2005; Barnard et al., 2007). Within the Figure 41 map area, shelf sediments are mainly sand.

Sea level has risen about 125 to 130 m (410 to 427 ft) since the Last Glacial Maximum (LGM) about 21,000 years BP (Stanford et al., 2011), leading to the progressive eastward migration of the shoreline and associated development of a wave-cut transgressive surface of erosion. In the Figure 41 map area, shelf and delta sediment thickness above this transgressive surface of erosion ranges from 0 m in areas of bedrock exposure to as much as 57 m (187 ft) in the San Andreas graben (Figure 43; Johnson et al., 2015a).

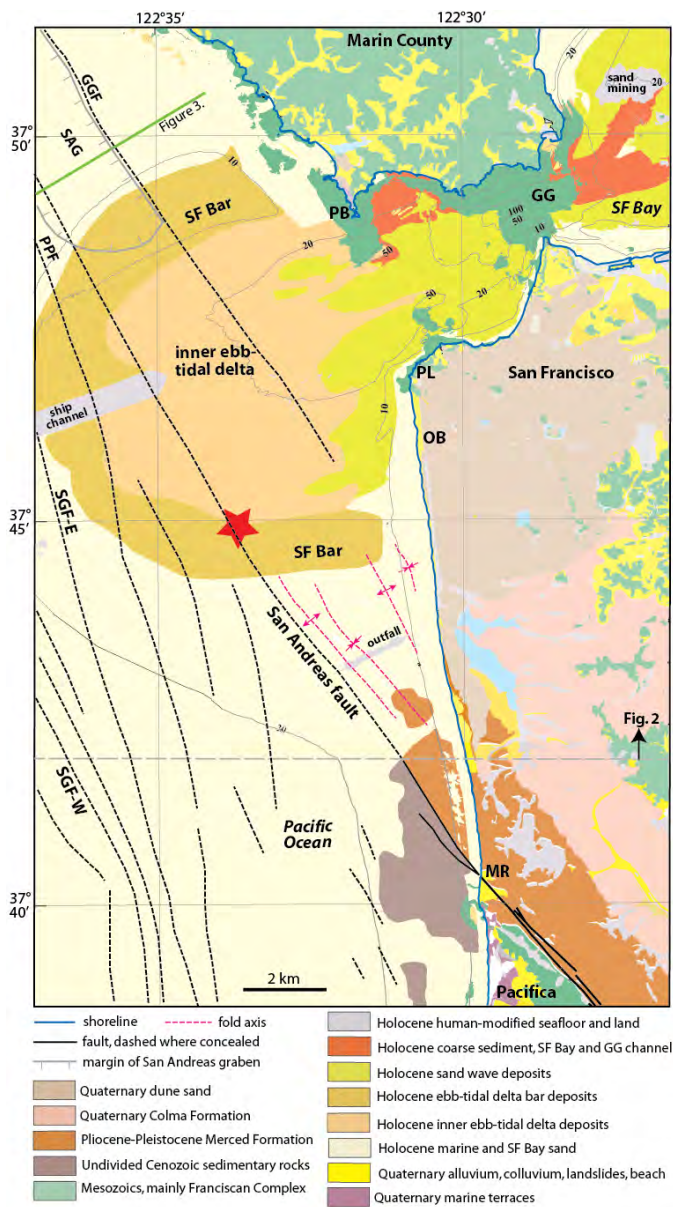


Figure 41. Onshore-offshore geologic map (simplified from Greene et al., 2014, 2015). Red star shows approximate location of epicenter of 1906 San Francisco earthquake (U.S. Geological Survey, 2018). Depth contour intervals are 10 m (33 ft), 20 m (66 ft), 50 m (164 ft), and 100 m (328 ft). GG, Golden Gate channel; GGF, Golden Gate fault; MR, Mussel Rock; OB, Ocean Beach; PB, Point Bonita; PL, Point Lobos; PPF, Potato Patch fault; SAG, San Andreas graben; SF Bar, San Francisco bar; SF Bay, San Francisco Bay; SGF-E, east strand of San Gregorio fault; SGF-W, west strand of San Gregorio fault. Dashed gray line is southern boundary of shaded-relief map shown in Figure 42.

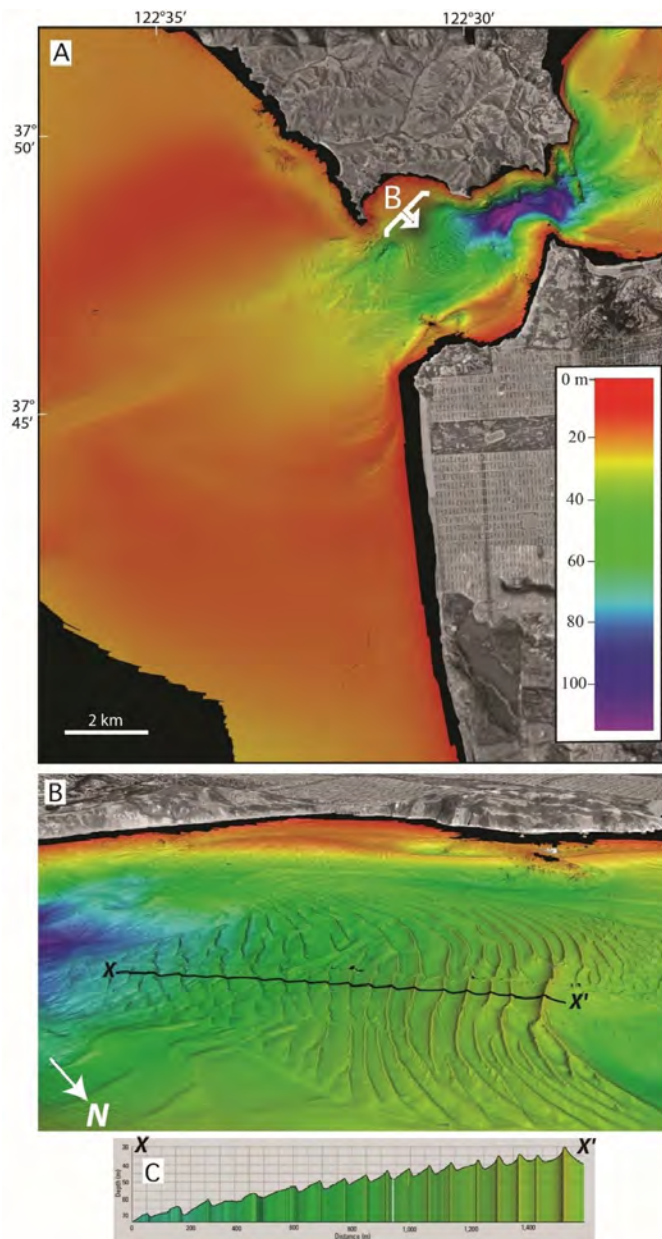


Figure 42. A. Colored, shaded-relief bathymetry of the offshore of San Francisco (map area shown in Figure 41). High-resolution bathymetry is not available in the black areas (nearshore and southwest part of map). B. Perspective view looking southeast (location in A) across field of sand waves generated by strong tidal currents at the mouth of San Francisco Bay. C. Bathymetric profile across field of sand waves on line X-X' in B. Note sand-wave asymmetry suggesting western sediment transport and significant westward shoaling. (Images from Dartnell, 2015, and Dartnell et al., 2015b.)

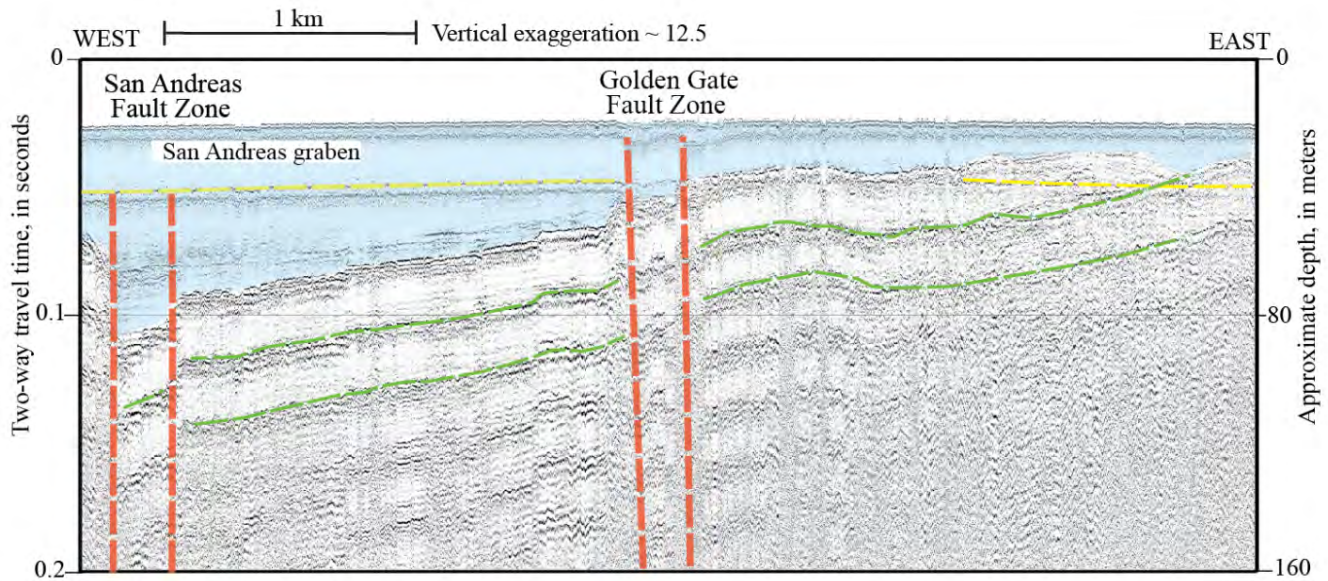


Figure 43. U.S. Geological Survey high-resolution, mini-sparker seismic-reflection profile GG-004, which crosses the shelf and eastern portion of the San Andreas graben northwest of San Francisco (location shown in Figure 41). Dashed red lines show San Andreas fault and Golden Gate fault (Cooper, 1973; Bruns et al., 2002; Ryan et al., 2008). Blue shading shows inferred uppermost Pleistocene and Holocene strata, deposited since last sea-level lowstand about 21,000 years ago. Dashed yellow line is seafloor multiple (echo of seafloor reflector). Dashed green lines are echoes of the first arrival from the top of basement rocks (the base of the blue unit) and are not stratigraphic markers.

Artificial (i.e., anthropogenic) seafloor has several distinct map occurrences (Figure 41), including: (1) sites of active sand mining inside San Francisco Bay; (2) a dredged shipping channel at the central crest of the San Francisco Bar; and (3) the sewage outfall pipe, associated riprap, and surrounding scour channel offshore Ocean Beach.

The Figure 41 map area is cut by several active northwest-striking, right-lateral strike-slip faults that cumulatively form a distributed shear zone. These structures include the San Andreas fault (SAF), the eastern and western strands of the San Gregorio fault zone, the Golden Gate fault, and the Potato Patch fault (Cooper, 1973; Bruns et al., 2002; Ryan et al., 2008; Johnson et al., 2015b). These faults are generally covered by Holocene sediments, have no seafloor expression, and are mapped using seismic-reflection data (e.g., Figure 43). The San Andreas graben (Figure 41 and Figure 43) is an extensional basin that formed within this zone and contains the thickest latest Pleistocene to Holocene (post LGM) sediment accumulation in central California—as much as 57 m (187 ft). The graben is about 7 km long (4.3 miles) and about 2 km wide (1.2 miles).

The San Andreas fault extends northwest across the Figure 41 map area and is the primary structure in the boundary between the Pacific and North American plates. It intersects the shoreline to the south at Mussel Rock (Figure 41); to the north it passes onshore at Bolinas Lagoon about 10 km (6 miles) north of the Figure 41 map area. The San Andreas fault in this area has an estimated slip rate of 17 to 24 mm/yr (U.S. Geological Survey and California Geological Survey, 2010). The devastating 1906 California earthquake M 7.9 is thought to have nucleated on the San Andreas fault a few kilometers offshore of San Francisco (Figure 41; U.S. Geological Survey, 2018). At a regional scale, it forms the boundary between two distinct basement terranes: Upper Jurassic and Lower Cretaceous rocks of the Franciscan Complex to the east, and Cretaceous granitic and older metamorphic rocks of the Salinian block to the west. In the local map area (Figure 41), however, Franciscan Complex rocks are present on both sides of the San Andreas fault. Seafloor bedrock outcrops east of the fault are present in the deep scour channel beneath the Golden Gate (Figure 41 and Figure 42), offshore of Point Lobos on the northwest San Francisco Peninsula, and offshore of Point Bonita in

Marin County. In the southern part of the map area, the San Andreas forms the southwestern boundary between the Franciscan Complex and the Pliocene and Pleistocene Merced Formation.

Geologic History of San Francisco⁴

by Russell W. Graymer

Because San Francisco is in a tectonically active part of the world, it is important to define just what one means by “geologic history of San Francisco,” as geology that is here now was someplace else earlier. Herein we will take “San Francisco” to mean the position of the city relative to the Sierra–Great Valley microplate, which is the piece of continental crust that now includes the Sierra Nevada batholith. By doing so, we neglect the westward motion of the microplate relative to cratonic North America, as well as the motion of North America itself, in order to focus on the relative interactions and offsets along the western North American continental margin. Note that this is different than the standard “rock-attached” frame of reference for geologic histories which would track with the rocks in San Francisco today, but would be limited to the history of those rocks. Nor is this a fixed latitude and longitude, as that would require accounting for movement of North America and the opening of the Basin and Range, distracting from the focus on story of plate interaction and continental growth at the margin. The relatively fixed San Francisco point of view allows the reader to imagine the changing geology flowing by with the passing of geologic time.

Rocks Passing Through

Prior to about 150 Ma, the western North American continental margin was a subduction zone located east of San Francisco, roughly at the position of the Melones fault zone in the Sierra Nevada Foothills (Figure 27A), give or take later deformation. At that time, part of the subducting oceanic plate was moving through the

location of San Francisco. As summarized by Graymer (2005), a suite of Permian, Triassic, and Early to Middle Jurassic rocks were accreted to the continental margin in the Middle Jurassic (172–165 Ma), and these rocks would have passed through San Francisco earlier on their way to the subduction zone. At about 165–158 Ma, San Francisco would have been roughly the location of an ocean island arc (Figure 44) formed above an east-dipping oceanic subduction zone outboard of the continental margin subduction zone (Blake et al., 2002).

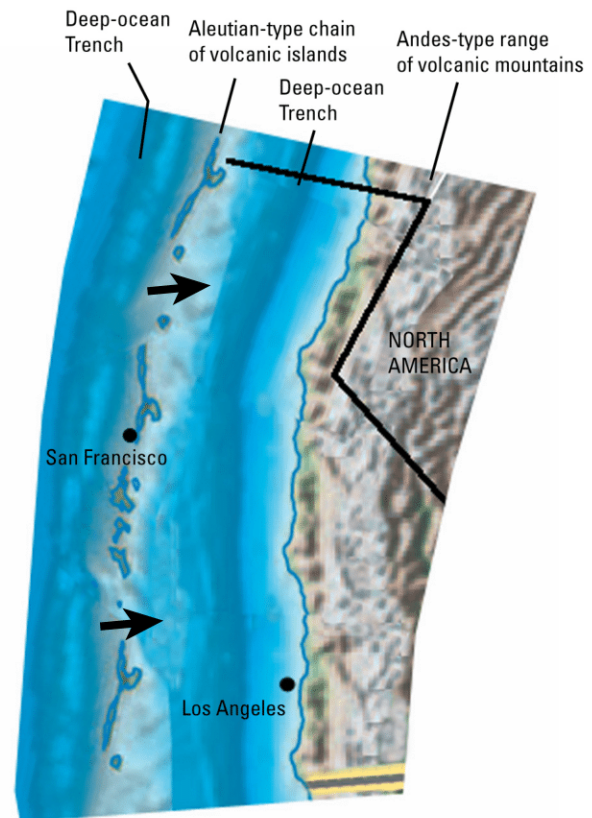


Figure 44. Diagrammatic physical map of part of the Middle Jurassic western North American continental margin and adjacent ocean floor, superimposed with the present day locations of the cities of San Francisco and Los Angeles, along with the California state line (black) and U.S.–Mexico border (yellow and gray). As suggested by the black arrows, in Middle and Late Jurassic time, an island arc moved through the position of San Francisco and was accreted to western North America. The subduction zone related to the trench shown west of San Francisco became the new continental margin. (Graymer et al., 2006b.)

As described above, the Coast Range Ophiolite formed at this time in the oceanic forearc to the west of San

⁴What follows is an interpretive narrative of some aspects of tectonic history of western North America and the oceanic plates to the west of it from the Mesozoic to the Quaternary. There is no scientific consensus on many aspects of that history; thus, much of the narrative touches on ideas that remain controversial, and the story presented conflicts with other published ideas. It would be impossible here to catalog all of the publications that present alternative narratives, but it is important to note that the history described here is that preferred by the author and in no way should be considered the generally accepted view (there is, for most of it, no generally accepted view).

Francisco. The oldest metamorphic ages for high-grade blocks in the Franciscan Complex are of this time frame as well (see the summary of radiometric ages from Franciscan Complex rocks in Ukar et al., 2012), and given the structural position of the blocks beneath and outboard of the Coast Range Ophiolite, this oceanic subduction zone was probably the locus of earliest Franciscan Complex subduction and metamorphism. By roughly 150 Ma, the island arc had moved east from the location of San Francisco to the continental margin subduction zone in the Sierra Nevada Foothills, where accretion of the arc volcanics and associated sedimentary rocks accompanied widespread regional metamorphism (the Nevadan orogeny). The continental margin subduction zone was blocked and abandoned, and the outboard oceanic subduction zone became the new continental margin subduction zone (see Tetreault and Buitter, 2012, for a recent look at the process of island arc accretion and subduction zone reorganization). By that time, plate motion would have moved the Coast Range Ophiolite through San Francisco to the east, and San Francisco would have been located roughly at the trench of the new continental margin subduction zone.

Rocks From Somewhere Else

Almost all the rocks in San Francisco today belong to the Franciscan Complex. As described above, these are a suite of terranes that represent several packages of upper oceanic crust and/or seamount volcanics and overlying pelagic and clastic sedimentary rocks, that have been accreted at the continental subduction margin. Previous authors (e.g., Wahrhaftig, 1984a; 1984b; Murchey and Jones, 1984; Karl, 1984; Murray et al., 1991; Hagstrum and Murchey, 1993) have used paleontological, paleomagnetic, and geochemical observations to describe how the seafloor volcanic rocks formed hundreds or thousands of kilometers away, accumulated pelagic sediments during their tectonic transport toward North America, with those sediments in turn overlain by continentally sourced detrital sediments upon their approach to the continental subduction margin.

Because the graywacke member of each terrane is continentally sourced, its age of deposition should roughly correspond to the timing of a terrane's approach to the continental margin. Unfortunately, fossils are sparse in Franciscan graywacke, so until recently many terranes lacked strong age control. However, detrital zircon studies (e.g., Snow et al., 2010; Wakabayashi, 2013; McPeak, 2015; Dumitru et al., 2016; Apen et al., 2016)

have added significant constraints to the depositional age of the various terranes. Of those Franciscan Complex terranes present today in San Francisco, the Angel Island terrane probably approached the continent first, around 110 Ma. (The very first Central Belt terrane to approach, around 145 Ma, was probably the Cazadero terrane, now in Sonoma County to the north.) Alcatraz and Marin Headland terranes probably approached at around the same time (100 Ma), although differences in sandstone lithology and geochemistry suggest different detrital source areas, so they probably approached different points along the continental margin. Of the Franciscan Central Belt terranes present today in San Francisco, the last to approach was the Bolinas Ridge terrane, about 90 Ma. Other Central Belt terranes, Novato Quarry and Permanente, now to the northeast and south of San Francisco, probably approached a bit later, around 85 Ma. Massive submarine landslides in the trench may have incorporated olistostromes into the graywacke section, locally beginning the process of mixing blocks into sedimentary-matrix *mélange*.

Following their approach to the continental margin, each terrane was subducted (Figure 45), with Angel Island terrane being first and going deepest, as evidenced by its higher grade of metamorphism. Following subduction, a portion of the downgoing oceanic plate was shaved off and added to the base of the overlying continental plate. This created an accretionary prism, with previously accreted Coast Range Ophiolite and subsequently deposited Great Valley Group structurally above the newly accreted Franciscan Complex terranes. During and after subduction and accretion, the terranes underwent metamorphism in the relatively high pressure/low temperature environment of the subduction zone, mostly to prehnite-pumpellyite facies, but to glaucophane-schist (blueschist) facies in the case of Angel Island terrane. Deformation in the subduction zone and between accreted terranes probably started the formation of *mélange* by tectonic mixing as well as shearing up olistostromes.

However, as shown by earlier workers (Murchey and Jones, 1984; Hagstrum and Murchey, 1993) for the Marin Headlands terrane, subduction/accretion of terranes in San Francisco today probably did not take place there, but much farther south. At some time, probably following the subduction/accretion of the youngest Central Belt terranes (Campanian, or 70.6–83.5 Ma), oblique convergence at the plate boundary produced a zone of right-lateral deformation. Large

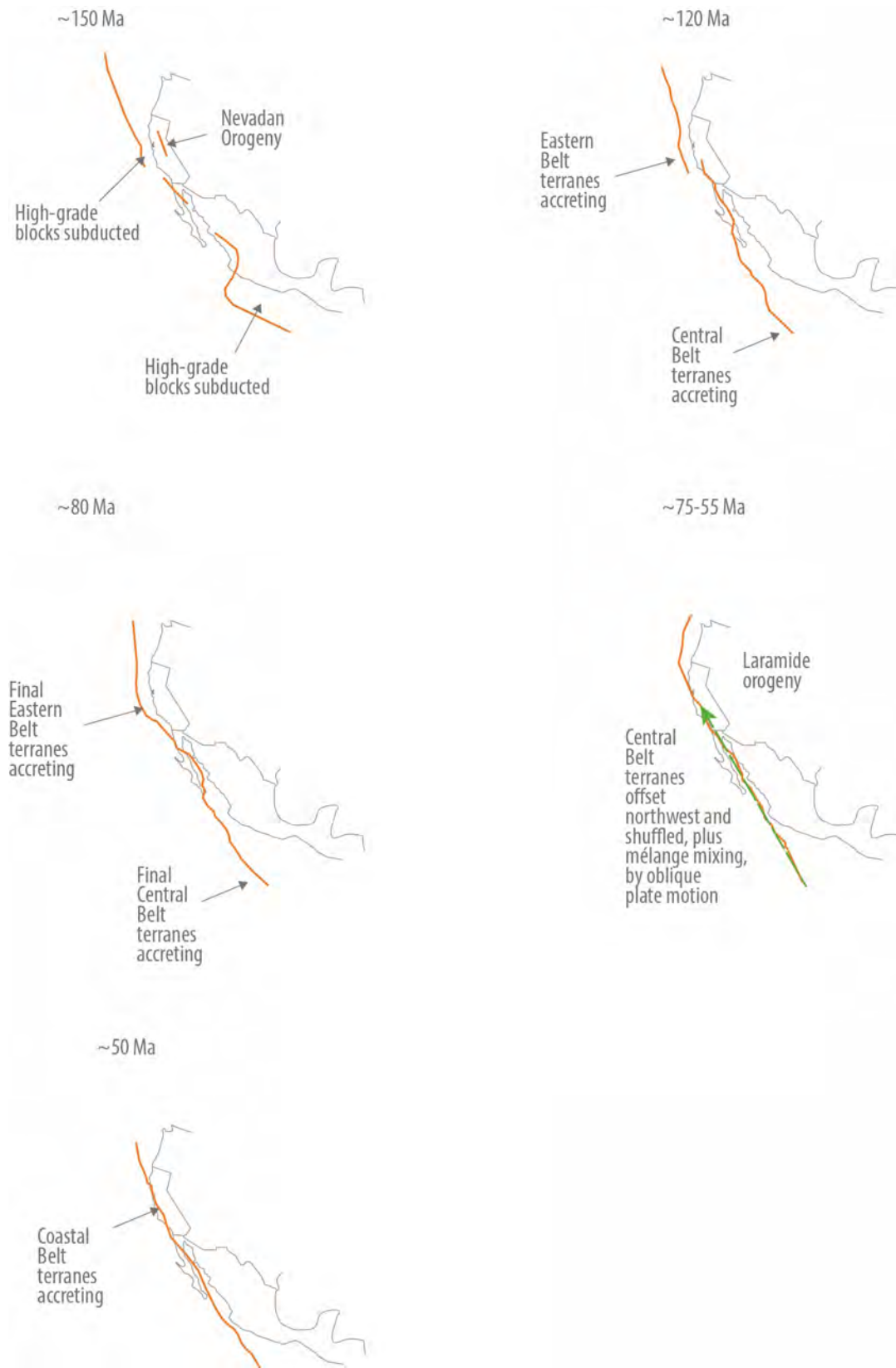


Figure 45. Cartoon maps showing Franciscan Complex terrane accretion and offset relative to present day North America at various times. Paleo subduction zone trenches shown as orange lines. Green arrow along the subduction zone at ~75–55 depicts transpressional transport along the subduction margin of Central Belt terranes.

bodies of Franciscan Complex terranes, together with the overlying Coast Range Ophiolite and Great Valley Group, were sheared from the accretionary prism and transported northward between latest Cretaceous and early Eocene time. These large slabs were further broken and shuffled during transport to form the interleaved coherent bodies and surrounding mélangé characteristic of the Central Belt Franciscan terranes and associated Coast Range Ophiolite and Great Valley Group in the San Francisco region. There are no latest Cretaceous (Maastrichtian) or Paleocene graywackes in the Franciscan Central Belt because of the transition away from subduction/accretion to transpressional offset. The Late Cretaceous and Paleogene period of transpressional offset rather than subduction/accretion is roughly coeval with the start of the Laramide orogeny and associated change in the structure of the subduction zone (Coney, 1976).

Early Eocene time marked the resumption of terrane approach to the continental margin, with San Bruno Mountain terrane graywacke deposition around 52 Ma based on detrital zircon (Snow et al., 2010). About the same time, following uplift and erosion during transpressional offset, Central Belt terranes were unroofed and locally overlain by Eocene strata (today only preserved as the Whiskey Hill Formation in San Mateo County; Pampeyan, 1993). Today, to the north of San Francisco, Coastal Belt terranes underlie Central Belt terranes along an east-dipping low angle (thrust) fault (Jones et al., 1978) that has been modestly deformed by subsequent compressive deformation (folding and reverse faulting). This suggests that in Eocene time, the North American continental margin shifted back from large scale right-lateral offset to subduction/accretion. The Central Belt terranes today in San Francisco stopped their northward voyage, were underplated by the San Bruno Mountain terrane, and were uplifted and locally overlain by shallow marine strata. These rocks were not yet in San Francisco, however.

The final stage in the voyage of the Franciscan rocks to San Francisco involves offset at a transform plate boundary. About 30 Ma, the Pacific plate first encountered the North American margin when a transform-spreading ridge boundary between the Pacific and Farallon plates moved into the subduction zone (Atwater, 1970). As is probably known to all geologists (and many others), subsequent convergent motion of the oceanic plates resulted in two triple junctions, the northward migrating transform/transform/subduction

Mendocino Triple Junction, and the southward migrating transform/spreading/subduction Rivera Triple Junction, connected by a new right-lateral transform plate margin between the North American and Pacific plates. What is less well known is that the transform margin initially occupied the trend of the old subduction margin, not that of the present San Andreas fault system. Because the basement rocks today in San Francisco were east of the new transform margin, they did not experience appreciable offset along it (relative to our Sierra–Great Valley microplate frame of reference). However, about 12 Ma, the transform offset jumped eastward to initiate the present-day San Andreas fault system. The basement rocks today in San Francisco resumed their northward motion, traveling about 175 km (109 miles), from around where Pinnacles National Park is today to their present position.

Geologically speaking, the rocks of San Francisco just got there, and they aren't staying for long. Slip on faults to the east continues at about 2 cm/yr (0.8 in/yr), so that the rocks presently at the southern boundary of San Francisco will have moved north past the northern boundary of the city in just 750,000 years if fault slip continues at the present pace.

Neogene Paleogeography

As Neogene and Quaternary fault offset brought the rocks that are now in San Francisco northward, other changes to the landscape in and around the position of San Francisco were taking place as well, including changing river systems, marine embayments, and volcanic fields. These changes are illustrated in Figure 46 and described below.

Prior to about 12 Ma, the accretionary prism of the Juan de Fuca–North American plate boundary subduction zone was in the position of San Francisco, although actual Neogene accretion probably occurred well to the north. The subduction zone trench was probably just offshore to the west, much as it is off northwestern California today. Between about 10 and 12 Ma, the Mendocino Triple Junction moved northward past the position of San Francisco (Atwater and Stock, 1998). At that time, volcanic activity that followed behind the triple junction (Fox et al., 1985) was initiated about 150 km southeast of the position of San Francisco (Burdell Mountain–Quien Sabe volcanics; Jones and Curtis, 1991; Drinkwater et al., 1992). All the San Andreas fault system offset through the region took place after 12 Ma (Dickinson and Snyder, 1979; Clark

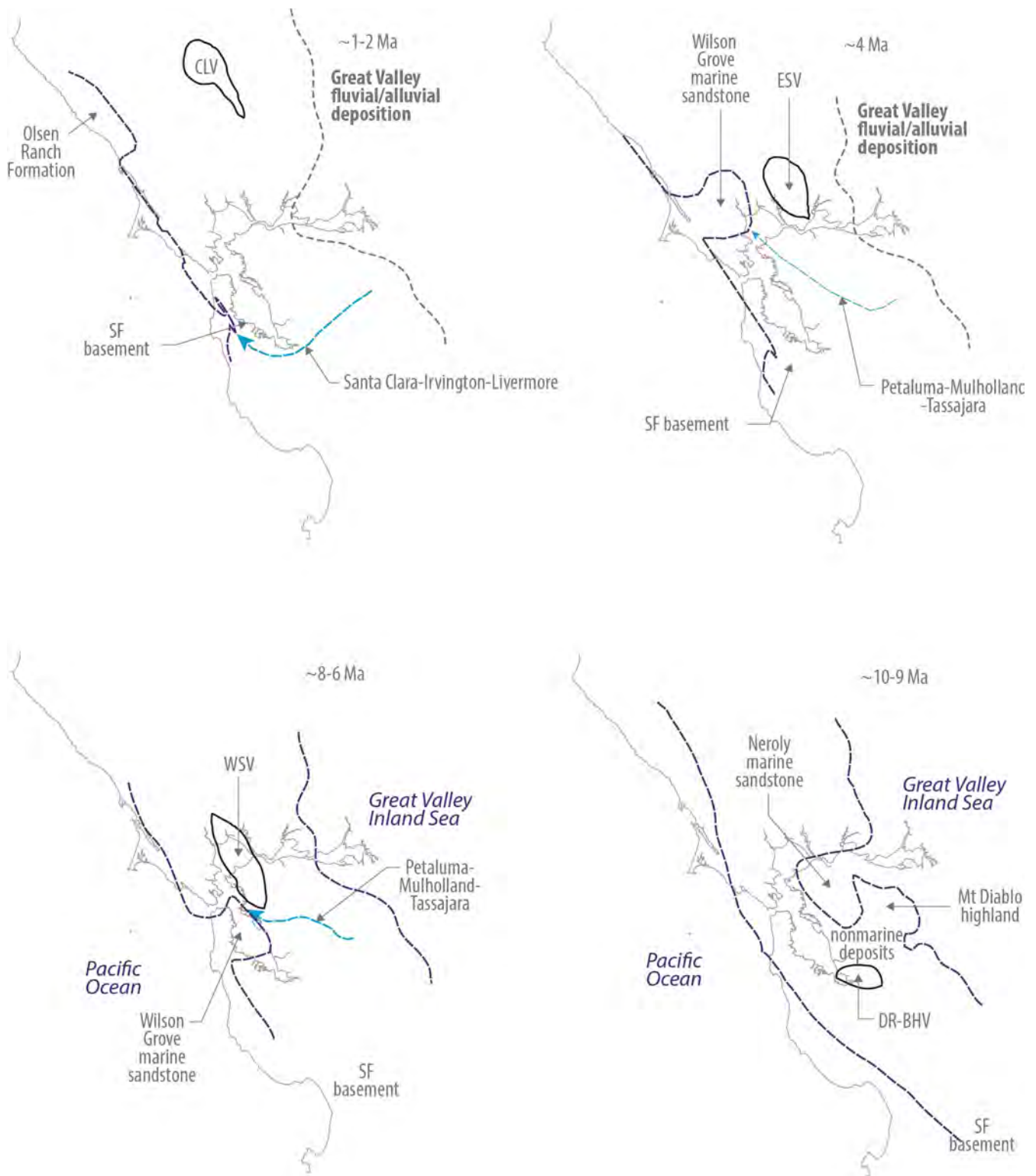


Figure 46. Cartoon palinspastic reconstructions of shorelines (purple dashed lines), major drainages (cyan dashed arrows showing flow direction), volcanic fields (black outlines; CLV=Clear Lake Volcanics; ESV=Eastern Sonoma Volcanics; WSV=Western Sonoma Volcanics, DR-BHV=Donnell Ranch–Berkeley Hills Volcanics), and the location of basement rocks that are in San Francisco today (SF basement), overlain on the present-day shoreline to show relative position. Paleodrainages and embayments are labeled with the name of geologic units formed there. Timing and amount of fault offsets and subdivision of volcanic fields from Graymer et al. (2002); Wagner et al. (2011).

et al., 1984; Graymer et al., 2002). Throughout this time, the position of San Francisco was geographically on an elongate upland separating an inland marine basin (characterized by marine Neroly, Cierbo, and Briones Sandstone deposition) to the east from the Pacific Ocean to the west.

About 9–10 Ma, the geography of the region remained very different than today. There were no major drainages connecting westward to the Pacific. Instead, the region continued to be characterized by a northwest trending upland separating the Pacific Ocean on the west from a shallow inland sea in the Great Valley to the east that is marked in the region by the deposition of the marine Neroly Sandstone. The inland sea joined the Pacific Ocean well to the south, south of the present-day Diablo Range, where marine Santa Margarita Sandstone, coeval with Neroly Sandstone, extends from the Great Valley westward to the San Andreas fault (and beyond, although deposits west of the San Andreas fault have been far offset by slip on the San Andreas fault). The restored distribution of Neroly Sandstone suggests a large westward embayment of the inland sea. Beach deposits in the Neroly on the north flank of Mount Diablo and coeval nonmarine deposits on the southwest flank suggest that there was a large island or peninsula in the embayment around today's mountain. At that time, volcanic activity (Donnell Ranch–Berkeley Hills volcanics; Youngman, 1989) was centered to the southwest of the shallow marine embayment (Graymer et al., 2002). A basement ridge through the position of San Francisco separated the Neroly embayment from the Pacific Ocean.

By about 8 Ma, the western embayment of the inland sea was cut off from the Central Valley, and the Mulholland–Petaluma fluvial/estuarine drainage into the estuarine/marine Wilson Grove Pacific Ocean embayment was established, as described by Liniacki-Laporte and Anderson (1988) and Sarna-Wojcicki (1992). Liniacki-Laporte and Anderson (1988) point out that the lower Mulholland Formation lacks Sierran detritus, so the Central Valley must have emptied well to the south (Woodring et al., 1940), and the Mulholland–Petaluma drainage separated from the great valley by uplands that ran through the location today of Mount Diablo and the Diablo Range. Estuarine strata in the Mulholland Formation indicate that at times the drainage was probably similar to the elongate estuary of the southern San Francisco Bay drainage of today. Between about 8 and 6 Ma,

volcanic activity (western Sonoma Volcanics; Wagner et al., 2011) was centered directly northeast of the fluvial/estuarine drainage, such that volcanic layers are found interfingering with sedimentary layers. The northern part of the Wilson Grove estuarine/marine embayment and the Franciscan, Coast Range Ophiolite, and Great Valley Group basement of its northern shore were in the location of San Francisco at that time.

About 4 Ma, the Mulholland–Petaluma–Wilson Grove drainage was still in place, as paleontologic evidence shows that the units deposited in the nonmarine fluvial system and the marine embayment extend into the early Pliocene (Bartow et al., 1973; Davies, 1986; Powell et al., 2004). However, fault offset on the Hayward and other faults of the East Bay fault system had moved the Wilson Grove embayment northward relative to the location of San Francisco (Sarna-Wojcicki, 1992; Graymer et al., 2002). This drainage system remained cut off from the Great Valley, which by this time had transitioned to a nonmarine depocenter in the area east of the location of San Francisco, based on the age of the Lawlor Tuff at the base of the nonmarine section (Sarna-Wojcicki et al., 2011). There was an active volcanic field (eastern Sonoma Volcanics; Wagner et al., 2011) roughly 20 km to the east of the Wilson Grove marine embayment. The position of San Francisco about 4 Ma was occupied by Franciscan basement uplands that extended as far east as the position today of the Berkeley Hills, forming the western boundary of the Mulholland–Petaluma fluvial/estuarine drainage. The Pacific coast was probably directly west of the position of San Francisco, roughly following the San Andreas fault as it does today north of the city, although the southern part of the Gualala Block was also to the west, and there are no Pliocene strata there, so perhaps it was emergent and lying between the location of San Francisco and the coast. The Salinian granitic basement and the San Gregorio fault were well south of San Francisco at that time.

By about 2 Ma, the Mulholland–Petaluma–Wilson Grove drainage was cut off, and a different drainage to the Pacific was established through the Merced Formation pull-apart basin. The distribution of Pleistocene fluvial deposits (Santa Clara, Irvington, and Livermore) suggests that the fluvial system wrapped around to the southeast from the embayment, then back northeast to Livermore Valley. At that time a large eastward embayment in the coastline was present to the north of the location of San Francisco, as represented by the shallow

marine and estuarine Olsen Ranch Formation (Higgins, 1960; Peck, 1960; Sarna-Wojcicki, 1976). At the same time, an active volcanic field (Clear Lake volcanics; Hearn et al., 1995) was present to the northeast. The position of San Francisco was occupied by Franciscan basement uplands, with a northwest trending Salinian granitic ridge (now Inverness Ridge in Point Reyes National Seashore) just to the west.

About 800,000 years ago, as noted above in the discussion of the Merced Formation, the Great Valley began to drain into the Lake Merced embayment associated with the Merced depocenter. The connection to the Great Valley may have been an eastward extension of the early Pleistocene drainage through the Altamont gap between Mount Diablo and the main Diablo Range, or Great Valley drainage may have been via a new fluvial system roughly following the present Sacramento River drainage into San Francisco Bay.

GEOTECHNICAL AND ENGINEERING GEOLOGY CHARACTERISTICS OF GEOLOGIC UNITS

by Kenneth A. Johnson

Numerous significant site investigation projects have been conducted throughout San Francisco; however, much of the data from these investigations originate from major engineering projects in and around San Francisco that are summarized in a later section of this paper. A great deal of other subsurface data is typically not published or available as much of the work has been done for private landowners or developers. One early publication that attempts to address the challenges of engineering and construction on soft bay margin sediments is the *Geologic and Engineering Aspects of San Francisco Bay Fill* 1969 (California Division of Mines and Geology (CDMG) Special Report 97, 1969). The CDMG report addresses experience in performance of foundations and bay margin sediments from early San Francisco development through the 1960s and also includes some of the earliest work on seismic performance of soft ground around the bay margin.

This section of this publication aims to briefly summarize the geotechnical and engineering characteristics of certain geologic units that have been well investigated. The information is largely drawn from personal experience, and while the intention of this section is to frame the properties of these units, all future projects

should include a thorough site investigation to arrive at appropriate engineering decisions for each specific need.

Artificial Fill

Artificial Fill is widely distributed across San Francisco, but especially in the downtown and South of Market area (See Plate 1). Artificial fill generally consists of very loose to medium dense sand (SP), silty sand (SM), medium stiff sandy clay (CL), categorized using the Unified Soil Classification System. Artificial fill occasionally contains gravels, and locally it typically contains miscellaneous debris (bricks, wood, metal, concrete, glass, crushed rock, etc.). Along the eastern side of San Francisco where over time the coastline has changed considerably due to fill placement, a wide variety of materials were used to reclaim or expand usable land. In many of these areas filling commenced by placing material below sea level and directly on top of Young Bay Mud and/or dune sand. The former Yerba Buena Cove and Mission Creek areas along the eastern shore were places where ships were converted from vessels to stationary structures. After years of fires, and landfill placement, including construction of the San Francisco seawall, portions of these wooden vessels have now become part of the stratigraphy of modern San Francisco.

In addition to the artificial fill placed in the eastern shores of San Francisco, another large area of artificial fill was placed on the northern tip of San Francisco in what is now known as the Marina District. This area was filled to prepare it to host the 1917–1918 Pacific Panama exhibition, where a number of structures were constructed on un-engineered fill. One structure that remains from the Exhibition is the Palace of Fine Arts, an important architectural example from that time period. The primary engineering consequence of extensive fill placement during those times is that these portions of San Francisco are highly susceptible to liquefaction during seismic events. The Marina District in San Francisco experienced significant liquefaction damage during the recent 1989 Loma Prieta earthquake (Seed et al. 1991), even with the epicenter some 88 km (54.6 miles) to the south in the Santa Cruz Mountains.

Eolian Deposits and Dune Sands

As illustrated in Figure 39, dune sand has been mapped over an extensive portion of San Francisco, from the

west coast to the northeastern coast. Typical for dune sands, the deposits generally consist of loose to medium dense, poorly-graded fine to medium grained sand (SP).

Relative densities of the dune sands are typically estimated based on the correlation with the field N-values. In general, the sands are characterized as loose ($N = 4-10$) to medium dense ($N = 10-30$). Following from the typically low relative densities, dune sand deposits are likely to have low shear wave velocities and be subject to settlement and slope deformation during seismic events. In the portions of San Francisco where dune sands occur below the water table or near the coastline, liquefaction potential is expected to be quite high, as shown on California Geological Survey (CGS) seismic hazard maps published on the Association of Bay Area Governments Earthquake Resilience website (<http://resilience.abag.ca.gov/earthquakes/>).

Young Bay Mud

Young Bay Mud is commonly encountered around the margins of San Francisco Bay. Because a great deal of construction and development has been performed in these areas, particularly in San Francisco, the engineering properties of Young Bay Mud have been extensively studied by Trask and Ralston (1951), Mitchell and Bonaparte (1979), and Koutsoftas (1999), for example.

Within San Francisco, Young Bay Mud/Marsh Deposits are typically found in the eastern, and to an extent the northern, parts of the city. Two distinguishing types of Bay Mud are commonly encountered as follows:

- **Soft Clay of Bay Mud:** This type of Young Bay Mud primarily consists of soft, organic-rich clay (CH-OH-MH). The soft clay is generally characterized by high plasticity, high water contents, low density, and lower shear strength.
- **Sandy/Silty Clay and Silty Sand:** In some areas where deposition might have been closer to an onshore environment, the component of silt or sand in the Bay Mud deposits can increase. These deposits primarily consist of soft to medium stiff sandy clay (CL) or medium dense silty sand (SM). Young Bay Mud in these borings generally have low plasticity, low water contents, high density, and higher shear strength. In addition to these coarser grained Bay Mud deposits, thin, generally discontinuous stringers or lenses of fine grained sand have also been observed within this unit.

The Young Bay Mud is considered quite compressible, and thus foundations and infrastructure that encounter this material need to be designed to tolerate the consolidation deformations or, as is more typical, need to be built on pile foundations or drilled shafts that are supported by deeper more dense, less deformable strata.

Colma Foundation

The Colma Formation generally consists of well-bedded, dense to very dense, medium- to fine-grained sand (SP or SM) with interbedded stiff to very stiff clay and sandy clay (CL). The geotechnical and engineering geology characteristics of the Colma Formation are distinct among Quaternary deposits in San Francisco. In particular, its rusty orange color, strength and density make it relatively easy to identify in boreholes and outcrops. Much of the sand and silty sand that comprise the Colma Formation has been slightly cemented with interstitial calcium carbonate.

Index Properties

The Colma Formation is typically a dense to very dense sand or stiff to very stiff clay and sandy clay. Total densities for the Colma Formation commonly range from 17.3 to 22 kN/m³ (110 to 140 pcf). Common field test that supporting this characterization include standard penetration test (SPT) blowcount measurements and the cone penetrometer test (CPT) logs.

- N-values commonly range between 20 and 80, frequently indicating medium dense to very dense sandy soils, with blowcounts of 50 or over.
- Clayey strata within the Colma typically have N-values from 8 to 30 indicating stiff to very stiff clayey soils.
- CPT results for Colma Formation indicate tip resistances from 9.6 to 37.5 MPa/m² (90 to 350 tsf) and sleeve resistances from 0.375 to 1.0 MPa/m² (3.5 to 10 tsf), which confirms that the soils encountered are relatively dense or stiff.

Hydraulic Conductivity

The hydraulic conductivity of the Colma Formation is generally lower than would be expected based on the typically fine to medium grain size of the strata. This probably results from the material in the interstitial space between the sand grains that can contain silt or clay particles, in addition to calcium carbonate cementation and iron oxide precipitation. Hydraulic

conductivity values for the Colma Formation typically range between 1×10^{-5} and 1×10^{-3} cm/s (Johnson, personal communication). While sandy zones at the higher end of the hydraulic conductivity range are common, the overall character of the Colma Formation is that it more often exhibits conductivity values toward the lower end of this range.

General Engineering Practice

The density and general continuity of the Colma Formation in eastern and northern San Francisco have provided excellent foundation-bearing capacity for nearly all the high-rise structures in downtown San Francisco. These foundations have performed well over time and in response to seismic shaking (most notably from the 1989 Loma Prieta earthquake).

The long-standing role of the Colma Formation as a foundation bearing unit is presently changing as a result of increasing building heights, heavier structural systems, and also due to the unsatisfactory performance of the foundation for the building known as the Millennium Tower. This building has settled over 43.2 cm (17 in) and is tilting slightly toward the northwest with a deep foundation partly resting on the Colma Formation and partly on deeper strata of the Yerba Buena Mud/Old Bay Deposits. While the precise cause of the unsatisfactory performance has yet to be determined, as a result of this deformation, newer high-rise buildings are utilizing deep foundations that extend through the Colma Formation and Yerba Buena Mud to rest on the underlying Franciscan Complex Bedrock.

Yerba Buena Mud (Old Bay Deposits)

The Yerba Buena Mud/Old Bay Deposits generally consist of interbedded dense to very dense sand (SP) and silty sand (SM) and stiff to very stiff clay (CL). The sand and clay layers in this unit are generally not continuous laterally or vertically due to the interbedding nature of the fine- and coarse-grained deposits.

Index Properties

Fine-grained strata within the Yerba Buena Mud/Old Bay Deposits generally have Atterberg limits values with liquid limits range from 20 to 85 and plasticity index range from 5 to 56. In situ water contents in this unit are typically close to the lower bound of the plastic limits of the soils, indicating the clayey soils are relatively stiff. Total densities range from 15.7 to 21.2 kN/m³ (100 to 135 pcf).

Relative Density and Consistency

The Yerba Buena Mud/Old Bay Deposits are typically interbedded dense to very dense sand (SP) and silty sand (SM) and stiff to very stiff clay (CL). Field test commonly performed that support this classification are the SPT measurements and the CPT logs, as summarized below:

- N-values for the sandy strata in Yerba Buena Mud/Old Bay Deposits are generally greater than 10, and most range from 30 to 100 or refusal indicating dense to very dense sandy soils.
- For the clayey strata, N-values commonly range from 10 to 60, indicating stiff to hard clayey soils.
- CPT results for Yerba Buena Mud/Old Bay Deposits indicate tip resistances range from 19.8 to 38.6 MPa/m² (185 to 360 tsf) and sleeve resistances from 0.6 to 0.86 MPa/m² (6 to 8 tsf), which confirms that the soils encountered are relatively dense or stiff.

Hydraulic Conductivity

The hydraulic conductivity of Yerba Buena Mud/Old Bay Deposits strata will depend on the textural variations in the strata (i.e., sand or clay). While the overall depositional setting for the Yerba Buena Mud/Old Bay Deposits was a marine environment resulting in predominantly fine-grained deposits, significant yet discontinuous lenses of sandy material are quite common. As such, the sandy horizons generally exhibit hydraulic conductivity values between 6×10^{-4} and 2×10^{-3} cm/s (Johnson, personal communication). These values are relatively large; however the limited extent of these lenses cause the overall hydraulic conductivity of the deposit to be dominated mostly by the clayey strata where the hydraulic conductivity is typically lower, with values ranging between of 10^{-7} and 10^{-5} cm/s (Johnson, personal communication).

Franciscan Complex Rocks

As described earlier, the bedrock underlying San Francisco is almost exclusively comprised of rocks of the Franciscan Complex. Rock types can vary widely, but the predominant rocks include chert, sandstone, shale, metasedimentary rocks, basalt, serpentinite and mélange. The structure and fracture characteristics of these rock types is also quite variable even while comprising many of San Francisco's famous hills.

Quarries

During San Francisco's early years, many of the rock outcrops on hills were quarried and supplied rock fill and aggregate for construction projects around the city. The remnants of some of these quarries still exist where steep rock slopes are exposed, for example on the north and east sides of Telegraph Hill (Figure 16), where the infamous Gray Brothers operated. Quarries were also located in the Diamond Heights area and along the north side of what is now Corona Heights Park (Figure 15), among others.

Much of the rock quarried provided excellent construction material and fill. Construction of the San Francisco seawall that formally established the northeastern and eastern San Francisco waterfront was constructed with large volumes of rock fill from quarries owned by the Gray Brothers.

On the other hand, as concrete became a more popular choice for construction, it became apparent that certain aggregates from certain quarries were not compatible with cement mixes used. This was primarily due to the presence of opal-family minerals in the chert rocks along the Diamond Heights region of San Francisco, which had deleterious effects in concrete products it was mixed with.

Rock Falls and Slope Stability

With the growth of San Francisco in the late 20th century, scarcity of open land caused development to move nearer and on top of some of the rock outcrops in the city. Rock slopes around Telegraph Hill, in particular, are some of the steepest and most susceptible to rock falls and instability. Even in recent years, these slopes have been the source of rockfalls that have impacted structures and businesses along Sansome Street, Broadway, and eastern Chestnut and Lombard Streets, where quarried slopes are adjacent to relatively new structures. An excellent discussion of the failure mechanisms and stabilization measures is presented in Wallace and Marcum (2015).

As property prices have continued to increase in San Francisco and available space to build has diminished, more and more structures are being built on steeper rock slopes. For these locations, it is essential to perform detailed engineering geologic analysis of the rock quality, discontinuity structure, and slope stability. Rock types need to be identified and rock mass prop-

erties need to be quantified. Such studies are critical to identify and mitigate risks to the project and adjacent properties connected to development.

GEOLOGIC ASPECTS OF NATURAL HAZARDS

by Keith L. Knudsen

Earthquake Hazards

San Francisco lies within the San Andreas fault system, which accommodates a significant fraction of the tectonic motion between the Pacific and North American plates. Although active faults of the San Andreas fault system do not transect city boundaries, the inexorable slip on these nearby faults will cause future large earthquakes that will shake San Francisco and produce strong ground motions damaging to the city's built environment. The shaking caused by these earthquakes will also induce liquefaction and landslides, with the most extensive ground failure likely to be caused by liquefaction around the margins of the city.

Historical seismicity, active fault maps, paleoseismic studies, and regional hazard assessments all indicate that nearby faults will host large earthquakes and that San Franciscans should expect to experience strong ground shaking from future large earthquakes. Such ground shaking will damage buildings, lifelines, and other infrastructure, and cause economic losses and fatalities. A number of historic earthquakes are testament to the damaging effects of seismic slip on nearby faults. The 1906 earthquake and others are described in sections below.

In the 1980s, groups of experts began to make use of historical seismicity data (similar to those in Figure 47 and Table 2), paleoseismological data (constraining estimates of prehistoric earthquake timing and rupture extent), and fault slip-rate data (Table 3), to produce earthquake rupture forecasts in which the likelihood and magnitude of future earthquakes is estimated (e.g., Figure 48). The first of these statewide forecasts, with estimates of earthquake magnitudes and recurrence time for individual faults, was released in 1988 by the Working Group on California Earthquake Probabilities. The most recent probabilistic earthquake rupture forecasts, shown in Figure 48, were developed and published in UCERF3, the Third Uniform California Earthquake Rupture Forecast (WGCEP, 2013; Field et

al. 2013) and summarized in a U.S. Geological Survey (USGS) Fact Sheet by Aagaard et al. (2016). UCERF3 studies concluded that there is a 72% chance of at least one $M \geq 6.7$ earthquake striking the San Francisco Bay Area over the 30-year time period 2014–2043. The San Andreas fault (22%) and the Hayward–Rodgers Creek fault (33%) are the most likely to produce a large earthquake damaging to San Francisco over this time. Although the methodology used in producing the most recent statewide rupture forecast is new and different from prior approaches, the aggregated rupture forecasts for the Bay Area (e.g., 72%) have not changed considerably over the last couple of Working Group cycles.

The earthquake rupture forecasts are used to produce probabilistic hazard maps, which provide estimates of the intensity of future ground shaking when all seismic sources that might affect an area or site are considered. Separate estimates are calculated for various frequencies of ground motion and for a range of return periods, for all of California. Such maps are referenced by building codes. Figure 49 is an example ground shaking hazard curve calculated for a site near the west end of the Bay Bridge. This site was assumed to be a soft soil site (having a representative shear wave velocity in the top 30 m (100 ft) (V_{S30}) of 180 m/s), and the calculations for a return period of 2,475 years (2% chance of exceedance in 50 years) can be obtained at the USGS website (see <https://earthquake.usgs.gov/hazards/>). For this location, a peak ground acceleration on the order of about 1.3g is shown in Figure 49 for the 2,475-year return period. The USGS hazards website also provides deaggregated hazard results, so that one can identify the seismic sources that contribute most to the hazard at any site of interest. For the site at the west end of the Bay Bridge, the controlling seismic sources are the San Andreas fault and the Hayward fault, with minor contributions from the San Gregorio fault.

Within the confines of the City and County of San Francisco, surface rupture from faulting is not likely, as active faults have not been mapped or identified within San Francisco’s boundaries and the State’s Official Maps of Alquist-Priolo Earthquake Fault Zones do not include areas in San Francisco. However, possible Holocene activity has been described by Hengesh et al. (1996, 2004) and Kennedy (2004) along the Serra Fault, which crosses the southwestern corner of the city. If the Serra Fault does rupture to the ground surface, it may do so only during large earthquakes on the nearby

San Andreas fault. Those faults within the San Andreas fault system that are likely to produce strong ground shaking that damages San Francisco are described below, along with historic earthquakes that have occurred along these faults and produced significant shaking in San Francisco. Other faults shown in Figure 48 (e.g., Green Valley/Concord fault) will not shake the city as intensely due to their greater distance from San Francisco, and thus are not described here.

San Andreas Fault

The San Andreas fault extends from the Gulf of California, Mexico, to Cape Mendocino on the Mendocino Coast in northern California, a distance of about 1,200 km (745 miles). The San Andreas fault system forms the boundary that separates the North American tectonic plate from the Pacific plate. In the San Francisco region, the North American Plate consists mainly of Franciscan Complex, Coast Range Ophiolite, and Great Valley Group basement. The Pacific Plate in the region is mostly granitic rock and associated metamorphic rocks, with fault slivers of other rock types. See the “Geologic Overview of the San Francisco Bay Region” section for more details.

The San Andreas fault system accommodates the majority of the motion between the Pacific and North American plates, about 41 mm/yr (DeMets et al., 1994), or a rate similar to the rate at which our fingernails grow. Movement on the San Andreas fault system has accumulated a total of about 475–490 km of right-lateral offset in the Neogene (Hill and Dibblee, 1953; Matthews, 1976; Clark et al., 1984; Jachens et al., 1998). See the “Geologic Overview of the San Francisco Bay Region” section for more details. The San Andreas fault is responsible for the largest known earthquake in northern California, the 1906 M 7.9 San Francisco earthquake (Wallace, 1990). The San Andreas fault is located on land for most of its length, but lies just offshore where it passes San Francisco; it intersects the coast south of the southwestern border of San Francisco.

In northern California, the San Andreas fault is clearly delineated, striking northwest, parallel to the vector of plate motion between the Pacific and North American plates. Over most of its extent in central California, the San Andreas fault is a relatively simple, linear fault trace (e.g., Wallace, 1990). Across the San Francisco Bay Area, however, the fault splits into a number of branch faults or splays.

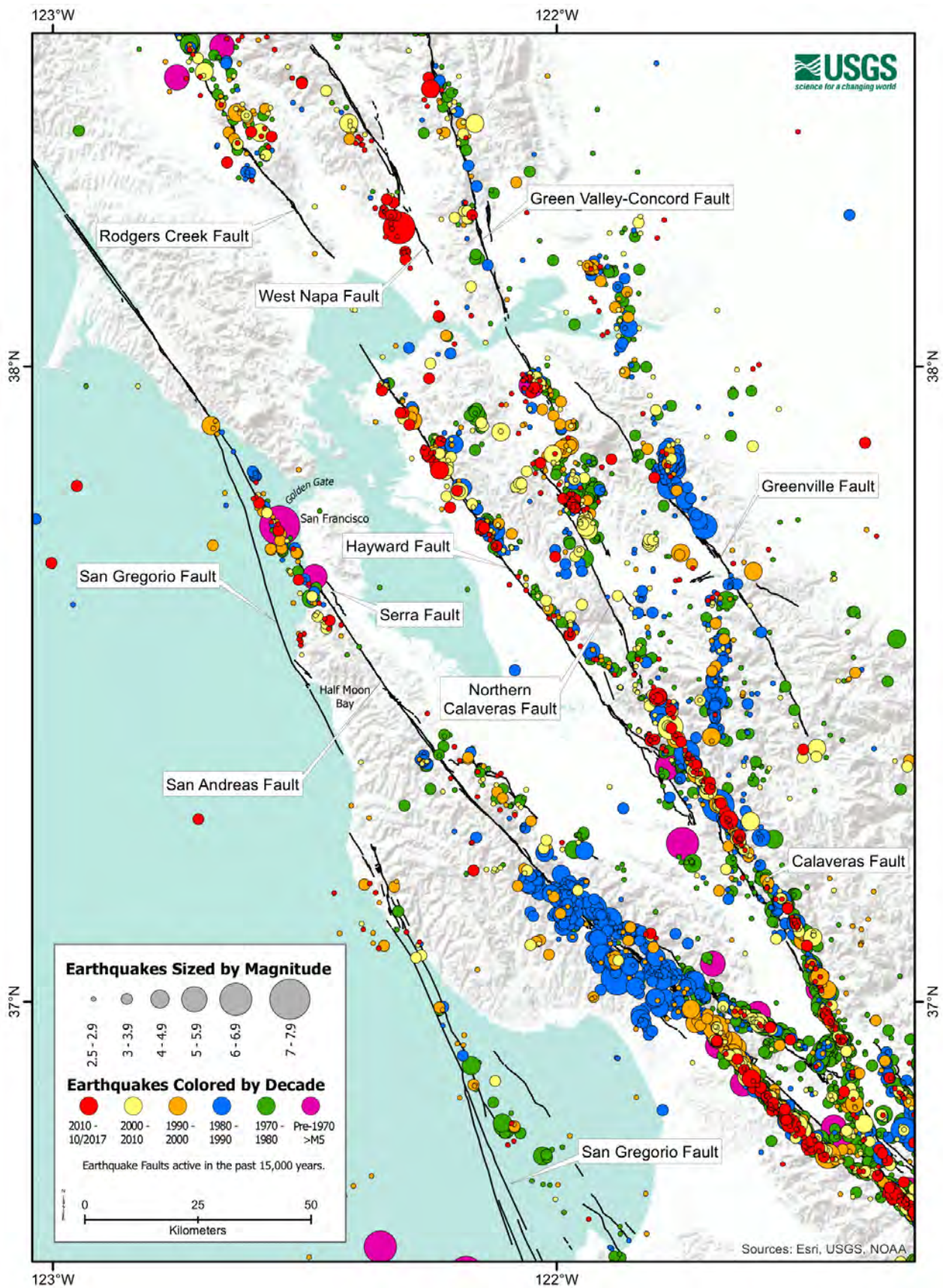


Figure 47. Map of historical ($M > 2.5$) seismicity from the Northern California Earthquake Data Center (NCEDC, 2014) catalogue, with known active faults of the San Francisco Bay Area (from USGS Quaternary fault and fold database; <https://earthquake.usgs.gov/hazards/qfaults/>).

Table 2. M>5 Earthquakes in the area shown on Figure 47 from the Advanced National Seismic System catalogue (1906–present).

| DateTime (UTC) | Latitude | Longitude | Depth (km) | Magnitude | Magnitude Type | Source | Event ID |
|---------------------------|-----------------|------------------|-------------------|------------------|-----------------------|---------------|-----------------|
| 1906/04/18 | 37.75 | -122.55 | | 7.9 | | | |
| 1911/07/01 22:00:00 | 37.25 | -121.75 | | 6.6 | Unk | BK | |
| 1949/03/09 12:28:39 | 37.02 | -121.48 | | 5.2 | ML | BK | |
| 1951/07/29 10:53:45 | 36.58 | -121.18 | | 5 | ML | BK | |
| 1954/04/25 20:33:28 | 36.93 | -121.68 | | 5.3 | ML | BK | |
| 1955/09/05 02:01:18 | 37.37 | -121.78 | | 5.5 | ML | BK | |
| 1955/10/24 04:10:44 | 37.97 | -122.05 | | 5.4 | ML | BK | |
| 1957/03/22 19:44:21 | 37.67 | -122.48 | | 5.3 | ML | BK | |
| 1959/03/02 23:27:17 | 36.98 | -121.6 | | 5.3 | ML | BK | |
| 1960/01/20 03:25:53 | 36.78 | -121.43 | | 5 | ML | BK | |
| 1961/04/09 07:23:16 | 36.68 | -121.3 | | 5.6 | ML | BK | |
| 1961/04/09 07:25:41 | 36.7 | -121.3 | | 5.5 | ML | BK | |
| 1963/09/14 19:46:17.00 | 36.87 | -121.63 | | 5.4 | ML | BK | |
| 1964/11/16 02:46:41.70 | 37.06 | -121.69 | | 5 | ML | BK | |
| 1969/10/02 04:56:45.30 | 38.4978 | -122.664 | 0.15 | 5.6 | ML | NC | 1003129 |
| 1969/10/02 06:19:56.39 | 38.45 | -122.7535 | 5.04 | 5.7 | ML | NC | 1003132 |
| 1972/02/24 15:56:50.99 | 36.5903 | -121.1905 | 3.87 | 5.1 | ML | NC | 1009257 |
| 1974/11/28 23:01:24.59 | 36.9202 | -121.4673 | 5.34 | 5.2 | ML | NC | 1021949 |
| 1979/08/06 17:05:22.93 | 37.1038 | -121.5123 | 8.31 | 5.8 | ML | NC | 1046962 |

SAN FRANCISCO – GEOLOGY OF THE CITIES OF THE WORLD

| | | | | | | | |
|---------------------------|---------|-----------|-------|------|-----|----|----------|
| 1980/01/24 19:00:08.58 | 37.84 | -121.7678 | 14.49 | 5.8 | ML | NC | 1050040 |
| 1980/01/24 19:01:01.54 | 37.811 | -121.775 | 6.52 | 5.1 | ML | NC | 1050041 |
| 1980/01/27 02:33:35.34 | 37.749 | -121.7063 | 14.17 | 5.4 | ML | NC | 1050437 |
| 1984/04/24 21:15:18.76 | 37.3097 | -121.6788 | 8.19 | 6.2 | ML | NC | 17204 |
| 1986/01/26 19:20:50.95 | 36.8043 | -121.285 | 8.15 | 5.5 | ML | NC | 64626 |
| 1986/03/31 11:55:39.81 | 37.4792 | -121.6867 | 8.5 | 5.7 | ML | NC | 68932 |
| 1988/02/20 08:39:57.26 | 36.7958 | -121.3112 | 9.18 | 5.1 | ML | NC | 10086194 |
| 1988/06/13 01:45:36.53 | 37.3927 | -121.7415 | 9.09 | 5.3 | ML | NC | 10087352 |
| 1988/06/27 18:43:22.33 | 37.1283 | -121.895 | 12.63 | 5.3 | ML | NC | 10139668 |
| 1989/08/08 08:13:27.39 | 37.1482 | -121.9268 | 13.41 | 5.4 | ML | NC | 10089897 |
| 1989/10/18 00:04:15.19 | 37.0362 | -121.8798 | 17.21 | 6.9 | Unk | NC | 216859 |
| 1989/10/18 00:41:23.77 | 37.1902 | -122.052 | 15.31 | 5.1 | ML | NC | 10090725 |
| 1990/04/18 13:53:51.30 | 36.9323 | -121.6568 | 5.49 | 5.4 | ML | NC | 20091154 |
| 1990/04/18 15:46:03.45 | 36.9588 | -121.6845 | 6.64 | 5.1 | ML | NC | 20091155 |
| 1998/08/12 14:10:25.14 | 36.7545 | -121.4615 | 8.82 | 5.1 | Mw | NC | 30190473 |
| 2007/10/31 03:04:54.81 | 37.4335 | -121.7743 | 9.74 | 5.45 | Mw | NC | 40204628 |
| 2014/08/24 10:20:44.07 | 38.2152 | -122.3123 | 11.12 | 6.02 | Mw | NC | 72282711 |

Notes:

NCEDC (2014), Northern California Earthquake Data Center. UC Berkeley Seismological Laboratory. Dataset. doi:10.7932/NCEDC
 Origin time of the earthquake in Coordinated Universal Time (UTC) in the format hh:mm:ss.ss, where hh is the hour, mm is the minute, and ss.ss is the second. UTC is 8 hours ahead of PST and 7 hours ahead of PDT
 Depths not provided for earthquakes before 1969

Magnitude type: UNK—unknown; ML—local magnitude; Mw—moment magnitude
 (see <https://earthquake.usgs.gov/learn/glossary/?term=magnitude>)

Source or Network Code: BK—UC Berkeley; NC—Northern California

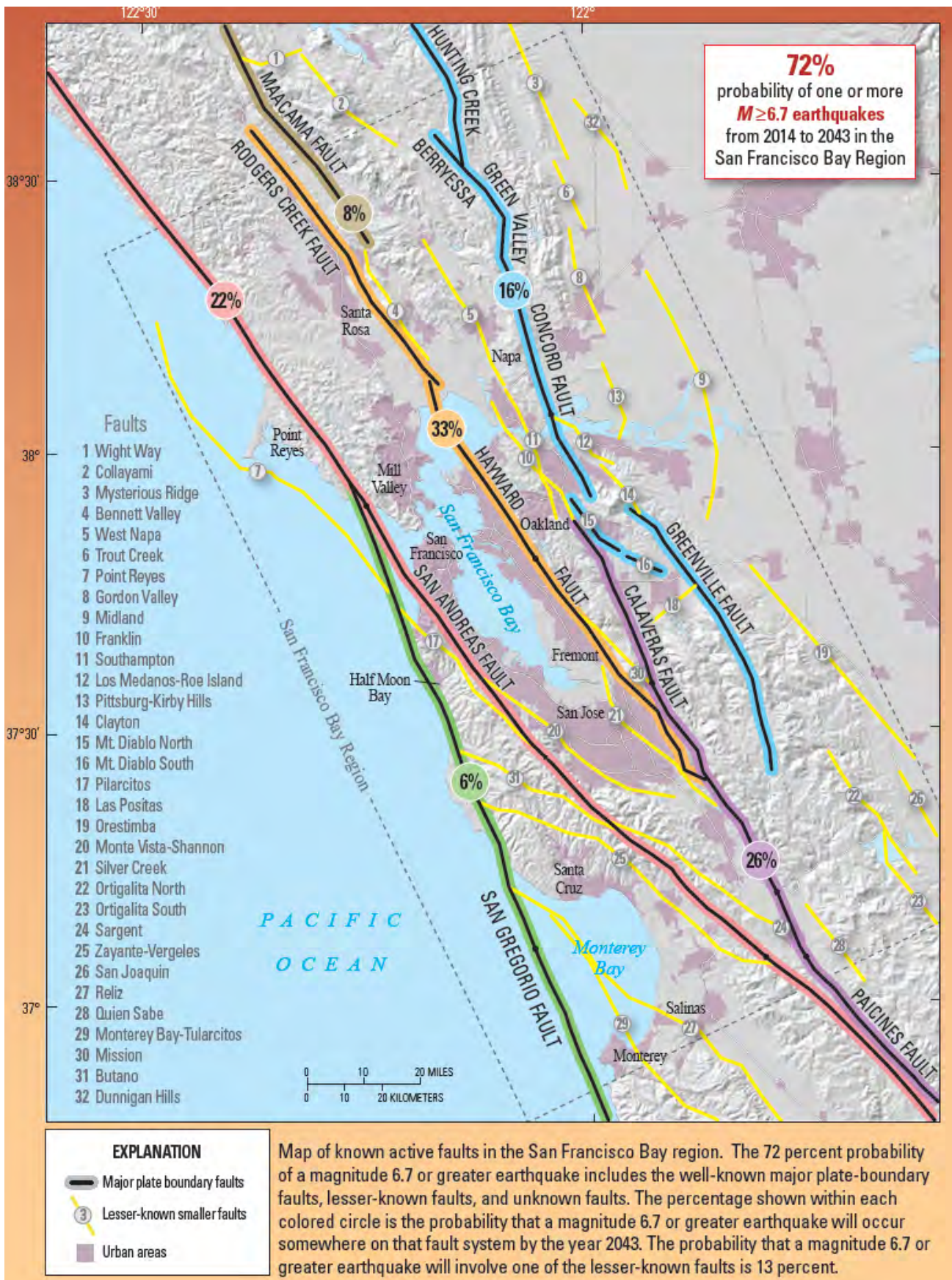


Figure 48. Map of active faults in the San Francisco Bay area, with probabilities that a $M \geq 6.7$ earthquake will occur along each major fault over the 30-year time period 2014–2043 (Aagaard et al., 2016).

Table 3. Major Quaternary active faults in the San Francisco Bay Area (slip rates and calculated recurrence intervals from UCERF3; Field et al., 2013).

| Fault Name | Slip rate in mm/yr; Range (best estimate) | Mean recurrence interval (yrs) for $M \geq 6.7$ |
|------------------------------------|--|--|
| Bartlett Springs | 1.0–9.0 (4.0) | 386 |
| Calaveras (north) | 3–8 (6.0) | 482 |
| Calaveras (central) | 9–20 (15) | 191 |
| Concord | 3–9 (4.3) | 1,220 |
| Green Valley | 2–9 (4.0) | 610 |
| Greenville (north) | 1–5 (3.0) | 648 |
| Greenville (south) | 1–5 (3.0) | 1090 |
| Hayward (north) | 7–11 (9.0) | 243 |
| Hayward (south) | 7–11 (9.0) | 168 |
| Rodgers Creek | 6–11 (9.0) | 309 |
| San Andreas (north coast) | 16–27 (24) | 160 |
| San Andreas (Peninsula) | 13–21 (17.0) | 210 |
| San Andreas (Santa Cruz Mountains) | 13–21 (17) | 143 |
| San Gregorio (north) | 4–10 (7) | 481 |
| West Napa | 1–5 (1) | 151 |

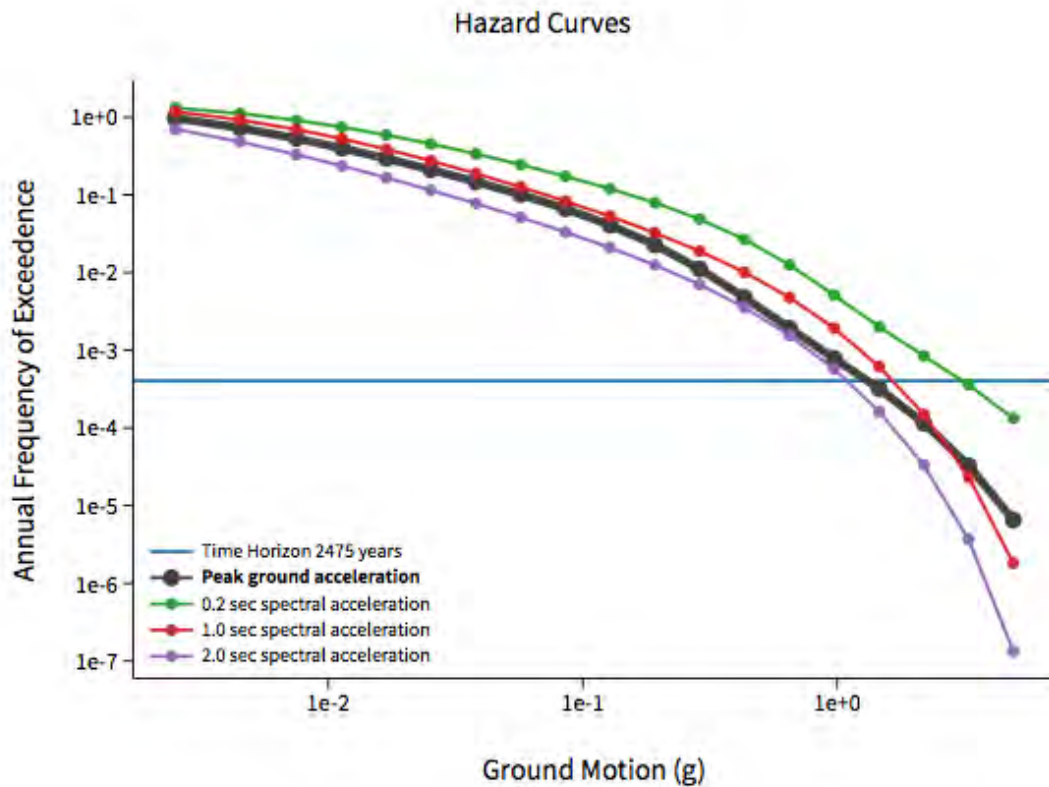


Figure 49. Shaking hazard curve for a site near the western end of the Bay Bridge. Plot is for a site with a V_{S30} of 180 m/s (site class D/E boundary). Horizontal blue line is for a 2% in 50 years chance of exceedance (2,475 year return period). Data and curves from <https://earthquake.usgs.gov/hazards/>.

These include the Calaveras fault and the Hayward–Rodgers Creek faults (Figure 47). In the San Francisco Bay Area, the main trace of the San Andreas fault forms a linear depression along the San Francisco Peninsula, occupied by the Crystal Springs and San Andreas Lake Reservoirs. Geomorphic evidence for Holocene faulting along the peninsula includes fault scarps in Holocene deposits, right-laterally offset streams, shutter ridges, and closed linear depressions (Wallace, 1990).

Based on differences in geomorphic expression, fault trace geometry, paleoseismic history, slip rate, seismicity patterns, and historical fault ruptures, the San Andreas fault has been divided into a number of fault segments. Each of these segments may be capable of rupturing independently or in conjunction with adjacent segments. In the San Francisco Bay Area, these segments include the North Coast, Peninsula, and Santa Cruz Mountain segments. The lengths of the fault segments imply that they are capable of earthquakes of $M \sim 7.45$, 7.15, and 7.0, respectively (WGCEP, 2003). The 1906 earthquake ruptured the Offshore (northernmost segment north of Point Arena), North Coast, Peninsula, and Santa Cruz Mountains segments. Two- or three-segment ruptures may also be possible (WGCEP, 2003), and a main difference between the most recent rupture model (WGCEP, 2013) and earlier ones is the relaxation of the fault segmentation concept, with more throughgoing ruptures incorporated into the model. Based on geodetic, geologic and paleoseismic data constraints, the fault slip rate for the San Andreas fault south of the Golden Gate is 14–24 mm/yr, with a preferred value of 17 mm/yr (Hall et al., 1999). North of the Golden Gate, the slip rate increases to 24 ± 5 mm/yr (Pease and Hall, 1992). Investigations by Niemi (2002) indicated that the repeat time for large earthquakes on the North Coast segment is likely less than 200–250 years. UCERF3 (WGCEP, 2013) assigned a mean recurrence interval of 143 to 210 years for M 6.7 earthquakes for different parts of the northern San Andreas fault (Table 3). They estimated a 22% probability of occurrence for a M 6.7 or larger earthquake on the San Andreas fault in northern California in the time period 2014 to 2043 (Figure 48).

1906 San Francisco Earthquake

At 5:12 a.m. local time on April 18, 1906, a M 7.9 earthquake ruptured the San Andreas fault and shook much of northern California. The epicenter of the earthquake was west and offshore of San Francisco

(Figure 47), and rupture propagated away from the epicenter in two directions (bilaterally) along the San Andreas fault (e.g., Boore, 1997; Lomax, 2005). The earthquake resulted in a fault rupture that extended from San Juan Bautista north to Cape Mendocino, approximately 475 km (295 miles) (Dengler, 2008). The average slip on the fault was 5.1 m (16.7 ft) north of the Golden Gate and 2.5 m (8.2 ft) along the San Francisco Peninsula and Santa Cruz Mountains, yielding an average slip for the entire rupture of 4.1 m (13.5 ft) based on geodetic modeling (Thatcher, 1975; Thatcher et al., 1997; Song et al., 2008). Strong shaking from the 1906 earthquake lasted from 45 to 60 seconds. For more information about the damage caused by the earthquake and the three days of fire that followed, see “The 1906 Earthquake” in the “History and Founding” section above.

Effects of the 1906 earthquake have been extensively documented in many publications, with the post-earthquake report by Lawson et al. (1908) being the most extensive and comprehensive. Ground surface displacement measurements and other data from the earthquake led Reid (1910) to formulate his elastic rebound theory, which is still the basis for our understanding of the “earthquake cycle” today. To explain the paucity of earthquakes in the area since 1906, Ellsworth et al. (1981) described a cycle in which quiescence follows large earthquakes, owing to stress relief (or stress “shadow”) in the region surrounding the causative fault. There were many more large Bay Area earthquakes in the decades leading up to the 1906 earthquake than there have been since 1906 (e.g., Ellsworth et al. 1981; Working Group on California Earthquake Probabilities, 2003; Schwartz et al., 2014).

1957 Daly City Earthquake

The Daly City earthquake, M 5.3, struck on March 22, 1957. It was the largest to be felt on the San Francisco Peninsula since the 1906 earthquake, although it was superseded in 1989 by the Loma Prieta earthquake (Figure 47). The epicenter of this 1957 event was near Mussel Rock (Oakeshott, 1959), where the San Andreas fault intersects the Pacific Ocean shoreline. Damage associated with this earthquake was minor, mainly restricted to nonstructural components of buildings. Bonilla (1959) described coseismic ground failure in the form of minor landsliding and liquefaction but found no evidence of fault surface rupture.

1989 Loma Prieta Earthquake

At 5:04:15 p.m. local time on October 17, 1989, a M 6.9 earthquake was felt throughout the San Francisco, Santa Cruz, and Monterey Bay regions. It is perhaps best known by those outside of California as the earthquake that interrupted the 1989 World Series between the San Francisco Giants and the Oakland Athletics. The earthquake's epicenter was near Loma Prieta Peak in the Santa Cruz Mountains, approximately 14 km (8.7 miles) northeast of Santa Cruz and about 100 km (62 miles) south of San Francisco. Strong shaking from the Loma Prieta earthquake lasted only about 6 to 15 seconds (Spudich, 1996), but the earthquake caused 63 deaths and about \$6 billion in direct losses. Two-thirds of the deaths occurred in the collapse of the Cypress Structure freeway in Oakland. A simple early earthquake warning system was deployed to warn rescuers working on the collapsed Cypress Structure of aftershocks (Bakun et al., 1994). Damage occurred at some distance from the epicenter (e.g., Cypress structure, the Bay Bridge, Oakland Airport, and the Marina District), reinforcing the concern that damage can occur at large distances from an earthquake's epicenter. This earthquake also underscored the effect of local geology on shaking intensity, with many observations of the amplification effects of soft soils on strong ground motion. This phenomenon was first documented following the 1906 earthquake (Lawson et al., 1908). The Loma Prieta earthquake stimulated studies of fault interaction and stress changes caused by earthquakes in general. Shortly after the earthquake, the State of California's Seismic Hazard Mapping Act was put into place by the state legislature.

A series of four U.S. Geological Survey Professional Papers (1550–1553), each with multiple chapters, was published describing the earthquake and its impacts. Numerous journal articles have also been published on this earthquake. One of the interesting questions debated in the literature is whether the 1989 earthquake was caused by the main San Andreas fault, or a nearby related, dipping fault. Part of this discussion was focused on a set of disparate surface features that were formed at the time of the 1989 earthquake, as some of these scarps and other features were also active in the 1906 earthquake (e.g., Cotton et al., 1990; Ponti and Wells, 1991; Prentice and Ponti, 1996; Prentice and Schwartz, 1991; Johnson and Fleming, 1993). Some authors interpreted geodetic data, three-dimensional mapping of earthquake hypocenters (mainshock and

aftershocks), and strong motion data as indications that a dipping fault, not associated with the surface trace of the San Andreas fault, was the earthquake's causative structure (e.g., Segall and Lisowski, 1990; Beroza, 1996). Spudich (1996) argued that the controversy over rupture location from different geodetic and seismic data analyses has been resolved with the availability of more recent geodetic data and analyses, with the conclusion that the rupture was deeper than early geodetic models showed. Recent reexamination of aftershock data, active seismic experiment data, and magnetic data by Zhang et al. (2018) addresses the question of geometry of the causative fault, and concludes that the San Andreas fault was responsible for this earthquake, as it changes to a shallower dip below the upper crust (i.e., the fault dips more steeply near the surface). Hanks and Krauwinkler (1991), in their introduction to a special issue of the Bulletin of the Seismological Society of America on the Loma Prieta earthquake, wrote that much work remains to be done integrating multiple data sets to form a robust depiction of the earthquake. This may remain true, about 27 years later.

Hayward–Rodgers Creek Fault

The Hayward fault extends on land for about 100 km (62 miles) from east of San Jose to Point Pinole on San Pablo Bay (Figure 47 and Figure 48). At Point Pinole, the Hayward fault continues beneath San Pablo Bay, and then connects with the Rodgers Creek fault. Recent studies by Watt et al. (2016) suggest that the two faults are connected at depth, and provide evidence of Holocene deformation along the connecting structure beneath the bay. The southern end of the Hayward fault has recently been shown to be more directly linked to the Calaveras fault than previously thought (Chaussard et al., 2015). The most recent major earthquake on the Hayward fault, in October 1868 (described below), occurred along the southern part of the fault (Figure 47).

As well as slipping during earthquakes, the Hayward fault also slips by aseismic creep between large earthquakes. Systematic right-lateral geomorphic offsets and creep offset of cultural features have been well documented along the entire length of the fault (e.g., Lienkaemper, 1992, 2006). Measurements along the fault over the last two decades indicate a creep rate of 5–9 mm/yr (Lienkaemper and Galehouse, 1997; McFarland et al., 2009; McFarland et al., 2016). Lienkaemper

et al. (2012) argued that the aseismic creep serves to reduce the magnitude and increase recurrence time of expected large earthquakes. Other models have been proposed for the distribution of creep along the fault (e.g., Schmidt et al., 2005; Shirzaei and Burgmann, 2013) with each model yielding different future hazard estimates. The effect of creep on potential earthquake magnitude has been incorporated into rupture forecasts for the Hayward fault by the Working Groups on California Earthquake Probabilities.

Studies by Lienkaemper et al. (2010) document 12 earthquakes on the southern Hayward fault since about 91 A.D., yielding an average recurrence interval of 161 +/- 65 years. Paleoseismic trenching along the northern Hayward fault indicates that the last surface-rupturing earthquake along this part of the fault was in the late 1600s to early 1700s (Lienkaemper et al., 1999; Schwartz et al., 2014). A study by Lienkaemper et al. (1999) also documented at least four surface-rupturing earthquakes in the last ~2,250 years for the northern part of the fault. UCERF3 calculated recurrence intervals of 161 and 243 years for the southern and northern parts of the fault, respectively (Table 3), and estimated a 33% chance of a M 6.7 earthquake occurring before 2043 on the Hayward–Rodgers Creek fault system.

The Rodgers Creek fault is at least 73 km (45 miles) long (Figure 48) and compared to the Hayward fault, its geomorphic expression is complex (Hecker and Randolph-Loar, 2018). North of Santa Rosa, the Rodgers Creek fault is also known as the Healdsburg fault (see Figure 28), and recent work by Hecker et al. (2016) has confirmed that the Rodgers Creek and Healdsburg faults are directly connected. The Rodgers Creek–Healdsburg fault is separated from the Maacama fault at its northern end (Figure 48) by a right step 10 km (6 miles) wide. (Wagner and Bortugno, 1982), but the two faults may be connected through the Bennett Valley fault, which lies about 3 km (1.8 miles) east of the Rodgers Creek fault south of Santa Rosa (Hecker and Randolph-Loar, 2018). Holocene activity along the Rodgers Creek fault is indicated by a series of fault scarps in Holocene deposits, side-hill benches, right-laterally offset streams, and closed linear depressions. Paleoseismic investigations by Schwartz et al. (1992) revealed three surface-rupturing events in the past 925 to 1,000 years. The most recent large earthquake occurred no earlier than A.D. 1690 and most likely after A.D. 1715 with a preferred mean date of A.D. 1745 (Hecker et al., 2005). The calculated slip rate

for the Rodgers Creek fault is 9 ± 2 mm/yr (Table 3) and the fault creeps interseismically as well (Funning et al., 2007; Lienkaemper et al., 2014, McFarland et al., 2016, Jin and Funning, 2017). Microseismicity is nearly absent along the southern part of the Rodgers Creek fault (Wong, 1991), where creep has not been documented. WGCEP models (2003; 2013) incorporate the possibility of the Hayward fault rupturing along with the Rodgers Creek fault. Rupture of the entire length of both faults would generate an earthquake of about M 7.3; rupture of the Rodgers Creek fault with only the northern segment of the Hayward fault would generate an earthquake of about M 7.1 (WGCEP 2003).

1868 Earthquake

The October 21, 1868, M ~6.8 Hayward fault earthquake toppled buildings in Hayward and other eastern San Francisco Bay Area communities, with strong shaking lasting about 40 seconds. Buildings were damaged in Oakland, San Francisco, Santa Rosa, San Jose, Napa, and Hollister (Lawson et al., 1908; Brocher et al., 2008; Boatwright and Bundock, 2008). About 30 people were killed by the earthquake. Based on historical reports, the surface rupture associated with this earthquake is thought to have extended for approximately 30 km (19 miles), from Warm Springs in Fremont to San Leandro, with a maximum reported displacement of about 1 m (3.3 ft) (Radbruch, 1967). However, reevaluation of survey data suggested that the fault may have ruptured as far north as Berkeley, with as much as 2 m (6.6 ft) of slip (Yu and Segall, 1996). Bakun (1999) estimated the epicenter to be located near San Leandro, and calculated a magnitude of 6.8 based upon pre-instrumental intensity reports. Boatwright and Bundock (2008) compiled and interpreted reports of damage and developed a map of the intensity of shaking. Hough and Martin (2015) reviewed previous estimates of the magnitude of the earthquake, and used the felt reports of Boatwright and Bundock (2008), to derive a somewhat smaller magnitude estimate of 6.5 for this earthquake.

San Gregorio Fault

The northwest-striking San Gregorio fault is the principal active fault west of the San Andreas fault in coastal central California, and lies largely offshore. The fault extends from offshore of Point Sur, northward to Bolinas Lagoon, where it merges with the San Andreas fault (Figure 47 and Figure 48). WGCEP (2003) divided the fault into northern and southern

rupture segments with the boundary at a prominent step in the middle of Monterey Bay (Jennings, 1994). Only two short sections, from Moss Beach/Seal Cove to Pillar Point and from Mussel Rock/Pescadero to Point Año Nuevo, lie on land, and both are on the northern segment of the fault. Because of the limited onshore extent of the fault, the fault is relatively poorly characterized. Simpson et al. (1997, 1998) carried out a paleoseismic investigation along the Seal Cove section of the fault, where they documented late Holocene right-lateral offset. They calculated a slip rate on the Seal Cove section over the past 80,000 years of 3.5–4.5 mm/yr from an offset stream channel. In the Point Año Nuevo section, the San Gregorio fault consists of several subparallel strands, and slip rates have only been measured across some strands, leading to high uncertainties in the slip rate across the entire fault zone. Weber and Cotton (1981), Weber (1994) and Weber et al. (1995) reported slip rates of 4–11 mm/yr for the entire fault zone in this section based on offsets of creeks and marine shoreline angles over the last 100,000 years. UCERF3 used a slip rate of 7 ± 3 mm/yr for the northern part of the fault. This rate is consistent with a model in which slip from the San Andreas fault is partially transferred to the San Gregorio fault, as the San Andreas slip rate decreases from 24 mm/yr north of the faults' intersection near Bolinas to 17 mm/yr south of the intersection.

Little paleoseismic data for the San Gregorio fault has been collected. The most recent surface-faulting event on the Seal Cove strand occurred sometime between A.D. 1270 and A.D. 1775, and the penultimate event occurred between A.D. 680 and A.D. 1400 (Simpson et al., 1997, 1998). Recent analyses of marsh stratigraphy along the same fault strand at Pillar Point Marsh constrain the most recent event to have occurred between about A.D. 1500 and present (Koehler et al., 2005), with a preferred date between A.D. 1667 and 1802 (Simpson and Knudsen, 2000). Koehler et al. (2005) estimate an average recurrence interval of 1,500 to 3,000 years from the marsh data at Pillar Point. Paleoseismic data from the Año Nuevo onshore section of the fault are similarly limited. Weber and Thornburg (1999) conducted a paleoseismic study at Cascade Ranch near Point Año Nuevo and found evidence for three to four events in deposits at most 6,000 to 8,000 years old, yielding a minimum average recurrence interval of 1,500 to 2,000 years.

Calaveras Fault

The Calaveras fault traverses the Hollister Plain and the Diablo Range east of the Santa Clara Valley, forming a structural boundary between the Diablo Range and the San Francisco Bay structural depression (Page, 1982). The Calaveras fault exhibits prominent geomorphic expression along its entire active length of 130 ± 10 km (81 ± 6 miles), and has generated small and moderate earthquakes during historical time. Abundant microseismicity and several historical moderate-magnitude earthquakes characterize the central Calaveras fault (Bakun, 1980; Bakun et al., 1984; Bakun and Lindh, 1985; Cockerham and Eaton, 1987; Oppenheimer et al., 1990; Schaff et al., 2002) (Figure 47 and Table 2).

Between 1949 and 1988, four $M > 5$ earthquakes ruptured the central Calaveras fault in a northward progression as post-seismic relaxation following one event triggered the next event (Du and Aydin, 1992). The earthquake cycle included the following sequence: 1949 Gilroy earthquake (M 5.2), 1979 Coyote Lake earthquake (M 5.9), 1984 Morgan Hill earthquake (M 6.2), and ending with the 1988 Alum Rock earthquake (M 5.1) (Oppenheimer et al., 1990).

The Coyote Lake and Morgan Hill rupture areas appear to be a repeat of previous events in 1897 and 1911, respectively (Toppozada et al., 1981; Toppozada and Parke, 1982; Oppenheimer et al., 1990). Oppenheimer et al. (1990) analyzed spatial patterns of microseismicity along the central Calaveras fault and inferred that the central Calaveras fault releases strain predominantly through aseismic creep and small to moderate ($\leq M$ 6.2) magnitude earthquakes.

The northern part of the Calaveras fault, north of where it intersects the Hayward fault, exhibits less historical seismicity (Figure 47), with only one moderate magnitude event along the fault north of Calaveras Reservoir: the 1861 M 5.8 San Ramon Valley earthquake (Oppenheimer and Lindh, 1992). This earthquake produced surface cracking in San Ramon for a length of either 4 km (2.5 miles) (Jennings, 1994) or 10–13 km (6.2–8 miles) (Rogers and Halliday, 1992). Others attribute this cracking to landsliding (Hart, 1981) and possibly strong ground shaking (WGCEP, 2003) rather than fault rupture to the ground surface. Over the past 35 years, numerous swarms of earthquakes have occurred on or near the northern Calaveras fault: 1970 (Danville), 1976 (Danville), 1990 (Alamo), 2002 (Las Trampas), 2003 (San

Ramon), 2015 (San Ramon), and 2018 (Danville; see <https://earthquake.usgs.gov/earthquakes/events/2018danville/>). These swarms appear to occur on minor faults that strike nearly orthogonal to the northern Calaveras fault, with the exception of the 2003 San Ramon swarm, which occurred parallel to and may be on, the Calaveras fault.

UCERF3 (WGCEP, 2013) calculated a 26% probability of a $M \geq 6.7$ earthquake on the Calaveras fault between 2014 and 2043 (Figure 48). Earlier Working Group reports estimated lower probabilities and evaluated each “segment” separately. For example, WGCEP (2003) analyzed available local and regional information, constructing multiple fault-rupture models and rupture scenarios involving three fault segments, to calculate a 2% probability between 2002 and 2031 for an earthquake rupture of $M \geq 7.0$ anywhere on the Calaveras fault.

Faults of San Francisco

City College Fault

Bonilla (1965, 1971, 1998) and Schlocker (1974) identified northwest-striking shear zones within the city limits of San Francisco, and named these shear zones the City College fault, or City College shear zone, and the Fort Point–Potrero Hill–Hunters Point shear zone. Available geologic data suggests that neither shear zone has been active in the late Quaternary, nor is there seismicity associated with these zones. Schlocker (1974) describes sheared and shattered Franciscan Complex rocks along the trend of the City College shear zone, with abundant slickensides and gouge zones exposed in the shear zone. These zones are described further in the section titled “Geology and Geologic History” above.

Serra Fault

The Serra fault is mapped crossing the southwestern corner of San Francisco, west of Lake Merced, and intersecting the coastline at Fort Funston (Figure 47). The Serra fault is the northernmost fault in the Foothills thrust system, a northwest-striking system of active blind and emergent thrust faults bounding the range front along the San Francisco Peninsula adjacent to and northeast of the San Andreas fault (Brabb and Olson, 1986; Pampeyan, 1994; Bürgmann et al., 1994; Hengesh et al., 1996; Angell et al., 1997; Bullard et al., 2004). The thrust faults generally dip southwest towards the San Andreas fault and likely merge with it at depth. Coseismic deformation has been documented along fault traces in the southern portion of

the Foothills thrust system following the 1906 San Francisco earthquake (Lawson, 1908) and the 1989 M 6.9 Loma Prieta earthquake (e.g., Haugerud and Ellen, 1990).

The Serra fault was first observed in housing development cut slopes near San Bruno by Manuel Bonilla of the U.S. Geological Survey in 1954, who named the fault after the nearby Junipero Serra Boulevard (Bonilla, 1994). Bonilla subsequently included the Serra fault on his preliminary geologic map of the San Francisco South 7.5-minute quadrangle, where he showed the fault juxtaposing Franciscan Complex rocks against younger deposits of the Plio–Pleistocene Merced and Pleistocene Colma formations (Bonilla, 1965). Based on subsequent mapping by various workers, the Serra fault extends for over 20 km (12 miles) from Fort Funston on the coast south to Hillsborough, and consists of discontinuous northwest-striking traces ranging in length from approximately 1.5 to 8 km (0.93 to 5 miles) (Smith, 1960; Bonilla, 1971, 1998; Brabb and Olson, 1986; Yancey, 1978; Pampeyan, 1994; Hengesh et al., 1996; Barr and Caskey, 1999; Kennedy, 2002).

Between San Bruno and Daly City, the fault is expressed as a linear northeast-facing escarpment that forms the southwestern margin of Colma Valley. The fault locally juxtaposes Franciscan Complex rocks over younger deposits of the Merced Formation (Hengesh et al., 1996) and in turn folded Merced Formation strata over relatively undeformed flat-lying beds of the younger Colma Formation (Yancey, 1978). In the Fort Funston area, the fault appears to be blind and is inferred based on the presence of a northeast-vergent monoclinical fold within the Merced Formation and a prominent northeast-facing escarpment (Barr and Caskey, 1999; Kennedy, 2002, 2004).

Late Quaternary uplift along the Serra fault is indicated by uplifted and folded shallow marine and non-marine deposits of the Merced Formation (Bonilla, 1998, 1996; Yancey, 1978), which are faulted against the Colma Formation. Paleoseismic studies along the Serra fault have suggested possible Holocene activity. These studies include trenching by Hengesh et al. (1996) at Junipero Serra County Park in San Bruno, which documented at least three episodes of fault movement, with the most recent episode marked by shear fractures that extend into and offset the soil A-horizon, consistent with Holocene activity. Slickensides on the fault

surfaces indicated a right-lateral reverse-oblique sense of motion. Kennedy (2002, 2004) interpreted tilted peat beds in the sea cliff exposures at Fort Funston radiocarbon dated at $7,800 \pm 70$ and $5,890 \pm 120$ years BP as evidence of Holocene fault-propagation folding above the Serra fault, and conjectured that the Serra fault represents the only active fault within San Francisco's city limits. It is not known whether the Serra fault ruptures independently or moves only during events on the San Andreas fault. Although it was earlier included in the State of California's Alquist Priolo Special Study Zones, it has not been shown on a special studies zone map by the state since the 1980s.

Liquefaction and Lateral Spreading

Damaging liquefaction in San Francisco has been caused by a number of large historical earthquakes, including the 1868, 1906 and 1989 earthquakes described above (e.g., Youd and Hoose, 1978; <https://geomaps.wr.usgs.gov/sfgeo/liquefaction/effects.html>). Liquefaction occurs when loose sand and silt that is saturated with water behaves like a liquid when shaken by an earthquake (Youd, 1973). When liquefaction occurs the soil can lose its ability to support structures, flow down even very gentle slopes, and erupt to the ground surface to form sand boils. Many of these phenomena are accompanied by settlement of the ground surface, usually in uneven patterns that damage buildings, roads and pipelines (Figure 50). Areas most vulnerable to liquefaction in San Francisco are old marshlands that were filled with

pumped or dredged material to create land. Such areas have liquefied in multiple past earthquakes and are likely to liquefy again in future earthquakes. These susceptible areas have been mapped by a variety of researchers who have made use of information on past occurrences of liquefaction, early historical maps of the coastline, geologic maps, and geotechnical borings (e.g., Knudsen et al., 2000; California Geological Survey, 2000; and O'Rourke et al., 2006).

The California Geological Survey, Seismic Hazards Mapping Program produces regulatory maps for the hazards of surface rupture, liquefaction and earthquake-induced landsliding. Figure 51 shows the CGS map of liquefaction and earthquake induced landslides "zones of required investigation" (California Geological Survey, 2000). The CGS zones of required investigation (1) trigger disclosure during real estate transactions, and (2) require that proponents of new development investigate, characterize, and mitigate the hazard.

The CGS liquefaction zones of required investigation for San Francisco were mapped based primarily on the extent of artificial fill and the location of past occurrences of liquefaction, primarily in the 1906 and 1989 earthquakes (CGS, 2000). Thus, the boundary defining the zone of required investigation for liquefaction is based on early maps of the coastline from the U.S. Coast Survey in 1851 and 1857, before artificial fill was placed to fill wetlands. This artificial fill hosted nearly all of the liquefaction and ground failure that occurred in the 1868, 1906 and 1989 earthquakes (Youd



Figure 50. Liquefaction-related damage in San Francisco due to the 1906 earthquake. Photograph on left shows Dore Street (from Bancroft Library) and photograph on right shows an area near Howard & 17th Streets (G.K. Gilbert, USGS photo).



Figure 51. California Geological Survey’s Seismic Hazard zones map showing zones of required investigation for liquefaction and earthquake-induced landslides (map data from <http://maps.conservation.ca.gov/cgs/information/warehouse/index.html?map=regulatorymaps>).

and Hoose, 1978; Tinsley et al., 1998; Knudsen et al., 2000).

Mitigation of liquefaction hazard can be accomplished through a variety of approaches, including: (1) avoiding hazardous areas, (2) purchasing insurance to cover anticipated losses, (3) “improving” the ground so it is less susceptible to liquefaction or so that if liquefaction does occur the amount of surface deformation is reduced, and (4) fortifying structures to withstand liquefaction of underlying soils. Ground susceptible to liquefaction can be improved by a variety of means, including densification through compaction, and ground treatment to reduce porosity and increase cementation of grains by grouting or soil mixing. Structural solutions include construction of deep foundations or reinforced shallow foundations, or building berms or other systems to prevent lateral movement should the ground liquefy.

The CGS zones of required investigation for earthquake-induced landsliding (Figure 51) are based primarily on these factors: slope, presence of weak rock, locations of adverse bedding, and past occurrences of landsliding. The CGS report describing this mapping (CGS, 2000) provides information about past landsliding, shear strength of various rock units, and the mapping/zoning process. Landslides have occurred in San Francisco in past earthquakes (Youd and Hoose, 1978), although the extent of damage is much more limited than that occurring due to liquefaction.

WATER RESOURCES

by Jeffrey A. Gilman and Greg W. Bartow

San Francisco’s Water Supply

The history of San Francisco’s water supply is rich with colorful characters and remarkable engineering, and is well described in Spring Valley Water Company (1926), O’Shaughnessy (1934), Wurm (1990), SFPUC (2005), Simpson (2005), and Righter (2006) as summarized below.

Early Years

San Francisco is surrounded by saltwater on three sides but isolated from significant fresh surface waters by topography and has limited groundwater resources. (For more on the past and planned future use of groundwater, see “Groundwater” section below.) Prior to the Gold

Rush in 1849, the small creeks and lakes were sufficient to support the Spanish Missionaries, the Presidio fort, and early settlers. With the arrival of thousands of gold seekers, the local supplies were overtaxed. In 1851, the Sausalito Water and Steam Tug Company was barging water across the bay by tank steamer from springs on the Marin shore, using some 65 water carts to supply San Francisco households. Primitive companies were formed to tap sources south of San Francisco on the peninsula. Small diversion dams, flumes, and pipelines met the growing demand for several years, but grew insufficient.

Post Gold Rush

Frequent fires were common in the wooden boomtown, with six major fires between 1850 and 1852 alone. Residents wanted a municipal water supply for firefighting and to control the price gouging and poor service of the small primitive water supply companies. The private companies competed with each other for control of the growing market throughout the 1850s, with some companies merging and others going out of business.

The Spring Valley Water Company (SVWC) emerged as the largest of these suppliers in the late 1850s and established a monopoly on the city’s water supply that would last until the 1920s. The California legislature granted a water franchise to Spring Valley in 1858, giving it and other privately owned municipal water companies the power of eminent domain to acquire land and water rights, and to lay pipelines for the good of the people they served. The water works of the SVWC are described with numerous photographs in *San Francisco Water* (Spring Valley Water Company, 1926).

Search for a Sierra Source

SVWC developed new water supplies located on the peninsula south of San Francisco and in the East Bay (Figure 52). However, these supplies were projected to be insufficient for the growing Bay Area population. Numerous alternative sources in the Sierra Nevada Mountains had been considered by the City, Spring Valley, and competing water suppliers. Nothing worked out again and again on various alternate water supplies in the 1880s and 1890s. Political and public support waxed and waned with alternating dry years and wet years. After the 1906 earthquake and the resulting inability to deliver water to San Francisco, public support swelled in favor of the City purchasing the SVWC and making water a public utility. The City eventually

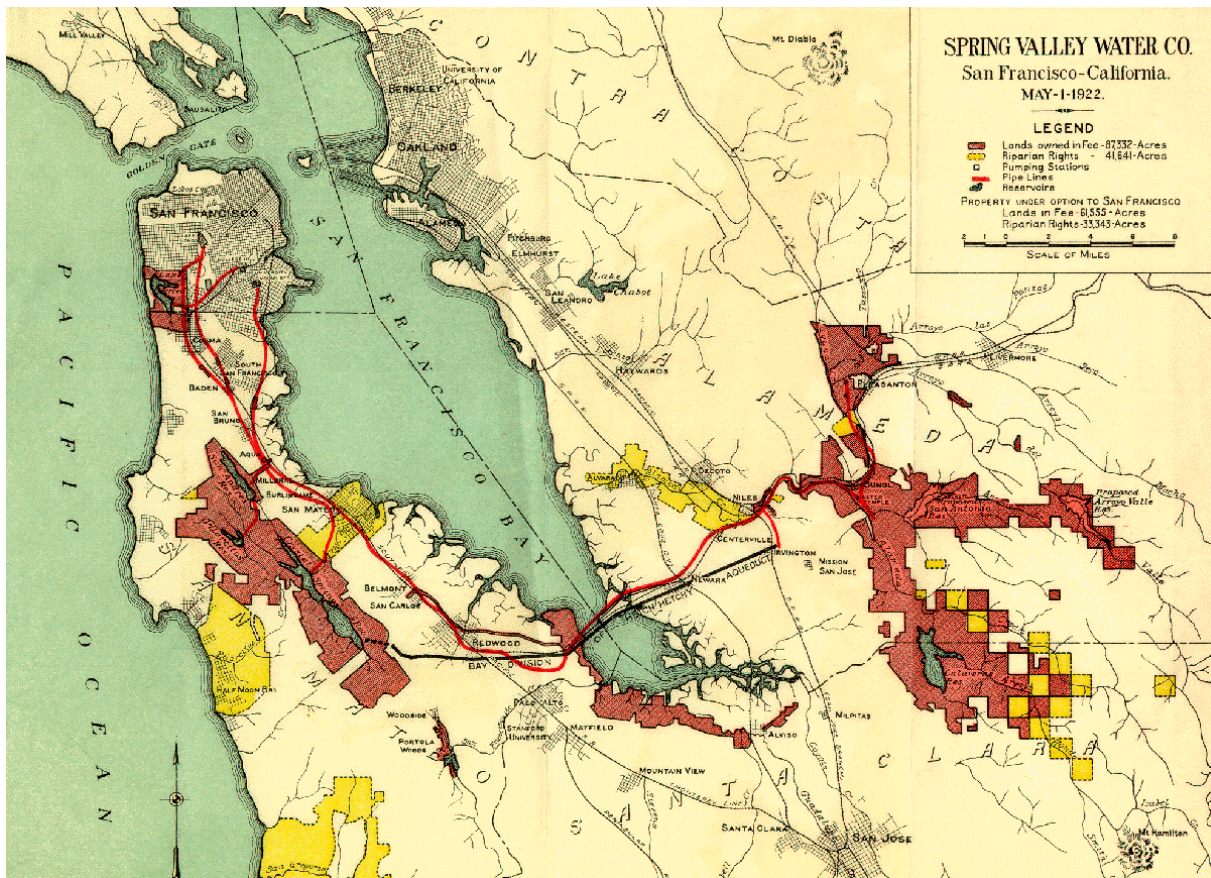


Figure 52. Spring Valley Water Company lands and water rights ca. 1922 (SFPUC, 2018a).

purchased the SVWC in 1930 for \$40 million.

The first plan to tap the Tuolumne River was apparently developed in 1882 by J.P. Dart, a water engineer in the Sierra foothills. The Tuolumne River has its source in glaciers on Mount Lyell, elevation 3,960 m (13,120 ft). The river drains 1,690 km² (652.5 square miles) of watershed in rugged granite mountains sloping west from the Sierra Nevada crest. Over 90% of the watershed is at elevations above 1,800 m (5,906 ft). In 1901, under the leadership of Mayor James D. Phelan, the city leaders finally decided to move forward and develop the Tuolumne River watershed. The Mayor and city engineers quietly and quickly put up their own money to send engineer J. B. Lippincott into the Sierra Nevada for the necessary surveys. On July 29, 1901, Mayor Phelan filed for water rights as a private citizen and on October 15, 1901, he applied for water rights and reservoir rights at Hetch Hetchy and Lake Eleanor. He assigned his interests to the City of San Francisco in 1903.

Concerns about meeting the growing water supply

needs, coupled with the memory of the 1906 earthquake and fire, highlighted the need to develop the Tuolumne River water source. Thus, began a 12-year fight for approval of the Hetch Hetchy Project that pitted San Francisco, competing irrigation districts, and environmentalists against each other. The controversy and eventual approval of Hetch Hetchy is well documented in O'Shaughnessy (1934), Righter (2005), San Francisco Public Utilities Commission (2005), and Simpson (2005). John Muir and the Sierra Club attacked through letters, pamphlets, and circulars, basing arguments on the claim that there was an adequate supply for San Francisco without the need to “destroy” Hetch Hetchy Valley. Muir famously wrote: “Dam Hetch Hetchy! As well dam for water-tanks the people’s cathedrals and churches, for no holier temple has ever been consecrated by the heart of man.”

Ultimately the Hetch Hetchy Grant, known as the Raker Act, was passed by Congress and signed by President Wilson in 1913. The Raker Act granted San Francisco the right of way and use of public lands in the areas concerned for purpose of constructing,

operating, and maintaining reservoirs, dams, and other structures necessary and use of the water and power. Work started on the dam in 1919 under the direction of Michael O’Shaughnessy. The dam, which was named for O’Shaughnessy, was the highest dam at the time and was largely completed in 1923. O’Shaughnessy Dam was raised to its current height of 131 m (430 ft) in 1938. Hetch Hetchy Reservoir is 13 km (8.1 miles) long, has a surface area of 8 km² (3.1 square miles), and a maximum water depth of 95 m (312 ft).

O’Shaughnessy, in his report on the history of Hetch Hetchy, wrote: “This is a large undertaking for a small city of the size of San Francisco. ‘The City That Knows How’ with courage and determination has brought the project to completion and I am proud to have been associated with the work so long” (O’Shaughnessy, 1934). In October 1934 the first water from the Hetch Hetchy Reservoir reached the San Francisco Peninsula and was celebrated at the Pulgas Water Temple in Woodside, California (Figure 53). Sadly, Michael O’Shaughnessy, the chief architect of this engineering marvel, passed just two weeks before this historic event.



Figure 53. October 1934 celebration at the Pulgas Water Temple of the delivery of the first water from the Hetch Hetchy Reservoir reaching the San Francisco Peninsula (SF-PUC).

Sunset Well Field

The Sunset Well Field was a group of 19 wells in western San Francisco that operated between October 25, 1930, and October 31, 1935 (San Francisco Public Utilities Commission, 1933; San Francisco Water Department, 1994). The wells were constructed in fiscal years 1929, 1930, and 1931 after below-normal rainfall. The dry years continued until fiscal year 1934, with the exception of a normal rainfall year in 1932 (Golden Gate Weather Services, 2017).

The average depth of these wells was about 75 m (245 ft). The pumping rate of the wells varied from 0.011 to 0.018 m³/s (170 to 280 gallons per minute, or gpm), depending on the capacity of the pumps. The wells pumped into a pipeline extending beneath 44th Avenue, terminating in a storage tank with a capacity of almost 1.9 million liters (500,000 gallons) at 44th Avenue near Santiago Street. A pump station at the tank location pumped the groundwater to Laguna Honda Reservoir.

The annual average groundwater production from the Sunset Well Field in m³/s and million gallons per day (mgd) was as follows (San Francisco Public Utilities Commission, 1933, 1934, 1935, 1936):

- Fiscal year 1930–1931 20,100 m³/d (5.3 mgd)
- Fiscal year 1931–1932 22,000 m³/d (5.8 mgd)
- Fiscal year 1932–1933 21,200 m³/d (5.6 mgd)
- Fiscal year 1933–1934 20,400 m³/d (5.4 mgd)
- Fiscal year 1934–1935 19,700 m³/d (5.2 mgd)
- Fiscal year 1935–1936 limited use

Reported observations of the pumping influence from the Sunset Well Field on groundwater levels and groundwater quality showed that the groundwater level remained the same, and the salinity of the water had not increased (San Francisco Public Utilities Commission, 1934, p. 42).

The San Francisco Water Department in the early 1990s began to investigate the groundwater potential of local aquifers, after a series of below-normal rainfall years from 1988 to 1992. These studies included the potential for rehabilitating the Sunset Well Field (Montgomery, 1991). This rehabilitation study concluded that the wells were in poor condition, casings were rusted with perforations rarely noticeable below the water level, and sand production was high during test pumping. Sixteen of the Sunset Well Field wells were decommissioned in June and July 2002 (ERRG, 2002). The decommissioning method consisted of filling the well casings with

sand-cement grout from bottom to top.

Hetch Hetchy Regional Water System

Today, the Hetch Hetchy Regional Water System, with its primary source in Yosemite National Park, provides drinking water to 2.7 million people living in the San Francisco Bay Area—including San Francisco County and parts of the counties of San Mateo, Santa Clara, and Alameda. In San Francisco, the system provides approximately 85% of the total water supply needs; the approximate remaining 15% comes from two local watersheds—the Alameda Creek and Peninsula. Hetch Hetchy is owned by the City and County of San Francisco and has been operated and maintained by the San Francisco Public Utilities Commission (SFPUC) since 1932. The Hetch Hetchy Reservoir stores up to 444.4 billion liters (360,000 AF) of high-quality mountain water that is transmitted entirely by gravity via 270 km (167 miles) of pipelines and tunnels all the way to San Francisco and also generates approximately 1.7 billion kWh of hydroelectricity per year (Polenghi-Gross, et al., 2014) (Figure 54, Figure 55, and Figure 56). The delivered water from Hetch Hetchy Reservoir is so clean and protected that it is exempt from filtration requirements by the U.S. EPA. In addition to Hetch Hetchy Reservoir, the Regional Water System includes eight other dams as listed on Table 4. Within San Francisco, the water distribution system is complicated by the uneven topography of the city. Consequently, the

city is divided into a large number of major and minor pressure zones controlled by tanks and valves to avoid excessive pressure variations.

Water System Improvement Program

Studies initiated by the SFPUC in 1997 indicated that without significant seismic improvements, the Hetch Hetchy System would likely be severely damaged in a major earthquake and parts of the SFPUC service territory could be out of water for up to two months. It was a striking finding that one of the United States' most iconic cities and the world's leading hub for the high-tech industry could be without an adequate water supply for an extended period of time.

In 2002, the SFPUC, together with its 26 San Francisco Bay Area wholesale customers launched what would become a \$4.8 billion Water System Improvement Program (WSIP) to repair, replace, and seismically upgrade the system's aging pipelines, tunnels, reservoirs, pump stations, storage tanks, and dams (Labonte, 2013). Crucial portions of the water system cross over or are near three major earthquake faults in the Bay Area. The program consists of 87 projects—35 local projects within San Francisco and 52 regional projects—spread over seven counties from the Sierra foothills to San Francisco. As of May 2018, the WSIP was approximately 95% complete (SFPUC, 2018b).

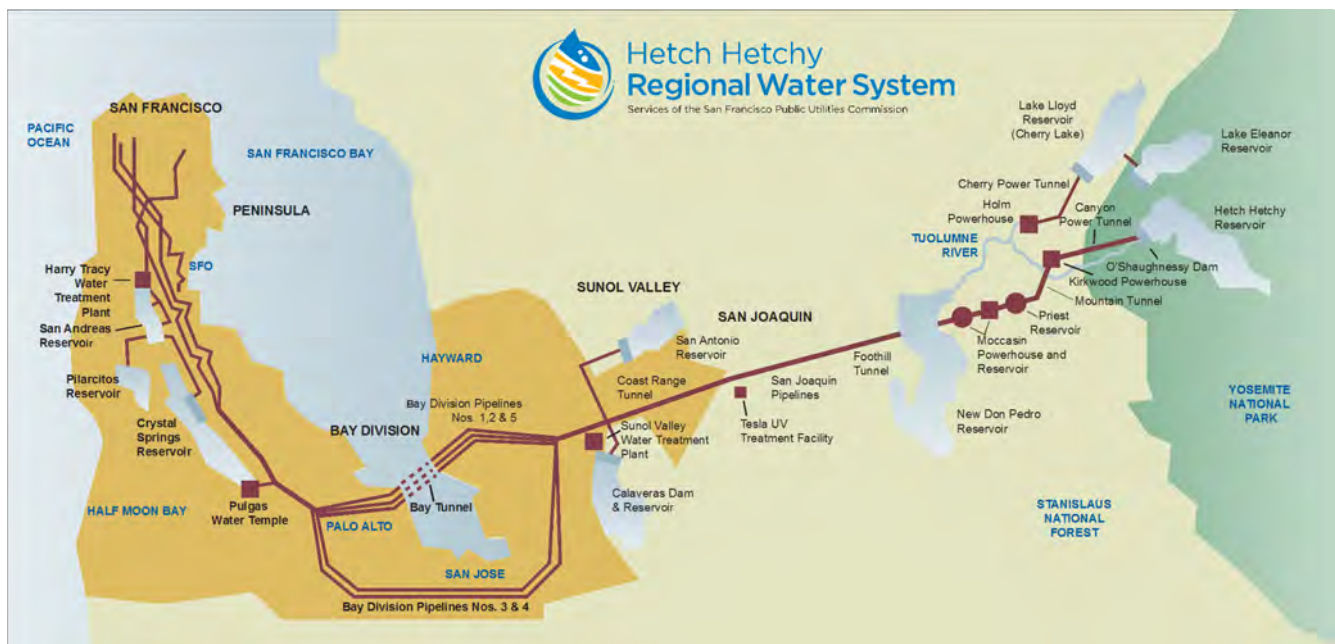


Figure 54. Overview of San Francisco Water System (SFPUC).



Figure 55. O'Shaughnessy Dam and Hetch Hetchy Reservoir (SFPUC).



Figure 56. Hetch Hetchy Valley, O'Shaughnessy Dam and Hetch Hetchy Reservoir (SFPUC).

Table 4. Summary of San Francisco Water Supply Reservoirs (SFPUC, 2005 and CA DWR, 2017).

| Dam and Reservoir Name | Year Construction Completed | Reservoir Capacity | Dam Type and Height |
|---|---------------------------------------|--|---|
| Pilarcitos Dam and Reservoir | 1866 (raised in 1867 and 1874) | 3.8 billion liters (3,100 acre-feet) | Earthen fill with a clay puddle core, height 31 m (103 ft) |
| San Andreas Dam and Reservoir | 1870 (raised in 1875) | 23.7 billion liters (19,207 acre-feet) | Earthen fill with a clay puddle core, height 33 m (107 ft) |
| Upper Crystal Springs Dam and Reservoir | 1877 (raised in 1891) | See Lower Crystal Springs Capacity | Earthen dam with a puddle core was raised once in 1891. |
| Lower Crystal Springs Dam and Reservoir | 1888 (raised in 1890, 1911, and 2018) | Upper and Lower Crystal Springs reservoirs operate as one system, and have a combined capacity of 71.4 billion liters (57,910 acre-feet) | Gravity arch dam consisting of interlocking concrete blocks that were poured in place, height 48 m (157 ft) |
| Eleanor Dam and Reservoir | 1918 | 35.3 billion liters (28,600 acre-feet) | Concrete multiple arch dam, height 19 m (61 ft) |
| Calaveras Dam and Reservoir | 1925 Rebuilt 2015–2019 | 119.4 billion liters (96,850 acre-feet) | Earthen fill, height 64 m (210 ft) |
| O’Shaughnessy Dam, Hetch Hetchy Reservoir | 1923 (raised in 1938) | 444 billion liters (360,000 acre-feet) | Concrete, height 95 m (312 ft) |
| Cherry Valley Dam and Lloyd Reservoir | 1956 | 337 billion liters (273,500 acre-feet) | Earthen and rock-fill, height 96 m (315 ft) |
| Turner Dam and San Antonio Reservoir | 1964 | 62 billion liters (50,500 acre-feet) | Earthen fill, height 59 m (193 ft) |

Auxiliary Water Supply System

Following the devastating damage from the fires associated with the 1906 San Francisco earthquake (described above), the City developed the Auxiliary Water Supply System (AWSS). The 1906 earthquake highlighted the vulnerability of the municipal water supply system and the need for an improved system. The design was originally proposed by San Francisco Fire Department chief engineer Dennis Sullivan in 1903, with construction beginning in 1909 and finishing in 1913. It was built as a high-pressure system with mains buried approximately 1.5 m (about 5 ft) below the ground surface, restrained pipeline joints, gate valves strategically placed within the system, and no domestic service connections, thus making it less vulnerable. The mains have a diameter of approximately 25 to 30 cm (10 to 12 in). The AWSS is used for large fires and as the secondary defense against fires in the event the municipal water supply system fails and is the only high-pressure network of its type in the United States (AECOM, 2014; San Francisco Fire Department, 2008).

The AWSS has been expanded and improved through several bond measures approved in the 1930s, the 1970s, the 1980s, 2010, and 2014 and today consists of approximately 230 cisterns, two saltwater pump stations, two storage tanks, one reservoir, and approximately 217 km (135 miles) of distribution piping (Figure 57).

The underground cisterns are located throughout the city and provide an emergency supply of water in the event of major damage to the municipal water supply and/or AWSS (Figure 58). The cisterns have an individual storage capacity of between 38,000 and 340,000 liters (10,000 and 90,000 gallons) of water with most having a capacity of 280,000 liters (75,000 gallons) (San Francisco Fire Department, 2008). The combined storage of all cisterns is over 42 million liters (11 million gallons).

As part of an AWSS planning study for the SFPUC, AECOM and AGS consultants provided a summary of the effects of the 1989 Loma Prieta earthquake on the AWSS and Municipal Water Supply System (MWSS) (AECOM, 2014) which is summarized as follows:

The performance of the AWSS remains untested in response to an earthquake of the same magnitude as the 1906 earthquake. The 1989 Loma Prieta earthquake was the largest earthquake affecting the Bay

Area since the construction of the AWSS in 1913. The 1906 earthquake had a magnitude of 7.9 which was significantly higher than the 6.9 magnitude of Loma Prieta. Even so, the damage done by the Loma Prieta earthquake was significant and resulted in approximately 69 main breaks and 54 service connection breaks in the Municipal Water Supply System (MWSS) in the Marina District. Additional repairs that were not documented may have also occurred. The repairs were spread throughout the area bounded by Marina Boulevard and Chestnut Street to the north and south and by Buchanan and Baker Streets to the east and west (USGS, 1992). The breaks in the system impaired water pressure and flow to the MWSS hydrants. The AWSS suffered damage due to liquefaction and lateral earth spread. There was one 12-inch AWSS main break in the South of Market (SOMA) area at 7th St. and Natoma St., and four AWSS fire hydrant breaks, with three located in SOMA and one in the Foot of Market area.

AECOM (2014) concluded that the Loma Prieta earthquake illustrated several points regarding these systems and the need for the AWSS following a major earthquake in the future:

- MWSS pipes will sustain damage in certain areas of the City, which will impair the ability to deliver water for firefighting.
- Due to the design features of the AWSS, it is likely to be more serviceable after an earthquake. However, it may still sustain some damage after an earthquake.
- In the Loma Prieta earthquake, the third line of defense, the Portable Water Supply System, and the fireboat, were successful in suppressing the fire in the Marina District.
- As expected, all AWSS damage was concentrated in the infirm (artificial fill) areas.
- While the majority of the AWSS network remained intact, specific portions of the system became inoperable as a result of the breaks and crews needed to be deployed to manually operate valves to isolate breaks.

AECOM (2014) also provides a roadmap for capital projects to further improve the system with funds from the 2010 and 2014 bond measures.

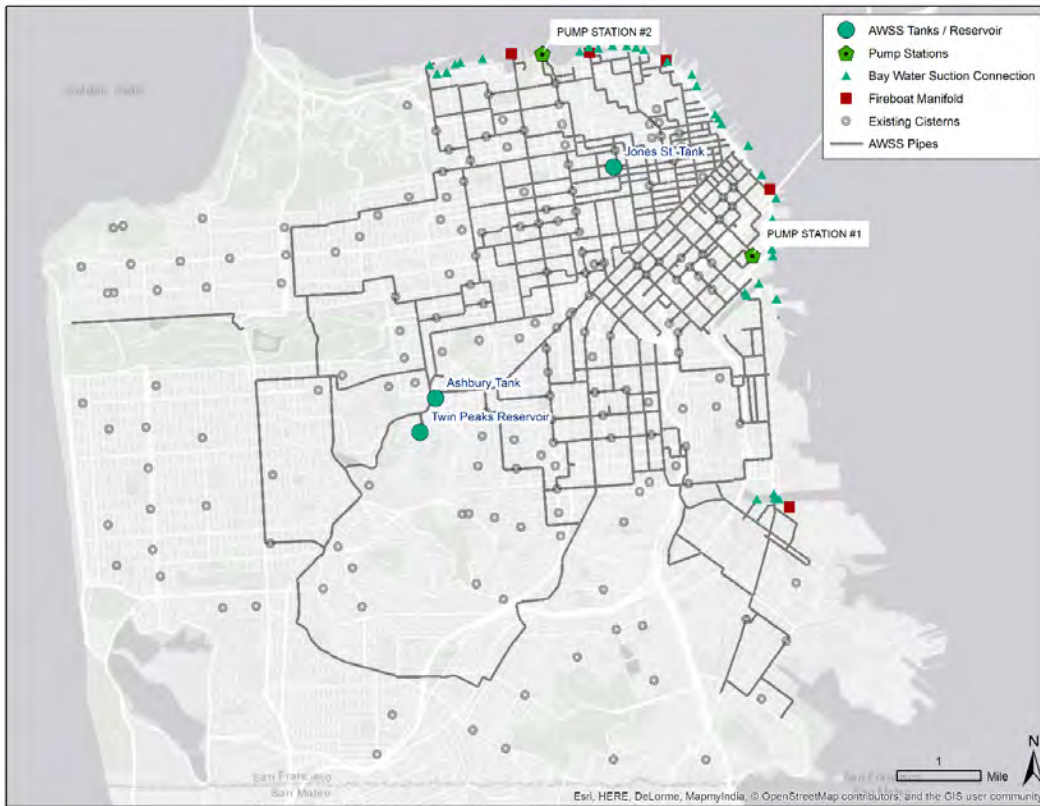


Figure 57. Map of San Francisco Auxiliary Water Supply System (SFPUC, 2016).



Figure 58. Typical emergency water supply cistern at intersection of Mariposa Street and Missouri Street (Mark Hogan).

Diversification of Water Supplies

Starting in the early 2000s, the San Francisco Public Utilities Commission (SFPUC) began work to diversify its water supply portfolio to address a variety of challenges regarding water supply reliability including climate variability and its impact on snowpack, the potential for earthquakes to disrupt water delivery, droughts, regulatory changes, and population growth. To address these challenges the SFPUC is developing groundwater, recycled water, and non-potable water supplies coupled with more water conservation (SFPUC, 2017).

Local Groundwater

SFPUC is implementing the San Francisco Groundwater Supply (SFGW) Project, which will produce an average of up to 15,120 m³/day (4 mgd) of local groundwater from the Westside basin (see “Groundwater” section below for more on the Westside basin). The objective of the SFGW Project is to diversify San Francisco’s municipal water supply, which from late 1935 to late 2017 has come mainly from surface water sources outside of San Francisco (the Regional Water System). The SFGW Project was approved by SFPUC in January 2014 following certification of the project’s Final Environmental Impact Report (San Francisco Planning Department, 2013).

The SFGW Project includes six groundwater well facilities, each consisting of a well and pump station. Four of the wells are new (phase 1 of the project) (Figure 62). Two of the wells are existing irrigation wells in Golden Gate Park that will be converted to potable use (phase 2 of the project), once recycled water becomes the primary irrigation supply for Golden Gate Park. Five of the wells will supply groundwater directly to Sunset Reservoir using a new groundwater pipeline constructed by the SFGW Project. The sixth well connects to the Lake Merced Pump Station supply. Groundwater is treated using chlorination, pH adjustment and blending with the Regional Water System supply, before the groundwater–surface water blend is distributed within San Francisco.

Groundwater production from the phase 1 wells began in 2017 and is anticipated to increase to an average annual rate of 3,800 m³/day (1 mgd) in 2018. After the first year of operation at that rate, groundwater production will increase in a stepwise manner by a maximum of 3,800 m³/day (1 mgd) per year, in

accordance with mitigation measures in the project’s Final Environmental Impact Report. The mitigation measures include monitoring for potential decline in lake levels and potential seawater intrusion. If conditions exceed specified trigger levels after one year of monitoring at each groundwater production step, SFPUC is required to alter or redistribute the amount and pattern of groundwater pumping and/or implement corrective actions such as supplementing Lake Merced with treated stormwater (San Francisco Planning Department, 2013). This adaptive management framework helps ensure that the SFGW Project will be operated in a sustainable manner.

Non-Potable Water

In 2012, San Francisco adopted the Onsite Water Reuse for Commercial, Multi-Family, and Mixed-Use Development Ordinance, allowing for the collection, treatment, and use of alternate water sources for non-potable uses in buildings. The alternate water sources include rainwater, stormwater, foundation drainage and most significantly, graywater and blackwater.

Since 2012, the Ordinance has been amended to allow for district-scale projects, where two or more parcels can share alternate water sources. Since 2015, the City has mandated that all new development projects over 23,200 m² (250,000 sq ft) install and operate an onsite non-potable water system. Onsite non-potable water systems, also referred to as alternate water source systems, provide numerous benefits such as reducing potable water use for toilet flushing and irrigation, meeting Stormwater Management Ordinance requirements, and helping San Francisco achieve greater water supply resiliency and reliability. A guidebook provides developers, architects, and engineers with the necessary steps to collect, treat, and use alternate water sources for non-potable uses. It also outlines the roles and responsibilities of each city agency involved in the approval and permitting process (Kehoe, 2014; SFPUC, 2018d).

Recycled Water

In 2017, the SFPUC started construction on the Westside Enhanced Water Recycling Project. The Project plans to save up to 7,600 m³/day (2 mgd) on average of potable groundwater water that is currently used for non-potable purposes such as irrigation and lake fill. Recycled water will be delivered for these uses through a system of pipelines, pump stations, storage tanks

and reservoirs. The system will bring recycled water from the recycled water treatment facility to Golden Gate Park, Lincoln Park Golf Course, the Presidio Golf Course, and other landscaped areas for irrigation.

A new recycled water treatment facility is being constructed to treat secondary effluent with an advanced treatment process using membrane filtration, reverse osmosis, and ultraviolet light disinfection to produce recycled water at a level that will exceed State of California standards. The project will produce up to 7,600 m³/day (2 mgd) on average of recycled water, with peak deliveries of up to 15,120 m³/day (4 mgd) during the summertime of recycled water that is suitable for all recycled water uses approved by the State of California (SFPUC, 2018e).

San Francisco Creeks and Lakes

Most of San Francisco's historic creeks, lakes, and wetlands (Figure 59) either no longer exist, or have been significantly modified, due to the construction of underground drains to replace creeks, and the filling of tidal marshes and lakes. The Oakland Museum of California has conducted extensive mapping of historic creeks, lakes, and wetlands in San Francisco and the surrounding Bay Area. The Oakland Museum's Creek & Watershed Map of San Francisco (Ramirez-Herrera, et al., 2007) provides an excellent overview of the remaining creeks and lakes, some of which are summarized below.

Lobos Creek

Lobos Creek is the only creek in San Francisco that largely remains in a natural condition. The creek flows through the southwestern Presidio draining into the Pacific Ocean at the southern tip of Baker Beach. Lobos Creek occupies a forested canyon and is one of San Francisco's last riparian corridors. In the early years of San Francisco, this creek was the city's main source of drinking water. Today it still supplies drinking water to the Presidio.

Mountain Lake

Mountain Lake, an approximately 0.0162 km² (4-acre) lake located in the Presidio, was previously named Laguna del Presidio. The Bautista de Anza expedition camped along its shore in 1776. In the mid-1800s, Mountain Lake provided part of San Francisco's drinking water supply. Approximately 40% of the lake area was filled, and the depth of the lake reduced by the

construction of Park Presidio Boulevard. In 2013 and 2014, polluted soil and invasive species were removed from the lake as described in the Mountain Lake Adaptive Management Plan (Presidio Trust, 2014).

Native species are now being reestablished including various underwater plants and the Western Pond Turtle. An aeration and water-mixing system has been installed to improve the overall water quality and reduce unhealthy algae blooms by minimizing stratification and increasing dissolved oxygen concentrations through all depths of the lake.

Lake Merced

Lake Merced consists of four interconnected lakes (North Lake, East Lake, South Lake, and Impound Lake), located in the southwest corner of San Francisco. Lake Merced is approximately 1.2 km² (300 acres) depending on its depth and is the largest coastal freshwater body between Pt. Reyes in Marin County and Pescadero Marsh in southern San Mateo County. Prior to the 1870s, Lake Merced was a coastal estuary; during large rain events, the lake would fill up with water and overflow, creating a channel which connected the lake to the ocean. The lake drained an area of approximately 26 km² (10 square miles) in size, which included Daly City, Westlake, and the Stonestown area of San Francisco.

Spring Valley Water Company purchased the water rights to Lake Merced in 1868, and began delivering Lake Merced water to the City of San Francisco in 1895. The connection to the ocean was closed off in 1895 by construction of Skyline Boulevard and the Great Highway. After the Spring Valley Water Company was purchased by the City of San Francisco, surface water from the newly constructed Hetch Hetchy Dam replaced Lake Merced water in 1934 as San Francisco's primary potable water source. Subsequently, Lake Merced was designated an emergency non-potable water supply for the city.

Lake Merced is hydraulically connected to the Westside groundwater basin and is a surface expression of the Shallow aquifer. During the 20th century, droughts and extensive groundwater pumping in the Westside Basin by golf courses, local municipalities, and cemeteries developed in the post-War years, lowered groundwater levels within the basin and contributed to lower surface water levels in the lake. Drought conditions, and subsequent diversion of stormwater runoff due to increased

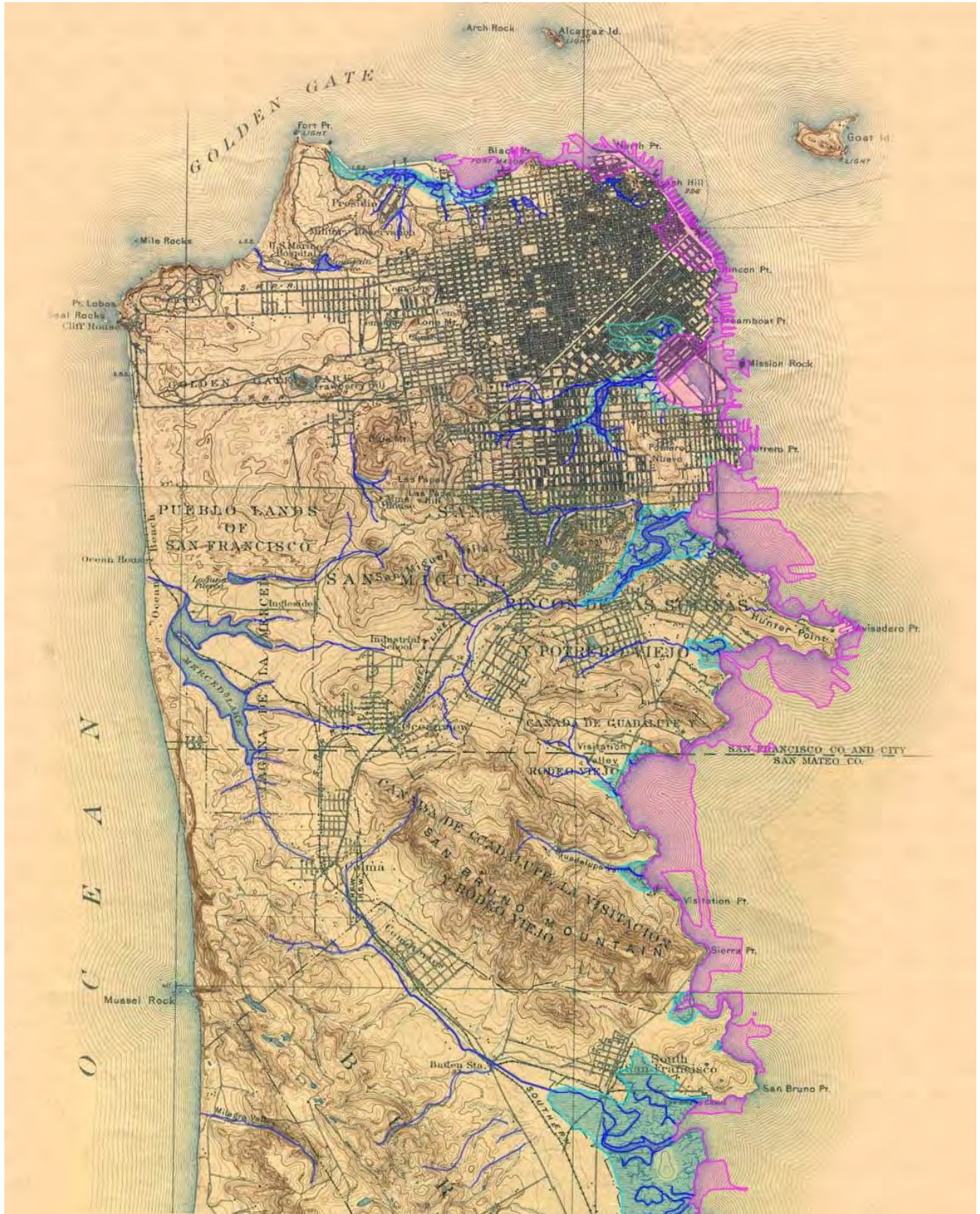


Figure 59. San Francisco Historical Creek and Shoreline Map, 1895 (Oakland Museum of California).

urbanization of the watershed further reduced runoff into the lake, resulting in lower levels. The lake hit its lowest levels during the drought between 1989 and 1993. Since that time, the lake level has rebounded, due to the efforts of CalTrout, the Committee to Save Lake Merced, and many other stakeholders and groups. Today, Lake Merced water levels are relatively stable, and the lake remains the city's emergency non-potable water supply. The lake provides incredible habitat for birds and other wildlife and is also home to a vibrant boating community (SFPUC, 2018a).

Vista Grande Drainage Basin Improvement Project

The Vista Grande Drainage Basin Improvement Project is a project being developed by the Daly City in collaboration with the SFPUC that would address storm-related flooding in Daly City, while providing the additional benefit of augmenting the level of Lake Merced in San Francisco. The project would include expansion of the existing outlet tunnel to the Pacific Ocean, matching the hydraulic capacity of the upstream canal; construction of a treatment wetland; and diversion of treated stormwater into the southern portion of Lake Merced. The project would also upgrade and replace the existing outflow structure at Fort Funston.

Groundwater

In San Francisco, a groundwater basin has been defined as a continuous body of unconsolidated sediments and the surrounding surface drainage area (Phillips et al., 1993). Seven basins have been identified on the basis of geological and geophysical data: Westside, Lobos, Marina, Visitacion Valley, Downtown, Islais Valley and South San Francisco. The Westside, Visitacion Valley and Islais Valley groundwater basins also extend into northern San Mateo County. The locations and aerial extent of these basins are shown in Figure 60. The unconsolidated sediments that comprise the groundwater-yielding units are the Merced Formation, Colma Formation, dune sand, hillslope deposits (colluvium), alluvium along existing and former stream channels, and bay muds.

All groundwater basins are open either to the Pacific Ocean or San Francisco Bay. The landward parts of these basins generally are bounded laterally and vertically by Franciscan bedrock, which is assumed to be relatively impervious. Groundwater flow may occur between basins where the bedrock ridge constituting the boundary is subterranean. There are numerous springs

and seeps issuing from bedrock areas as best identified on the “Seep City Water Exploration Map” (Pomerantz, 2015). Some of these springs and seeps help sustain natural areas in San Francisco, while others discharge directly into the city's combined sewer system.

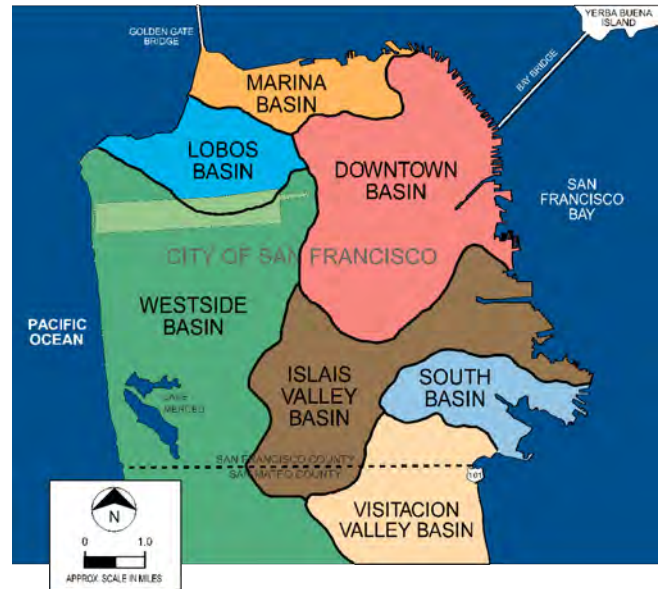


Figure 60. Groundwater basins in San Francisco (San Francisco Water Power and Sewer, 2016).

Sources of groundwater recharge for the San Francisco area are infiltration of rainfall and applied irrigation water, and leakage of water and sewer pipes (Phillips et al., 1993).

The California Department of Water Resources (DWR) has identified all seven groundwater basins and assigned each a basin number (California DWR, 2003). All basins except Visitacion Valley have participated in the DWR's California Statewide Groundwater Elevation Monitoring (CASGEM) Program (California DWR, 2017). The CASGEM Program also has ranked the priority of the basins, and all seven currently have a “very low” overall priority (California DWR, 2016). The California Regional Water Quality Control Board, San Francisco Bay Region, has recognized all seven groundwater basins as having existing or potential use for municipal and domestic water supply (California Water Boards, San Francisco Bay—R2, 2017).

Westside Groundwater Basin

The Westside groundwater basin is located in the northwestern part of San Francisco (Figure 60), and it is the largest groundwater basin in San Francisco and the northern San Francisco Peninsula. Its DWR-assigned basin number is 2-35. The surface area of the

basin is 103 km² (39.7 square miles) (California DWR, 2003).

In San Francisco the basin is located primarily within the Sunset district and parts of Golden Gate Park and the Richmond district. The Westside basin extends into San Mateo County and trends southeastward toward the San Francisco International Airport and the cities of Millbrae and Burlingame. The Westside basin has been divided informally by the San Francisco–San Mateo county line (jurisdictional boundary) into the North Westside basin (subbasin) in San Francisco, and the South Westside basin (subbasin) in northern San Mateo County.

Bedrock topographic highs separate the Westside basin from the Lobos groundwater basin to the north, the Downtown, Islais Valley and Visitacion Valley groundwater basins to the east, and the San Mateo Plain subbasin of the Santa Clara Valley groundwater basin to the south. The San Andreas fault forms the western boundary and it serves as the onshore boundary of the South Westside basin. However, the fault extends offshore west of San Francisco so that a portion of the basin lies under the Pacific Ocean. The Pacific Ocean is defined as the administrative western boundary for the North Westside basin.

The primary water-yielding formations within the Westside groundwater basin are the Pliocene to Pleistocene Merced Formation, the Pleistocene Colma Formation, and Quaternary dune sand, which overlay bedrock of the Franciscan Complex (Schlocker, 1974). Lake Merced is the primary surface water body within the groundwater basin (Figure 60). It consists of four individual but connected water bodies (North, South, East and Impound lakes), with a combined surface area of about 1.2 km² (0.46 square miles). Pine Lake (also known as Laguna Puerca), located about 1.3 km (0.8 miles) northeast of Lake Merced, is a shallow, natural lake with an area of about 0.01 km² (0.004 square miles) (Ramirez-Herrera et al., 2007). Groundwater development has primarily occurred in the Colma and Merced Formations, although the deeper Merced Formation is the principal water-producing aquifer in the basin. The shallower Colma Formation is also of interest because Lake Merced and Pine Lake are incised within this formation.

The subsurface configuration of the various geologic units in the Westside basin has been delineated in a series of geologic cross sections based on a combina-

tion of lithologic logs, water well drillers' reports, and geophysical logs (Luhdorff & Scalmanini Consulting Engineers, Inc., 2010). The primary water-yielding units and other significant hydrogeological features in the basin are illustrated schematically in the cross section in Figure 61.

In the North Westside basin, there are up to three aquifer units separated by two distinctive fine-grained units (aquitards): the -30-meter (-100-foot) clay and the W-Clay (LSCE, 2010). The aquifer units are generally designated as Shallow, Primary Production, and Deep:

- The Shallow (S) aquifer, which is present to an elevation of approximately -30 m (-100 ft) North American Vertical Datum of 1988 (NAVD88) (located above the -30-meter (-100-foot) clay) in the vicinity of Lake Merced and in the southern portion of the Sunset District of San Francisco
- The Primary Production (PP) aquifer overlies the W-Clay
- The Deep (D) aquifer underlies the W-Clay

In the Daly City area of the South Westside Basin, the -30-meter (-100-foot) clay is absent, and the aquifer system is primarily composed of the Primary Production aquifer and the Deep aquifer (Figure 61). In the South San Francisco area, the W-Clay is absent and the Primary Production aquifer is split into shallow and deep units, separated by a fine-grained unit at an elevation of approximately -91 m (-300 ft) NAVD88. The Primary Production aquifer in the San Bruno area is located at an elevation less than -61 m (-200 ft) NAVD88, and it underlies a thick, surficial fine-grained unit comprised of clay, sandy clay and sand beds (LSCE, 2010). A southward-extending ridge of Franciscan bedrock appears to separate San Bruno from the San Francisco Bay to the east. The upper fine-grained beds in the San Bruno area appear to be Holocene to late Pleistocene estuarine deposits of the San Francisco Bay (LSCE, 2004).

Groundwater generally occurs in the Shallow aquifer under water table (i.e., unconfined) conditions. Semi-confined conditions occur with increasing depth within the Primary Production aquifer. Groundwater occurs in the Deep aquifer under confined conditions (LSCE, 2010; San Francisco Water Power Sewer, 2016).

In the North Westside basin, the primary groundwater flow direction in both the Shallow and Primary Production aquifers is to the west, following the topography.

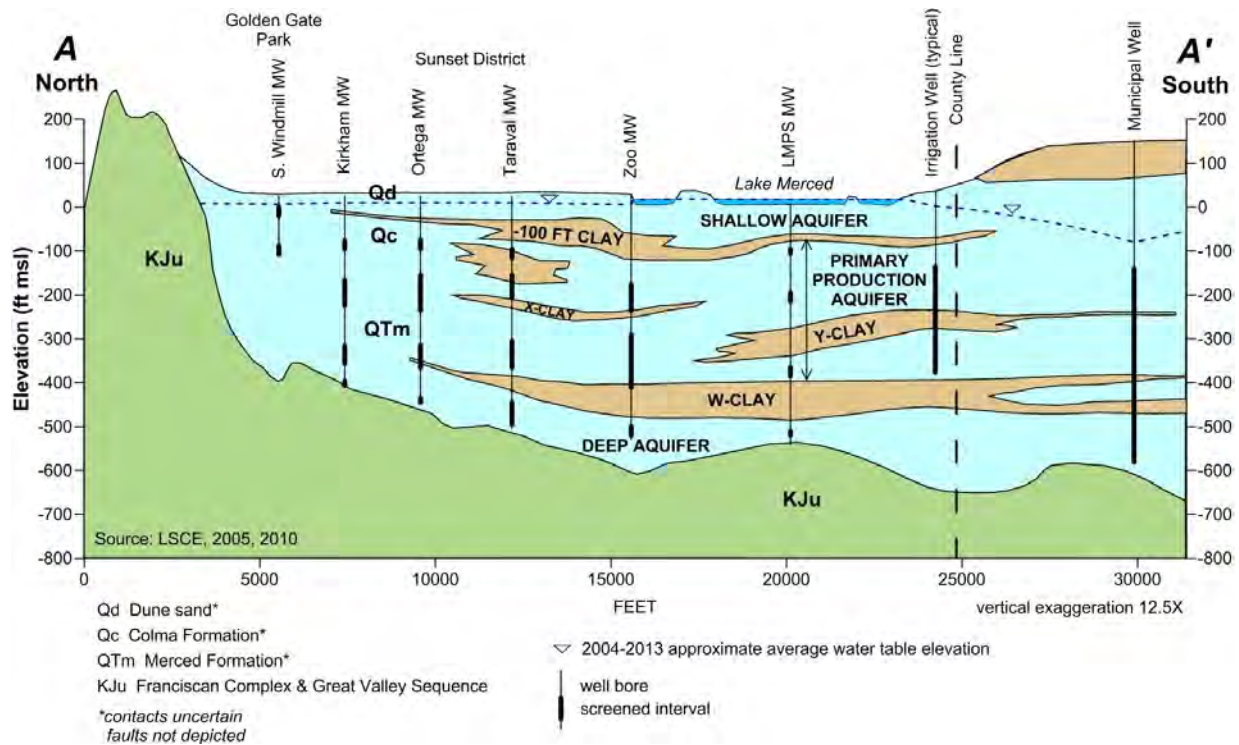


Figure 61. Geologic cross section of North Westside basin. See line of cross section on Figure 62 (San Francisco Water Power Sewer, 2016).

In the Shallow aquifer from the northern part of Lake Merced to the county line, the general groundwater flow direction trends to the southwest. In the Primary Production aquifer, the general groundwater flow direction trends to the southwest in the northern part of Lake Merced and then to the south-southeast in the southern part of Lake Merced and Daly City (SFPUC, 2018f). In the South Westside basin, the primary groundwater flow direction in the Primary Production aquifer is toward areas where municipal groundwater pumping is concentrated and away from non-pumping areas (SFPUC, 2018f).

Sources of groundwater recharge to the Westside groundwater basin include infiltration of rainfall, infiltration of irrigation water, and leakage from water and sewer pipes. The best information on groundwater recharge in the Westside basin is the volumetric water budget analysis found in the most recent version of the “Westside Basin Groundwater-Flow Model” (HydroFocus, 2017). Groundwater recharge in the North Westside basin for the period of 2003 to 2014 was approximately 9 million m³/yr (7,300 acre-ft/yr). In contrast a groundwater recharge estimate in the North Westside basin for water years 1987 and 1988, a drier than normal period, was about 5.9 million m³/yr (4,800

acre-ft/yr) (Phillips et al., 1993). Groundwater recharge in the South Westside basin for the period of 2003 to 2014 was approximately 5.4 million m³/yr (4,400 acre-ft/yr) (HydroFocus, 2017).

The volumetric water budget in the Westside basin model also provides estimates of subsurface outflow and the net change in groundwater storage (HydroFocus, 2017). Approximately 4.1 million m³/yr (3,300 acre-ft/yr) of groundwater left the North Westside basin as subsurface outflow beneath the Pacific Ocean, for the period of 2003 to 2014. Also, about 2.2 million m³/yr (1,800 acre-ft/yr) of groundwater flowed from the North Westside basin to the South Westside basin as subsurface outflow for the same time period. Groundwater storage in the North Westside basin increased by approximately 580,000 m³/yr (470 acre-ft/yr) for the period of 2003 to 2014. Groundwater storage in the South Westside basin increased by about 2.5 million m³/yr (2,010 acre-ft/yr) for the same time period.

Groundwater in the Westside basin has been pumped for municipal water supply for over 100 years (Bartell, 1913). The historical development of municipal groundwater pumpage is discussed in the annual Westside basin groundwater monitoring reports (SF-

PUC, 2018f). In the North Westside basin, the principal groundwater use has been by the San Francisco Recreation and Park Department for irrigation and other non-potable uses in Golden Gate Park and the San Francisco Zoo. However, groundwater from the Sunset Well Field was used for domestic water supply during a dry period of approximately five years in the 1930s. In the South Westside basin, the cities of Daly City, South San Francisco (supplied by the California Water Service Company, known as Cal Water), and San Bruno have relied on groundwater for a substantial part of their municipal supply. Municipal groundwater pumping in these areas increased in the 1950s as a result of increased suburban development.

Groundwater also has been produced by private pumpers for irrigation use. Three golf clubs in the Lake Merced area (one in San Francisco, two in Daly City) relied exclusively on groundwater to irrigate their golf courses until late 2004, when Daly City began furnishing tertiary-treated recycled water for irrigation. This recycled water supply has largely substituted for groundwater, although some groundwater is still pumped (SFPUC, 2018f). In addition, approximately 2.4 km² (0.93 square miles) of cemeteries in Colma and two additional golf clubs in the South Westside Basin use groundwater for irrigation. Their estimated groundwater use is summarized in the annual Westside basin groundwater monitoring reports (SFPUC, 2018f).

The municipal use of groundwater by San Francisco, Daly City, Cal Water (South San Francisco) and San Bruno is summarized in the annual Westside basin groundwater monitoring reports (SFPUC, 2018f). The volumetric water budget analysis in the Westside basin model also provides an average estimate of groundwater pumpage for both municipal and private pumpers (HydroFocus, 2017). The average groundwater pumpage in the North Westside basin was approximately 5,700 m³/day (1.5 mgd) for the period of 2003 to 2014. The average groundwater pumpage in the South Westside basin was approximately 19,000 m³/day (5.0 mgd) for this same period.

In the North Westside basin, the SFPUC is implementing the San Francisco Groundwater Supply Project, which eventually will produce an average of up to 15,120 m³/day (4 mgd) of groundwater. Groundwater production under this project began in 2017. The six municipal wells that are part of this project are shown on Figure 62. In the South Westside basin, the SFPUC

in partnership with Daly City, Cal Water (South San Francisco) and San Bruno are developing the Regional Groundwater Storage and Recovery Project. This is a conjunctive use project designed to supplement dry-year water supplies. It will rely on *in lieu* recharge during normal and wet years and tapping of banked groundwater storage during dry years.

Groundwater in the vicinity of Lake Merced and north to Golden Gate Park is encountered at relatively shallow depths, ranging from approximately 1.5 to 18 m (5 to 60 ft) below ground surface (bgs). South of Lake Merced, the depth to groundwater can exceed 91 m (300 ft) bgs. Since 2000, SFPUC in cooperation with Daly City, Cal Water and San Bruno have conducted monitoring of groundwater levels and quality using a comprehensive well network (SFPUC, 2018f). The monitoring wells in the North Westside basin that are part of this network are shown on Figure 62. Eleven wells in San Francisco (IDs 47806 through 47816) and eight wells in northern San Mateo County (IDs 48974 through 48980 and 49246) are included in the CASGEM program for this basin (CASGEM, 2018). They have been monitored as part of the CASGEM program from fall 2011 to present. These CASGEM wells have been part of the Westside basin groundwater monitoring program for a longer time period (SFPUC, 2018f).

Because the wells in the Westside basin groundwater monitoring program are located throughout the basin and monitor different depths/aquifers, groundwater levels and their fluctuations over time are quite variable. Water level hydrographs help illustrate these conditions, which are a function of the hydrogeologic framework of the Westside groundwater basin and the net change in groundwater storage over time. The net change in storage varies as a function of changes in groundwater recharge, subsurface inflow and outflow, and groundwater pumpage. The annual Westside basin groundwater monitoring reports display hydrographs for all active wells in the groundwater-level monitoring program (SFPUC, 2018f). A comprehensive hydrograph analysis of several sets of monitoring well “clusters” in the North Westside basin is provided in the draft “North Westside Basin Groundwater Sustainability Plan” (San Francisco Water Power Sewer, 2016). A monitoring well cluster consists of multiple wells targeting discrete depth intervals at a single location. Figure 63 illustrates hydrographs for three well clusters near the Pacific Ocean in the North Westside basin. Each cluster

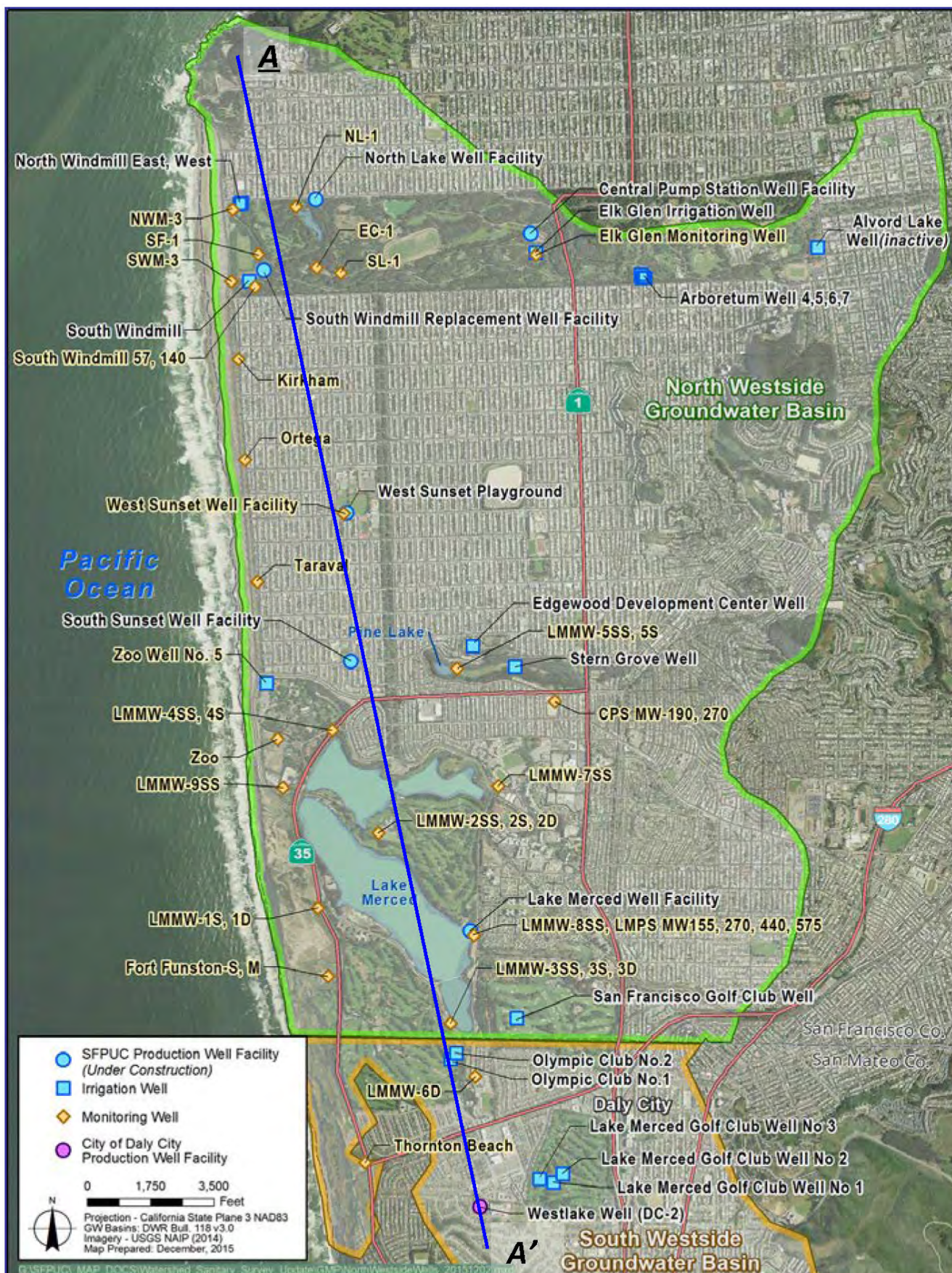


Figure 62. North Westside groundwater basin (San Francisco Water Power Sewer, 2016).

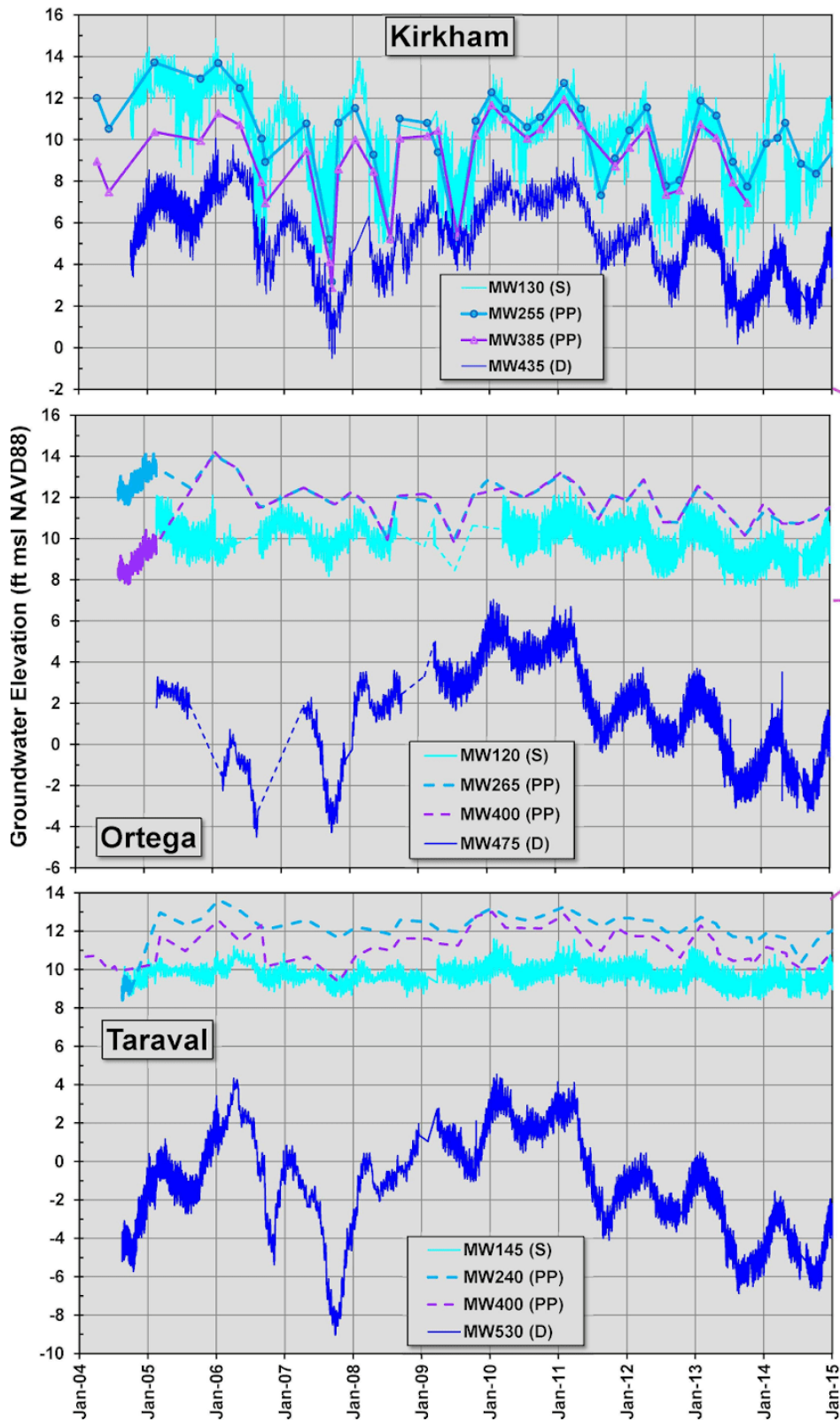


Figure 63. Hydrographs for selected coastal groundwater monitoring wells (location shown in Figure 62) (SFPUC, 2018f).

contains one well screened in the Shallow aquifer, two wells screened at different depths in the Primary Production aquifer, and one well screened in the Deep aquifer. The locations of these well clusters are shown in Figure 62. Figure 64 shows hydrographs of two wells with longer well screens (compared to a cluster well) in the Primary Production aquifer, one at the West Sunset Playground in the central part of the North Westside basin (Figure 62) and the other in South San Francisco.

Groundwater quality data for monitoring wells in the Westside basin groundwater monitoring program, as well as some active and inactive production wells, are

presented in the annual Westside basin groundwater monitoring reports (SFPUC, 2018f). In addition, the draft “North Westside Basin Groundwater Sustainability Plan” (San Francisco Water Power Sewer, 2016) provides groundwater quality data collected during initial testing of SFPUC municipal production wells in the North Westside Basin, as well as an analysis of groundwater ionic types (San Francisco Water Power Sewer, 2016). In general, groundwater in the North Westside basin is a magnesium–bicarbonate or a mixed cation (i.e., calcium, magnesium or sodium not dominant)–bicarbonate type, and is generally hard. Groundwater in the South Westside basin generally

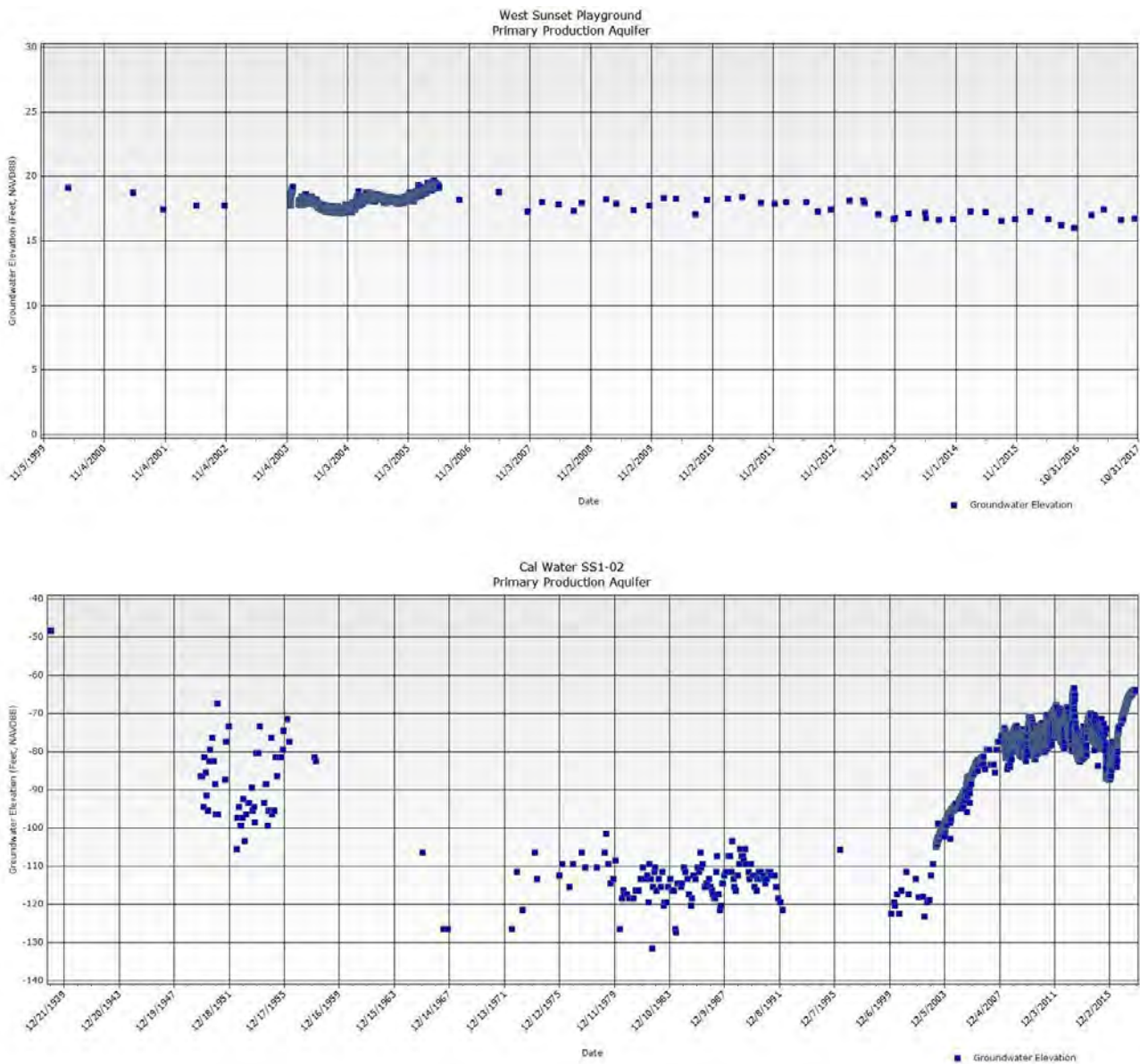


Figure 64. Long term hydrographs for long screened wells in Primary Production Aquifer (SFPUC, 2018f).

shows no dominant cation, and the majority anion is either bicarbonate or chloride. The groundwater in the South Westside basin commonly is more mineralized (i.e., higher concentrations of total dissolved solids and major ions) and harder than groundwater in the North Westside basin (SFPUC, 2018f).

Elevated concentrations of nitrate are common in the Shallow aquifer (SFPUC, 2018f) and some areas of the South Westside basin in the Primary Production aquifer. Nitrate in groundwater from the SFPUC production wells will be diluted when it is blended with surface water municipal supplies well below the maximum contaminant level (MCL).

Manganese is found in some wells screened in the Primary Production and Deep aquifers at concentrations that exceed the MCL. Blending of groundwater from the SFPUC production wells with surface water municipal supplies will lower manganese concentrations to well below the secondary MCL.

There is a general lack of evidence of seawater intrusion in the North Westside basin (SFPUC, 2018f). Chloride levels in SFPUC municipal production wells and Golden Gate Park irrigation wells in the North Westside basin have not exceeded 48 milligrams per liter (mg/L), well below the recommended secondary MCL of 250 mg/L (San Francisco Water Power Sewer, 2016). Monitoring wells in the North Westside basin will be monitored for chloride in conjunction with the San Francisco Groundwater Supply Project, because of proximity of this increased project pumpage to the Pacific Ocean.

A relatively narrow zone near the Pacific Ocean in San Francisco, as well as around Stow Lake in Golden Gate Park, is very highly susceptible to liquefaction during earthquake shaking. Some areas near Lake Merced are considered highly susceptible to liquefaction during earthquake shaking (USGS, 2018). This susceptibility is due to the relatively shallow depth to groundwater and weakly-consolidated sand deposits in these areas.

Lobos Groundwater Basin

The Lobos groundwater basin is located in the northwestern part of San Francisco (Figure 60). The basin is located primarily within parts of the Richmond district and Presidio neighborhoods. Bedrock topographic highs separate the Lobos basin from the Westside groundwater basin to the south, the Marina groundwater basin to the northeast, and the Downtown groundwater

basin to the east. The Pacific Ocean forms the northwestern boundary of the basin. Its DWR-assigned basin number is 2-38. The surface area of the basin is 9.6 km² (3.7 square miles) (California DWR, 2003).

The primary water-yielding formations within the Lobos groundwater basin are dune sand and the Colma Formation (Phillips et al., 1993), which overlie bedrock of the Franciscan Complex (Schlocker, 1974). Lobos Creek is the primary surface water body within the groundwater basin, and Lobos Creek's flow of 6,050 m³/day (1.6 mgd) is fed almost entirely by groundwater seepage (SFPUC, 1997).

The primary groundwater flow direction in the basin is northwest, following the topography. The total recharge for the Lobos groundwater basin was estimated as 1.9 million m³/yr (1,570 acre-ft/yr) for water years 1987 and 1988, with recharge due to leakage from municipal water and sewer pipes accounting for about half of the total recharge (Phillips et al., 1993). One well in this basin is included in the CASGEM program (ID 47801). It has been monitored from fall 2011 to present, and groundwater levels have fluctuated by about 4 m (13 ft) over this time period. This well is also permitted as an active groundwater production well. For the most recent readings in 2017, the depth to water in this well was approximately 13 m (42 ft) below ground surface (CASGEM, 2018). Another active permitted production well in the Lobos Basin is a backup supply well for Kaiser Hospital (DeMarr, 2018). The quantity of groundwater use from these production wells has not been estimated.

The groundwater-fed Lobos Creek is used, after treatment, as the main domestic water supply for the Presidio of San Francisco. Lobos Creek provides about 70 to 80% of the Presidio's potable water needs. Water from Lobos Creek is hard, and it contains nitrate at concentrations less than the MCL. Monitoring of raw water from Lobos Creek has detected low levels of tetrachloroethylene (PCE), although samples of finished water (i.e., post-treatment) have not detected PCE (Presidio Trust, 2018a).

Marina Groundwater Basin

The Marina groundwater basin is the northernmost of the seven groundwater basins in San Francisco (Figure 60). It is separated by bedrock ridges from the Lobos basin to the south and southwest and the Downtown basin to the south and east. San Francisco Bay forms

the northern boundary of the basin. Its DWR-assigned basin number is 2-39. The surface area of the basin is 8.8 km² (3.4 square miles) (California DWR, 2003).

The primary water-yielding formations within the Marina groundwater basin are alluvial fan deposits, hillslope deposits (colluvium), dune sand, and artificial fill (Phillips et al., 1993), which overlay bedrock of the Franciscan Complex (Schlocker, 1974). There are no significant streams or creeks in the basin.

The primary groundwater flow direction is to the north, following the topography. The total recharge for the Marina groundwater basin was estimated as 1.6 million m³/yr (1,341 acre-ft/yr) for water years 1987 and 1988, with recharge due to leakage from municipal water and sewer pipes accounting for about half of the total recharge (Phillips et al., 1993). One well in this basin is included in the CASGEM program (ID 47804). It was monitored from November 2011 to August 2012, and groundwater levels fluctuated by about 0.3 m (1 ft) over this time period. This well is no longer active. For the most recent readings in 2012, the depth to water in this well was approximately 11 m (35 ft) below ground surface (CASGEM, 2018).

There are no known active production wells in the Marina groundwater basin at present (DeMarr, 2018). Based on the general similarity of groundwater quality for all basins beneath the San Francisco Peninsula (Phillips et al., 1993), the groundwater is expected to be a mixed cation–bicarbonate type, and generally hard. Elevated concentrations of nitrate are common, especially at shallower depths (Phillips et al., 1993).

The shallow depth to groundwater expected in the northern part of the Marina groundwater basin, as well as along historical stream channels, makes parts of the Marina basin very highly susceptible to liquefaction during earthquake shaking (USGS, 2018). This area experienced severe property damage due to liquefaction during the 1989 Loma Prieta earthquake.

Visitacion Valley Groundwater Basin

The Visitacion Valley groundwater basin is located in the far southeastern part of San Francisco (Figure 60). San Bruno Mountain bounds it on the southwest. Bedrock ridges that extend northward from San Bruno Mountain to McLaren Park separate the basin from the Islais Valley basin to the northwest and the South San Francisco basin to the north. San Francisco Bay forms the eastern boundary of the basin. Its DWR-assigned

basin number is 2-32. The surface area of the basin is 23.6 km² (9.1 square miles) (California DWR, 2003).

The primary water-yielding formations within the Visitacion Valley groundwater basin are dune sand, the Colma Formation, bay muds, and artificial fill (Phillips et al., 1993), which overlie bedrock of the Franciscan Complex (Schlocker, 1974). There are no significant streams or creeks in the basin.

The primary groundwater flow direction is expected to be toward the east, following the topography. The total recharge for the portion of the Visitacion Valley groundwater basin in San Francisco was estimated as 332,000 m³/yr (269 acre-ft/yr) for water years 1987 and 1988. Sources of recharge include rainfall, landscape irrigation, and leakage from water and sewer pipes (Phillips et al., 1993). No wells in this basin have been included in the CASGEM program (CASGEM, 2018).

There are two active permitted production wells in the Visitacion Valley groundwater basin, one located at a residence and the other for irrigation of a city greenway (DeMarr, 2018). The quantity of groundwater use from these production wells has not been estimated. Based on the general similarity of groundwater quality for all basins beneath the San Francisco Peninsula (Phillips et al., 1993), the groundwater is expected to be a mixed cation–bicarbonate type, and generally hard. Elevated concentrations of nitrate are common, especially at shallower depths (Phillips et al., 1993).

The expected shallow depth to groundwater and artificial fill in the eastern part of the Visitacion Valley groundwater basin, east of Bayshore Boulevard, makes this part of the Visitacion Valley basin very highly susceptible to liquefaction during earthquake shaking (USGS, 2018).

Downtown Groundwater Basin

The Downtown groundwater basin is located in the northeastern part of San Francisco (Figure 60). Bedrock ridges and subsurface bedrock highs separate the Downtown basin from the Lobos and Westside groundwater basins to the west, Marina basin to the north, and Islais Valley basin to the south. San Francisco Bay forms the eastern boundary of the basin. Its DWR-assigned basin number is 2-40. The surface area of the basin is 30.8 km² (11.9 square miles) (California DWR, 2003).

The primary water-yielding formations within the

Downtown groundwater basin are dune sands and the Colma Formation with a maximum saturated thickness of approximately 53 m (175 ft) (King and Zamboanga, 1994). These formations overlie bedrock of the Franciscan Complex (Schlocker, 1974). Aquifers are primarily silty sand (King and Zamboanga, 1994).

Mission Creek and its tributaries historically were the primary surface water bodies within the Downtown groundwater basin, and they extended eastward into extensive tidal marshes along San Francisco Bay. Hayes Creek was another historical creek that flowed intermittently and into a tidal marsh. Today these creeks are underground (Ramirez-Herrera et al., 2007).

The primary groundwater flow direction is northeast, following the topography (California DWR, 2003). The total recharge for the Downtown groundwater basin was estimated as 7.3 million m³/yr (5,931 acre-ft/yr) for water years 1987 and 1988, with recharge due to leakage from municipal water and sewer pipes accounting for about half of the total recharge (Phillips et al., 1993). One well in this basin is included in the CASGEM program (ID 47805). It was monitored from October 2011 to April 2013, and groundwater levels fluctuated by less than 0.3 m (1 ft) over this time period. This well is no longer active. For the most recent reading in 2013, the depth to water in this well was approximately 10 m (33 ft) below ground surface (CASGEM, 2018). Historically, groundwater levels measurements taken from 1988 to 1992 in other wells indicated little to no seasonal fluctuations (California DWR, 2003).

There are three active permitted production wells in the Downtown groundwater basin: one is a backup supply well for a hospital, another is a backup supply well for a car wash, and the third is located at the Yerba Buena Gardens city park (DeMarr, 2018). The quantity of groundwater use from these production wells has not been estimated. A field investigation of the Downtown groundwater basin conducted in 1993–1994 as part of the San Francisco Groundwater Master Plan Project identified 22 active wells and sumps. The sumps were for dewatering, and all of the wells were for non-potable uses, including toilets, boilers, laundry, fountains, and irrigation. Pumping rates from the wells ranged from 164 to 273 m³/day (30 to 50 gpm) in the deeper portions of the basin, and from 27 to 54 m³/day (5 to 10 gpm) near the bedrock boundaries of the basin. The largest water use in the Downtown groundwater basin was the dewatering sump at the Powell Street

BART station, which averaged about 490,000 m³/yr (400 acre-ft/yr). Other groundwater uses at the time of the investigation totaled about 123,000 m³/yr (100 acre-ft/yr)⁵ (King and Zamboanga, 1994).

Groundwater samples were collected and analyzed from 20 wells and sumps. Based on these samples, the groundwater was mixed cation–bicarbonate type, and generally hard. Low to moderate concentrations of nitrate were present. Total coliform was present in 3 of 18 wells that were sampled for coliform; fecal coliform was not present. Iron and/or manganese concentrations that exceeded the secondary maximum contaminant level (MCL) were found in 11 of the 20 wells that were sampled (King and Zamboanga, 1994).

An additional water quality evaluation of the Downtown groundwater basin was conducted in 2000 to support the California Regional Water Quality Control Board’s proposal (at that time) to de-designate the beneficial domestic use of the basin’s groundwater (Pezzetti and Waer, 2000). The general water quality observed in samples from wells representative of background groundwater conditions was similar to that found in the San Francisco Groundwater Master Plan Project. Exceptions included detections of barium and volatile organic compounds, all at concentrations below their respective MCLs (Pezzetti and Waer, 2000).

Dewatering sumps at six locations in the Downtown groundwater basin were studied further to evaluate the feasibility of beneficially using these supplies for non-potable purposes to offset potable water use (Parulekar and Kennedy, 2011). Groundwater quality conditions were similar to those found in the previous field investigations discussed above. Groundwater production at each site was evaluated based on records of discharges to the San Francisco combined sewer system. The groundwater production from the dewatering sump at the Powell Street BART station averaged about 657 m³/day (120 gpm), which is about half the 1994 rate noted above from the San Francisco Groundwater Master Plan Project.

The part of the Downtown groundwater basin generally south of Market Street is very highly susceptible to liquefaction during earthquake shaking (USGS, 2018). This susceptibility is due to the expected shallow depth to groundwater and areas underlain by bay mud,

⁵Groundwater use does not include about 370,000 m³/yr (300 acre-ft/yr) for construction dewatering at the (new) San Francisco Library site in the Civic Center area.

other marsh deposits, artificial fill, and alluvium along Mission Creek, Hayes Creek, and other historical creek channels (Figure 51).

Islais Valley Groundwater Basin

The Islais Valley groundwater basin is located in the south-central part of San Francisco (Figure 60). Bedrock ridges that include Mt. Davidson and Twin Peaks separate the basin from the Westside basin to the west. Bedrock topographic highs separate the Islais Valley basin from the Downtown groundwater basin to the north and the Visitacion Valley and South San Francisco groundwater basins to the south. San Francisco Bay forms the eastern boundary of the basin. Its DWR-assigned basin number is 2-33. The surface area of the basin is 24 km² (9.3 square miles) (California DWR, 2003).

The primary water-yielding formations within the Islais Valley groundwater basin are dune sand, the Colma Formation, bay muds, and artificial fill (Phillips et al., 1993), which overlie bedrock of the Franciscan Complex (Schlocker, 1974). Islais Creek historically was the primary surface water body within the Islais Valley groundwater basin, and it extended southwestward along the general area that today is Alemany Boulevard. A branch of Islais Creek is free-flowing in Glen Canyon Park in the northwestern part of the basin; however, downstream of the park Islais Creek flows underground to San Francisco Bay (Ramirez-Herrera et al., 2007).

The primary groundwater flow direction is expected to be toward the east, following the topography. The total recharge for the Islais Valley groundwater basin was estimated as 2.2 million m³/yr (1,836 acre-ft/yr) for water years 1987 and 1988. Sources of recharge include rainfall, landscape irrigation, and leakage from water and sewer pipes (Phillips et al., 1993). One well in this basin is included in the CASGEM program (ID 47802). It has been monitored from fall 2011 to present, and groundwater levels have fluctuated by about 0.6 m (2 ft) over this time period. For the most recent readings in 2017, the depth to water in this well was approximately 15 m (48 ft) below ground surface (CASGEM, 2018).

There is one active permitted production well in the Islais Valley groundwater basin, located at a residence (DeMarr, 2018). The quantity of groundwater use from this production well has not been estimated. Based on the general similarity of groundwater quality for all

basins beneath the San Francisco peninsula (Phillips et al., 1993), the groundwater is expected to be a mixed cation–bicarbonate type, and generally hard. Elevated concentrations of nitrate are common, especially at shallower depths (Phillips et al., 1993).

Parts of the Islais Valley groundwater basin generally east of U.S. Highway 101 are very highly susceptible to liquefaction during earthquake shaking (USGS, 2018). This susceptibility is due to the expected shallow depth to groundwater, and poor geotechnical properties of the underlying bay muds, other marsh deposits, and extensive areas of artificial fill (Figure 51).

South San Francisco Groundwater Basin

The South San Francisco groundwater basin (also known as South groundwater basin) is located in the south-central part of San Francisco (Figure 60). Bedrock topographic highs separate the South San Francisco basin from the Islais Valley groundwater basin to the north and west and the Visitacion Valley groundwater basin to the south. San Francisco Bay forms the basin boundary along its entire eastern extent. Its DWR-assigned basin number is 2-37. The surface area of the basin is 8.8 km² (3.4 square miles) (California DWR, 2003).

The primary water-yielding formations within the South San Francisco groundwater basin are dune sand, the Colma Formation, bay muds and artificial fill (Phillips et al., 1993), which overlie bedrock of the Franciscan Complex (Schlocker, 1974). Yosemite Creek historically was the primary surface water body within the South San Francisco groundwater basin, and it extended eastward to San Francisco Bay. Today most of this creek is underground, although there are small free-flowing tributaries in John McLaren Park in the western part of the basin. Springs issuing from bedrock in McLaren Park feed McNab Lake and Yosemite Marsh (Ramirez-Herrera et al., 2007).

The primary groundwater flow direction is expected to be toward the east, following the topography. The total recharge for the South San Francisco groundwater basin was estimated as 859,000 m³/yr (696 acre-ft/yr) for water years 1987 and 1988. Sources of recharge include rainfall, landscape irrigation, and leakage from water and sewer pipes (Phillips et al., 1993). One well in this basin is included in the CASGEM program (ID 47803). It has been monitored from fall 2011 to present, and groundwater levels have fluctuated by about 1 m (3

ft) over this time period. For the most recent readings in 2017, the depth to water in this well was approximately 0.3 m (1 ft) below ground surface (CASGEM, 2018).

There is one active permitted production well in the South San Francisco groundwater basin, located at a residence (DeMarr, 2018). The quantity of groundwater use from this production well has not been estimated. Based on the general similarity of groundwater quality for all basins beneath the San Francisco peninsula (Phillips et al., 1993), the groundwater is expected to be a mixed cation–bicarbonate type, and generally hard. Elevated concentrations of nitrate are common, especially at shallower depths (Phillips et al., 1993).

Parts of the South San Francisco groundwater basin generally east of 3rd Street are very highly susceptible to liquefaction during earthquake shaking (USGS, 2018). This susceptibility is due to the expected shallow depth to groundwater in the lower elevations parts of the Bayview and Hunters Point districts, and poor geotechnical properties of the underlying bay muds and artificial fill (Figure 51).

ENVIRONMENTAL CONCERNS

by Greg W. Bartow, Lori A. Simpson, Dorinda Shipman, Sally Goodin, Darrell Klingman, William E. Motzer, George Ford

San Francisco contains a variety of environmental cleanup sites that include leaking underground fuel tanks, historic manufactured gas plants, historic railroad operations, and closed military bases. This section summarizes the general regulatory setting and provides an overview of some of the major sites and cleanup issues.

Regulatory Setting

Environmental cleanup sites in San Francisco are regulated by a combination of local, state, and federal agencies. Investigation and cleanup of leaking underground fuel storage tanks is regulated by the San Francisco Department of Public Health, which is delegated this responsibility from the State Water Resources Control Board.

Non-Fuel Cleanup Program Sites (formerly known as Spills, Leaks, Investigations, and Cleanups [SLIC] sites) are typically overseen by the San Francisco Bay Regional Water Quality Board, a state agency under the

State Water Resources Control Board. However, both the California Department of Toxic Substances Control and Regional Water Quality Boards have overlapping jurisdiction for such sites, including so-called “brown-field sites,” which can be any property where reuse or redevelopment is hampered because of known or perceived environmental contamination. Both agencies have Voluntary Cleanup Programs that allow owners of contaminated properties to petition for a lead agency and pursue voluntary oversight of site cleanup.

There are three large closed military bases in San Francisco that are undergoing investigation and cleanup (former Hunters Point Naval Ship Yard, former Treasure Island Naval Ship Yard, and former Presidio Army Base). These sites are described below and are under the oversight of the U.S. EPA in coordination with the California Department of Toxic Substances Control, San Francisco Bay Regional Water Quality Board and San Francisco Department of Public Health.

GeoTracker

GeoTracker is the State Water Resources Control Board’s Internet-accessible database system used by the State Board, regional boards, and local agencies to track and archive compliance data from authorized or unauthorized discharges of waste to land, or unauthorized releases of hazardous substances from underground storage tanks (<http://geotracker.waterboards.ca.gov/>). This system contains online compliance reports, a geographical information system interface, and other features utilized by regulatory agencies, the regulated industry, and the public to input, manage, or access compliance and regulatory tracking data (See Figure 65 for example).

Maher Ordinance

The Maher Ordinance originally applied to cleanup sites in San Francisco located in areas of historic bay fill. However, in 2015, the Maher Ordinance was expanded and now applies to the characterization and mitigation of hazardous substances in soil and groundwater in designated areas zoned for industrial uses, sites with industrial uses or underground storage tanks, sites with historic bay fill, and sites in close proximity to freeways or underground storage tanks (Figure 66). The Maher Ordinance is implemented by the San Francisco Department of Public Health pursuant to San Francisco Health Code, Article 22A.

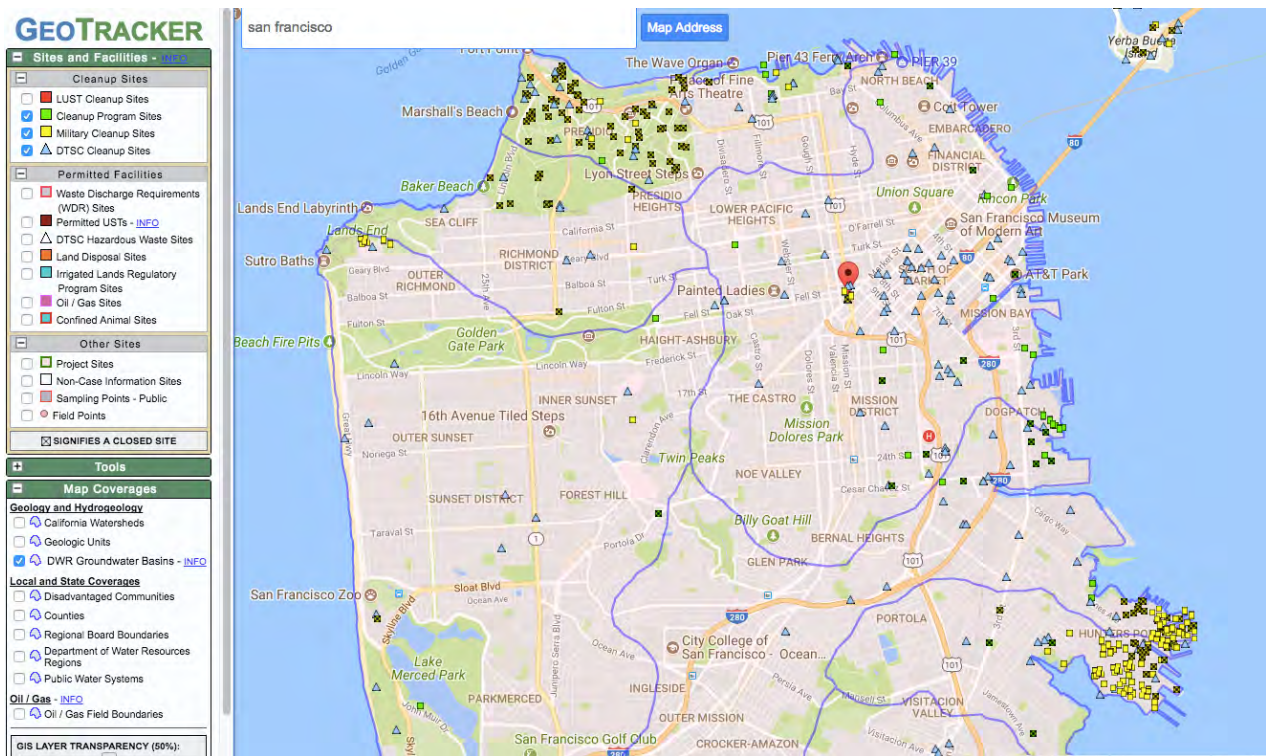


Figure 65. Map generated from GeoTracker showing location of Cleanup Program Sites, Military Cleanup Sites, and DTSC Cleanup Sites (<http://geotracker.waterboards.ca.gov>).

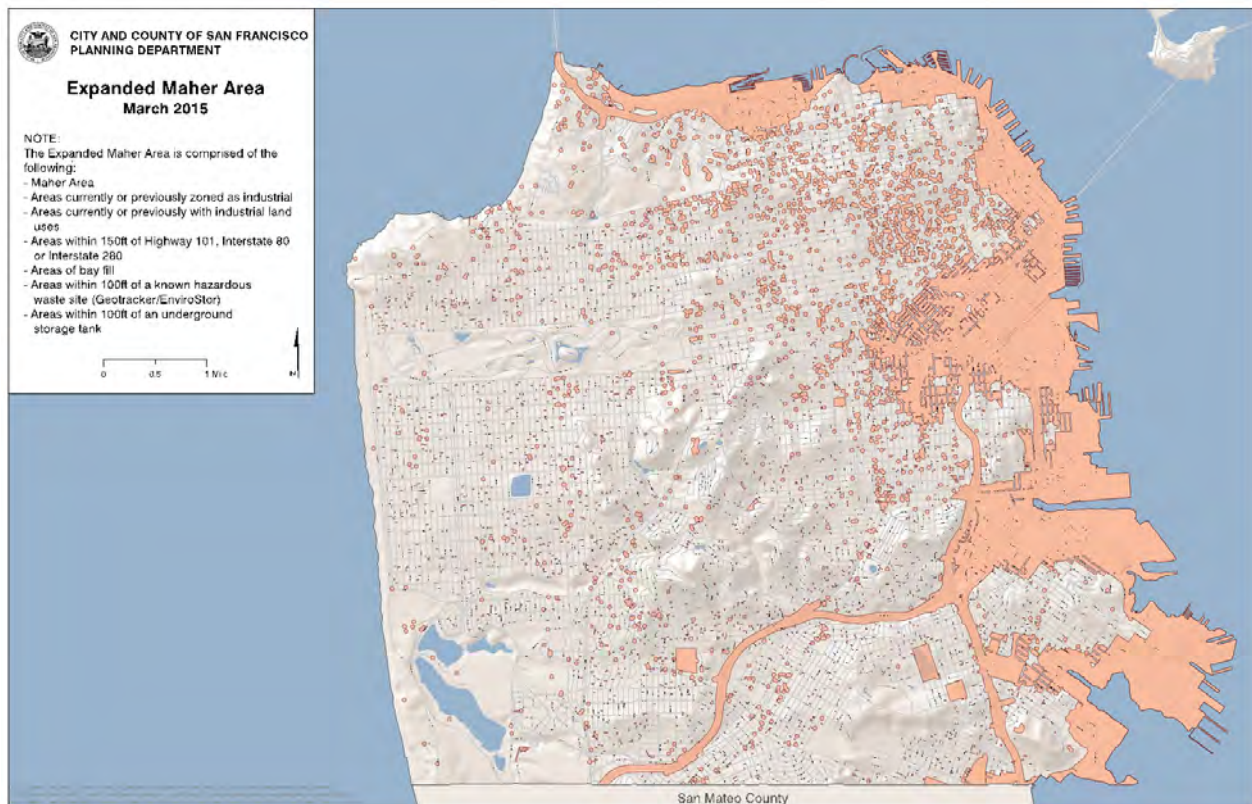


Figure 66. Map of areas of San Francisco subject to the Maher Ordinance for characterization and mitigation of hazardous substances in soil and groundwater (City and County of San Francisco Planning Department).

Hunters Point Naval Shipyard

The Hunters Point Naval Shipyard is located in southeastern San Francisco, adjacent to San Francisco Bay. The Shipyard consists of 3.5 km² (1.35 square miles): 1.7 km² (0.66 square miles) on land and 1.8 km² (0.69 square miles) under water in San Francisco Bay. The U.S. EPA (2017) provides extensive background on the history of the Hunter’s Point Naval Shipyard and environmental cleanup.

Hunters Point was originally a private, commercial dry dock facility from 1869 to 1939, when the Navy purchased the property. The natural landscape of Hunters Point was significantly changed by extensive grading and flattening of the rocky hills and filling of the shoreline areas during the World War II and postwar periods. From 1945 until 1974, the Navy predominantly used the shipyard as a naval submarine and ship repair facility. At the height of operations, approximately 8,000 civilian workers were employed at the Shipyard. In addition to serving as a repair facility, the Shipyard was also the site of the Naval Radiological Defense Laboratory (NRDL) from 1948 to 1969. The purposes of the NRDL included radiological decontamination of ships exposed to atomic weapons testing as well as research and experiments on radiological decontamination, the effect of radiation on living organisms, and the effects of radiation on materials. In 1974, the Navy ceased shipyard operations, placing the Shipyard in industrial reserve. From 1976 to 1986, the Navy leased most of the Shipyard to a commercial ship repair facility.

Cleanup Program at the Shipyard

In 1989, the U.S. EPA placed the Shipyard on its National Priority List which is a list of Federal Superfund Sites in the United States. The cleanup program at the Shipyard is conducted by the Navy. After each parcel is cleaned up, it is transferred to the local reuse authority, the San Francisco Office of Community Investment and Infrastructure, to allow for development for public and private uses. At many locations throughout the Shipyard, groundwater, bay sediments, and soil are contaminated with petroleum fuels, pesticides, heavy metals (such as lead and zinc), polychlorinated biphenyls (PCBs), or volatile organic compounds (VOCs). Much of the soil at the Shipyard originated from grading and flattening the nearby hills containing rock and soil known as serpentinite. Serpentinite rock contains naturally occurring asbestos and metals such as iron,

nickel, zinc, and manganese. Likely due to the activities of the NRDL, radionuclides such as radium-226, cesium-137, and strontium-90 have been detected in low concentrations and small quantities in soil, presumably from leakage from storm drains and sewers used by NRDL or, in the case of commodities removed from vessels and mostly disposed of in discrete identified areas, from the radionuclide-containing paint (i.e., either radium-226 or strontium-90) that was used to make the commodities glow-in-the-dark.

The investigation and cleanup of contamination at the Shipyard is a multi-phase project that has been ongoing for more than 30 years. Investigations and testing of soil and groundwater at the Shipyard are targeted at known industrial operational areas and where Navy records indicate a known or potential release of hazardous substances. The Navy has issued the Record of Decision (ROD) documents detailing the planned cleanup actions for all but one parcel (i.e., Parcel F-ROD planned for end of 2018) across the Shipyard to address known soil and groundwater contamination. As of mid-2017, these cleanup actions have resulted in the transfer of four parcels to the City of San Francisco, removal of 45 km (28 miles) of sewer and storm drain lines, removal of more than 31,000 truckloads of soil from cleanup operations, and treatment of 32.5 million liters (8.6 million gallons) of groundwater.

The latest Draft Hunters Point Shipyard Redevelopment Plan (Figure 67) calls for a mix of residential, open space, commercial, and an artist complex (San Francisco Redevelopment Agency, 2018).

Treasure Island Naval Shipyard

Treasure Island Naval Shipyard consists of two contiguous islands: Treasure Island to the north, and Yerba Buena Island to the south. As described in the “Major Engineering Projects” section below, Treasure Island is a man-made island and was constructed of sediments dredged from San Francisco Bay. Yerba Buena Island is a natural island. The Navy acquired Treasure Island by condemnation in 1942. Military activities at Treasure Island date back to 1866 when the U.S. Government took possession of Yerba Buena Island for defensive fortifications. During World War II, Treasure Island became a major naval facility, processing approximately 12,000 military personnel per day for service overseas and upon their return to the United States. Treasure Island Naval Shipyard was closed in 1997 as part of



Figure 67. Draft 2018 Hunters Point Shipyard Redevelopment Plan (City and County of San Francisco Office of Community Investment and Infrastructure, 2018).

the nationwide Base Realignment and Closure Program (Naval Facilities Engineering Command, 2018, US EPA, 2018).

The initial facility-wide Preliminary Assessment/Site Investigation was conducted in 1987 to identify areas on Treasure Island that required further investigation due to possible contamination in soil, sediment, and/or groundwater. As of 2015, the Navy has identified 33 environmental sites on Treasure Island and Yerba Buena Island including a former fire training area, a landfill, a former dry-cleaning facility, an old bunker area, fuel farms, and a service station (Figure 68). Contamination in these areas is largely the result of releases of petroleum products from fueling operation/storage areas, training, and storage/disposal of hazardous waste materials. As of 2015, there are 13 closed non-petroleum (Superfund) sites, and 11 open non-petroleum (Superfund) sites. In addition, there are 112 closed petroleum sites and 9 open petroleum sites (Tetra Tech EM Inc., 2015).

The Treasure Island Development Authority (TIDA) is a state agency staffed by the San Francisco mayor’s office and is the entity responsible for planning the

reuse and redevelopment of the former installation. Treasure Island property is transferred from the Navy to TIDA in phases as environmental cleanup actions are completed by the Navy.

Presidio of San Francisco

The Presidio has a rich history spanning back to the time of the native Ohlone people. The Spanish arrived in 1776 to establish the northernmost outpost of their empire in western North America. The Presidio was administered by Mexico for 24 years before the U.S. Army took control in 1846. The U.S. Army administered the property for 148 years from 1846 until 1994, when the land was turned over to the National Park Service (NPS). The post was designated a National Historic Landmark in 1962. The Park Service ceded the interior portions of the park to the newly-formed Presidio Trust in 1998, but retained authority over a narrow strip of coastal land. The Trust and the Park Service continue to administer the park, which totals 6 km² (2.3 square miles) (Figure 69).

The Army’s nearly 150-year tenure had significant

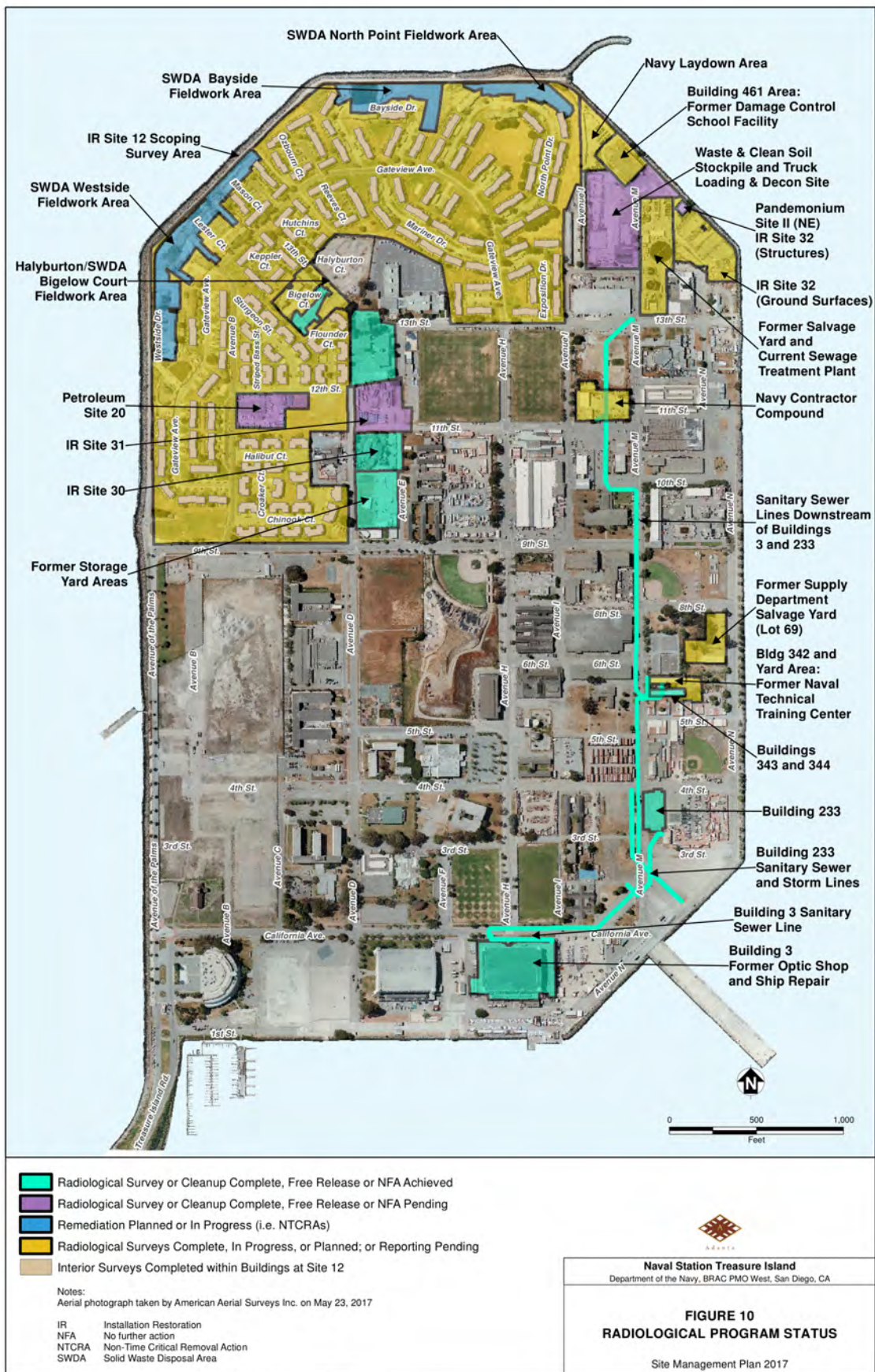


Figure 68. Treasure Island cleanup sites (2017).

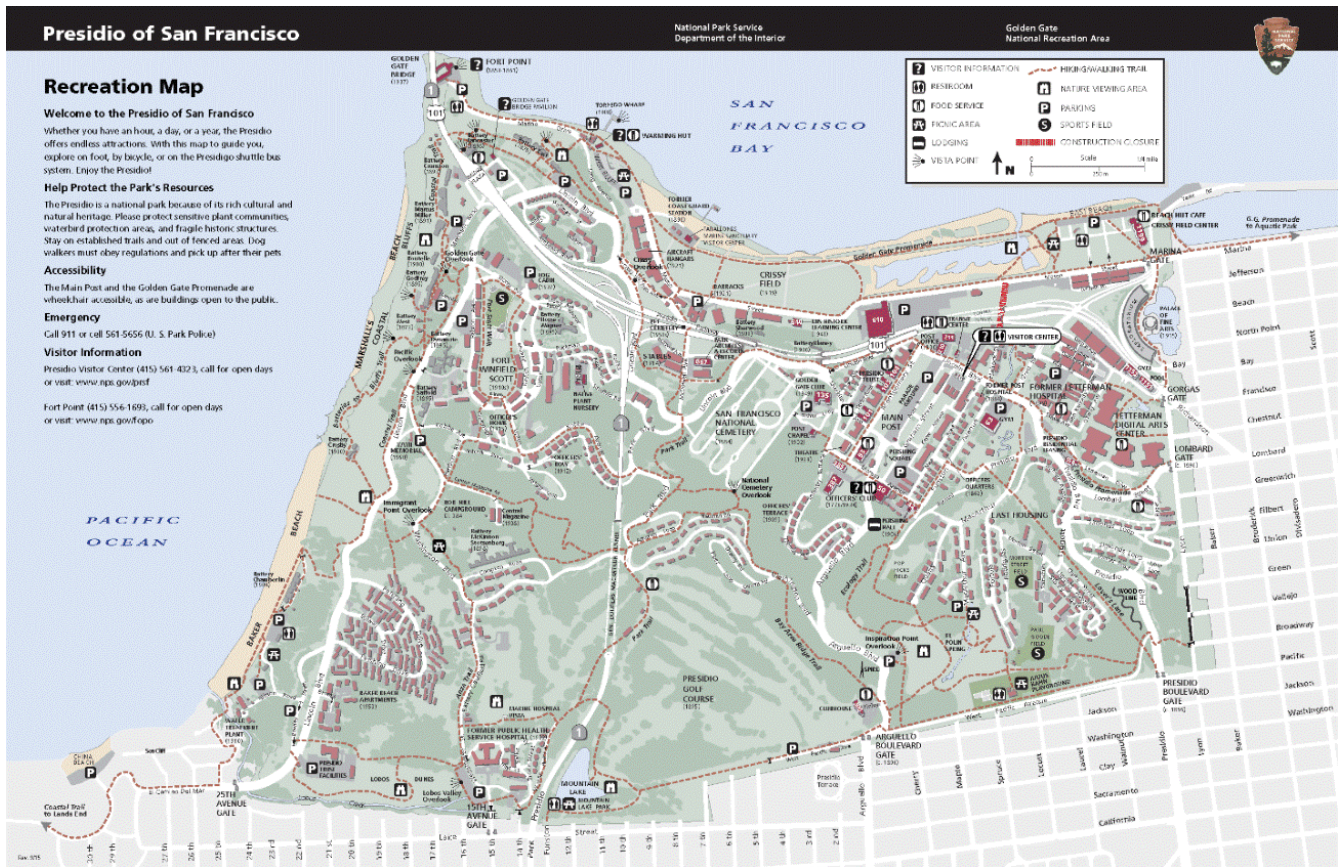


Figure 69. Map of Presidio of San Francisco.

effects on the land. During this period the Army:

- Planted thousands of eucalyptus and Monterey cypress trees, creating forest where scrub-covered dunes once existed;
- Built several generations of coastal artillery batteries to defend the Golden Gate. Many of these batteries remain well-preserved within the park;
- Built nearly 1,000 structures ranging from out-houses to multi-story hospitals and over 500 residential units;
- Operated two separate military bases on the property, resulting in the construction of two of nearly everything—chapels, bowling alleys, officer’s clubs, parade grounds, motor pools, maintenance departments and the like;
- Preserved the post from commercial development; and
- Inadvertently preserved continuous swaths of native vegetation and habitat.

Environmental Issues

The Army began cleaning up environmental hazards in the mid-1990s, starting with removal of many underground tanks and the demolition and removal of many buildings on Crissy Field. These cleanups continued between 1994 and 1998 when the NPS administered the post. In 1999 the Army and the Presidio Trust signed a Memorandum of Agreement transferring responsibility for the cleanup to the Trust upon payment of \$100 million to the Trust. The Trust purchased two environmental insurance policies to cover possible costs exceeding \$100 million. The entire cleanup program took 14 years and eventually cost \$165 million.

Landfills

In the 20th century, the Army began placing demolition debris in canyons within the Presidio. Household garbage was burned in the early days. Later, the Army contracted with local garbage haulers to remove household garbage, but it continued to dispose of construction debris in various canyon and stream-fills. Over the years this practice resulted in 17 identified

landfills, plus smaller accumulations of debris.

Notable landfills include:

- Landfill E in Tennessee Hollow: This former burn-dump (where trash was burned and buried) contained over 38,200 m³ (50,000 yd³) of waste. It was capped in 2012 and a baseball field was restored on top of the cap.
- Landfill 2 at El Polin Spring: 550 non-native trees and 32,900 m³ (43,000 yd³) of waste removed.
- Baker Beach Landfills 1 and 2 on the Baker Beach bluffs: 41,300 m³ (54,000 yd³) removed.
- Baker Beach Landfill 3: 21,400 m³ (28,000 yd³) of construction debris removed.
- Landfill 4 and Fill Site 5: 19,100 m³ (25,000 yd³) of waste removed. Landfill 4 planted as experimental restoration forest, Fill Site 5 restored as native dune scrub habitat.
- Fill Site 6: 6,900 m³ (9,000 yd³) of waste removed, creek daylighted and restored as Thompson Reach natural area.
- Landfills 8 and 10 at head of Lobos Creek drainage: 30,600 m³ (40,000 yd³) of construction debris capped in place.

Petroleum Leaks

The Army used oil heat for most buildings in the Presidio beginning in the 1930s. To supply oil, the Army built an oil distribution system that connected to nearly every occupied building. Fuel oil barges would dock at the west end of Crissy Field and the heavy bunker oil would be cut with diesel to improve flowability. The thinned oil was then pumped up to a tank located on top of a hill adjacent to Lincoln Boulevard. The oil was then fed by gravity through kilometers of small-diameter galvanized pipe leading to each building. Most buildings had a small day tank in the basement or outside. As the distribution system aged, it caused petroleum contamination in many locations:

- Along the feeder pipeline running from the dock to the storage tank,
- Around and below the storage tank,
- Along most of the galvanized distribution pipelines, and
- Around and below the day tanks at most buildings.

Fortunately, the heating oil tended to bind up in the soil immediately surrounding the tank or pipes. In

most cases these spills could be cleaned up by simply digging out the oily soil with an excavator. Long segments of the distribution pipes were capped in place.

Crissy Field

The Army built a large motor pool (vehicle maintenance and storage area) along the south edge of Crissy Field, around the site of the current Sports Basement. The usual leaks of gasoline, diesel motor oil and chlorinated solvents occurred over this area. The Trust performed cleanups in and around this area on several occasions in the 1990s and 2000s.

Another major environmental project undertaken by the Army in 1998–2000 was the removal of 90,000 tons of fill and contaminated soil, which was performed as the initial effort to restore the tidal wetlands that is now known as Crissy Marsh (<https://www.nps.gov/goga/learn/nature/crissy-field.htm>). As part of this work, the Army and Presidio Trust also performed remediation of polynuclear aromatic compounds and lead contaminated soil associated with a former skeet range located on the beach adjacent to Crissy Field.

On the western edge of Crissy Field, a number of contamination issues were identified and addressed in the area around Building 637. This area was termed a Petroleum, Oil and Lubricants area that supported the motor pool for the Army at Crissy Field. Contaminants in this area included solvents, fuels and other hydrocarbon materials. A thorough summary of the issues at the Building 637 Site is presented in Eler and Kalinowski (2004). In addition to this site, a number of other locations in the Presidio were impacted from gas tanks, hydraulic lift cylinders, and a gas station at the foot of Halleck Street near Mason Street.

Shooting Ranges and Artillery Batteries

The Army maintained and operated a number of shooting ranges at the Presidio including the Barnard Avenue protected range, ranges at south edge of Crissy Field, Building 1369 in the Fort Scott area, and near East Battery. These sites were evaluated for lead contamination as a result of their historical use. In most cases the cleanup of lead-contaminated soil was performed by digging out contaminated soil and disposing it offsite.

On the bluffs around the south side of the Golden Gate bridges, artillery batteries were installed as part of the overall defense scheme for San Francisco (Martini,

2016). Many of the batteries have been destroyed; however others remain and are maintained to this day to serve as reminders of the history of the western part of the Presidio (Figure 70).

Mountain Lake

Mountain Lake contained pesticides (probable golf-course runoff) and lead washed into lake from storm drains on adjacent Highway 1. The lake was also affected by years of disposal of non-native animals (goldfish, carp, and even a small alligator) by local residents. The Presidio received a \$10 million settlement from the California Department of Transportation (Caltrans) to help fund the cleanup, which was notable because Caltrans rarely acknowledges responsibility for lead washed off Caltrans roads. In 2013, the lake was hydraulically dredged and the lead-bearing sediment was dewatered, stabilized and disposed offsite. Approximately 10,000 m³ (13,000 yd³) of soil were removed from the lake bed. Sediment-trapping catch basins have since been installed on the storm drains on Highway 1 to prevent contaminated sediments from entering the lake. The lake shore is now being restored as native riparian habitat and the lake has been stocked with native fish and amphibians (Presidio Trust, 2018b).

Mission Bay

Mission Bay is an approximately 1.2 km² (0.46 square miles) parcel in a former industrial part of San Francisco that is currently being redeveloped. The new neighborhood in San Francisco will offer a new UCSF research campus, the UCSF medical center, the new Chase Center and Golden State Warriors arena, 410,000 m² (4.4 million sq ft) of commercial office space, 40,000 m² (430,000 sq ft) of retail space, 6,514 new housing units, a 250-room hotel, and 0.17 km² (42 acres) of open space (Office of Community Investment and Infrastructure (OCII), 2018), as shown on Figure 71.

Mission Bay was originally comprised of a shallow bay, tidal flats, and marshlands (Figure 72). The bay is underlain by soft, compressible clay, known locally as Young Bay Mud, which is as much as 45 m (147.6 ft) thick in Mission Bay. Dense to very dense sand of the Colma Formation and medium stiff to very stiff Old Bay Deposits underlie the Young Bay Mud. Other stratigraphic layers include colluvium and alluvium. Bedrock of the Franciscan Formation is about 1.2 to 76 m (4 to 250 ft) deep. Groundwater is shallow; it is generally encountered about 1.5 to 3 m (5 to 10 ft) below the ground surface, and is tidally influenced.



Figure 70. Endicott batteries at Fort Scott along the former location of West Battery. L to R: Batteries Boutelle, Marcus Miller, Cranston, and Lancaster (John A. Martini Collection).



Figure 71. Mission Bay Land Use Plan (San Francisco Office of Community Investment and Infrastructure).



Figure 72. 1852 United States Coast Survey Map of Mission Bay and eastern San Francisco.

Reclamation of Mission Bay began in the 1850s and continued until the mid-1910s to the shoreline we see today (Figure 73). A timber pile-supported bridge that crossed Mission Bay from north to south named the Long Bridge was present along what is now 3rd Street.

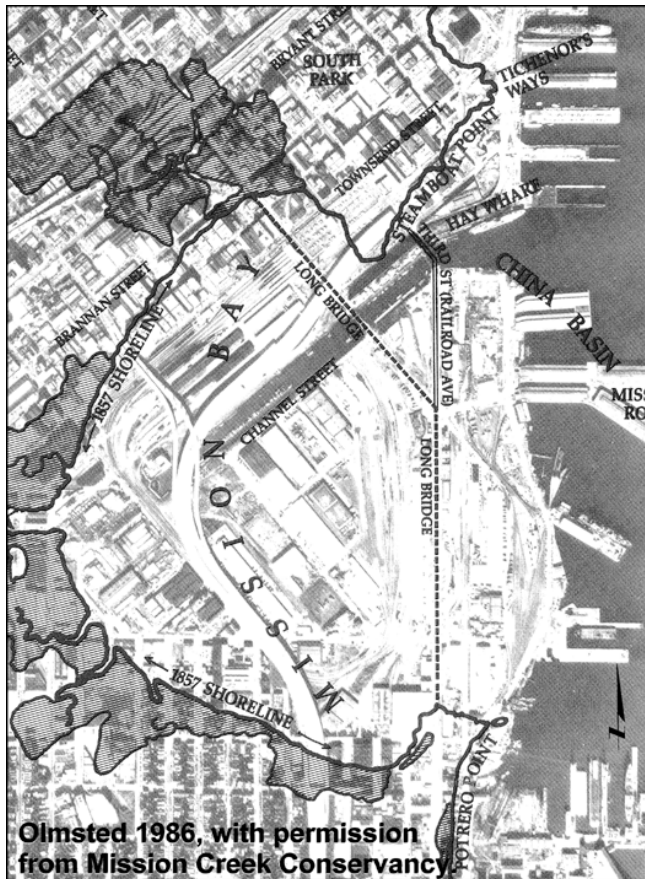


Figure 73. Historical and Current Shoreline in Mission Bay.

Sources of fill included sand from the removal of a 30-meter (100-foot) high sand dune on Townsend Street, rock from the cutting of San Francisco's hills, rubble from the 1906 earthquake and fire, and residential garbage. Much of the rock material used is serpentine that contains naturally occurring asbestos and heavy metals. Reclamation was generally performed by dumping the materials into the bay; little to no effort was made to compact the material. Subsequent to land reclamation, there were a variety of land uses, including a city dump, lumber yards, railroad operations, shipyards, petroleum blending, storage, conveyance, and a variety of industrial operations, manufacturing facilities, tanneries, and gas plants (ESA, 1990).

Geologic Hazards

Mission Bay is located in between the San Andreas and Hayward faults. Strong ground shaking is expected dur-

ing a major earthquake. No faults have been mapped in Mission Bay; however, Mission Bay is in a liquefaction hazard zone, as mapped by the California Geological Survey (2001).

Subsurface conditions in Mission Bay vary based on distance from the original shoreline, the former presence of marshlands, the formation of mud waves during dumping of the material to reclaim the land, and geologic conditions. The undocumented fill is heterogeneous, comprised of clay, silt, sand, gravel, cobbles, boulders, rubble, and garbage, and varies in thickness from about 2.5 to 12 m (8 to 40 ft) thick. It is notable that there are variations in thickness within short distances due to the occurrence of bearing capacity failure of the weak Young Bay Mud when too much material was placed during reclamation. In these areas, the weight of the load caused "mud waves" where the Young Bay Mud was pushed down under the load and displaced upward adjacent to the load. Where the fill is predominantly granular and/or has low plasticity, it is potentially liquefiable. Portions of Mission Bay have a high potential for lateral spreading as well. Ground improvement has been performed at a number of parcels in Mission Bay to mitigate liquefaction and/or lateral spread potential.

Young Bay Mud is compressible. Historic records show that about 2.7 m (8.9 ft) of settlement occurred between the early 1900s to the 1990s near the corner of 3rd and 4th Streets (they formerly intersected south of Mission Creek Channel). Where Young Bay Mud is thicker than about 18 to 24 m (60 to 80 ft), it is still consolidating under the fill placed in the late 1800s to early 1900s. Where recent fill has been placed as part of site development, a new cycle of consolidation settlement is occurring. Some sites in Mission Bay have undergone a surcharge program with the use of wick drains to pre-settle the site and reduce the amount of settlement to accommodate for site improvements. Deep foundations have most commonly been used for support of structures in Mission Bay.

Environmental Hazards and Regulatory Framework

Based on the historical land uses in Mission Bay, a variety of contaminants are present. Lead and other metals are typically present in soil at levels that can exceed California and Federal hazardous waste criteria. Petroleum hydrocarbons and associated volatile and semi-volatile organic compounds are also commonly

present in the fill. Naturally occurring asbestos and heavy metals are found where serpentinite rock fragments are present. Petroleum hydrocarbons and metals are often encountered in groundwater and construction dewatering can require groundwater treatment prior to permitted discharge.

Construction and development activities at Mission Bay are subject to the Mission Bay Subsequent Environmental Impact Report (EIR, City and County of San Francisco Planning Department and San Francisco Redevelopment Agency, September 17, 1998). In response to certain EIR mitigation measures, a Risk Management Plan (RMP) was prepared to mitigate potential risks associated with the construction and development planned for the Mission Bay Project Area (Environ, 1999). The California Environmental Protection Agency designated the San Francisco Regional Water Quality Control Board (Water Board) as the Administering Agency under California Assembly Bill (AB) 2061. As the Administering Agency, the Water Board has exclusive responsibility and jurisdiction for providing direction on the environmental aspects of Mission Bay Site development activities. The Administering Agency also coordinates its decisions and actions with state, regional and local agencies. Locally, the San Francisco Department of Public Health (SFDPH) assists with overseeing RMP implementation and compliance activities and oversees compliance with Articles 22A (Maher Ordinance) and 22B (Construction Dust Control Requirements) of the San Francisco Public Health Code.

The RMP presents the decision framework and specific protocols for managing the chemicals in the soil and groundwater in a manner that is protective of human health and the ecological environment, consistent with the existing and planned future land uses, and compatible with long-term phased development. The RMP delineates the specific risk management measures that must be implemented prior to, during, and after development of each parcel within the Mission Bay area. In 2000, the City and County of San Francisco established the Covenant and Environmental Restriction for the entire Mission Bay development site. This covenant states that site must be developed in accordance with the 1999 Mission Bay RMP.

Soil gas testing has encountered the presence of methane gas at some parcels likely present from decaying waste material. Each project at Mission Bay

is evaluated on a site-by-site basis for management of methane gas. When soil gas methane sample results exceed 1.25% by volume, the project applicant must notify the Water Board to determine whether any additional investigation or mitigation measures are warranted. Methane mitigation typically involves installing a passive vapor mitigation system, consisting of perforated pipe placed within a gravel layer beneath the building slab and connected to risers that sweep the methane up to a discharge point above the roof. The system design and operation and maintenance plan are reviewed and approved by the Water Board.

As shown in Figure 73, Mission Bay is located bayward of San Francisco's historic shoreline. Article 22A of the San Francisco Public Health Code states that construction projects in San Francisco that are bayward of the historic 1852 high tide line and disturb more than 38.2 m³ (50 yd³) of soil are required to assess the site history and subsurface soil quality. Many sites in Mission Bay contain fill with lead and other metals that exceed hazardous waste threshold concentrations which require special handling and disposal. Article 22A requires that site mitigation and health and safety plans be prepared before construction and followed prior to off-haul of fill material to designated landfills.

The RMP and Article 22B require that construction projects follow an approved Dust Control Plan to prevent dust from leaving the construction sites. Additionally, Title 17 of the California Code of Regulations (17 CCR) Section 93105, Airborne Toxic Control Measure (ATCM), requires that for projects that disturb more than an acre of land in areas where naturally occurring asbestos is present, an Asbestos Dust Mitigation Plan must be prepared, approved by the Bay Area Air Quality Management District (BAAQMD). Control measures, air sampling and reporting be implemented under BAAQMD oversight to minimize asbestos dust.

Manufactured Gas Plants

In the mid-1800s and early 1900s, before natural gas was available as an energy source, manufactured gas plants (MGPs) existed throughout California and the United States. These plants used coal and oil to produce gas for lighting, heating, and cooking. At that time, this technology was a major step forward, revolutionizing street lighting, enhancing public safety, and enabling businesses to work into the night.

Gas manufacturing in San Francisco originated in the

Gold Rush era, in the early 1850s, when San Francisco was the key urban, commercial and financial center for the United States western territories. Several of the MGPs in San Francisco went out of business in 1906 due to damage from the earthquake and subsequent fires. All had closed by 1930 when the plants became obsolete due to readily available natural gas.

There were 12 MGPs located in San Francisco. Table 5 identifies the original owner/operator and the dates of operation; the locations are shown on Figure 74.

The original process used to manufacture gas was coal carbonization. In this process, coal was heated in closed retorts. Inside these ovens, the coal was kept from burning by limiting its contact with outside air. Volatile constituents of the coal would be driven off as a gas, which was collected, cooled, and purified prior to being piped into the surrounding areas for use. The solid portion of the coal would become a black, granular material called coke. Coke was a valuable fuel for many industrial uses and for home heating, because it burned hotter and more cleanly than ordinary coal. As the gas manufacturing industry developed and expanded, new processes (oil gas and carbureted water gas) were developed which produced gas mixtures that burned hotter and brighter.

As mentioned above, in addition to gas, MGPs produced a variety of byproducts, some of which were useful and marketable, such as coke, coal tar, and lampblack. The byproducts that could not be sold were removed for disposal or remained at the MGP site. The most common residues found at historic MGP sites are coal tar and lampblack. Coal tar is a black substance that looks like and is chemically similar to roofing tar. Lampblack looks like and is chemically similar to soot from a candle. These materials sometimes smell like roofing tar or fresh asphalt. MGP residues are comprised of many chemicals, including polycyclic aromatic hydrocarbons (PAHs) and volatile organic compounds (VOCs). Naphthalene, which smells like mothballs, is often associated with the coal tar.

All of the MGP sites in San Francisco were out of service and dismantled by the 1930s. Subsequent development covers all of the former MGP sites. Some of the residual subsurface structures/MGP wastes may have been removed during redevelopment. Others may remain but there is no indication that these sites pose any health concerns to the public under current conditions because, in most cases, the MGP residues are located below the ground surface where direct contact exposure is unlikely. However, if redevelopment occurs, the possible presence of MGP residues needs to

Table 5. Location and dates of operation of San Francisco’s manufactured gas plants

| Original Owner/Operator | Name/Location | Dates of Operation |
|--|----------------------|---------------------------|
| San Francisco Gas Company | Howard Street | 1854–1891 |
| Aubin Patent Gas Company | Sheraton Palace | 1857–1858 |
| Citizens Gas Company | King Street | 1866–1887 |
| Metropolitan Gas Company | Channel Street | 1872–1878 |
| San Francisco Gas Company | Potrero | 1872–1930 |
| Central Gas Company | Townsend Street | 1881 |
| Central Gas Light Company | Fillmore | 1881–1906 |
| San Francisco Gas Light Company | North Beach | 1891–1906 |
| Equitable Gaslight Company | Cannery | 1898–1906 |
| San Francisco Coke and Gas Company | Beach Street | 1900–1930 |
| Independent Gas and Power Corporations | Adjacent to Potrero | 1902–1915 |
| Baldwin Gas Company | Station T | 1882–1906 |

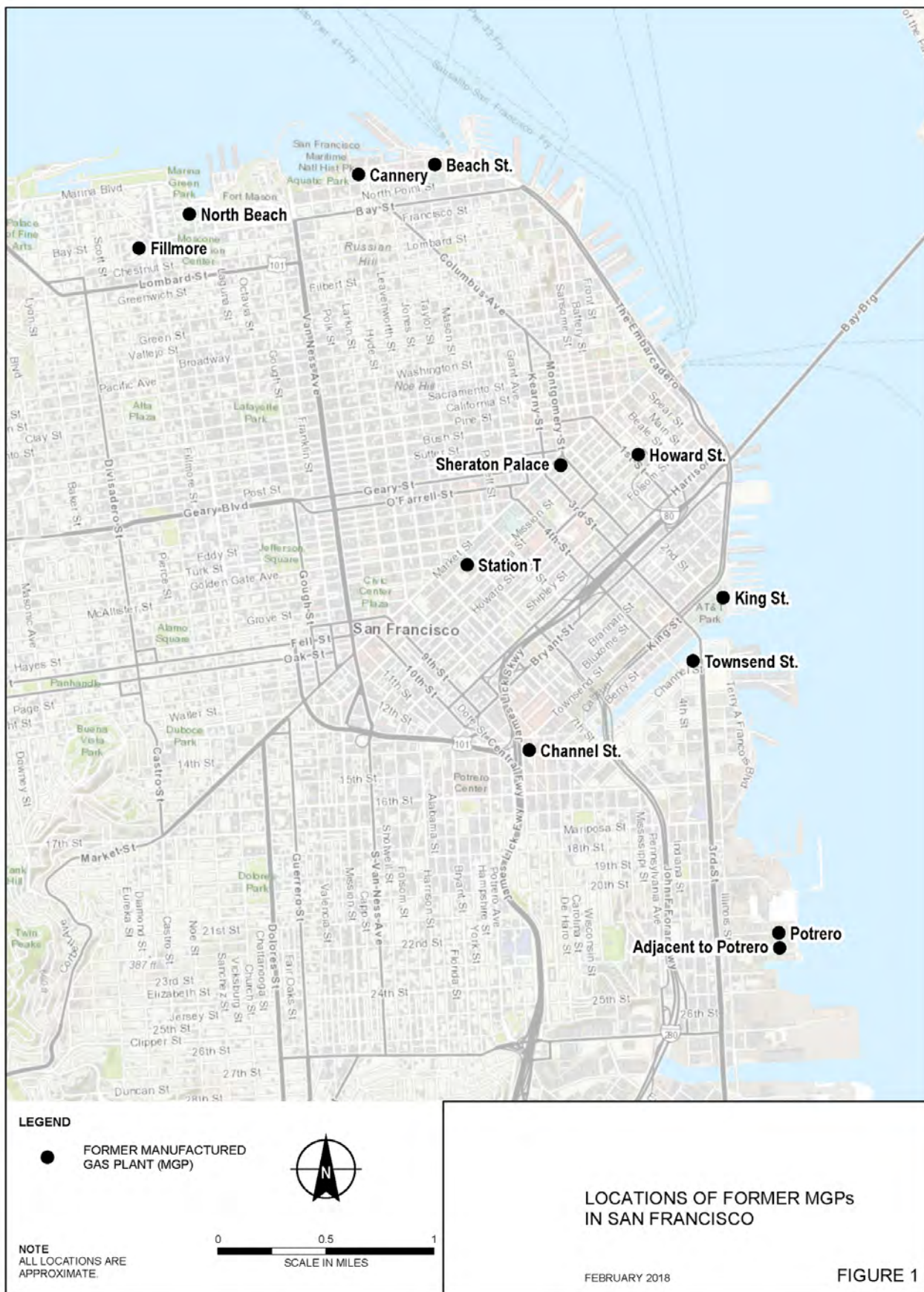


Figure 74. Locations of former manufactured gas plants in San Francisco.

assessed and appropriate plans for handling the residues developed and implemented as part of redevelopment.

In the late 1800s/early 1900s, many industries located along the Bay shoreline, including MGPs, discharged some waste into the Bay. Some of these discharge areas have subsequently been filled in as San Francisco expanded its footprint; however, at some MGP sites (including Potrero, Beach Street, and North Beach), MGP impacts have been observed in near shore Bay sediments. The California Water Quality Control Board, San Francisco Bay Region (the Water Board) is requiring sediment investigation and cleanup as necessary to protect aquatic life at all three of these MGP sites.

The Water Board and its sister agency, the California Department of Toxics Substances Control (DTSC), oversee investigation and cleanup at a subset of these 12 MGP sites. Cleanup generally involves removal of accessible soil contamination, management of non-accessible soil contamination, and removal or stabilization of any sediment contamination. At the North Beach and Beach Street MGP sites, DTSC oversees upland soils and the Water Board oversees non-upland sediments. At the Potrero MGP site, the Water Board oversees both soils and sediments.

MAJOR ENGINEERING PROJECTS

by Kenneth A. Johnson and Philip J. Stuecheli

Golden Gate Bridge

The Golden Gate Bridge, built between 1933 and 1937, is an engineering structure unique to San Francisco. It captures much of the spirit of innovation and transcendence that have become part of the California cultural landscape. Like most major projects, the construction of the Golden Gate Bridge was not without controversy. While a number of controversial issues in the politics and administration of the project have been described in other publications, the focus of this article is on the engineering geologic controversy of the project.

Major Structural Foundation Elements

The narrowest part of the Golden Gate was selected for the bridge alignment. It is not clear whether other locations for the crossing were ever considered. It may be that the scale of the engineering feat to bridge this narrow location was so formidable that other configurations were perceived as even more audacious and

unlikely. The major foundation elements of the bridge include the north anchorage structure, the north tower foundation, the south tower foundation, and the south anchorage structure.

The geology of the north and south termini of the bridges both included rocks of what was then called the Franciscan Series. Despite being part of the same formation, the character of the rock on each side was quite distinct. On the north side, which was called Lime Point, the rocks consisted of massive, hard basalt, chert, sandstone, and limestone, whereas the southern terminus at Fort Point included a mixture of basalt, serpentinite, and sandstone.

The controversy stemmed from the serpentinite, which even then was recognized as a rock type that in places displayed a tendency of weak, unreliable strength behavior. The primary controversy revolved around the views of Andrew Lawson, the esteemed professor of geology at the University of California and Bailey Willis, professor emeritus from Stanford University. The physiographic evidence that informed the divergent opinions of these two experts were (1) the presence of an apparently erosion resistant ridge forming the southern terminus of the bridge where sandstone and serpentinite were mapped, and (2) the apparent instability of the slopes south and west of the bridge terminus where the serpentinite rock was exposed and perceived to be weathering, disintegrating and sloughing unstably into the Pacific Ocean between the proposed bridge foundation and Baker Beach. Lawson believed the geology at the south tower and anchorage structure was strong based on initial information, and proceeded to confirm his opinion with detailed attention to geology encountered during construction. Willis, on the other hand, maintained that the rock was entirely unsuitable to sustain a structure as large and important as the Golden Gate Bridge because serpentinite was known to be a rock of questionable strength, and further that the cliffs south of the bridge exhibited tremendous instability. Additional details about the resolution of this dispute are presented below.

North Anchorage Structure and Tower

The North Anchorage Structure is located near Lime Point on the north side of the bridge. The foundation of the anchorage structure is comprised of hard sandstone and chert, with inclusions of limestone (Figure 75).

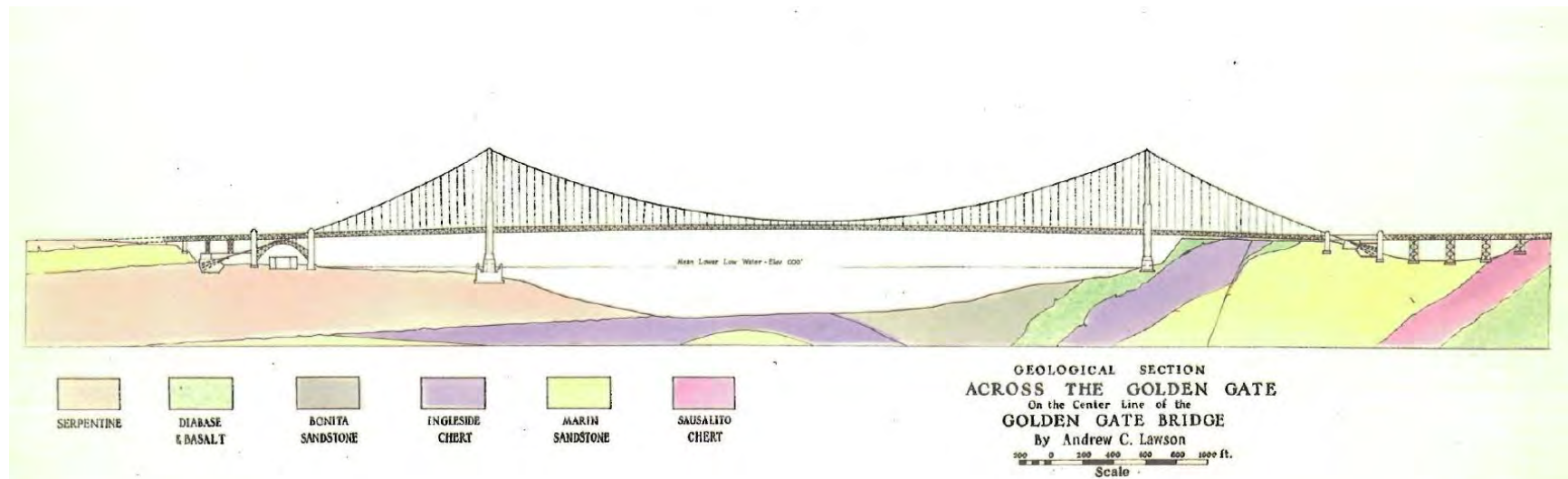


Figure 75. Cross section of the Golden Gate looking west prepared by Andrew Lawson, no vertical exaggeration. From Golden Gate Bridge and Highway District, Investigation of criticism of foundation by Bailey Willis, November 27, 1934.

As described by A.E. Sedgwick in his 1931 report, the geology of the north pier tower foundation is comprised of hard massive basalt (or diabase) that intrude chert. Excavation of the rock to a depth of 6 m (20 ft) below mean low tide was recommended to remove weathered and fractured portions of the rock. Schlocker (1974) describes the foundation geology of the north tower as comprised of greenstone on the west portion of the pier and chert and shale on the east portion.

South Tower

The geology of the south tower foundation was described by A.E. Sedgwick based on findings from 6 coreholes that were advanced into rock at this location. The upper rock section was comprised of basalt with an average thickness of about 5 m (16.4 ft) that was underlain by serpentinite to the depths explored, which was greater than 30 m (100 ft) below the bay bottom. Lawson inspected the excavation bottom for the south

pier and his observations are summarized in a letter to the Chief Engineer Joseph Strauss on December 9, 1934. Regarding the rock encountered 32.6 m (107 ft) below grade at the depth of the foundation Lawson stated, “The rock of the entire area, which I take to be typical of the surface upon which the pier rests, is compact strong serpentine remarkably free from any seams of any kind. When struck with the hammer it rings like steel, significant of its sound highly elastic condition. As a foundation for the pier the rock is all that could be desired...” (Figure 76).

South Approach and Anchorage Structure

According to Sedgwick, the geology of Fort Point and the southern anchorage structure is similar to that encountered for the South Tower. The serpentinite generally appeared to be strong, with thin weaker zones intermittently. In his report, he noted that the



Figure 76. Engineer team at the bottom of the south pier excavation; note the stylish hard hats of the time (Willis, 1934). From Golden Gate Bridge and Highway District, Investigation of criticism of foundation by Bailey Willis, November 27, 1934.

serpentinite exposed to the elements (presumably along the cliffs west and south of Fort Point) was prone to slaking and poor strength, whereas the rock that had not been weathered was quite strong. He recommended therefore that the foundation rock be sealed off from the elements with concrete in the future bridge structure.

The character of the serpentinite in the Fort Point area on the south side of the Golden Gate was described by Schlocker (1974). He indicates that the serpentinite is apparently resistant to erosion, despite its sheared character. This observation stems from the presence of serpentinite in many of the hills of San Francisco along the belt of serpentinite rocks connecting Potrero Hill with Fort Point.

As noted above, the slope instability along the coast south of the proposed bridge foundation suggested to Willis that the serpentinite rock was not suitable for a bridge foundation. Lawson, on the other hand, understood the difference between the weathered serpentinite on the surface along the coast and the rocks that had been cored as part of the foundation investigation of the bridge (Engineering News Record, 1930). The bridge construction was completed and the foundation has stood the test of time thus far.

San Francisco–Oakland Bay Bridge

The San Francisco–Oakland Bay Bridge is comprised of three separate structures: the eastern bridge, the western bridge, and the Yerba Buena tunnel that connects the two. The eastern bridge was originally built as an extensive truss structure with foundation pads resting on driven piles and a long cantilever section between Yerba Buena Island and the Oakland shoreline. The eastern span of the bridge is approximately 3.10 km (1.92 miles) long and was originally constructed using a complex cantilever section connected to a girder-truss structure. The original structure suffered significant damage during the 1989 Loma Prieta earthquake and after years of debate whether to retrofit the bridge or build a new span, it was decided to build the current eastern span comprised of a single-tower self-anchored suspension section linked to a viaduct section to complete the span.

The western bridge is a suspension structure with anchorages at Yerba Buena Island on the eastern end and Rincon Hill on the San Francisco side. In the middle of the western bridge is the central anchorage structure that was built to moderate the length of the

suspension structure over the approximately 3.14 km (1.95 miles) spanned by that bridge.

The different types of bridges on each side were largely dictated by the geology of each reach, as described in more detail below.

When the bridge opened on November 12, 1936, six months before the Golden Gate Bridge opened, it was the longest and tallest modern overwater structure in the world. The original two-deck configuration had the upper deck dedicated to two-way automobile traffic and the lower deck dedicated to rail and truck traffic. Conversion to the current configuration with westbound traffic on the upper deck and eastbound traffic on the lower deck was completed in 1963.

Western Span

Eastern and Western Anchorages

The geology of the western and eastern anchorages of the western span of the bridge are quite similar. Rincon Hill and Yerba Buena Island are both comprised of massive Franciscan Complex sandstone from the Alcatraz terrane of the Central Belt. This competent, erosion resistant rock provides an excellent foundation conditions for the eastern and western anchorages for the bridge.

Central Anchorage

The central anchorage for the western span of the bridge was the key to successful construction because it was not possible to build a suspension bridge spanning more than about 1.6 km (1 mile), and this span was close to 3.2 km (2 miles). By building the anchorage, the western span would essentially be comprised of two 1.6-kilometer (1-mile) long bridges. This anchorage was built in 61 m (200 ft) of water and then sunk an additional 61 m (200 ft) through the bay sediments to bedrock. This extraordinary structure was built by constructing a caisson system comprised of 55 caissons, of 4.5-meter (15-foot) diameter, that were assembled and barged out to the site location, sunk and mined out incrementally in sections (Figure 77 and Figure 78). Once the caissons were mined, they were then backfilled with concrete. This composite structure then provided the foundation for the massive concrete structure visible above the water today where the cables from each side of the western span are joined.

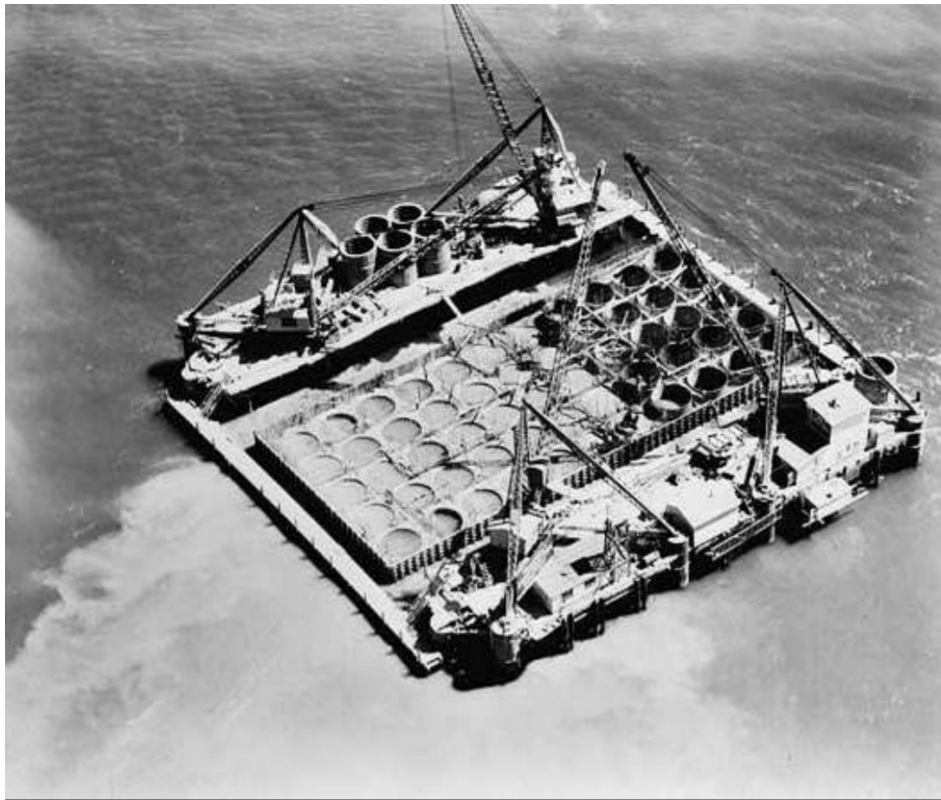


Figure 77. Construction of the caisson system for the central anchorage on the western span of the San Francisco–Oakland Bay Bridge (Bancroft Library Collection).



Figure 78. Excavation of central anchorage caissons on the western span of the San Francisco–Oakland Bay Bridge (Bancroft Library Collection).

Yerba Buena Tunnel

As mentioned above, Yerba Buena Island is comprised of generally competent sandstone rocks of the Alcatraz terrane of the Franciscan Complex Central Belt. While the island is not exactly part of the bridge structure, it does serve as the landing point for the western and eastern spans of the bridge. Due to the elevation of this prominent landform, the connection for the two bridge spans was completed as a tunnel through the competent rock.

Construction of the tunnel, which would be 160 m (525 ft) in length, began in 1933 with portal excavation on each side of the island (Figure 79). Excavation then proceeded by driving three adits, one at the crown of the tunnel and one at the invert on each side of the final tunnel profile. Following completion of these adits, the rock was excavated between the adits and steel supports were placed to form the structural core of the final crown of the tunnel. The remaining tunnel core was then excavated, and the middle deck and final lining were constructed. The tunnel was completed in 1936. Tunnel construction proceeded without significant cave-ins or instability problems. With excavated dimensions of 23 m (75 ft) wide and 18 m (59 ft)

high, the Yerba Buena tunnel continues to be the largest vehicular tunnel constructed in the world.

Eastern Span

The eastern span of the San Francisco–Oakland Bay Bridge was initially constructed with a combination of a cantilevered section connected to a truss section due to the length of the span and absence of firm material for a suspension foundation on the east end of the bridge. While not part of the geology of San Francisco, a brief description of the geology and foundation considerations for the eastern span are warranted (Figure 80).

The depth to bedrock along the alignment of the eastern span increases significantly just east of Yerba Buena Island. The first pier east of Yerba Buena Island encountered bedrock at a depth greater than 100 m (328 ft) and is the last foundation element of the span on bedrock. Other foundation elements to the east were founded on pile foundations within Neogene sediments comprised of sand, silt and clay. From youngest to the oldest these deposits begin with Young Bay Mud, Merritt Sand, and Posey Formations, which are underlain by the predominantly fine-grained San Antonio Formation. The Alameda Formation is encountered below the San

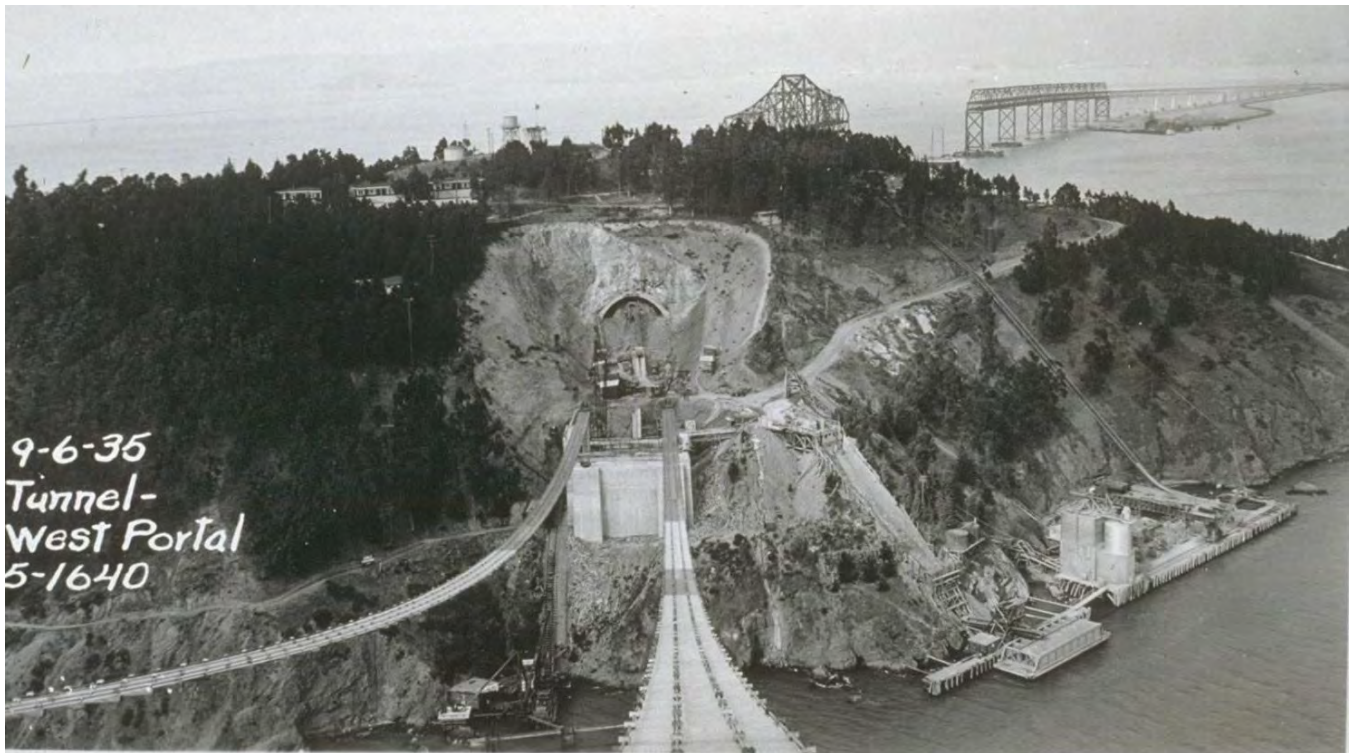


Figure 79. West Portal of the Yerba Buena Tunnel during construction of the San Francisco–Oakland Bay Bridge, as seen from the first tower of the western span; notice eastern span in background (Bancroft Library Collection).

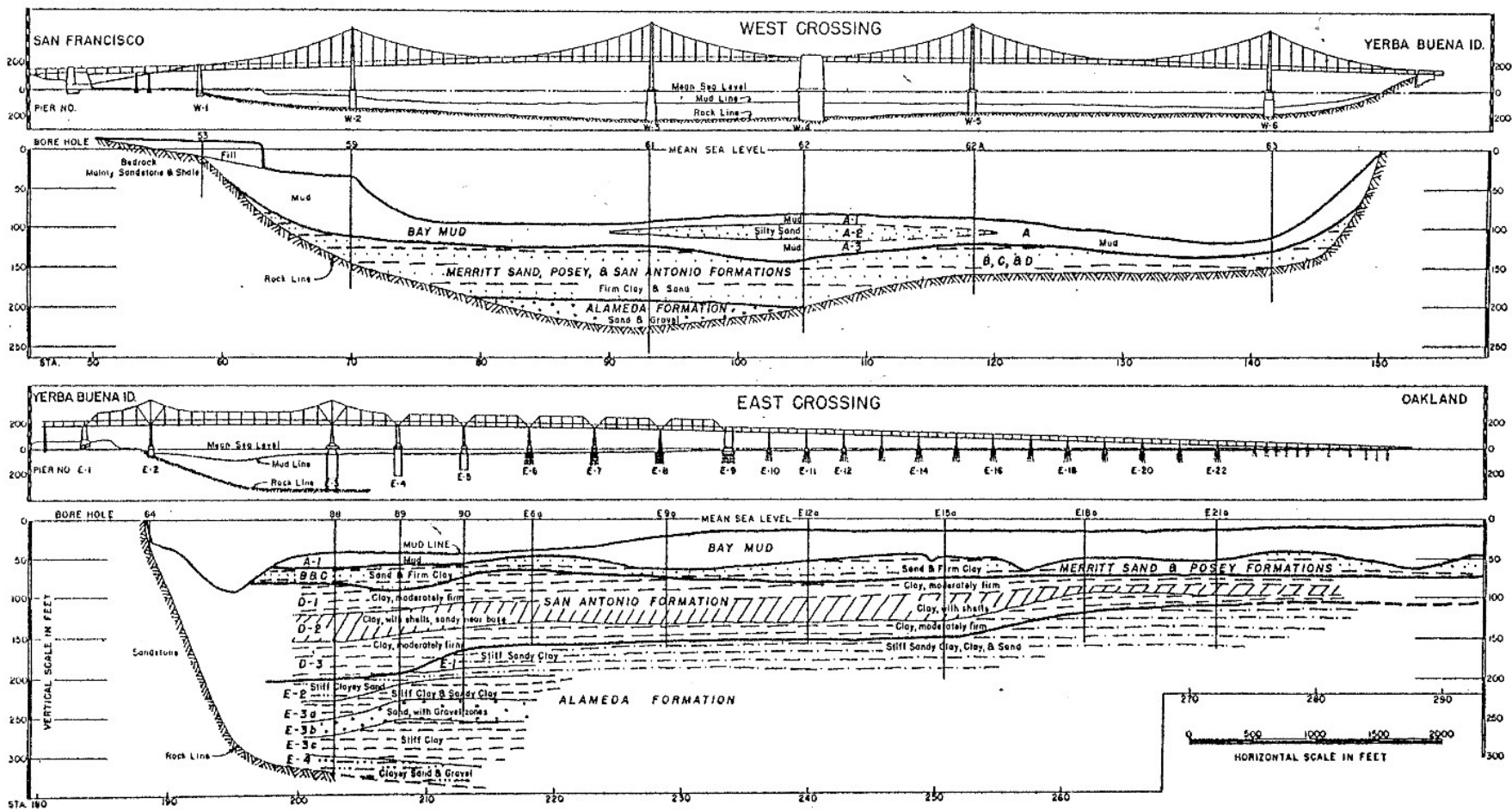


FIGURE 4.—PROFILE OF SEDIMENTS, PARALLEL CROSSING, SAN FRANCISCO BAY

Figure 80. Sedimentary deposits beneath the San Francisco–Oakland Bay Bridge, from Trask and Rolston (1951).

Antonio, and these two units are believed to correlate with the Santa Clara Formation and possibly the Merced Formation (previously described).

A decision to forego retrofit and repair of the original cantilever and truss structures following damage from the Loma Prieta earthquake in 1989 led to the design and construction of a new eastern span. The new span features the geology of Yerba Buena Island once again with the completion of a self-anchored suspension section connected to a traditional causeway. The new span opened in 2013.

Port of San Francisco—San Francisco Seawall at Embarcadero

In its natural condition, San Francisco was not a particularly well-suited port location. Despite the protection afforded by the San Francisco Peninsula as ships entered San Francisco Bay, the shoreline off what is now the Embarcadero was comprised of tidal marsh and mudflats and had very little deep water. The history of the city was linked to the development and growth of the Port, and the single biggest engineering structure that solidified the Port of San Francisco was the San Francisco seawall.

The need for modification of the coastline in the downtown area was recognized as a result of the boom-time of the Gold Rush. In 1863, the California legislature created the California Board of State Harbor Commissioners that first advanced the idea of a seawall construction. Not unlike new development ideas today, the seawall design and construction was delayed by about 4 years due to legal challenges. The commission established a contest to develop the best design for the first wall, awarding the project to W.J. Lewis who was appointed chief engineer for the project.

The original wall was designed to be built by dredging an excavation 18.3 m (60 ft) wide below the low tide level and dumping loads of rock into the excavation to become the foundation for the wall. Cofferdams were constructed so that the base of the wall could be constructed on the rock fill. The rock fill was then capped with a concrete slab 0.60 m (2 ft) thick by 3 m (10 ft) wide, upon which a masonry wall was constructed that was 2.1 m (7 ft) wide at its base and 2.7 m (9 ft) tall. The water in the region behind the wall was then pumped out and replaced with rubble fill, garbage, and any other material available to bring the grade up.

The seawall was constructed in 22 different sections along the waterfront, totaling 4.8 km (3 miles) (Figure 81). The construction began in 1879 and was not completed until 1916, a span of 37 years. There were a number of reasons the construction was intermittent through the late 19th and early 20th century.

Land title in the relatively new state of California was extremely difficult and tedious to acquire in a growing metropolis and while the plan was conceived in 1863 it wasn't until 1871 that the California Board of State Harbor Commissioners had control of all the wharves along the waterfront, except those along the Mission Bay side. In 1869, the construction of the transcontinental railroad diverted much infrastructure attention away from the seawall, delaying construction. Construction continued in the ensuing years on the waterfront to the south, with the China Basin seawall construction being completed in 1929. That same year, legislation to create the San Francisco Harbor Bond Finance Board was established as a means to finance State Harbor Commissioners work with the ongoing operation of the harbor by the State of California. It wasn't until 1959 that the California Board of State Harbor Commissioners for San Francisco Harbor was renamed the San Francisco Port Authority. Even more recently the Port Authority was a state sponsored agency until 1968 when legislative measures were used to transfer the jurisdiction and control of the Port Authority to the City and County of San Francisco.

The actual design of the various section of the seawall varied dramatically with the specific site conditions and planned uses. Various levels of sophistication were employed in the engineering from dumped rock fill all the way to pile-supported structures with sandy backfill placed behind a bulkhead. (Figure 82, Figure 83, and Figure 84). Considering the approximately 4.8-kilometer (3-mile) length of the seawall and the volume of rock required, it is easy to see how an industrious quarry could do very well during this period of seawall construction in San Francisco. One of the greatest natural opportunities for supplying the seawall construction materials was the quarry owned and operated by the Gray Brothers at Telegraph Hill. See “Quarries in San Francisco” in the history section above for more details regarding the infamous Gray Brothers. Other quarries around the bay were also well situated to provide rock fill including, for example, the Ford Quarry in Richmond. Also close to the bay, their quarry provided rock fill to the construction sites via barge transport

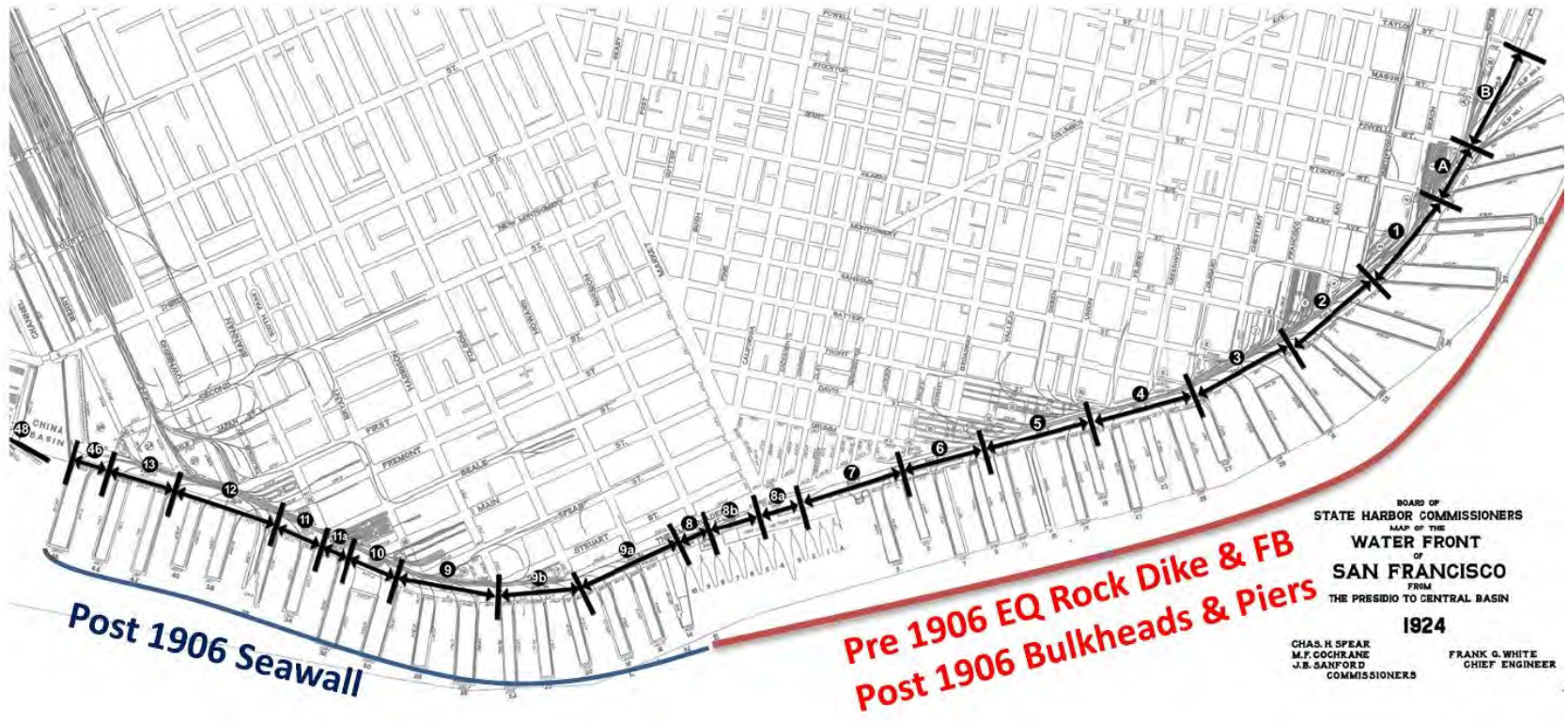


Figure 81. Overview of San Francisco seawall layout (Port of San Francisco).



TRANSVERSE SECTION of SEA WALL and THOROUGHFARE.

Figure 82. San Francisco seawall typical early construction (Courtesy of Port of San Francisco).

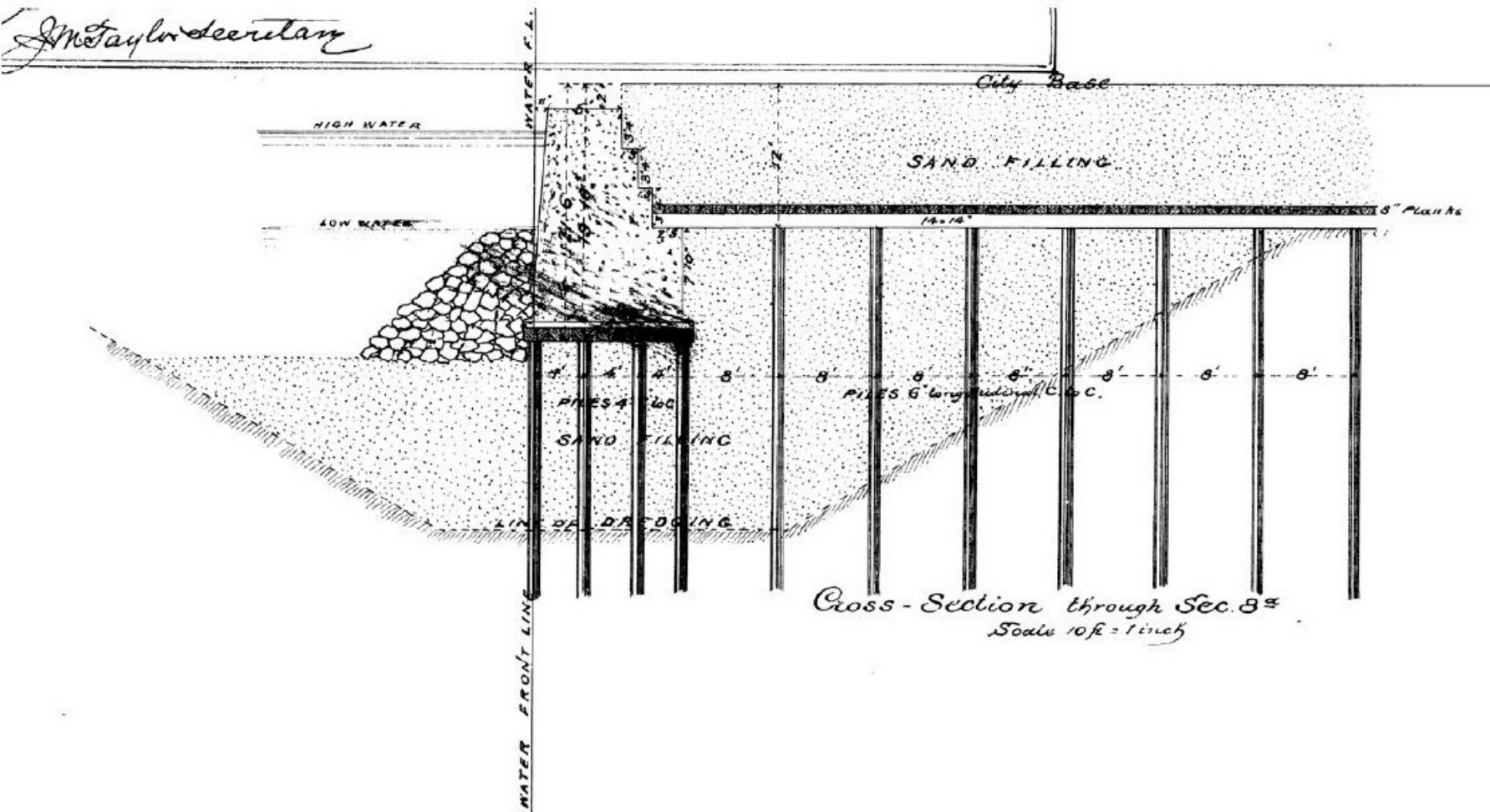
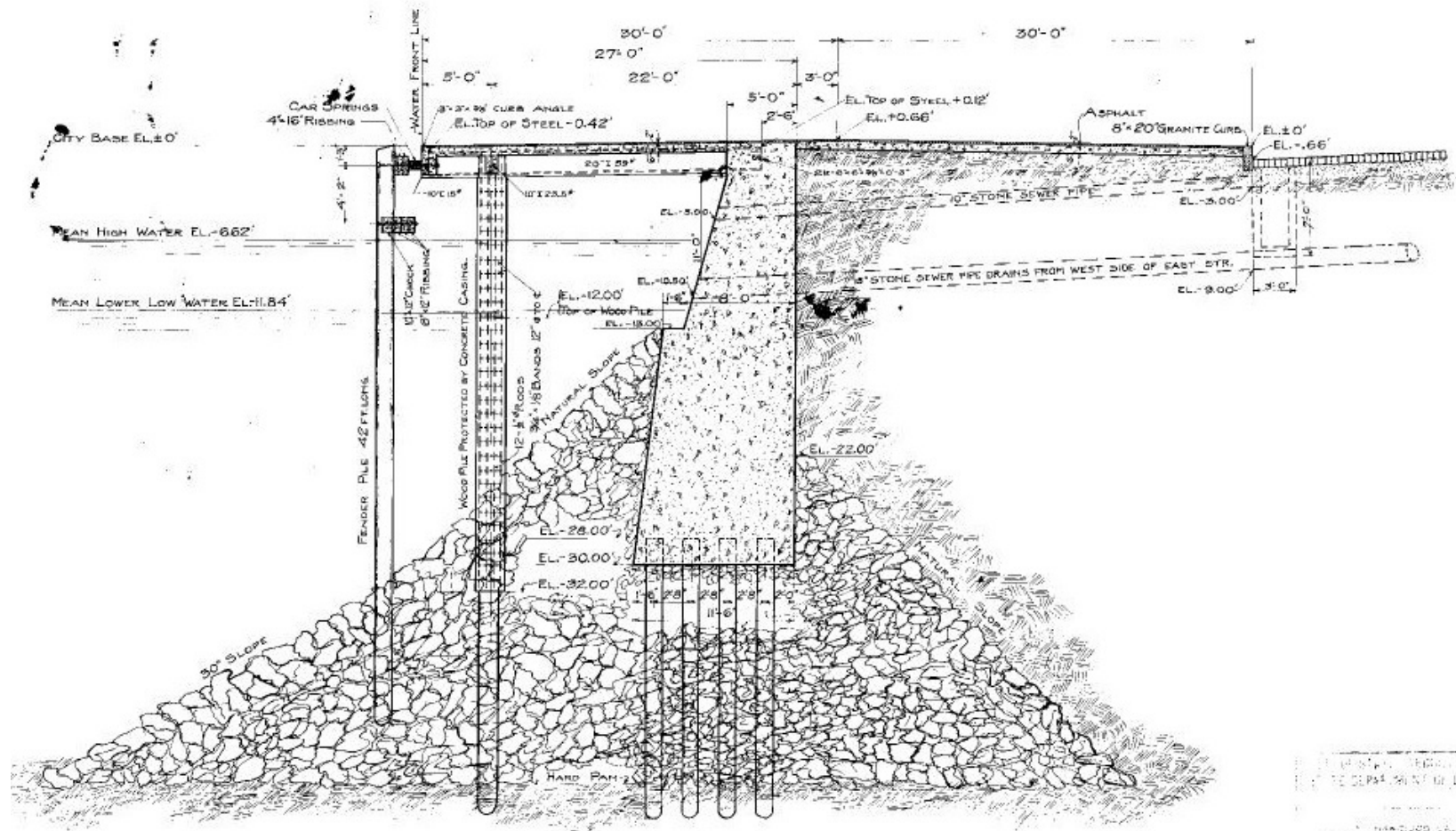


Figure 83. Section 8a (1891–1893) and 8b (1888–1890). See Figure 81 for section location (Courtesy of Port of San Francisco).



CROSS SECTION OF SEAWALL SECTION 10

1993-39

Figure 84. Section 10, ca. 1910. See Figure 81 for section location (Courtesy of Port of San Francisco).

that was easily and efficiently placed.

Much of the Embarcadero waterfront property suffered damage from the 1906 earthquake; however the Ferry Building near Sections 8a and 8b (Figure 81) of the seawall survived the earthquake intact. The Ferry building was already a major hub of transportation and commerce, and it was tremendously significant that the building and Ferry operations could quickly recover after the earthquake. Other portions of the wall were less fortunate. The State legislature responded to the disaster by passing the San Francisco Harbor Improvement Act in 1909 and a total of \$9 million dollars was allocated for the repair of the seawall and additional construction to the south in the area of Islais Creek and India Basin.

With the emergence of the Ports of Los Angeles, Oakland, and Seattle in the latter half of the 20th century, the Port of San Francisco experienced a significant drop in cargo volume. The construction of the Embarcadero Freeway, which opened in 1959 running as a double-deck viaduct from the Bay Bridge around the Embarcadero to Washington Street, served to isolate the waterfront from the rest of the adjacent bustling business district. During the Embarcadero Freeway era, the waterfront wharves to the east seemed stuck in limbo as the history of the Waterfront faded from everyday experience. All of this changed after the Loma Prieta earthquake in 1989. The Embarcadero viaduct design was essentially the same as that of the Cypress Structure in Oakland, which partially collapsed with loss of life during the earthquake. Thus, the Embarcadero Freeway was doomed. The freeway was demolished in the early 1990s and the waterfront and Embarcadero experienced an extremely popular reconnection with the rest of the downtown area. The Ferry building and many businesses are presently thriving in the waterfront area. With the complete renovation of the Ferry Building and Plaza, construction of the Giants stadium at AT&T Park, construction of the state-of-the-art cruise ship terminal, the new home of the Exploratorium science museum, and soon the completion of the Chase Center for the Golden State Warriors, the seawall is increasingly essential to one of the most dynamic areas of San Francisco.

The Port of San Francisco has initiated a major upgrade of the seawall infrastructure and is currently implementing the Seawall Earthquake Safety Program to bolster the stability of the waterfront to withstand

seismic events, but also to incorporate global sea level change as an essential element of the program to protect the stability and resilience of the city's waterfront.

Treasure Island

Treasure Island is located in the central portion of San Francisco Bay and within the City and County of San Francisco. The island is connected to Yerba Buena Island by an engineered fill causeway at the southwest corner of the Treasure Island. Treasure Island was constructed in 1936 and 1937 for the 1939 Golden Gate International Exposition, after originally being conceived as an airport for San Francisco. Treasure Island and the causeway connecting it to Yerba Buena Island were created by placing over 16 million m³ (21 million yd³) of hydraulic fill at the site of the Yerba Buena Shoals, a sandy shallow subtidal platform that formerly extended a little over a mile north of Yerba Buena Island (Figure 85 and Plate 2). The project was jointly funded by the Works Progress Administration (WPA) and the backers of the International Exposition, and constructed by the U.S. Army Corps of Engineers. Lee (1969), Hagwood (1980) and Power et al., (1998) provide detailed descriptions of the conception, design and construction of the Island.

In 1941, both islands were acquired by the U.S. Navy to establish the Treasure Island Naval Station, which remained active until base closure in 1997. Following base decommissioning and environmental cleanup operations, most of the base was transferred to the Treasure Island Development Authority (TIDA), a nonprofit organization managed by the City of San Francisco. The master plan calls for construction of several thousand new dwelling units, retail and commercial space centered in an urban core of mid- to high-rise buildings, and a new marina and ferry terminal. The redevelopment construction is anticipated to extend over 20 to 30 years and would create 8,000 new households for approximately 20,000 people.

Hydraulic Fill

Hydraulic fills at Treasure Island are between about 4 and 12 m (13 and 40 ft) thick with the base of the fill, generally reflecting the pre-filling bathymetry. The fills were placed inside rock fill dikes that delineate the island shape, and consist of generally loose, poorly graded to silty sand with thin, sharply defined layers of silt and clay (Figures 86 and 87). Ground shaking from the 1989 Loma Prieta caused numerous sand boils



Figure 85. Treasure Island fill, April 1937. (Wikimedia Commons: https://commons.wikimedia.org/wiki/Category:NARA_images_of_Treasure_Island,_San_Francisco)



Figure 86. Fill sample from 9.1 to 9.4 m (30 to 31 ft) showing poorly graded sand with sharply defined clay and silt laminations (ENGE0, 2015).

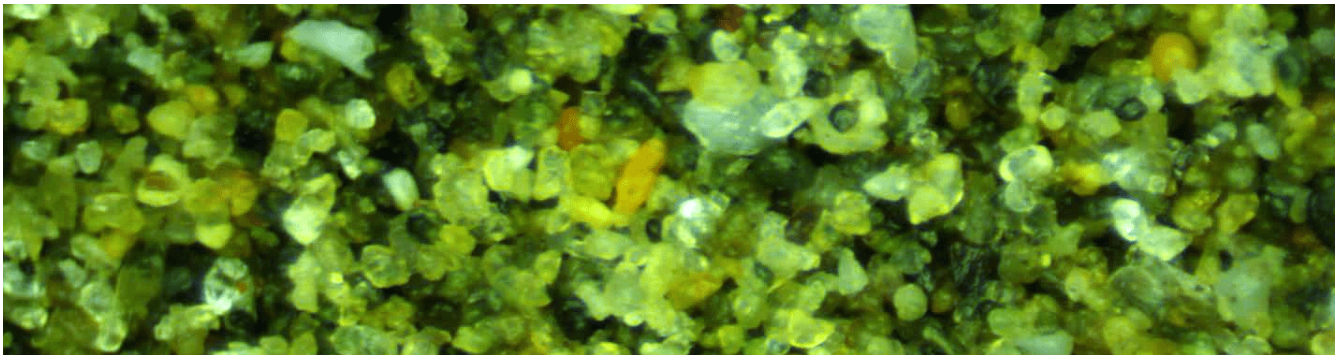


Figure 87. Photomicrograph of clean sand at 9.6 m (31.5 ft) (grain size predominantly 0.4 mm to 0.1 mm) (ENGE0, 2015).

and ground settlements of up to several inches, as well as ground fissures from incipient lateral spreading. The earthquake effects on the island were documented by Power, et al., (1998) and Bennet, (1998).

Shoal Deposits (Estuarine Sands)

The Yerba Buena Shoals underlying the hydraulic fill consist of complexly interbedded and highly bioturbated silty to clayey sand and clay (Figures 88 and 89). Bioturbation has destroyed much of the original fine stratification, and the sands are weakly cemented by interstitial clays.

Young Bay Mud (Estuarine Clays)

Soft, normally consolidated fine-grained estuarine clays (Young Bay Mud) underlie the shoal sands. Beneath the southern portion of the island, the lower portions of the Young Bay Mud contain a large volume of interbedded, fine-grained, dense to medium dense, clayey estuarine sand similar to the shoal sands (Figure 90). The compressible estuarine clays reach a maximum thickness

of over 30 m (100 ft) near the northwest corner of the island. The large volume of sand interbedded with the Young Bay Mud is unlikely to have originated from the mainland, since the area is isolated by relatively deep-water tidal channels on the east and west. The grain-size distribution and texture of the sand closely matches that of the adjacent eolian sand deposits on adjacent wave-cut bluffs on Yerba Buena Island. It appears likely that most of the shoal sand was eroded from the bluffs and re-deposited by wave action and tidal currents.

The base of the Young Bay Mud is marked within many borings by the presence of oxidized layers and horizons containing plant debris and roots. This suggests deposition in intertidal conditions or weathering profiles developed during the sea-level low stand. Based on information compiled from the existing subsurface data, we prepared a contour map of the interpreted base of Young Bay Mud deposits (Plate 2). The compiled data show that the pre-Holocene land surface had up to about 30 m (100 ft) of topographic relief. An

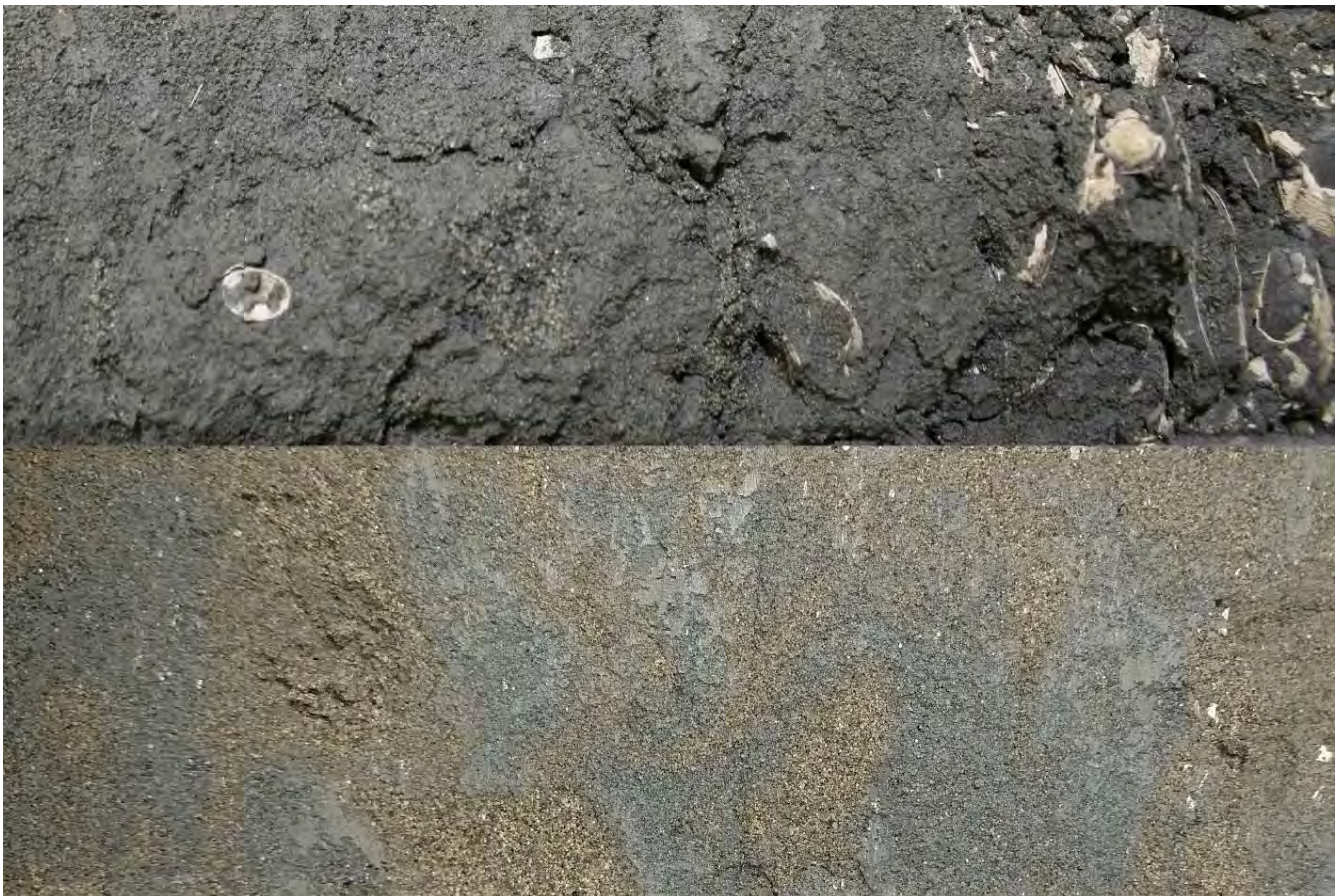


Figure 88. Shoal sample images: Top; fine-grained shoal; poorly stratified clayey sand with shells; Bottom; coarser shoal sand with clay-cemented regions (gray) disrupted by sand-filled bioturbated regions (brown) (ENGE0, 2015).

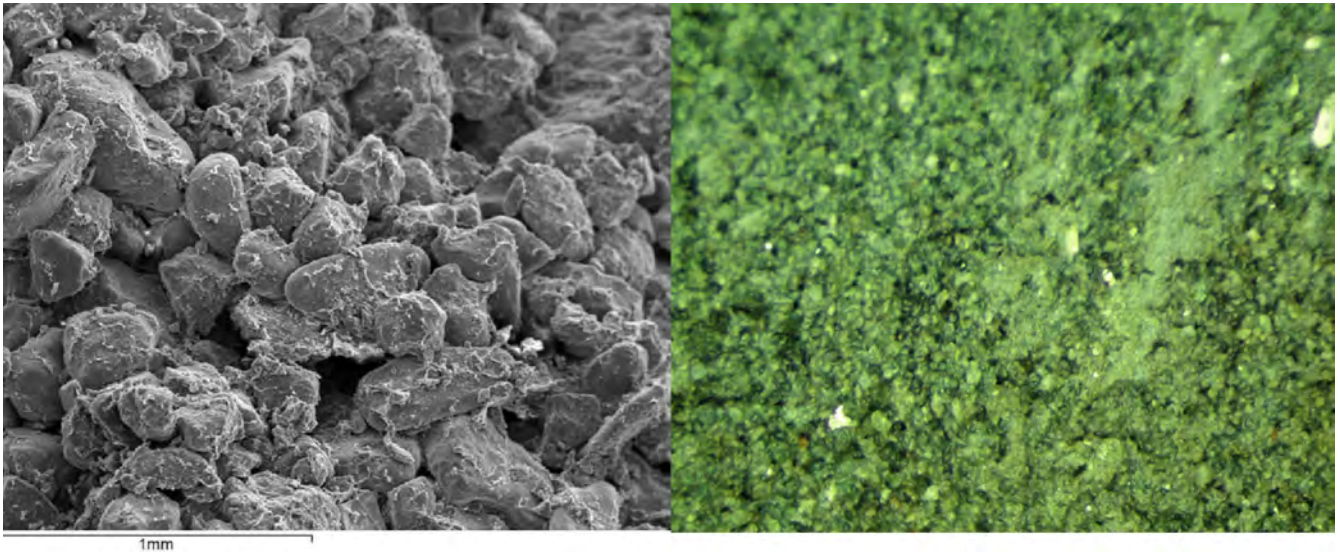


Figure 89. Left: SEM image of tightly packed sand with abundant fines and clay cement; Right: photomicrograph of shoal sand with thin clay lenses (ENGEO, 2015).

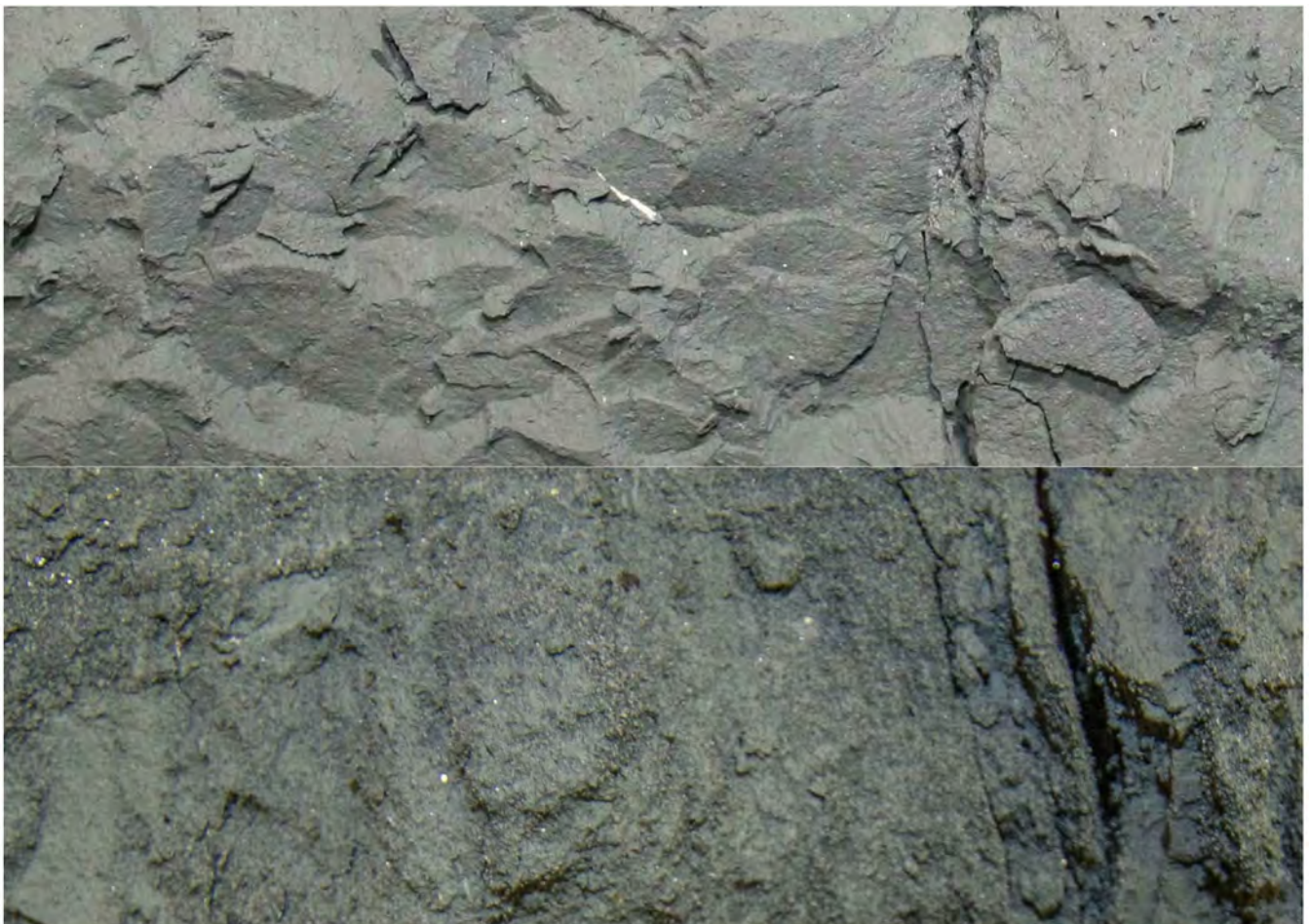


Figure 90. Top: Typical Young Bay Mud clay (15 m, 50 ft), Bottom: Typical estuarine clayey sand (29 m, 95 ft) (ENGEO, 2015).

apparent paleo-channel separated high-standing areas at the southwest corner of the island and along the east shoreline. Radiocarbon dates recovered near the base of the Young Bay Mud yielded dates of about 9,500 years BP (before present) to 10,500 years BP. Two samples obtained from older estuarine clays were dated as greater than 43,500 years BP.

Older Bay Deposits (Undifferentiated)

Older (Pleistocene-age) estuarine deposits underlie the Young Bay Mud across the entire island. These older estuarine deposits consist of slightly over-consolidated clays and sands that are very similar to the deposits of the modern estuary. At Treasure Island, neither eolian nor alluvial deposits have been identified on the unconformity at the base of the Holocene section or within the Pleistocene estuarine section. The few borings that have penetrated the entire 30- to 40-meter (100- to 130-foot) thickness of estuarine Older Bay Deposits have encountered sandy to gravelly older alluvium directly above the Franciscan bedrock.

Geotechnical Mitigation Measures for Treasure Island Redevelopment

In preparation for redevelopment of Treasure Island, potential ground deformation from consolidation of the soft (Holocene) Young Bay Mud due to new loads, seismically induced liquefaction, and lateral spreading hazards at Treasure Island will require mitigation. As noted by Powers, et al. (1997) areas of the island that were previously improved using vibro-compaction methods performed well during the Loma Prieta earthquake. Recent full-scale vibro-compaction ground improvement testing showed that the hydraulic fills were significantly improved by this method, but that the underlying shoal sands were not improved. Detailed study of the shoal sands (which included multiple cyclic direct simple shear testing and detail microscopy logging) showed that they are not highly susceptible to flow failure from liquefaction, but tend to have more of a “cyclic mobility” behavior due to interbedded fines and natural clay cementation (Figure 88 and Figure 89). Seismically induced movements or failure of the island shoreline will be mitigated by construction of deep-soil mixing (DSM) shear panels where vertical improvements are relatively close to the shoreline or by setbacks occupied by open space and parkland. The hydraulic fills underlying the entire proposed development area (excluding areas surrounding historic structures) will be improved by vibro-compaction.

Areas proposed for development, site access, and utility corridors will be surcharged to accelerate consolidation of compressible Young Bay Mud. The surcharge program will include wick drains pushed through the Bay Mud to depths of up to 40 m (131 ft) and surcharge fills up to 6 m (20 ft) thick in order to meet project construction deadlines.

Transportation Tunnels in San Francisco

San Francisco is a city with a natural affinity to tunnels. Its hilly terrain and broadly developed urban footprint make mobility a priority and tunnels facilitate that significantly for both transportation and other infrastructure projects. Below we summarize some of the more significant tunnel project in San Francisco and highlight the geological elements of each (Figure 91).

Southern Pacific Tunnels to the Peninsula

Railroad transportation between San Francisco and San Jose was first established in the late 1850s with a series of poorly funded railroad companies that failed frequently and were reestablished within a year or two. The route of these lines followed closely the path of the current El Camino Real (California State Highway 82), entering San Francisco west of San Bruno Mountain and through the Mission District into the downtown area. As the financing of the operations were stabilized by investments from some of the most famous railroad “barons” of the time (Stanford, Crocker, Hopkins, Huntington, and Harriman), the use of railroads grew and the high amount of locomotive traffic through the now densely populated Mission district spurred the development of an alternate coastal route out of the city. The Bayshore Cutoff with a series of five tunnels was conceived, designed, constructed, and operational by 1907, despite the setback posed by the 1906 earthquake. These tunnels are named uncreatively numerically with Tunnel 1 being closest to the San Francisco Terminus and Tunnel 4 being the southernmost tunnel still in operation. Tunnels 1 through 4 were excavated using conventional mining method in rock composed primarily of the Franciscan Complex rocks from Potrero Hill south to the area formerly occupied by Candlestick Park. Tunnel 5 was eliminated from service in the 1950s when U.S. Highway 101 was constructed as a freeway and the railroad line was relocated west of its previous alignment, making the tunnel obsolete.



Figure 91. Transportation tunnels in San Francisco.

Fort Mason Tunnel

The Fort Mason Tunnel extends from its west portal just east of the intersection of Laguna and Beach Streets, underneath the promontory of Fort Mason emerging at the east portal at the north end of Van Ness Avenue at Aquatic Park. This tunnel served as a single track light rail/street car line from its construction in 1914. It was originally utilized to transport materials and people to the Pacific Panama Exhibition of 1915, which was located west of the tunnel in what has now been reconstructed as the residential Marina District. The tunnel line continued to be used by the Army in its expansion of military operations in the early and mid-20th century and was then operated by the State Belt Railroad until it was closed in 1993.

The tunnel transects a section of the Franciscan Complex that matches structurally with some of the more

resistant sandstone beds of the Central Belt that lie between the Hunters Point Mélange on the west and the more coherent Alcatraz terrane on the east.

Stockton Street Tunnel

The Stockton Street Tunnel was also constructed to facilitate transportation to the Pacific–Panama Exhibition of 1915, and was completed on December 28, 1914. The tunnel portals begin on the south at Stockton and Bush Streets, and on the north end at Stockton Street between California and Sacramento Streets. The tunnel was notable in that it was conceived as the largest span single tunnel in the world at the time with an inside dimension at its base of 15 m (49 ft) clear at the base of its foundation walls. Another innovation that caused a significant stir in the labor market for masons was the decision to utilize a cast-in-place concrete lining. A concrete tunnel lining of this size and complexity

had not previously been successfully built and the bricklayers union protested loudly against the “folly” of a concrete lining that “couldn’t be built.” Indeed the method of delivering the concrete to the lining forms through pressurized piping was also quite innovative at the time. Termed Pneumatic Concreting at the time, this was one of the first applications of using compressed air and hoses to deliver concrete to difficult-to-reach forming.

The tunnel encountered shale members of the Franciscan Complex near each portal and the records indicate a schistose rock was encountered in the center reach of the tunnel. The tunnel was conventionally mined using explosives and heavy equipment, much to the dismay of the neighbors. Undesirable ground movement was significant at the early stages of construction, causing the contractor to innovate excavation by excavating smaller side tunnels with supplemental support prior to excavating the central portion of the tunnel, making it the first sequential excavation tunnel in California.

Twin Peaks Tunnel

The construction of the Twin Peaks tunnel, which is 3.65 km (2.27 miles) long, was begun on November 30, 1914 and completed on July 14, 1917. The final lining consisted of a cast-in-place reinforced concrete lining. Two underground stations were originally constructed including the Forest Hill Station (originally called the Laguna Honda Station) and the Eureka Station, which was closed in 1972 when the underground Market Street subway and its nearby Castro Station were built. With two sets of tracks installed, light rail service between the Castro neighborhood and what is now known as West Portal began in February of 1918. Much of the support for this project came from landholders in the newly developed West of Twin Peaks neighborhood, where a great deal of housing was being built in the aftermath of the 1906 earthquake and fire. Commuter rail service in this tunnel continues to this day with service to hundreds of thousands of citizens riding the K-, L-, and M-Lines of the San Francisco Municipal Railroad.

While no specific information about the geology of the Twin Peaks Tunnel has been found, it is likely comprised of chert, sandstone, greenstone, and shale of the Franciscan Complex. As noted above, construction was completed in just under three years, largely due to a very experienced tunneling contractor and the relative stability of the rock mass.

Sunset Tunnel

The Sunset Tunnel was constructed between June 1926 and February 1928, as a light rail link for the N-Line of the San Francisco Municipal Railway. The tunnel, also called the Duboce Tunnel, connects the east portal at Duboce and Noe streets, with the west portal near Cole and Carl streets. The tunnel traverses underneath the hill capped by Buena Vista Park. The tunnel was constructed with conventional mining methods and has final cast-in-place reinforced concrete liner, similar to that of the Twin Peaks Tunnel. The dimensions of the tunnel are slightly smaller than the Twin Peaks Tunnel with a crown height of 37 m (121.4 ft) and a width at the invert of approximately 7 m (23 ft). Geologically, the rock encountered during the excavation of the tunnel are within the same portion of the Franciscan Complex that comprise Twin Peaks and Mt. Olympus where the rock types consist of chert, sandstone, greenstone and some shale.

Broadway Tunnel

Construction of the Broadway Tunnel, officially known as the Robert C. Levy Tunnel after the former San Francisco City Engineer and Superintendent of Building Inspection, was begun in May 1950 and was completed in December 1952. The Broadway Tunnel is comprised of two parallel tunnels each carrying two lanes of traffic with a pedestrian lane walkway. The tunnel is approximately 580 m (1,900 ft) long and was intended to link the Embarcadero Freeway and Central Freeway, which were being constructed around and through the city, respectively, to connect with the Golden Gate Bridge. These freeway connections were never completed—indeed they were demolished after the 1989 Loma Prieta earthquake revealed their design to be seismically inadequate—but the tunnel itself remains a valued rapid link between the eastern neighborhoods of North Beach and Chinatown with the Van Ness and Pacific Heights neighborhoods on the west.

The Broadway Tunnel alignment lies beneath a portion of Russian Hill. The geology in this portion of San Francisco is comprised of shale and sandstone of the Franciscan Complex Alcatraz terrane.

Bay Area Rapid Transit

The Bay Area Rapid Transit district (BART) is the primary heavy rail commuter system in the Bay Area and was built in the late 1960s and early 1970s. Within

San Francisco, the system is generally underground, except in the southwest portion of the city. Construction of the system included shielded tunnel excavations beneath Market Street and cut-and-cover station excavations in the downtown San Francisco area and Mission District. All BART access to the downtown area from the east currently comes through the Transbay Tube, an immersed tube that was constructed on land and then assembled and submerged in the bay. Four transbay lines use the Tube. Heading south from the Mission District, the twin tunnels enter a portion of the project called the Fairmont Tunnel, which goes through Franciscan Complex rock as the tunnel approaches the Glen Park Station. The tunnels then extend from Glen Park to Balboa Park Station where, as the tracks head southward, they emerge from underground onto an elevated structure that carries the trains out of San Francisco and on to Daly City and points south.

Excellent descriptions of the BART tunnels in San Francisco are presented in Rogers, (2001a and 2001b).

San Francisco Municipal Railroad (Muni)

The first public transportation rail system to go into broad service in San Francisco was the cable car system that began in 1873. The system was devised by Andrew Hallidie, a Scottish immigrant and manufacturer of wire cables. Early acceptance was likely due to the ability of the cable cars to negotiate San Francisco's famously steep hills.

The San Francisco Municipal Railway (Muni) began streetcar (light rail) service in 1912 with the establishment of the A- and B-Line routes between downtown and the Richmond District. Over the next 5-10 years streetcar lines were added throughout many areas of the city, with routes identified from the original A-Line through the M-Line that served southwest San Francisco through the Twin Peaks Tunnel. The N-Line was added in 1928 with the completion of the Sunset Tunnel, described above.

Muni Metro—Market Street Subway

The Market Street Subway system moved many of the street cars that ran on the surface of Market Street (J-, K-, L-, M- and N- Lines) to underground tracks built in twin tunnels constructed on top of the BART system tunnels (Figure 92 and Figure 93).

T-Third Street Line/Central Subway

The newest municipal railroad line in San Francisco is the T-Third Street Line which is being constructed in phases. The first phase extended from the Sunnysdale District in southeastern San Francisco to King Street where the trains join other lines that run along the Embarcadero waterfront. Phase 1 began operating in April 2007 and serves the growing Bayview and Dogpatch Districts as well as Sunnysdale. Phase 1 was constructed entirely at grade and provides excellent service connecting these neighborhoods with the downtown area.

Phase 2 of the T-Line is also known as the Central Subway project. This extension of the T-Line is currently under construction, and when complete will take the existing T-Line from 4th and King streets north into Chinatown. There will be one new surface station at 4th and Brannan and three new underground stations: Yerba Buena/Moscone Station (YBM), Union Square/Market Street (UMS) Station and Chinatown Station (CTS). Along this alignment, the underground portion of the project begins on 4th Street underneath the I-80 viaduct where the track will enter the south portal facility with northbound and southbound trains operating in separate side-by-side tunnels. The tunnels extend to YBM station before lowering the alignment to pass under the existing BART tunnels and rise into UMS station. The tunnels continue to CTS station and while that will be the final station in Phase 2, the tunnel-boring machine (TBM) tunnels extend into North Beach to facilitate extraction of the TBMs and set the project up for the Phase 3 extension that is currently in the planning process.

The project was structured to begin with construction of the twin tunnels, followed by the excavation and construction of the underground stations, removing tunnel segments within the station footprint. Construction began in 2011 with utility relocation and tunnel construction. The twin tunnels were completed in April 2015, and station construction is presently ongoing.

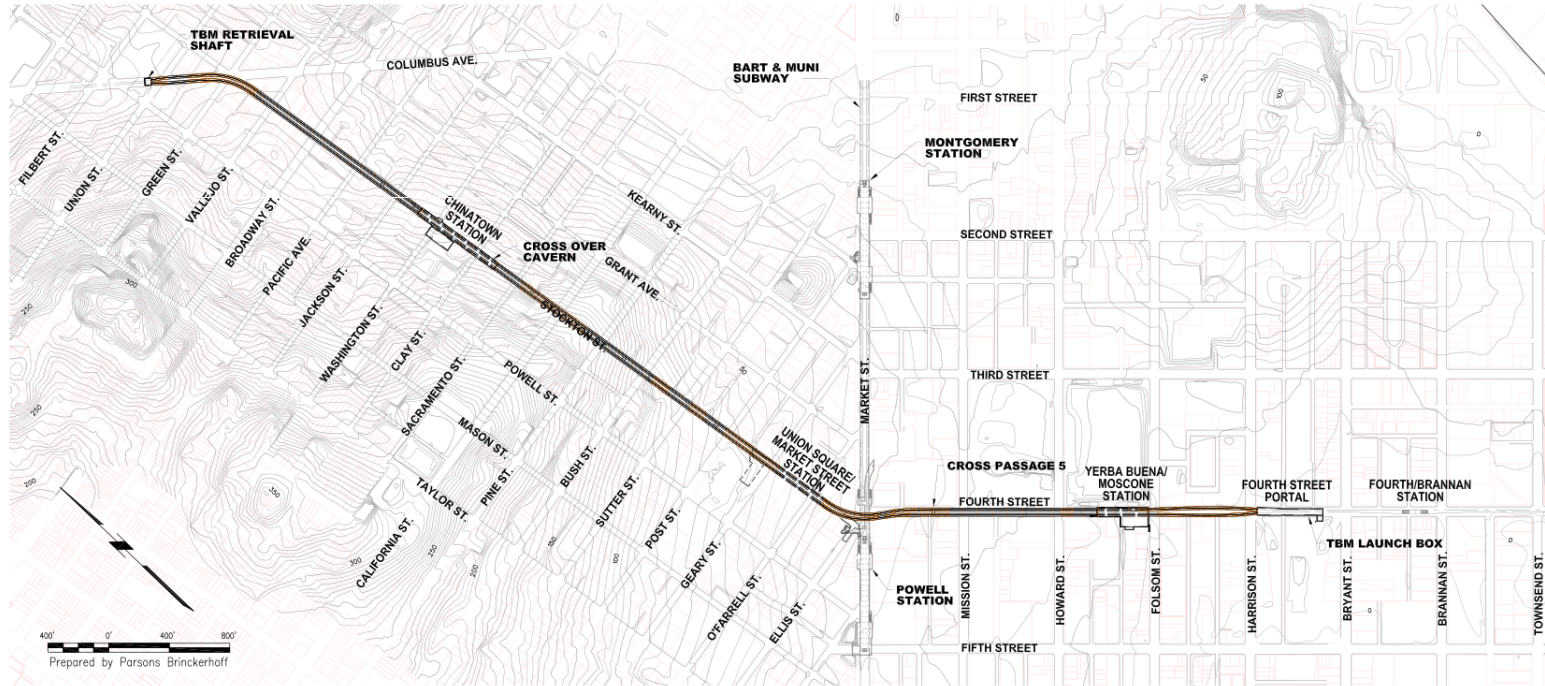
A plan and geologic profile of the tunnel alignment is presented in Figure 94. Geologic units encountered along the project alignment range from artificial fill, dune sand, Young Bay Mud, Colma Formation, Yerba Buena Mud, Colluvium and Franciscan Complex rock. As shown on the profile, the Central Subway tunnels pass directly beneath the older Stockton Street Tunnel that was described above.



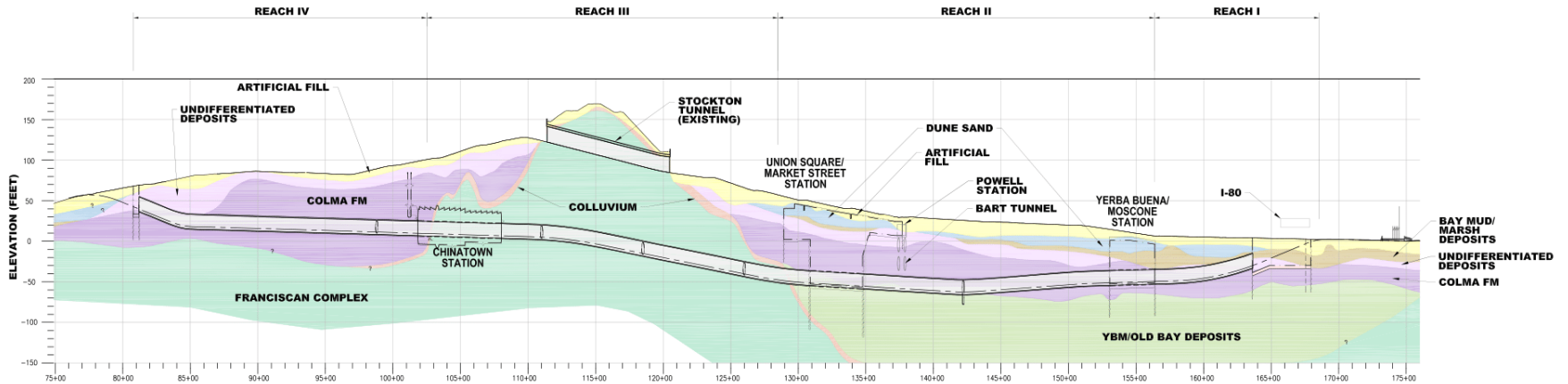
Figure 92. Construction of BART and Muni subways in 1970: Montgomery Street Station, Market Street looking northeast (Photo from SFMTA).



Figure 93. Construction of BART and Muni subways 1970: Civic Center Station, Market Street looking northeast (Photo from Market Street Railway, www.streetcar.org).



PLAN



PROFILE

Figure 94. Plan and Profile for the Phase 2 of the Central Subway project. Dk green—Franciscan bedrock; orange—Colluvium; Lt green—YBM/Old Bay deposits; purple—Colma Fm; Lt purple—Undiff. deposits; Ochre—Young Bay Mud; blue—dune sand; Yellow—fill. (Figure from WSP USA, 2018).

SFPUC Sewer System

The San Francisco Public Utilities Commission operates and maintains the 1,450-kilometer (900-mile) long combined sewer system and 17 pump stations that collect sewage and stormwater, moving the wastewater to the three treatment plants for treatment and discharge to the San Francisco Bay and Pacific Ocean.

The San Francisco wastewater collection and treatment system has been developed over the past 110 years. The current San Francisco sewer system effectively collects, conveys, treats, and discharges all of the dry-weather domestic wastewater and urban runoff flows

and most of the wet-weather runoff (Figure 95 and Figure 96). This dual function allows the system to treat both point and nonpoint sources of pollution. The system utilizes natural watershed areas wherever possible to take advantage of gravity flow for the collection, transport, treatment, and discharge of wastewater and stormwater. The current configuration is largely the result of implementing the recommendations from a 1972 Master Plan (San Francisco Department of Public Works, 1972). The city is primarily served by combined sewers that collect both wastewater and stormwater for treatment at one of three San Francisco treatment facilities. There are two centralized dry-weather treat-



Figure 95. San Francisco Sewer System Drainage Basins and Major Sewer System Infrastructure. (SFPUC, 2018c).

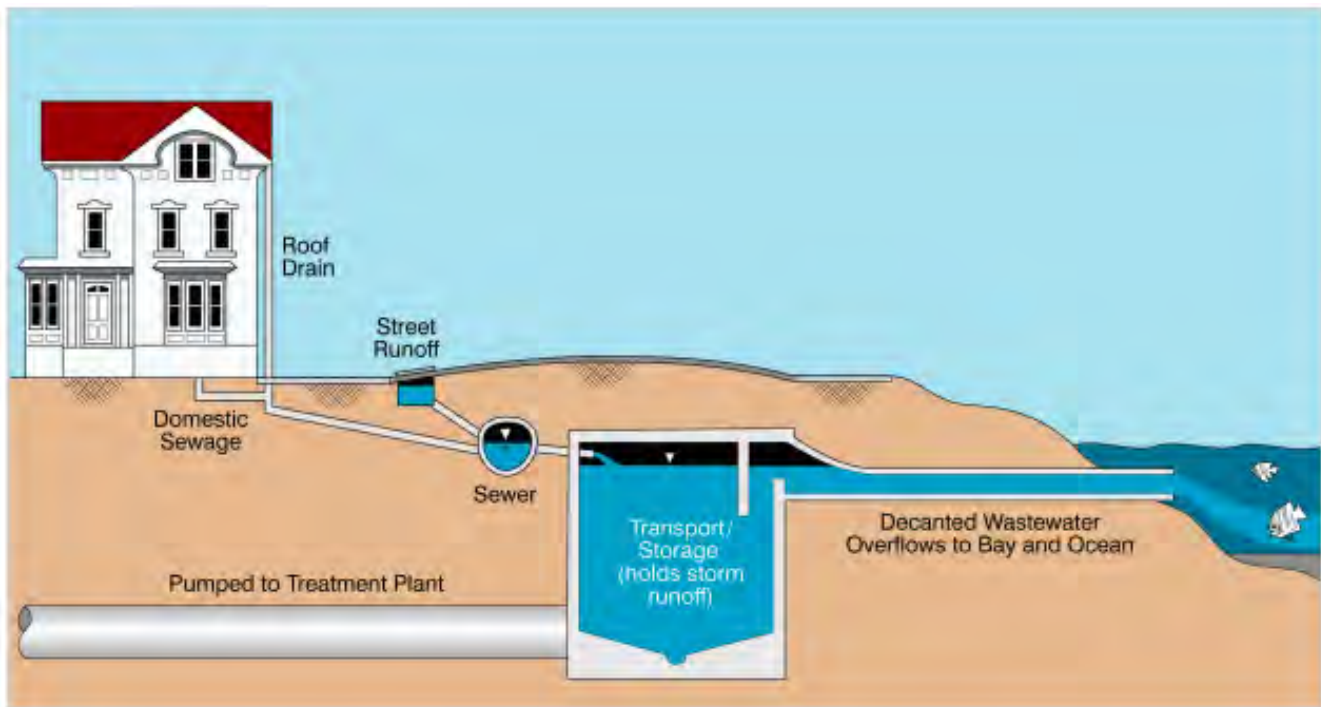


Figure 96. Typical features of San Francisco’s Combined Sewer System (SFPUC, 2018c).

ment plants, the Southeast Water Pollution Control Plant and the Oceanside Water Pollution Control Plant, and one wet-weather facility, the North Point Wet-Weather Facility. There are three currently functioning deepwater outfalls locations: the Southeast Outfall, the North Point Outfall, and the Southwest Ocean Outfall. The Oceanside Plant serves the Westside Watershed, the Southeast Plant serves the Bayside Watershed, and the North Point Plant operates only during wet weather to provide supplementary treatment capacity for the Bayside.

The SFPUC is moving forward with a Sewer System Improvement Program to address the aging infrastructure, seismic vulnerability, climate change impacts, localized flooding and to improve water quality in the bay and ocean. Over 60% of San Francisco sewer pipes are over 80 years old and the system gets overwhelmed during heavy rains with uncontrolled discharges of sewage into the bay. In 2012 SFPUC Commission authorized the planning and development of Phase 1 projects estimated at \$2.7 billion of proposed sewer system capital improvement projects (SFPUC, 2010).

Wastewater Tunnels

Major tunnels have been constructed to convey and control wastewater within San Francisco, and have resulted in a network of conveyance and combined

sewer outfall structures around the city. Early in the development of the city a combined sewer–stormwater system was chosen to minimize the amount of conveyance structures that would have to be constructed. It was also thought that the system had the “benefit”

that stormwater would periodically flush out the sewer system. These Transport and Storage facilities essentially ring the city shores to facilitate conveyance of wastewater and stormwater to the three treatment plants, namely the Southeast Treatment Plant, Oceanside Treatment Plant and the North Point Wet Weather Facility. These large Transport and Storage facilities have been constructed as cut and cover box culverts and where necessary mined or bored tunnels. Below is a summary of the primary mined or bored tunnels in the system.

Mile Rock Tunnel

The Mile Rock Tunnel was constructed between 1914 and 1915 to convey stormwater and sewage from the near the intersection of Cabrillo and 48th Avenue to the outfall in the Pacific Ocean near Mile Rock Beach. This tunnel, approximately 1,280 m (4,200 ft) long, was built using conventional mining methods with initial support ranging from none where hard rock was encountered to extensive wooden cribbing where

needed. The final tunnel lining consisted of cast-in-place reinforced concrete.

Richmond Transport Tunnel

The Richmond Transport Tunnel was completed in 1996 and connected sewer and stormwater systems in the northwest portion of San Francisco with the Westside and Lake Merced Transport and Storage Facilities that supply the Oceanside Treatment Plant in the southwest portion of the city. It is 3,100 m (10,170 ft) long, and extends from the east portal near the west end of Baker Beach to the West Portal at the north end of Ocean Beach. The geology along the alignment includes primarily rocks of the Franciscan Complex, but also Colma Formation, dune sand and Fill (Klein et al., 2001). The Franciscan Complex rocks encountered included sandstone, shale, greenstone, chert, and serpentinite. In the central portion of the alignment a section of *mélange* approximately 1,200 m (3,900 ft) long was encountered.

Lake Merced Tunnel

The Lake Merced Transport Tunnel was completed in 1993 and provides collection of combined flows in the southwestern corner of San Francisco for conveyance to the Oceanside treatment plant. The tunnel has an inside diameter of 4.3 m (14.1 ft) and was excavated using an open-face shielded tunnel-boring machine. The geology along the alignment consisted of generally soft ground including Colma Formation and loose sand dune deposits (Abramson and Kobler, 2001). Local groundwater control was required as part of the excavation due to the permeable nature of the excavated material and relatively high water table.

Northshore Transport and Storage Facility

The Northshore Transport and Storage (T/S) facility is comprised of a number of subprojects including the Marina T/S, North Point Tunnel, and Jackson T/S facilities. Construction of the North Point Tunnel was performed in the early 1980s. This project marked the first time an earth pressure balance tunnel-boring machine was used in the U.S. As most of this tunnel traversed the northeastern shore line of San Francisco, the geologic conditions encountered were comprised primarily of fill, Young Bay Mud, and unconsolidated sand deposits.

Channel Tunnel

As part of the Central Bayside System Improvement Project, the San Francisco Public Utilities Commission is planning a comprehensive update of stormwater and sewer conveyance and storage systems throughout east-central San Francisco. The Channel Tunnel is one of the elements of this system. This tunnel will be a large-diameter force main that links combined flow management and treatment facilities from the Southeast Treatment Plant to the Northpoint Wet-Weather treatment plant in the northeast part of the city.

PROFESSIONAL PRACTICES

by Greg W. Bartow and Kenneth A. Johnson

Engineering geology has been an important element of the development of San Francisco and will continue to have an important role in the future. Some of the key projects that have helped shape San Francisco have been well chronicled in the 2001 AEG Special Publication 12, *Engineering Geology Practice in Northern California*, edited by Horacio Ferriz and Robert Anderson. As commonly occurs in our society, the development of the professional practice is often triggered by specific events. For example, the professional practice and codes for seismic design for structures and buildings in California were motivated by major earthquake damage from the 1906 San Francisco, 1935 Long Beach and 1994 Northridge earthquakes in California. As discussed below, the San Francisco ordinances for Soft Story retrofits and unreinforced masonry building retrofits were implemented following the Loma Prieta earthquake in the San Francisco Bay Area. Other current issues facing the engineering geology community within San Francisco include structural resilience in building responses to seismic shaking, resilience related to global climate change and sea level rise, and naturally occurring asbestos. Each of these topics is briefly discussed in this section.

Seismic Building Codes: Early Motivations and First Seismic Provisions

Nothing advances the science of seismology so much as a great earthquake. –C. Davidson, 1936

At the time of the 1906 San Francisco earthquake, many California municipalities had building codes, but none considered seismic effects. Not surprisingly,

the 1906 earthquake sparked discussion of improving earthquake engineering design and incorporating those improvements in regulatory codes. Professional organizations, particularly the Seismological Society of America, which formed in 1906, and later, the Structural Engineers Association of California, were persistent advocates of code provisions for earthquake-resistant construction (Stanford University, 2006). However, the building code changed very little in the aftermath of the earthquake and fire. In fact, not only were the defects in earthquake and fire resistance repeated in the rebuilding, but building code standards were actually reduced from those in effect before the Great Fire (Hansen, 1989).

In a report titled “Retrospective on the 1906 earthquake’s impact on Bay Area and California public policy” (Perkins, 2006), the authors found that the “1906 earthquake’s influence has been both a blessing and curse on the Bay Area’s and California’s progress to effectively manage earthquake risk.” This earthquake, and its impacts noted in the historical record, have both motivated and discouraged policymakers to act through mitigation and improved emergency response.

Because of the 1906 earthquake, California state and local governments no longer consider earthquakes and their effects as acts of God, beyond human control. The State Earthquake Investigation Commission’s report on the 1906 earthquake is one of the first products of that perspective. The concept was embraced by the progressives of the time, including John Muir, colleague of the report’s principal author, Andrew Lawson, and other Bay Area residents active in the formation of the Seismological Society of America and the Sierra Club.

After the 1906 event, San Francisco officials adjusted local construction codes to increase wind design criteria because engineers could not agree on how to design for earthquakes, and the officials believed that higher wind resistance would enhance earthquake resistance. It was not until 1947 that San Francisco adopted earthquake safety requirements in the city building code (Geschwind, 2001).

In 1961, elected officials from the region’s local governments came together to form the Association of Bay Area Governments, a joint powers agency of the cities and counties of the region, and California’s first council of governments. As a voluntary association of cities and counties, ABAG brought the region’s elected officials together to examine and propose solutions for major

regional issues. From the beginning, earthquakes were recognized as an issue to be addressed by region-wide strategies, a conclusion supported by the impacts of the 1906 earthquake throughout the Bay Area rather than in San Francisco alone. ABAG’s involvement in earthquake hazards planning began with its collaboration with the U.S. Geological Survey in the report, “Regional Geology—The Geology of San Francisco Bay Area and Its Significance in Land Use Planning” (USGS 1968), which was prepared for and published by ABAG. The report includes maps of generalized geology, including active faults, and describes earthquake hazards, but falls short of its promise to provide land use planning guidance. It confirmed the reality of 1906 that the entire Bay Area is “earthquake country” (Perkins, 2006).

The 1906 earthquake gave clues to what would happen in future earthquakes, although the most spectacular damage and ensuing fires in the major cities tended to obscure other effects. For example, collapsed or severely damaged bridges over the Gualala River, the Garcia River, the Salinas River, and Moss Landing provided clear evidence that bridges throughout California, particularly those on soft soils, were highly vulnerable to earthquakes (Lawson et al. 1908). But it was not until the 1989 Loma Prieta earthquake that comprehensive steps would be taken by policymakers to evaluate and reduce bridge vulnerability. The partial collapse of both the Cypress Overpass in Oakland and the San Francisco–Oakland Bay Bridge, as well as others, prompted the legislature to demand major reforms in the funding and capital outlay priorities within the California Department of Transportation. The Loma Prieta earthquake would later be dubbed the “Bridge earthquake.” Similarly, 1933 Long Beach is labeled the “Schools earthquake,” and 1971 is the “Hospitals earthquake” (Perkins, 2006).

Mandatory Soft Story Retrofit Program

In 2013, San Francisco created the Mandatory Soft Story Retrofit Program (MSSP) to ensure the safety and resilience of San Francisco’s housing stock by retrofitting soft-story buildings. Soft-story buildings are those with large openings for windows, doors, or garages that cause the ground floor to be weak and vulnerable to damage or even collapse in an earthquake. The MSSP is enforced by the San Francisco Department of Building Inspection (DBI) and focuses on wood-frame apartment buildings with three or more

stories and five or more units that were built before modern code changes adopted in 1978. As part of the MSSP, all affected property owners were required submit screening forms to DBI by September 15, 2014, and 99% have done so. (San Francisco Department of Building Inspection, 2018; San Francisco Planning and Urban Research Association (SPUR), 2011).

City of San Francisco Unreinforced Masonry Program

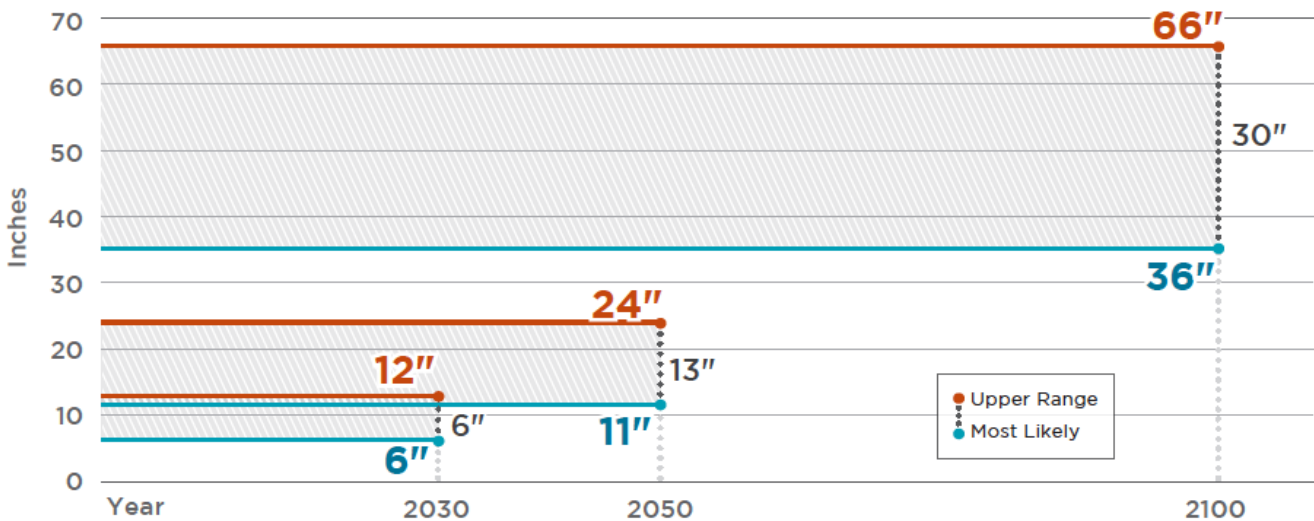
Beginning in 1993, the City took a proactive step in requiring the retrofit of 2,000 brick buildings through the Unreinforced Masonry Building (UMB) program because of their known vulnerability to shaking and collapse from earthquake forces (David Leung, San Francisco Department of Building Inspection, personal communication). The City was able to obtain a 95% compliance rate—the highest recorded throughout California. The UMB Ordinance, 225-92, was adopted on July 14, 1992, and incorporated into San Francisco Building Code as its Chapters 14 and 15 in the 1992 edition. In current code editions, these became San Francisco Existing Building Code Chapters 4A and 4B.

Sea Level Rise: Forecasts, Adaptation Plans, and Policy

San Francisco has 39 km (24 miles) of shoreline and is thus vulnerable to rising sea levels. In the last century, sea levels have risen 0.2 m (8 in) around the San Francisco Bay and Pacific Coast. With continued warming, sea level rise will accelerate for at least the remainder of this century. The National Research Council’s (NRC) 2012 report *Sea-Level Rise for the Coast of California, Oregon, and Washington* (NRC, 2012) projected that San Francisco will likely experience about 0.91 m (36 in) of sea level rise by the end of this century, with up to 1.7 m (66 in) possible. Storm surge for a 100-year extreme weather event could add 1 m (42 in) of temporary flooding on top of sea level rise, resulting in sea levels that are potentially 2.7 m (108 in) higher than today (Figure 97 and Figure 98). Meanwhile, a new report commissioned by the state of California found median projections remain around the same but the upper plausible range of sea level rise alone by end of century may be over 3 m (10 ft). (*Rising Seas in California*, 2017).

The scale of total risk to public and private property

SEA LEVEL RISE PROJECTIONS FOR SAN FRANCISCO RELATIVE TO THE YEAR 2000



Source: NRC (2012). Lower range projections are excluded as they are not recommended for planning purposes.

NOTE: SLR projections do not include extreme tides or coastal storms, which could add up to 42 inches of temporary flooding, for a total of 108 inches above today’s average high tide.

Figure 97. Sea level rise projections for San Francisco relative to the year 2000 (City and County of San Francisco, March 2016).



Legend

— Sea Level Rise Vulnerability Zone



NOTE: SLR Vulnerability Zone represents upper range (unlikely, but possible), end-of-century projections for permanent SLR inundation (up to 66 inches) plus temporary flooding due to a 100-year extreme storm (up to 42 inches) for a total of 108 inches above today's MHHW.

Map Disclaimer: The inundation maps and the associated analyses are intended as planning level tools to illustrate the potential for inundation and coastal flooding under a variety of future sea level rise and storm surge scenarios. The maps depict possible future inundation that could occur if nothing is done to adapt or prepare for sea level rise over the next century. The maps do not represent the exact location of flooding. The maps relied on a 1-m digital elevation model created from LIDAR data collected in 2010 and 2011. Although care was taken to capture all relevant topographic features and coastal structures that may impact coastal inundation, it is possible that structures narrower than the 1-m horizontal map scale may not be fully represented. The maps are based on model outputs and do not account for all of the complex and dynamic San Francisco Bay processes or future conditions such as erosion, subsidence, future construction or shoreline protection upgrades, or other changes to San Francisco Bay or Open Coast. For more context about the maps and analyses, including a description of the data and methods used, please see the Climate Stressors and Impacts Report: Bayside Sea Level Rise Inundation Mapping Technical Memorandum, March 2014 and FEMA Open California Coast Sea Level Rise Pilot Study, San Francisco County, 2015.

Data Source: Bayside—SFPUC SSIP Inundation Mapping, 2015. Westside—FEMA Sea Level Rise Pilot Study, 2015.

Figure 98. San Francisco sea level rise vulnerability zone (City and County of San Francisco, March 2016).

value in San Francisco due to sea level rise is considerable. Estimating expected losses in public and private property value informs decisions about balancing costs of post-disaster relief with those of upfront adaptation. With a sea level rise of 1.7 m (66 in), the total property value at risk is \$55 billion and a sea level rise of 2.7 m (108 in) yields a total property value risk of \$77 billion (Risk Management Solutions, 2015).

In 2016, the City prepared a San Francisco Sea Level Rise Action Plan (City and County of San Francisco, March 2016) as a “call to action for City departments and stakeholders to work together to make San Francisco a more resilient city in the face of rising sea levels. The Plan defines an overarching vision and set of objectives for future sea level rise and coastal flood planning and mitigation in San Francisco.” The Action Plan is a first step in developing a Citywide Sea Level Rise Adaptation Plan, expected to be completed by summer 2018, which will incorporate the adaptation strategies identified in the Action Plan and set a planning framework to prioritize investments to best improve climate resilience, while protecting economic and environmental value. The Sea Level Rise Adaptation Plan will also identify potential funding sources, governance structures, and implementation timelines.

A six-step process is outlined in the Action Plan for adaptation planning and implementation: Review Science, Assess Vulnerability, Assess Risk, Develop Adaptation, Implement Adaptation, and Monitor Implementation. The process begins by selecting the most reliable climate information to use for planning. Next, vulnerability and risk assessments identify the potential physical damage an asset may incur when exposed to a hazard (e.g., flooding), as well as the consequences and likelihood of said damage. Once assets have been prioritized for adaptation, comprehensive planning evaluates the best strategies to reduce vulnerability and risk.

Current adaptation implementation in San Francisco will continue to address imminent risk while larger interventions will be developed and implemented over longer time frames. Finally, ongoing monitoring identifies which actions are most effective, any unintended consequences, and new data that may change direction or inspire additional strategies. In general, sea level rise adaptation requires one or more of the following three options: accommodate (raise or waterproof assets in place), protect (create natural or engineered barriers, such as wetlands or levees), or retreat (relocate sensitive

assets to low-risk areas and/or transition high-risk areas to lower-risk uses) (Figure 99). The Citywide Adaptation Plan is expected to focus on governance related strategies (e.g., zoning, design standards, maintenance procedures) and innovative physical strategies (e.g., green infrastructure, structure elevations, and flood barriers). Solutions may be implemented at multiple scales and timeframes, and in combination in order to optimize performance and efficiency.

INTERVENTION OPTIONS

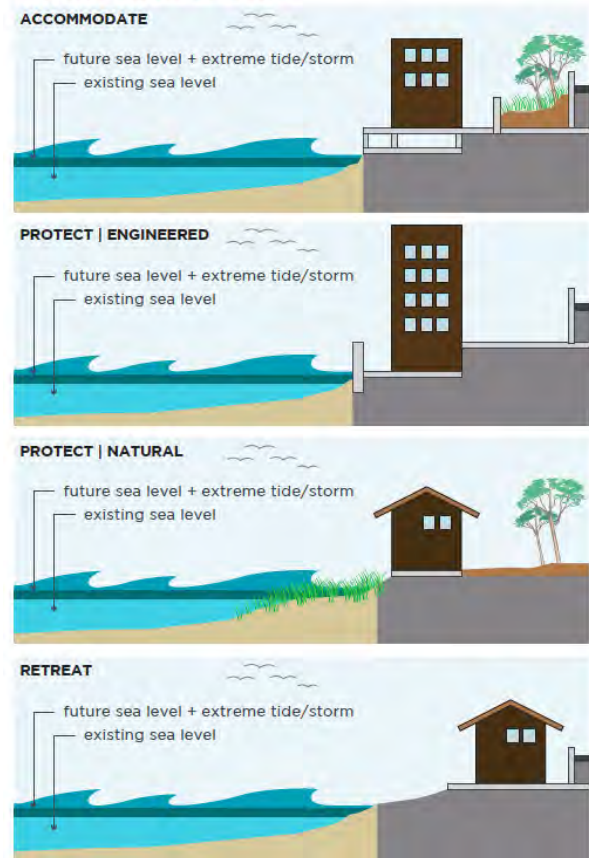


Figure 99. San Francisco sea level rise intervention options (City and County of San Francisco, March 2016).

One well-understood difficulty in planning resilience to climate change effects in general and sea level rise in particular derives from uncertainty. While sea levels are virtually certain to rise for decades and likely centuries, the rate at which seas rise will remain uncertain. As the science advances, projections are actually getting wider rather than narrower (Griggs et al., 2017). As a result, planners, including those in San Francisco, are increasingly turning to approaches that plan for a “most likely” sea level rise scenario defined by best available science while also accounting for the possibility that sea level

rise could accelerate more rapidly. In this environment, design of flexible adaptation approaches and monitoring become essential. In coming decades, we will know more about how international agreements curtail or fail to curtail global greenhouse gas emissions, which will have a significant effect on sea level rise. We will also learn more about how sensitive key components of sea level rise are to warming, such as thermal expansion of oceans and land ice melt in Antarctica and Greenland. These types of knowledge will inform how adaptation response can best be phased.

Naturally Occurring Asbestos (NOA)

The term *asbestos* refers to a group of serpentine and amphibole group minerals having a fibrous (asbestiform) crystal habit that were commonly used to manufacture a number of different building materials (Erskine and Bailey, in press). One of those minerals, chrysotile asbestos, has been documented in association with the serpentine in the foundation of the south tower and anchorage for the Golden Gate Bridge. Given that the California official State Rock is serpentine, it should not be surprising that San Francisco would be true to the state and have widespread exposure of this rock. The common occurrence of serpentine in San Francisco, coupled with current state legislation that regulates asbestiform minerals makes naturally occurring asbestos an important concern in San Francisco.

The minerals in the asbestos group that were typically used in manufacturing included chrysotile and five narrowly defined minerals of the amphibole group including actinolite, anthophyllite, riebeckite (also called crocidolite), tremolite, and cummington-grunerite (also called amosite). It is these mineral species that have been most studied in health exposure and toxicological studies, and as a result these specific minerals are specified in regulations promulgated by the U.S. Occupational Safety and Health Administration (OSHA) and the U.S. Environmental Protection Agency (EPA). These five amphiboles were also specified in California's Airborne Toxic Control Measures (ACTM) and required analytical testing methods for naturally occurring asbestos.

Despite the regulatory definitions of asbestos described above, a number of researchers in NOA are considering all asbestiform (fibrous) amphiboles that are crystallographically related to these regulated amphiboles together with their mineralogic relatives. For example,

minerals such as chrysotile polymorphs antigorite or lizardite or solid-solution series minerals glaucophane-riebeckite sequence are also being included in the literature for NOA. In addition to widely distributed serpentine in San Francisco, glaucophane-bearing rocks are now therefore being considered as potentially qualifying as NOA within the city as policies around NOA evolve.

Specific analytical testing methods have been required for asbestos-containing materials to evaluate the level of asbestos in the materials. These methods were originally targeting building materials (e.g., drywall) being regulated as described above rather than NOA. Methods for documenting and addressing NOA for site investigations, such as polarized light microscopy, transmission electron microscopy, scanning electron microscopy, and x-ray diffraction, have been described by the California Geological Survey (CGS) in their Special Technical Publication 124 – Guidelines for Geologic Investigations of Naturally Occurring Asbestos in California (CGS, 2002).

SUMMARY

As in most major cities of the world, the natural and geologic setting strongly influence the history and development of the city of San Francisco. This paper attempts to address the most significant issues for San Francisco presented in an overall geologic framework of the Bay Area. As San Francisco continues to evolve and develop, the geology will continue to affect the city, even as it continues to be a center of culture, finance, trade and technology.

ACKNOWLEDGMENTS

This paper was inspired by the work of three legendary San Francisco Bay Area geologists. Julius Schlocker, Doris Sloan, and Clyde Wahrhaftig advanced the geologic understanding of San Francisco throughout their careers and some of their key contributions are referenced in this paper, including the following outstanding summaries: Schlocker (1974), Sloan (2006), and Wahrhaftig (1984a).

The Editors and the Association of Engineering Geologists wish to thank the many reviewers including Robert Anderson, Kelly Archer, David Behar, Stephen Hill, Mark Johnson, Manisha Kothari, Ravi Krishnaiah, David Leung, Michele Liapes, Tina Low, Mike Maley,

Garry Maurath, Alec Naugle, Jack Meyer, Obiajulu Nzewi, Steven Reel, Nick Sitar, Ross Steenson, Ray Sullivan, Jessica Tibor, John Wakabayashi, Carl Wentworth, and Sam Young.

Drew Kennedy generously provided information on the Serra Fault and Luke Blair kindly developed many of the seismic hazards figures and tables used herein. Reviewers Jack Boatwright, Patricia McCrory, Suzanne Hecker, Stephen Hickman, David Schwartz, and Carl Wentworth each provided valuable comments and suggestions on the seismic hazards section. Clark Fenton, Susan Olig, and Judith Zachariassen contributed to descriptions of the faults that served as the basis for the fault descriptions included in the seismic hazards section.

This report greatly benefitted from the work of Courtney Pasco, who assisted with the many aspects of production and coordination. The report would not have been finished in time for the September 2018 IAEG Congress in San Francisco without her efficient assistance. Mary-Russell Roberson provided exceptional overall editorial and technical review; and much help in providing continuity to this multi-authored report. Michael B. Henry provided tremendous support in preparing and refining many of the graphics within the paper. Danial Walsh provided valuable GIS assistance in producing the generalized geologic map. The Editors wish to acknowledge WSP USA for their support in producing the paper as well, especially its Geotechnical and Tunneling Group.

CONTRIBUTING AUTHORS

John Baldwin, CEG
Lettis Consultants International
baldwin@lettisci.com

Greg W. Bartow, CEG, CHg
California State Parks
greg.bartow@parks.ca.gov

Peter Dartnell
U.S. Geological Survey
pdartnell@usgs.gov

George Ford, CEG
Geosyntec, Inc.
gford@geosyntec.com

Jeffrey A. Gilman, CEG, CHg
Private Consultant
jgilman72@comcast.net

Robert Givler, CEG
Lettis Consultants International
givler@lettisci.com

Sally Goodin, PG
Pacific Gas & Electric Co
SEGC@pge.com

Russell W. Graymer, PhD
U.S. Geological Survey
rgraymer@usgs.gov

H. Gary Greene, PhD
Center for Habitat Studies
Moss Landing Marine Labs
greene@mlml.calstate.edu

Kenneth A. Johnson, PhD, CEG, PE
WSP USA, San Francisco, CA
kenneth.johnson@wsp.com

Samuel Y. Johnson, PhD
U.S. Geological Survey
sjohnson@usgs.gov

Darrell Klingman
Pacific Gas & Electric Co
DSK5@pge.com

Keith L. Knudsen, CEG
U.S. Geological Survey
kknudsen@usgs.gov

William Lettis, CEG
Lettis Consultants International
lettis@lettisci.com

William E. (Bill) Motzer, PhD, PG, CHg, AIPG CPG
Forensic Geochemist/Geologist
bmotzer1986@att.net

Dorinda Shipman, CHg
Langan Engineering and Environmental Services, Inc.
dshipman@langan.com

Lori A. Simpson, PE, GE
Langan Engineering and Environmental Services, Inc.
lsimpson@langan.com

Philip J. Stuecheli, CEG
ENGEEO, Incorporated
pstuecheli@engeo.com

Raymond Sullivan, B.Sc, PhD
Professor Emeritus of Geology
San Francisco State University
sullivan@sfsu.edu

REFERENCES

- Aagaard, B.T., Blair, J.L., Boatwright, J., Garcia, S.H., Harris, R.A., Michael, A.J., Schwartz, D.P., and DiLeo, J.S., 2016, Earthquake outlook for the San Francisco Bay region 2014–2043 (ver. 1.1, August 2016): U.S. Geological Survey Fact Sheet 2016–3020, 6 p., <http://dx.doi.org/10.3133/fs20163020>.
- ABAG, 2009, Association of Bay Area Governments (ABAG) Liquefaction Maps and Information: <http://www.abag.ca.gov/bayarea/eqmaps/liquefac/liquefac.html>.
- Abramson, L. and Kobler, M., 2001, Lessons learned during construction of the Lake Merced stormdrain tunnel, *in* Engineering Geology Practice in Northern California, H. Ferriz and R. Anderson, eds., AEG Special Publication 12, pp. 465-474.
- AECOM, Inc., 2014, CS-199 Planning Support Services for Auxiliary Water Supply System (AWSS), Project Report Prepared for SFPUC.
- Alpers, C.N., Hunerlach, M.P., May, J.T., and Hothem, R.T., 2005, Mercury contamination from historical gold mining in California: U.S. Geological Survey (USGS) Fact Sheet 2005-3014 Version 1.1 Revised October 2005, USGS, Sacramento, CA, 6 p.
- Ambrose, S. E., 2000, Nothing Like it in the World: The Men Who Built the Transcontinental Railroad 1863-1869: Touchstone Publishers, New York, NY, 431 p.
- Amin, R. and Stokle, B., 2016, Designing the Bay Area's second transbay rail crossing: SPUR, The Urbanist, Issue 549, February 10, 2016.
- Andersen, D.W., Sarna-Wojcicki, A.M., Sedlock, R.L., 2001, San Andreas fault and coastal geology from Half Moon Bay to Fort Funston: Crustal motion, climate change, and human activity in Stoffer, P.W., and Gordon, L.C., eds., *Geology and National History of San Francisco Bay Area; A Field-Trip Guidebook*: U.S. Geological Survey Bulletin 2188, p. 87–104
- Angell, M.A., Hanson, K.L., and Crampton, T., 1997, Characterization of Quaternary contractional deformation adjacent to the San Andreas fault, Palo Alto, California: Final Report submitted to the U.S. Geological Survey, National Earthquake Hazards Reduction Program, Award No. 1434-95-G-2586.
- Apen, F.E., Day, H.W., Souders, K., and Roeske, S.M., 2016, Cretaceous depositional ages of blueschist facies metagraywacke, Tiburon Peninsula, CA; Implications for evolution of the Franciscan Complex in the San Francisco Bay Area: Geological Society of America Abstracts with Programs, v. 48, no. 7, Paper No. 267–8.
- Armstrong, C. F., and Gallagher, K., 1977, Fossils from the Franciscan assemblage, Alcatraz Island: California Geology, v. 30, p. 134.
- Atwater, B.F., Hedel, C.W., and Helley, E.J., 1977, Late Quaternary depositional history, Holocene sea-level changes, and vertical crustal movement, southern San Francisco Bay, California: U.S. Geological Survey Professional Paper 1014, 15 p.
- Atwater, T., 1970, Implications of plate tectonics for the Cenozoic tectonic evolution of western North America: Geological Society of America Bulletin, v. 81, p. 3,513–3,536.
- Atwater, T., and Stock, J., 1998, Pacific-North America plate tectonics of the Neogene southwestern United States; an update: International Geology Review, v. 40, p. 375-402.
- Bailey, E.H., Irwin, W.P., and Jones, D.L., 1964, Franciscan and related rocks and their significance in the geology of western California: California Division of Mines and Geology Bulletin 183, 177 p., 2 plates.
- Bailey, E.H., Blake, M.C., Jr., and Jones, D.L., 1970, On-land Mesozoic oceanic crust in California Coast Ranges: U.S. Geological Survey Professional Paper 700-C, p. C70-C81.
- Bakun, W.H., 1980, Seismic activity on the southern Calaveras fault in central California: Bulletin of the Seismological Society of America, v. 70, p. 1,181–1,197.
- Bakun, W.H., 1999, Seismic activity of the San Francisco Bay region, Bulletin of the Seismological Society of America, v. 89, no. 3, p. 764–784.
- Baldwin, J.N., Kelson, K.I., and Randolph, C.E.,

- 1998, Timing of the most-recent surface faulting event on the northern Calaveras fault near Sunol, California [abs]: EOS (Transactions, American Geophysical Union), v. 79, no. 45, p. F611.
- Baldwin, J.N., Kelson, K.I., Witter, R.C., Koehler, R.D., Helms, J.G., and Barron, A. D., 2002, Preliminary Report On The Late Holocene Slip Rate Along The Central Calaveras Fault, Southern San Francisco Bay Area, Gilroy, California, Final Technical Report, U.S. Geological Survey, Award 00-HQ-GR-0073, p. 1–28.
- Barbeau, D.L., Jr., Ducea, M.N., Gehrels, G.E., Kidder, S., Wetmore, P.H., and Saleeby, J.B., 2005, U-Pb detrital-zircon geochronology of northern Salinian basement and cover rocks: Geological Society of America Bulletin, v. 117, p. 466–481.
- Barnard, P. L., Eshelman, J., Erikson, L., and Hanes, D.M., 2007, Coastal processes study at Ocean Beach, San Francisco, CA—Summary of data collection 2004–2006: U.S. Geological Survey Open-File Report 2007–1217, 165 p., available at <http://pubs.usgs.gov/of/2007/1217/>.
- Barnard, P. L., Hanes, D.M., Kvittek, R.G., and Iampietro, P.J., 2006a, Sand waves at the mouth of San Francisco Bay, California: U.S. Geological Survey Scientific Investigations Map 2944, 5 sheets, available at <http://pubs.usgs.gov/sim/2006/2944/>.
- Barnard, P. L., Hanes, D.M., Rubin, D.M., and Kvittek, R.G., 2006b, Giant sand waves at the mouth of San Francisco Bay: Eos, v. 87, p. 285–289.
- Barnard, P. L., Schoellhamer, D. H., Jaffe, B. E., and McKee, L. J., 2013, Sediment transport in the San Francisco Bay coastal system: An overview: Marine Geology special issue (volume 345) released November, 2013.
- Barnes, J.D., Eldam, R., Lee, C.A., Errico, J.C., Loewy, S., Cisneros, M., 2013, Petrogenesis of serpentinites from the Franciscan Complex, western California, USA: Lithos, v. 178, p. 143–157.
- Barr, J., and Caskey, S. J., 1999, Northern continuation of the Serra fault to southwest San Francisco: constraints on uplift rates and style of deformation on the San Francisco Peninsula: Geological Society of America Abstracts with Programs, v. 31, no. 6.
- Bartell, M. J., 1913, Report on the underground water supply of San Francisco County, present yield, probable additional yield: Prepared under direction of M. M. O’Shaughnessy, City Engineer by M. J. Bartell, Department of Public Works, Bureau of Engineering, May 1913, 173 p.
- Barth, A.P., Wooden, J.L., Grove, M., Jacobson, C.E., and Pedrick, J.N., 2003, U-Pb zircon geochronology of rocks in the Salinas Valley region of California; a reevaluation of the crustal structure and origin of the Salinian block: Geology, v. 31, p. 517–520.
- Bartow, J.A., Sarna-Wojcicki, A.M., Addicott, W.O., and Lajoie, K.R., 1973, Correlation of marine and continental Pliocene deposits in northern California by tephrochronology: The American Association of Petroleum Geologists Bulletin, v. 57, no. 4, p. 769.
- Bean, L.J., ed., 1994, The Ohlone Past and Present: Native Americans of the San Francisco Bay Region. Ballena Press, 1994.
- Bennet, M. J., 1998, Sand boils and settlement at Treasure Island after the earthquake, *in* The Loma Prieta, California, earthquake of 1989—Liquefaction, U.S. Geological Survey Professional Paper 1551-B.
- Berkland, J.O., 1973, Rice Valley outlier—New sequence of Cretaceous–Paleocene strata in the northern Coast Ranges, California: Geological Society of America Bulletin, v. 84, p. 2,389–2,406.
- Bero, D.A., 2014, Geology of Ring Mountain and Tiburon Peninsula, Marin County, California: California Geological Survey Map Sheet 62, 34 p., 2 sheets.
- Berroza, G.C., 1996, Rupture history of the earthquake from high-frequency strong-motion data, *in* The Loma Prieta, California, earthquake of October 17, 1989—Main shock characteristics, Spudich, P., ed., U.S. Geological Survey Professional Paper 1550-A.
- Blackwelder, E., 1914, A summary of the orogenic

- epochs in the geologic history of North America: *Journal of Geology*, v. 22, p. 633–654.
- Blake, M.C., Jr., ed., 1984, Franciscan Geology of Northern California: Pacific Section, Society of Economic Paleontologists and Mineralogists, v. 43, 254 p.
- Blake, M.C., Jr., Graymer, R.W., and Jones, D.L., 2000, Geologic map and map database of parts of Marin, San Francisco, Alameda, Contra Costa, and Sonoma Counties, California: U.S. Geological Survey Miscellaneous Field Studies MF-2337, 31 p., 1 sheet, scale 1:75,000.
- Blake, M.C., Jr., Graymer, R.W., and Stamski, R.E., 2002, Geologic map and map database of western Sonoma, northernmost Marin, and southernmost Mendocino counties, California: U.S. Geological Survey Miscellaneous Field Studies Map MF-2402, 45 p., 1 sheet, scale 1:100,000.
- Blake, M.C., Jr., Harwood, D.S., Helley, E.J., Irwin, W.P., Jayko, A.S., and Jones, D.L., 1999, Geologic map of the Red Bluff 30' x 60' quadrangle, California: U.S. Geological Survey Geologic Investigations Series Map I-2542, 15 p., 1 sheet, scale 1:100,000.
- Blake, M.C., Jr., Howell, D.G., and Jayko, A.S., 1984, Tectonostratigraphic terranes of the San Francisco Bay region, *in* Blake, M.C., Jr., ed., Franciscan Geology of Northern California: Pacific Section, Society of Economic Paleontologists and Mineralogists, v. 43, p. 5–22.
- Blake, M.C., Jr., Howell, D.G., and Jones, D.L., 1982, Preliminary tectonostratigraphic terrane map of California: U.S. Geological Survey Open-File Report 82-593, 9 p., 3 maps, scale 1:750,000.
- Blake, M.C., Jr., Irwin, W.P., and Coleman, R.G., 1969, Blueschist-facies metamorphism related to regional thrust faulting: *Tectonophysics*, v. 8, p. 237–246.
- Blake, M.C., Jr., Jayko, A.S., Murchey, B.L., and Jones, D.L., 1992, Formation and deformation of the Coast Range Ophiolite and related rocks near Paskenta, California: *American Association of Petroleum Geologists Bulletin*, v. 76, p. 417.
- Blake, M.C., Jr., and Jones, D.L., 1974, Origin of Franciscan mélanges in Northern California, *in* Dott, R.H., Jr., and Shaver, R.H., Modern and ancient geosynclinal sedimentation: Society of Economic Paleontologists and Mineralogists Special Publication, no. 19, p. 345-357.
- Blake, W.P., 1853, Geology of the vicinity of San Francisco, *in* Joseph, H., and Baird, S.F., eds., Reports of explorations and surveys to ascertain the most practicable and economical route for a railroad from the Mississippi River to the Pacific Ocean: Washington, D.C., U.S. War Department, v. 5, part II, ch. XII.
- Bloxam, T.W., 1956, Jadeite-bearing metagraywackes in California: *American Mineralogist*, v. 41, p. 488–496.
- Bloxam, T.W., 1960, Jadeite-rocks and glaucophane-schists from Angel Island, San Francisco Bay, California: *American Journal of Science*, v. 258, p. 555–573.
- Boatwright, J., and Bundock, H., 2008, Modified Mercalli intensity maps for the 1868 Hayward earthquake plotted in ShakeMap format, U.S. Geological Survey Open-File Report 2008-1121.
- Bonilla, M.G., 1959, Geologic observations in the epicentral area of the San Francisco earthquake of March 22, 1957, *in* Oakeshott, G., ed., 1959, The San Francisco Earthquakes of March 1957, CDMG Special Report 57, p. 25–37.
- Bonilla, M.G., 1965, Geologic map of the San Francisco South quadrangle, California: U.S. Geological Survey Open-File Map, OF-65-18, 1:20,000.
- Bonilla, M.G., 1971, Preliminary geologic map of the San Francisco South quadrangle and part of the Hunters Point quadrangle, California: U.S. Geological Survey Miscellaneous Field Studies Map MF-311, 2 sheets, scale 1:24,000.
- Bonilla, M.G., 1994, Serra fault zone, San Francisco Peninsula, California [abs.]: EOS (Transactions, American Geophysical Union, Fall Meeting Supplement), v. 75, p. 681.
- Bonilla, M.G., 1996, Late Cenozoic folds and thrust faults, San Francisco South quadrangle, *in* Jayko, A.S., and Lewis, S.D., (compilers), Towards assessing the seismic risk associated with blind

- faults, San Francisco Bay Region, California: U.S. Geological Survey Open-File Report 96-267, p. 36–38.
- Bonilla, M.G., 1998, Preliminary geologic map of the San Francisco South 7.5-minute quadrangle and part of the Hunters Point 7.5-minute quadrangle, San Francisco Bay Area, California: A Digital Database: U.S. Geological Survey Open-File Report 98-354, scale 1:24,000.
- Boore, D.B., 1977, Strong-motion recordings of the California earthquake of April 18, 1906: Bulletin of the Seismological Society of America, v. 67, p. 561–578.
- Bowen, O.E., Jr., and Crippen, R.A., Jr., 1951, Geologic map of the San Francisco Bay Region, *in* Jenkins, O.P., ed., Geologic guidebook of the San Francisco Bay Counties: California Division of Mines and Geology Bulletin, no. 154, p. 161–174.
- Brabb, E.E., Graymer, R.W., and Jones, D.L., 1998, Geology of the onshore part of San Mateo County, California: Derived from the digital database Open-File 98-137, scale 1:62,500.
- Brabb, E.E., Graymer, R.W., and Jones, D.L., 2000, Geologic map and map database of the Palo Alto 30'X60' quadrangle, California: U.S. Geological Survey Miscellaneous Field Studies Map MF-2332, 30 p., 2 sheets, scale 1:100,000.
- Brabb, E. E., and Olson, J. A., 1986, Map showing fault and earthquakes epicenters in San Mateo County, California: U.S. Geological Survey, Map I-257-F, scale 1:62,500.
- Brabb, E.E., and Pampeyan, E.H., 1983; Geologic Map of San Mateo County, California: Miscellaneous Investigation Series Map I-1257-A, U.S. Geological Survey, scale 1:62,500.
- Brocher, T.M., Boatwright, J., Lienkaemper, J.J., Prentice, C.S., Schwartz, D.P., and H. Bundock, 2008, The Hayward Fault—Is it due for a repeat of the powerful 1868 earthquake? U.S. Geological Survey Fact Sheet 2008-3019, version 1.0
- Bruns, T.R., Cooper, A.K., Carlson, P.R., McCulloch, D.S., 2002, Structure of the submerged San Andreas and San Gregorio fault zones in the Gulf of the Farallones off San Francisco, California, from high-resolution seismic reflection data, *in* Parsons, Tom, ed., Crustal structure of the Coastal and Marine San Francisco Bay region, California: U.S. Geological Survey Professional Paper 1658, p. 77–118.
- Bryant, W.A., 1981, Calaveras, Coyote Creek, Animas, San Felipe, and Silver Creek faults, California Division of Mines and Geology, Fault Evaluation Report 122, 13 p.
- Bryant, W.A., Smith, D.P. and Hart, E.W., 1981, Sargent, San Andreas and Calaveras fault zone - evidence for recency in the Watsonville East, Chittenden and San Felipe quadrangles, California, California Division of Mines and Geology Open-File Report 81-7, 3 map sheets, 1:24,000 scale.
- Bullard, T.F., Hanson, K.L., and Abramson, H., 2004, Quaternary investigations to evaluate seismic source characteristics of the Frontal Thrust Belt, Palo Alto region, California: Desert Research Institute and Geomatrix Consultants, Final Report submitted to the U.S. Geological Survey, National Earthquake Hazards Reduction Program, Award No. 01HQGR0015 and 01HQGR0016.
- Bürgmann, R., Arrowsmith, R., Dumitru, T., and McLaughlin, R., 1994, Rise and fall of the southern Santa Cruz Mountains, California, from fission tracks, geomorphology, and geodesy: Journal of Geophysical Research, v. 99, no. B10, p. 20,181–20,202.
- Bürgmann, R., Schmidt, D., Nadeau, R.M., d'Alessio, M., Fielding, E., Manaker, D., McEvilly, T.V., and Murray, M.H., 2000, Earthquake potential along the northern Hayward fault: Science, v. 289, p. 1,178–1,182.
- Bürgmann, R., and Lei, Ling, 2009, TerraSAR InSAR Investigation of Active Crustal Deformation, Berkeley Seismological Laboratory, Annual Reports (2008-2009).
- Byrd, Brian F., Whitaker, A.R., Mikkelsen, P.J., and Rosenthal, J.S., 2017, San Francisco Bay-Delta Regional Context and Research Design for Native American Archaeological Resources, Caltrans District 4. Far Western Anthropological Research Group, Inc., Davis, California. Submitted to California Department of Transportation District

- 4, Oakland, California. Available online at <http://www.dot.ca.gov/ser/guidance.htm>.
- California Department of Water Resources (DWR), 2003, California's Groundwater: California Department of Water Resources, Bulletin 118, Update 2003: October 2003.
- California Department of Water Resources (DWR), 2016, California's Groundwater, Working Toward Sustainability: California Department of Water Resources, Bulletin 118, Interim Update 2016: December 22, 2016.
- California Department of Water Resources (DWR), 2017, California Statewide Groundwater Elevation Monitoring (CASGEM) Program: Available online at <https://www.casgem.water.ca.gov/OSS>, January 14, 2018.
- California Department of Water Resources (DWR), 2017, Dams Within the Jurisdiction of the State of California, 117 p.
- California Division of Mines and Geology, 1965, Potassium-argon age dates for some California localities: California Division of Mines and Geology Mineral Information Service, v. 18, no. 1, p. 16.
- California Geological Survey (CGS), California's Seismic Hazard Mapping Program: <http://www.conservation.ca.gov/cgs/shzp>
- California Geological Survey (CGS), California's Seismic Hazard Mapping Program, 2000, Seismic Hazard Zone Report for the City and County of San Francisco, California, 63 pgs., http://gmw.conservation.ca.gov/SHP/EZRIM/Reports/SHZR/SHZR_043_City_And_County_of_San_Francisco.pdf
- California Geological Survey (CGS), 2001, State of California Seismic Hazard Zones, City and County of San Francisco, Official Map, 17 November 2000.
- California Geological Survey (CGS), 2002, California Geomorphic Provinces: Note 36.
- California Geological Survey (CGS), 2018, Draft - Preliminary Simplified Geologic Map of California.
- California High Speed Rail Authority, 2017, High-Speed Rail: Connecting and Transforming California, California HSR, June 2017.
- California Water Boards, San Francisco Bay – R2, 2017, Water Quality Control Plan (Basin Plan) for the San Francisco Bay Basin: Chapter 2, Table 2-2, Available online at https://www.waterboards.ca.gov/sanfranciscobay/water_issues/programs/planningtmdls/basinplan/web/docs/bp_ch2+tables.pdf.
- Chapman, A.D., Ducea, M.N., Kidder, Steven, and Petrescu, L., 2014, Geochemical constraints on the petrogenesis of the Salinian arc, central California—Implications for the origin of intermediate magmas: *Lithos*, v. 200–201, p. 126–141.
- Chapman, A.D., Luffi, P.I., Saleeby, J.B., and Petersen, S., 2011, Metamorphic evolution, partial melting and rapid exhumation above an ancient flat slab—insights from the San Emigdio Schist, southern California: *Journal of Metamorphic Geology*, v. 29, p. 601–626.
- Chapman, A.D., Saleeby, J.B., Wood, D.J., Piasecki, A., Kidder, S., Ducea, M.N., and Farley, K.A., 2012, Late Cretaceous gravitational collapse of the southern Sierra Nevada batholith, California: *Geosphere*, v. 8, p. 314–341.
- Chaussard, E., Bürgmann, R., Fattahi, H., Nadeau, R.M., Taira, T., Johnson, C.W., and Johanson, I., 2015, Potential for larger earthquakes in the East San Francisco Bay Area due to the direct connection between the Hayward and Calaveras Faults: *Geophysical Research Letters*, v. 42, no. 8, p. 2,734–2,741, doi:10.1002/2015GL063575.
- Choi, S.H., Shervais, J.W., Mukasa, S.B., 2008, Supra-subduction and abyssal mantle peridotites of the Coast Range Ophiolite, California: *Contributions to Mineralogy and Petrology*, v. 155, p. 551–576.
- City and County of San Francisco, Office of Community Investment, 2018, Draft 2018 Hunters Point Shipyard Redevelopment Plan.
- City and County of San Francisco Planning Department and San Francisco Redevelopment Agency, 1998, Mission Bay Subsequent Environmental Impact Report, 17 September 1998.

- City and County of San Francisco, San Francisco Planning Department, 2017, Seawall Lot 337 and Pier 48 Mixed-Use Project Draft EIR: Cultural Resources, Seawall Lot 337 Associates, LLC, Apr. 2017. sfmea.sfplanning.org/MissionRock_Sec_4.D_Cultural.pdf.
- City and County of San Francisco, 2016, San Francisco Sea Level Rise Action Plan, San Francisco Planning and San Francisco Public Works, March 2016. Available online at http://default.sfplanning.org/plans-and-programs/planning-for-the-city/sea-level-rise/160309_SLRAP_Final_ED.pdf
- Clark, J.C., and Brabb, E.E., 1997, Geology of Point Reyes National Seashore and vicinity, California; a digital database: U.S. Geological Survey Open-File Report 97-456, 8 p., scale 1:48,000.
- Clark, J.C., Brabb, E.E., Greene, H.G., and Ross, D.C., 1984, Geology of Point Reyes Peninsula and Implications for San Gregorio Fault History, *in* Crouch, J.K., and Bachman, S.B., eds., Tectonics and Sedimentation Along the California Margin: Pacific Section, Society of Economic Paleontologists and Mineralogists, v. 38, p. 67–86.
- Clark, W.B., 1970, Gold Districts of California: California Department of Conservation, Division of Mines and Geology, Bulletin 193.
- Clarke, S.H., Jr., 1973, The Eocene Point of Rocks Sandstone: Provenance, mode of deposition and implications for the history of offset along the San Andreas fault in central California [Ph.D. thesis]: Berkeley, University of California, 302 p.
- Clary, R. H., 1984, The Making of Golden Gate Park, The Early Years: 1865-1906, (2d ed.): San Francisco, Don't Call It Frisco Press, 192 p.
- Clary, Raymond H., 1987, The Making of Golden Gate Park, 1906-1950: San Francisco, Don't Call It Frisco Press, 197 p.
- Clifton, H.E., Hunter, R.E., and Gardener, J.V., 1988, Analysis of eustatic, tectonic, and sedimentologic influences on transgressive and regressive cycles in the late Cenozoic Merced Formation, San Francisco, California, *in* Paola, C., Kleinspehn, K.L., eds., New Perspectives of Basin Analysis, Springer Verlag, New York, p. 109–128.
- Cloos, M., 1982, Flow mélanges; numerical modeling and geologic constraints on their origin in the Franciscan subduction complex, California: Geological Society of America Bulletin, v. 93, p. 330–345.
- Coleman, R. G., 2000, Prospecting for ophiolites along the California continental margin, *in* Dilek, Y. D., Moores, E. M., Elthon, D., and Nicolas, A., eds., Ophiolites and oceanic crust: New insights from field studies and the Ocean Drilling Program: Geological Society of America Special Paper 349, p. 351–364.
- Coleman, R.G., and Lee, D.E., 1962, Metamorphic aragonite in the glaucophane schists of Cazadero, California: American Journal of Science, v. 260, p. 577–595.
- Coney, P.J., 1976, Plate tectonics and the Laramide orogeny, *in* Woodward, L.A., and Northrop, S.A., eds., Tectonics and mineral resources of southwestern North America: New Mexico Geological Society Special Publication, no. 6, p. 5–10.
- Cooper, A.K., 1973, Structure of the continental shelf west of San Francisco, California: U.S. Geological Survey Open-File Report 73–48, 65 p., available at <http://pubs.er.usgs.gov/publication/ofr7348>.
- Corbett, M.R., 1979, Splendid Survivors, San Francisco Downtown Architectural Heritage: San Francisco, California Living Book, 270 p.
- Cotton, W. R., Fowler, W.L., and Van Velsor, J.E., 1990, Coseismic bedding plane faults and ground fissures associated with the Loma Prieta earthquake of 17 October 1989, *in* The Loma Prieta (Santa Cruz Mountains), California, earthquake of 17 October, 1989, ed. S.R. McNutt and R.H. Sydner, Special Publication, California Division of Mines and Geology, 104, p. 95–104.
- Crandall, R., 1907, The geology of the San Francisco Peninsula: American Philosophical Society, Proceedings, v. 46, no. 185, scale 1:325,000.
- Curry, F.B., Cox, Allen, and Engebretson, D.C., 1984, Paleomagnetism of Franciscan rocks in the Marin Headlands, *in* Blake, M.C., Jr., ed., Franciscan

- Geology of Northern California: Pacific Section, Society of Economic Paleontologists and Mineralogists, v. 43, p. 89–98.
- Curtis, G.H., Evernden, J.F., and Lipson, J., 1958, Age determination of some granitic rocks in California by the potassium-argon method: California Division of Mines and Geology Special Report 54, 16 p.
- Cutter, D. C., 1948, The Discovery of Gold in California, *in* Geologic Guidebook along Highway 49 – Sierran Gold Belt – The Mother Lode Country: California Division of Mines Bulletin 141, p. 13–17.
- Dallas, K.L., and Barnard, P.L., 2011, Anthropogenic influences on shoreline and nearshore evolution in the San Francisco coastal system: Estuarine Coastal and Shelf Science, v. 92, p. 195–204.
- Dartnell, P., 2015, Data integration and visualization, Offshore of San Francisco map area, California, sheet 4, *in* Cochran, G.R. and Cochran, S.A., eds., California State Waters Map Series—Offshore of San Francisco, California: U.S. Geological Survey Open-File Report 2015-1068, pamphlet 39 p., 10 sheets, scale 1:24,000, <http://dx.doi.org/10.3133/ofr20151068>. IP-052334.
- Dartnell, P., Barnard, P., Chin, J., Hanes, D., Kvitek, R., Iampietro, P., Gardner, J., 2006, Under the Golden Gate Bridge—Views of the Sea Floor Near the Entrance to San Francisco Bay, California: U.S. Geological Survey Scientific Investigations Map 2917; U.S. Geological Survey, 7 July 2006, pubs.usgs.gov/sim/2006/2917/
- Dartnell, P., Kvitek, R.G., and Bretz, C.K., 2014a, Colored shaded-relief bathymetry, Offshore of Pacifica map area, California, sheet 1, *in* Cochran, S.A. and Edwards, B.D., eds., California State Waters Map Series—Offshore of Pacifica, California: U.S. Geological Survey Open-File Report 2014-1260, pamphlet 38 p., 10 sheets, scale 1:24,000, <http://dx.doi.org/10.3133/ofr20141260>. IP-052391.
- Dartnell, P., Kvitek, R.G., Bretz, C.K., Erdey, M.D., and Phillips, E.L., 2014b, Acoustic backscatter, Offshore of Pacifica map area, California, sheet 3, *in* Cochran, S.A. and Edwards, B.D., eds., California State Waters Map Series—Offshore of Pacifica, California: U.S. Geological Survey Open-File Report 2014-1260, pamphlet 38 p., 10 sheets, scale 1:24,000, <http://dx.doi.org/10.3133/ofr20141260>. IP-052391.
- Dartnell, P., Erdey, M.D., Kvitek, R.G., and Bretz, C.K., 2015a, Acoustic backscatter, Offshore of San Francisco map area, California, sheet 3, *in* Cochran, G.R. and Cochran, S.A., eds., California State Waters Map Series—Offshore of San Francisco, California: U.S. Geological Survey Open-File Report 2015-1068, pamphlet 39 p., 10 sheets, scale 1:24,000, <http://dx.doi.org/10.3133/ofr20151068>. IP-052334.
- Dartnell, P., Kvitek, R.G., and Bretz, C.K., 2015b, Colored shaded-relief bathymetry, Offshore of San Francisco map area, California, sheet 1, *in* Cochran, G.R. and Cochran, S.A., eds., California State Waters Map Series—Offshore of San Francisco, California: U.S. Geological Survey Open-File Report 2015-1068, pamphlet 39 p., 10 sheets, scale 1:24,000, <http://dx.doi.org/10.3133/ofr20151068>. IP-052334.
- Davies, E.A., 1986, The stratigraphic and structural relationships of the Miocene and Pliocene formations of the Petaluma Valley area of California [M.S. thesis]: Berkeley, University of California, 96 p.
- Dawson, T.E., and R.J. Weldon, II, 2013, Appendix B—Geologic-Slip-Rate Data and Geologic Deformation Model; Uniform California Earthquake Rupture Forecast, Version 3 (UCERF3)—The Time-Independent Model: U.S. Geological Survey Open-File Report 2013-1165.
- DeLisle, M.J., and Real, C.R., 1994, Preliminary Seismic Hazard Zone Map, Liquefaction hazard zones for a portion of the San Francisco North quadrangle: California Division of Mines and Geology, scale 1:24,000.
- DeMarr, R., 2018, Personal communication between Robert DeMarr, San Francisco Department of Public Health, Environmental Health Branch, and Jeffrey Gilman, San Francisco Public Utilities Commission: January 24, 2018.
- DeMets, C., Gordon, R.G., Argus, D.F., and Stein, S., 1994, Effect of recent revisions to the geomagnetic reversal time scale on estimates

- of current plate motions: *Geophysical Review Letters*, v. 21, p. 2191–2194.
- Dengler, L., 2008, The 1906 earthquake on California's north coast: *Bulletin of the Seismological Society of America*, v. 98, p. 918–930, 10.1785/0120060406.
- Dibblee, T.W., Jr., 1966, Geologic map and sections of the Palo Alto 15' quadrangle, California: California Division of Mines and Geology Map Sheet 8, scale 1:62,500.
- Dibblee, T.W., Jr., 1974, Geologic map of the Shandon and Orchard Peak quadrangles, San Luis Obispo and Kern counties, California: U.S. Geological Survey Miscellaneous Investigations Series Map I-788, scale 1:62,500.
- Dickinson, W.R., Ducea, Mihai, Rosenberg, L.I., Greene, H.G., Graham, S.A., Clark, J.C., Weber, G.E., Kidder, Steven, Ernst, W.G., and Brabb, E.E., 2005, Net dextral slip, Neogene San Gregorio-Hosgri Fault Zone, Coastal California—Geologic evidence and tectonic implications: *Geological Society of America Special Paper* 391, 43 p.
- Dickinson, W.R., Hopson, C.A., Saleeby, J.B., Schweickert, R.A., Ingersoll, R.V., Pessagno, E.A., Jr., Mattinson, J.M., Luyendyk, B.P., Beebe, Ward, Hull, D.M., Munoz, I.M., Blome, C.D., 1996, Alternate origins of the Coast Range Ophiolite (California); introduction and implications: *GSA Today*, v.6, no. 2, p. 1–10.
- Dickinson, W.R., Ingersoll, R.V., and Graham, S.A., 1979, Paleogene sediment dispersal and paleotectonics in northern California: *Geological Society of America Bulletin*, v. 90, pt. I, p. 897–898; pt. II, p. 1,458–1,528
- Dickinson, W.R., and Rich, E.I., 1972, Petrologic intervals and petrofacies in the Great Valley Sequence, Sacramento Valley, California: *Geological Society of America Bulletin*, v. 83, p. 3,007–3,024.
- Dickinson, W.R., and Snyder, W.S., 1979, Geometry of triple junctions related to San Andreas transform: *Journal of Geophysical Research*, v. 84, no. B2, p. 561–572.
- Dolnick, E., 2014, The Rush—America's Fevered Quest for Fortune, 1848-1853: New York, NY, Little, Brown and Company, 350 p.
- Dow, G.R., 1973, Bay fill in San Francisco—A history of change [M.A. thesis]: San Francisco, California State University at San Francisco, 249 p.
- Drinkwater, J.L., Sorg, D.H., and Russell, P.C., 1992, Geologic map showing ages and mineralization of the Quien Sabe volcanics, Mariposa Peak Quadrangle, west-central California: U.S. Geological Survey Miscellaneous Field Studies Map MF-2200, 1 sheet, scale 1:24,000.
- Ducea, M.N., Kidder, S., Chesley, J.T., and Saleeby, J.B., 2009, Tectonic underplating of trench sediments beneath magmatic arcs; the central California example: *International Geology Review*, v. 51, p. 1–26.
- Dumitru, T.A., Elder, W.P., Hourigan, J.K., Chapman, A.D., Graham, S.A., Wakabayashi, J., 2016, Four Cordilleran paleorivers that connected Sevier thrust zones in Idaho to depocenters in California: *Geology*, v. 44, p. 75–78.
- Dumitru, T.A., Ernst, W.G., Wright, J.E., Wooden, J.L., Wells, R.E., Farmer, L.P., Kent, A.J.R., and Graham, S.A., 2013, Eocene extension in Idaho generated massive sediment floods into the Franciscan trench and into the Tyee, Great Valley, and Green River basins: *Geology*, v. 41, p. 187–190.
- Edelman, S.H., and Sharp, W.D., 1989, Terranes, early faults, and pre-Late Jurassic amalgamation of the western Sierra Nevada metamorphic belt, California: *Geological Society of America Bulletin*, v. 101, p. 1420–1433.
- Elder, W. P., 1998, Mesozoic molluscan fossils from the Golden Gate National Recreation Area and their significance to terrane reconstructions for the Franciscan Complex, San Francisco Bay Area, California, *in* Santucci, V. L., Lindsay, M., eds., National Park Service Paleontology Research, National Park Service Tech. Report NPS/NRGD/6RD78-98/01, p. 90–94.
- Elder, W.P., and Miller, J.W., 1993, Map and checklists of Jurassic and Cretaceous macrofossil localities within the San Jose 1:100,000 map sheet, California, and discussion of paleontolog-

- ical results: U.S. Geological Survey Open-File Report 93-503 map scale 1:100,000.
- Ellsworth, W.L., Lindh, A.G., Prescott, W.H., and Herd, D.G., 1981, The 1906 San Francisco earthquake and the seismic cycle: American Geophysical Union Maurice Ewing Series, p. 126–140.
- ENGEO, 2015, Geotechnical Data Report (GDR), Sub-Phase 1A, Treasure Island, San Francisco, California, Project No. 7091.000.000, December 31, 2015.
- ENGEO, 2009. Geotechnical Conceptual Design Report (GCDR), Treasure Island, San Francisco, California, Project No. 7091.600.103, February 2, 2009.
- Engineering News Record, 1930, Borings show foundation suitable for Golden Gate Bridge piers.
- Engineering/Remediation Resources Group, Inc. (ERRG), 2002, Well decommissioning report, Sunset Wells project, San Francisco, California: 8 p., 5 apps.
- ENVIRON Corporation (Environ), 1999, Risk Management Plan, Mission Bay Area, San Francisco, California, Environ, 11 May 1999.
- Environmental Protection Agency (EPA), 2017, Hunters Point Naval Shipyard, 13 Oct. 2017, Available online at: <https://yosemite.epa.gov/r9/sfund/r9sfdocw.nsf/vwsoalphabetic/Hunters+Point+Naval+Shipyard?OpenDocument>.
- Environmental Science Associates (ESA), 1990, Mission Bay Hazard Mitigation Program.
- Erikson, R., 2011, Petrology of a Franciscan olistostrome with a massive sandstone matrix; the King Ridge Road mélangé at Cazadero, California, in Wakabayashi, J., and Dilek, Y., eds., mélanges; processes of formation and societal significance: Geological Society of America Special Paper 480, p. 171–188.
- Erler and Kalinowski, 2004, Building 637 Area Completion Report, prepared for The Presidio Trust, 31 March 2003.
- Ernst, W.G., 1965, Mineral paragenesis in Franciscan metamorphic rocks, Panoche Pass, California: Geological Society of America Bulletin, v. 76, p. 879–914.
- Ernst, W.G., 1970, Tectonic contact between the Franciscan mélangé and the Great Valley Sequence—crustal expression of a late Mesozoic Benioff zone: Journal of Geophysical Research, v. 75, p. 886–901.
- Ernst, W.G., Martens, U., McLaughlin, R.J., Clark, J.C., and Moore, D., 2009, Significance of U-Pb zircon ages from the Pescadero and Cambria felsites, west-central California Coast Ranges: Geological Society of America Abstracts with Programs, v. 41, no. 7, p. 644.
- Ernst, W.G., Martens, U., McLaughlin, R.J., Clark, J.C., and Moore, D., 2011, Zircon U-Pb age of the Pescadero felsite; a Late Cretaceous igneous event in the forearc, west-central California Coast Ranges: Geological Society of America Bulletin, v. 123, p. 1,497–1,512.
- Field, E. H. Biasi, G. P., Bird, P., Dawson, T. E., Felzer, K.R., Jackson, D.D., Johnson, K.M., Jordan, T. H., Madden, C., Michael, A.J., Milner, K.R., Page, M.T., Parsons, T., Powers, P.M., Shaw, B.E., Thatcher, W.R., Weldon, R.J II, Seng, Yuehua, 2015, Long-term, time-dependent probabilities for the Third Uniform California Earthquake Rupture Forecast (UCERF3), Bulletin of the Seismological Society of America, v. 105, p. 511–543, doi: 10.1785/0120140093.
- Field, E.H., Biasi, G.P., Bird, P., Dawson, T.E., Felzer, K.R., Jackson, D.D., Johnson, K.M., Jordan, T.H., Madden, C., Michael, A.J., Milner, K.R., Page, M.T., Parsons, T., Powers, P.M., Shaw, B.E., Thatcher, W.R., Weldon, R.J., II, and Zeng, Y., 2013, Uniform California earthquake rupture forecast, version 3 (UCERF3)—The time-independent model: U.S. Geological Survey Open-File Report 2013–1165, 97 p., California Geological Survey Special Report 228, and Southern California Earthquake Center Publication 1792, <http://pubs.usgs.gov/of/2013/1165/>.
- Fox, K.F., Jr., Fleck, R.J., Curtis, G.H., and Meyer, C.E., 1985, Implications of the northwestwardly younger age of the volcanic rocks of west-central California: Geological Society of America Bulletin, v. 96, p. 647–654.

- Fradkin, P. L., 2006, *The Great Earthquake and Firestorm of 1906, How San Francisco nearly destroyed itself*: Berkeley, University of California Press, 418 p.
- Friedman, S.M., 2017, *The Inflation Calculator*: <https://westegg.com/inflation/infl.cgi>.
- Fuis, G.S. and Mooney, W.D., 1990, Lithospheric structure and tectonics from seismic-refraction and other data, *in* Wallace, R.E., ed., *The San Andreas Fault System, California*: U.S. Geological Survey Professional Paper 1515, p. 206–236.
- Funning, G.J., Burgmann, R., Ferretti, A., Novali, G., and Fumagalli, A., 2007, Creep on the Rodgers Creek fault, northern San Francisco Bay area from a 10 year PS-InSAR dataset: *Geophysical Research Letters*, v. 34, 5 p., <https://doi.org/10.1029/2007GL030836>.
- Galehouse, J.S., 1995, *Theodolite measurements of creep rates on San Francisco Bay region faults*: U.S. Geological Survey Open-file Report 95-210.
- Galloway, A.J., 1977, *Geology of the Point Reyes Peninsula, Marin County, California*: California Division of Mines and Geology Bulletin 202, 72 p., map scale 1:48,000.
- Gastil, R.G., 1975, Hypothesis suggesting 700 km of right slip in California along northwest-oriented faults; *Comment: Geology*, v. 3, p. 84.
- Geschwind, C.-H., 2001, *California Earthquakes: Science, Risk, and the Politics of Hazard Mitigation*. The Johns Hopkins University Press, p. 322
- Ghatak, A., Basu, A.R., and Wakabayashi, J., 2013, Implications of Franciscan Complex graywacke geochemistry for sediment transport, provenance determination, burial-exposure duration, and fluid exchange with cosubducted metabasites: *Tectonics*, v. 32, p. 1,480–1,492.
- GHD-GTC Joint Venture (GHD-GTC), 2016, *Earthquake Vulnerability Study for the Seawall Vulnerability Study of the Northern Seawall San Francisco, California: Phase 2 Report*, unpublished consulting report prepared for the Port of San Francisco, dated July 2016, 292 p.
- Givler, R. W., 2007, *Creek & Watershed Map of Daly City & Vicinity*, Oakland Museum of California, 2007.
- Gluskoter, H.J., 1964, Orthoclase distribution and authigenesis in the Franciscan Formation of a portion of western Marin County, California: *Journal of Sedimentary Petrology*, v. 34, no. 2, p. 335–343.
- Gluskoter, H.J., 1969, *Geology of a portion of western Marin County, California*: California Division of Mines and Geology, Map Sheet 11.
- Goebel, T, Waters, M.R., and O'Rourke, D.H., 2008, The late Pleistocene dispersal of modern humans in the Americas: *Science*, v. 319, no. 5869, pp. 1,497–1,502. doi: 10.1126/science.1153569
- Goldcalifornia.net, 2011b, *California Gold—The Discovery by John A. Sutter—Details from a letter written by John Sutter about the Discovery and Impact of the California Gold Rush*: <http://www.goldcalifornia.net>.
- Golden Gate Bridge and Highway District, 1934, *Investigation of criticism of foundation by Bailey Willis*, November 27.
- Golden Gate Weather Services, 2017, *Climate of San Francisco monthly rainfall 1949-present*: Available online at <http://ggweather.com/sf/monthly.html> , December 9, 2017.
- Golden, N.E., and Cochrane, G.R., 2015, Ground-truth studies, Offshore of San Francisco map area, California, sheet 6, *in* Cochrane, G.R. and Cochran, S.A., eds., *California State Waters Map Series—Offshore of San Francisco, California*: U.S. Geological Survey Open-File Report 2015-1068, pamphlet 39 p., 10 sheets, scale 1:24,000, <http://dx.doi.org/10.3133/ofr20151068>. IP-052334.
- Golden, N.E., Edwards, B.D., Cochrane, G.R., Phillips, E.L., Erdey, M.D., and Krigsman, L.M., 2014, Ground-truth studies, Offshore of Pacifica map area, California, sheet 6, *in* Cochran, S.A. and Edwards, B.D., eds., *California State Waters Map Series—Offshore of Pacifica, California*: U.S. Geological Survey Open-File Report 2014-1260, pamphlet 38 p., 10 sheets, scale 1:24,000, <http://dx.doi.org/10.3133/ofr20141260>. IP-052391.
- Goldman, H.B., ed., 1969, *Geologic and engineering*

- aspects of San Francisco Bay fill: California Division of Mines and Geology Special Report 97.
- GovMint.com, 2016, The San Francisco Mint: The 'Granite Lady': <https://www.govmint.com/coin-authority/post/the-san-francisco-mint-the-granite-lady/>
- Graymer, R.W., 2000, Geologic map and map database of the Oakland metropolitan area, Alameda, Contra Costa, and San Francisco Counties, California: U.S. Geological Survey Miscellaneous Field Studies MF-2342, 31 p., 1 sheet, scale 1:50,000
- Graymer, R.W., 2005, Jurassic-Cretaceous assembly of central California, *in* Stevens, Calvin, and Cooper, John, eds., Mesozoic tectonic assembly of California: Pacific Section, Society of Economic Paleontologists and Mineralogists Book 96, p. 21–64.
- Graymer, R.W., Bryant, W., McCabe, C.A., Hecker, S., and Prentice, C.S., 2006a, Map of Quaternary-active faults in the San Francisco Bay region: U.S. Geological Survey Scientific Investigations Map, SIM-2919, 1 sheet, scale 1:275,000.
- Graymer, R.W., Jones, D.L., and Brabb, E.E., 1996, Preliminary geologic map emphasizing bedrock formations in Alameda County, California: A digital database: U.S. Geological Survey Open-File Report 96-252, 2 sheets, scale 1:75,000
- Graymer, R.W., Langenheim, V.E., Roberts, M.A., and McDougall, K., 2014, Geologic and geophysical maps of the eastern three-fourths of the Cambria 30' x 60' quadrangle, central California Coast Ranges: U.S. Geological Survey Scientific Investigations Map 3287, 50 p., scale 1:100,000 (interactive pdf).
- Graymer, R.W., Moring, B.C., Saucedo, G.J., Wentworth, C.M., Brabb, E.E., and Knudsen, K.L., 2006b, Geologic map of the San Francisco Bay region: U.S. Geological Survey Scientific Investigations Map, SIM-2918, 1 sheet, scale 1:275,000.
- Graymer, R.W., Sarna-Wojcicki, A.M., Walker, J.P., McLaughlin, R.J., and Fleck, R.J., 2002, Controls on timing and amount of right-lateral offset on the East Bay Fault System, San Francisco Bay region, California: Geological Society of America Bulletin, v. 114, p. 1,471–1,479.
- Greene, H.G., Hartwell, S.R., Manson, M.W., Johnson, S.Y., Dieter, B.E., Phillips, E.L., and Watt, J.T., 2014, Offshore and onshore geology and geomorphology, Offshore of Pacifica map area, California, sheet 10, *in* Cochran, S.A. and Edwards, B.D., eds., California State Waters Map Series—Offshore of Pacifica, California: U.S. Geological Survey Open-File Report 2014-1260, pamphlet 38 p., 10 sheets, scale 1:24,000, <http://dx.doi.org/10.3133/ofr20141260>. IP-052391.
- Greene, H.G., Johnson, S.Y., Manson, M.W., Hartwell, S.R., Endris, C.A., and Bruns, T.R., 2015, Offshore and onshore geology and geomorphology, Offshore of San Francisco map area, California, sheet 10, *in* Cochran, G.R. and Cochran, S.A., eds., California State Waters Map Series—Offshore of San Francisco, California: U.S. Geological Survey Open-File Report 2015-1068, pamphlet 39 p., 10 sheets, scale 1:24,000, <http://dx.doi.org/10.3133/ofr20151068>. IP-052334.
- Griggs, G., árvai, J., Cayan, D., DeConto, R., Fox, J., Fricker, H.A., Kopp, R.E., Tebaldi, C., Whiteman, E.A., 2017, Rising Seas in California: An Update on Sea-Level Rise Science by the California Ocean Protection Council Science Advisory Team Working Group: California Ocean Science Trust..
- Guddle, E.G., 1997, California Gold Camps: Berkeley, University of California Press, 465 p.
- Hagstrum, J.T., 1997, Paleomagnetism, paleogeographic origins, and remagnetization of the Coast Range Ophiolite and Great Valley Sequence, Alta and Baja California: American Association of Petroleum Geologists Bulletin, v. 81, p. 686–687.
- Hagstrum, J.L., and Murchey, B.L., 1993, Deposition of Franciscan Complex cherts along the paleo-equator and accretion to the American margin at tropical paleolatitudes: Geological Society of America Bulletin, v. 105, p. 766–778.
- Hagwood, J.J., 1980, Engineers at the Golden Gate, A History of the San Francisco District, U.S. Army Corps of Engineers, 1866-1980, U.S. Army Corp of Engineers, San Francisco, California, p. 158–166.
- Hall, C.A., and Saleeby, J.B., 2013, Salinia revisited:

- a crystalline nappe sequence lying above the Nacimiento fault and dispersed along the San Andreas fault system, central California: *International Geology Review*, v. 55, p. 1,575–1,615.
- Hall, N.T., 1965, Late Cenozoic stratigraphy between Mussel Rock and Fleishhacker Zoo, San Francisco Peninsula: *International Association for Quaternary Research, VII Congress, Guidebook I: Northern Great Basin and California*, p. 151–158.
- Hall, N.T., 1966, Late Cenozoic stratigraphy between Mussel Rock and Fleishhacker Zoo, San Francisco Peninsula: *California Division of Mines and Geology Mineral Information Service*, v. 19, no. 11, p. S22-S25.
- Hall, N.T., Wright, R.H. and Clahan, K.B., 1999, Paleoseismic studies of the San Francisco Peninsula segment of the San Andreas fault zone near Woodside, California: *Journal of Geophysical Research*, v. 104, p. 23, 215–23, 236.
- Hamilton, W., 1969, Mesozoic California and the underflow of Pacific mantle: *Geological Society of America Bulletin*, v. 80, p. 2,409–2,430.
- Hanks, T. C. and Krawinkler, H., 1991, The 1989 Loma Prieta, California, earthquake and its effects: introduction to the special issue, *Bulletin of the Seismological Society of America*, v. 81, p. 1,415-1,423.
- Hansen, G., and Condon, E., 1989, Denial of Disaster, *The Untold Story and Photographs of the San Francisco Earthquake and Fire of 1906*: San Francisco, Cameron and Co. 160 p.
- Harris, R., and Simpson, R.W., 1998, Suppression of large earthquakes by stress shadows: A comparison of Coulomb and rate-and-state failure: *Journal of Geophysical Research*, v. 103, p. 24,439–24,451, doi: 10.1029/98JB00793.
- Haugerud, R. A., and Ellen, S. D., 1990, Coseismic ground deformation along the northeast margin of the Santa Cruz Mountains, *in* Schwartz, D. P., and Ponti, D. J., eds., *Field guide to neotectonics of the San Andreas fault system, Santa Cruz Mountains, in light of the 1989 Loma Prieta earthquake*, U.S. Geological Survey Open-File Report 90-274, p. 32–38.
- Hearn, B.C., Jr., Donnelly-Nolan, J.M., and Goff, F.E., 1995, Geologic map and structure sections of the Clear Lake Volcanics, northern California: U.S. Geological Survey Miscellaneous Investigations Series I-2362, 3 sheets, scale 1:24,000.
- Hecker, S., Langenheim, V.E., Williams, R.A., Hitchcock, C.S., and DeLong, S.B., 2016, Detailed mapping and rupture implications of the 1 km releasing bend in the Rodgers Creek fault at Santa Rosa, northern California: *Bulletin of the Seismological Society of America*, v. 106, no. 2, p. 575–594, <https://doi.org/10.1785/0120150152>.
- Hecker, S., and Randolph-Loar, C.E., 2018, Map of recently active traces of the Rodgers Creek Fault, Sonoma County, California: U.S. Geological Survey Scientific Investigations Map 3410, 7 p., 1 sheet, <https://doi.org/10.3133/sim3410>.
- Hecker, S., Pantosti, D., Schwartz, D.P., Hamilton, J.C., Reidy, L.M., and Powers, T.J., 2005, The most recent large earthquake on the Rodgers Creek fault, San Francisco Bay area: *Bulletin of the Seismological Society of America*, v. 95, no. 3, p. 844–860, <https://doi.org/10.1785/0120040134>.
- Heizer, R. F., 1951, Indians of the San Francisco Bay area: *California Div. Mines Bull.* 154, p.39–56
- Helley, E.J., Lajoie, K.R., Spangle, W.E., and Blair, M.L., 1979, Flatland deposits of the San Francisco Bay Region, California—Their geology and engineering properties, and their importance to comprehensive planning: U.S. Geological Survey Professional Paper 943.
- Hengesh, J.V., and Wakabayashi, J., 1995, Dextral translation and progressive emergence of the Pleistocene Merced Basin and implications for timing of initiation of the San Francisco peninsula segment of the San Andreas Fault, *in* Sangines, E.M., Anderson, D.W., and Busing, A.V., eds., *Recent geologic studies in the San Francisco Bay area*: Society of Economic Paleontologists and Mineralogists, Pacific Section Special Publication 76, p. 47–54.
- Hengesh, J. V., Wakabayashi, J., and Nolan, J. M., 1996, Paleoseismic investigation of the Serra

- fault, San Francisco Peninsula, California: U.S. Geological Survey, National Earthquake Hazards Reduction Program, Award No. 1434-95-2549, 17 p.
- Hengesh, J.V., Nolan, J.M., and Wakabayashi, J., 1996b, Holocene Displacement Along the Serra Fault, San Francisco Peninsula, California [abs]: EOS (Transactions, American Geophysical Union, Fall Meeting Supplement), v. 77, p. F744, Abstract T41B-16.
- Hengesh, J.V., Nolan, J.M., and Wakabayashi, J., 2004, Seismic hazards associated with the Serra fault, San Francisco Peninsula, California, *in* Kennedy, D. G., and Hitchcock, C. S., eds., Seismic Hazard of the Range Front Thrust Faults, Northeastern Santa Cruz Mountains/Southwestern Santa Clara Valley, Field Trip Guidebook, Association of Environmental & Engineering Geologists, San Francisco Section.
- Henn, W. G., Jackson, T. L., and Schlocker, J., 1972, Buried human bones at the “BART” site, San Francisco: California Geology, v. 25, no. 9, p. 208–209.
- Henn, W. G., and Schenk, R. E., 1970, An archaeological analysis of skeletal material excavated from the Civic Center of BART. San Francisco: Society for California Archaeology, R. E. Schenk Memorial Archives of California Archaeology 11.
- Hertlein, L.G., 1956, Cretaceous ammonite of Franciscan group, Marin County, California: American Association of Petroleum Geologists Bulletin, v. 40, p. 1,985–1,988.
- HiddenSF.com, 2017, Early San Francisco History: <http://www.hiddensf.com/400-san-francisco-attractions/brief-early-san-francisco-history.html>.
- Higgins, C.G., 1960, Ohlson Ranch Formation, Pliocene, northwestern Sonoma County, California: University of California Publications in Geological Sciences, v. 36, no. 3, p. 199–231
- Hill, M.L., and Dibblee, T.W., Jr., 1953, San Andreas, Garlock, and Big Pine faults, California—a study of the character, history, and tectonic significance of their displacements: Bulletin of the Geological Society of America, v. 64, p. 443–458.
- Hillhouse, J.W. and Godt, J.W., 1999, Map showing damaging landslides in San Francisco City and County, California: Resulting from 1997-1998 El Nino Rainstorms, U.S. Geological Survey Miscellaneous Field Studies Map MF-2325-G; scale 125,000.
- Hinds, N.E.A., 1934, The Jurassic age of the last granitoid intrusives in the Klamath Mountains and Sierra Nevada, California: American Journal of Science, v. 227, p.182–192.
- Hitchcock, C., Givler, R., DePascale, G., Dulberg, R., 2008, Detailed mapping of artificial fills, San Francisco Bay Area, California, Final Technical Report for U.S. Geological Survey National Earthquake Hazard Reduction Program Grant Number 07HQGR0078.
- Hitchcock, C.S., and Kelson, K.I., 1999, Growth of late Quaternary folds in southwest Santa Clara Valley, San Francisco Bay area, California: Implications of triggered slip for seismic hazard and earthquake recurrence, Geology, v. 27, no. 5, p. 391–394.
- Holzer, T.L., ed., 1998, The Loma Prieta, California, earthquake of October 17, 1989 - Liquefaction: U.S. Geological Survey Professional Paper 1551-B.
- Hopson, C.A., Mattinson, J.M., Luyendyk, B.P., Beebe, W.J., Pessagno, E.A., Jr., Hull, D.M., Munoz, I.M., and Blome, C.D., 1997, Coast Range Ophiolite; paleoequatorial ocean-ridge lithosphere: American Association of Petroleum Geologists Bulletin, v. 81, p. 687.
- Hopson, C.A., Mattinson, J.M., and Pessagno, E.A., Jr., 1981, Coast Range Ophiolite, western California, *in* Ernst, W.G., ed., The Geotectonic Development of California, Rubey volume 1: Prentice-Hall, Englewood Cliffs, N.J., p. 419–510.
- Hough, S.E., and Martin, S.S., 2015, The 1868 Hayward Fault, California, earthquake: Implications for earthquake scaling relations on partially creeping faults, Bulletin of the Seismological Society of America, v. 105, no. 6, p. 2,894–2,909, doi: 10.1785/0120140372
- Hsu, K.J., 1968, Principles of mélanges and their bearing on the Franciscan-Knoxville paradox:

- Geological Society of America Bulletin, v. 79, p. 1,063–1,074.
- Hunter, R.E., Clifton, H.E., Hall, N.T., Császár, G., Richmond, B.M., and Chin, J.L., 1984, Pliocene and Pleistocene coastal and shelf deposits of the Merced Formation and associated beds, northwestern San Francisco Peninsula, California: Society of Economic Paleontologists and Mineralogists, Field Trip Guidebook 3, p. 1–29.
- HydroFocus, Inc., 2017, Westside basin groundwater-flow model: extended and updated model simulation results, version 4.1 (1959-2014): Prepared for Mr. Patrick Sweetland, City of Daly City, March 21, 2017.
- Ingersoll, R.V., 2012, Composition of modern sand and Cretaceous sandstone derived from the Sierra Nevada, California, USA, with implications for Cenozoic and Mesozoic uplift and dissection: *Sedimentary Geology*, v. 280, p. 195–207.
- Irwin, W. P., 1960, Geologic reconnaissance of the northern Coast Ranges and Klamath Mountains, California: California Division of Mines Bulletin 179, 80 p.
- Iversen, E., 1989, Water supply at the Presidio of San Francisco, San Francisco County: California Geology, v. 42, no. 12, p. 267–270.
- Jachens, R.C., Wentworth, C.M., and McLaughlin, R.J., 1998, Pre-San Andreas location of the Gualala block inferred from magnetic and gravity anomalies, *in* Elder, W.P., ed., *Geology and tectonics of the Gualala block, Northern California: Pacific Section, Society of Economic Paleontologists and Mineralogists, Book 84*, p. 27–64.
- Jachens, R.C., Wentworth, C.M., Zoback, M.L., Bruns, T.R., and Roberts, C.W., 2002, Concealed strands of the San Andreas Fault System in the central San Francisco Bay region, as inferred from aeromagnetic anomalies, *in* Parsons, T., ed., *Crustal structure of the Coastal and Marine San Francisco Bay region, California: U.S. Geological Survey Professional Paper 1658*, p. 43–61.
- Jacobson, C.E., Grove, M., Pedrick, J.N., Barth, A.P., Marsaglia, K.M., Gehrels, G.E., and Nourse, J.A., 2011, Late Cretaceous-early Cenozoic tectonic evolution of the southern California margin inferred from provenance of trench and forearc sediments: *Geological Society of America Bulletin*, v. 123, p. 485–506.
- James M. Montgomery Consulting Engineers, Inc. (Montgomery), 1991, City and County of San Francisco Water Department, Sunset well rehabilitation study technical memorandum: November 1991, 24 p., 4 apps.
- Jayko, A.S., and Blake, M.C., Jr., 1984, Sedimentary petrology of graywacke of the Franciscan Complex in the northern San Francisco Bay region, California, *in* Blake, M.C., Jr., ed., *Franciscan Geology of Northern California: Pacific Section, Society of Economic Paleontologists and Mineralogists*, v. 43, p. 121–134.
- Jennings, C.W., comp., 1977, Geologic map of California: California Division of Mines and Geology Geologic Data Map, no. 2, scale 1:750,000.
- Jin, L., and Funning, G.J., 2017, Testing the inference of creep on the northern Rodgers Creek fault, California, using ascending and descending persistent scatterer InSAR data: *Journal of Geophysical Research Solid Earth*, v. 122, p. 2,372–2,389, <https://doi.org/10.1002/2016JB013535>
- Johnson, A. M., and Fleming, R.W., 1993, Formation of left-lateral fractures within the Summit Ridge shear zone, 1989 Loma Prieta, California, earthquake; *Journal of Geophysical Research*, v. 98, p. 21,823–21,837.
- Johnson, S.Y., Cochrane, G.R., Golden, N.E., Dartnell, P., Hartwell, S.R., Cochran, S.A., and Watt, J.T., 2017, The California Seafloor Mapping Program—Providing science and geospatial data for California’s State Waters: *Ocean and Coastal Management*, v. 140, p. 88–104. <http://dx.doi.org/10.1016/j.ocecoaman.2017.02.004>.
- Johnson, S.Y., Hartwell, S.R., Sliter, R.W., Watt, J.T., Phillips, E.L., Ross, S.L., and Chin, J.L., 2015a, Local (Offshore of San Francisco map area) and regional (offshore from Bolinas to Pescadero) shallow-subsurface geology and structure, California, sheet 9, *in* Cochrane, G.R. and Cochran, S.A. eds., *California State Waters Map Series—Offshore of San Francisco, California:*

- U.S. Geological Survey Open-File Report 2015-1068, pamphlet 39 p., 10 sheets, scale 1:24,000, <http://dx.doi.org/10.3133/ofr20151068>.
- Johnson, S.Y., Sliter, R.W., Bruns, T.R., Ross, S.L., and Chin, J.L., 2015b, Seismic-reflection profiles, Offshore of San Francisco map area, California, sheet 8, *in* Cochrane, G.R. and Cochran, S.A., eds., California State Waters Map Series—Offshore of San Francisco, California: U.S. Geological Survey Open-File Report 2015-1068, pamphlet 39 p., 10 sheets, scale 1:24,000, <http://dx.doi.org/10.3133/ofr20151068>. IP-052334.
- Jones, D.L., Blake, M.C., Jr., Bailey, E.H., and McLaughlin, R.J., 1978, Distribution and character of Upper Mesozoic subduction complexes along the west coast of North America: *Tectonophysics*, v. 47, p. 207–222.
- Jones, D.L., Cox, A., Coney, P., and Beck, M., 1982, The growth of western North America: *Scientific American*, v. 247, no. 5, p. 70–84.
- Jones, D.L., and Curtis, G.H., 1991, Guide to the geology of the Berkeley Hills, central Coast Ranges, California, *in* Sloan, D., and Wagner, D.L., eds., *Geologic excursions in northern California: San Francisco to the Sierra Nevada*: California Division of Mines and Geology Special Publication 109, p. 63–74
- Karl, S.M., 1984, Sedimentologic, diagenetic, and geochemical analysis of Upper Mesozoic ribbon cherts from the Franciscan Assemblage at the Marin Headlands, California, *in* Blake, M.C., Jr., ed., *Franciscan Geology of Northern California*: Pacific Section, Society of Economic Paleontologists and Mineralogists, v. 43, p. 71–88.
- Keefer, D.K. and Manson, M.W., 1998, Regional distribution and characteristics of landslides generated by the earthquake, *in* Keefer, D.K., ed., *The Loma Prieta, California, earthquake of October 17, 1989—Landslides*: U.S. Geological Survey Professional Paper 1551-C, p. C7-C32.
- Kehoe, P., et al., 2014, San Francisco Takes the Lead in Setting Standards for Onsite Reuse. California-Nevada Section American Water Works Association (AWWA), v. 28, no. 4, p. 22–23.
- Kelson, K.I., 2001, Geologic characterization of the Calaveras fault as a potential seismic source, San Francisco Bay area, California, *in* Engineering Geology Practice in Northern California, Ferriz, H. and Anderson, R., eds., AEG Special Publication 12 / California Geological Survey Bulletin 210, p. 179–192.
- Kennedy, D. G., 2002, Neotectonic character of the Serra fault, northern San Francisco peninsula [M.S. thesis]: San Francisco State University, 117 p.
- Kennedy, D. G., 2004, Evidence for Holocene activity on the Serra fault at Fort Funston, San Francisco, California, *in* Kennedy, D. G., and Hitchcock, C. S., eds., *Seismic Hazard of the Range Front Thrust Faults, Northeastern Santa Cruz Mountains/Southwestern Santa Clara Valley*, Field Trip Guidebook, Association of Environmental & Engineering Geologists, San Francisco Section.
- Kennedy, D. G. and Caskey, J., 2005, Late Pleistocene to Holocene Fold Growth above the Serra Fault, Northern San Francisco Peninsula, California: *Geological Society of America Abstracts with Programs*, v. 37, no. 4, p. 92.
- King, Michael J. and Zamboanga, Alan, 1994, Downtown basin field investigation program: Technical Memorandum 9 – Volume 1, prepared for San Francisco Water Department by AGS, Inc., January 31, 1994, 10 p., 4 figs., 11 tbls.
- Kircher, C.A., Seligson, H.A., Bouabid, J., and Morrow, G.C., 2006. When the Big One strikes again—Estimated losses due to a repeat of the 1906 San Francisco earthquake: *Earthquake Spectra*, v. 22, no.S2, p. 297–339.
- Kistler, R.W., and Champion, D.E., 1997, Granitoid intrusive suite in the Salinian composite terrane of coastal California: *Geological Society of America Abstracts with Programs*, v. 29, no. 6.
- Kistler, R.W., and Peterman, Z.E., 1978, Reconstruction of crustal blocks of California on the basis of initial strontium isotopic compositions of Mesozoic granitic rocks: U.S. Geological Survey Professional Paper 1071, 17 p.
- Klein, S., Kobler, M., and Strid, J., 2001, Overcoming difficult ground conditions in San Francisco – The Richmond transport tunnel, San Francisco

- County, California, *in* Engineering Geology Practice in Northern California, H. Ferriz and R. Anderson, eds., AEG Special Publication 12, pp. 433-442.
- Knudsen, K.L., Noller, J.S., Sowers, J.M., Lettis, W.R., Graham, S.E., Randolph, C.E., and May, T.E., 1997, Quaternary geology and liquefaction susceptibility, San Francisco, California 1:100,000 quadrangle: a digital database: U.S. Geological Survey Open-File Report 97-715, scale 1:100,000.
- Knudsen, K.L., Sowers, J.M., Witter, R.C., Wentworth, C.M., and Helley, E.J., 2000, Preliminary Maps of Quaternary Deposits and Liquefaction Susceptibility, Nine-County San Francisco Bay Region, California: A Digital Database, U.S. Geological Survey Open-File Report 00-444. Digital Database by Wentworth, C.M., Nicholson, R.S., Wright, H.M., and Brown, K.H. Online Version 1.0.
- Koehler, R. D., R. C. Witter, G. D. Simpson, E. Hemphill-Haley, and W. R. Lettis (2005). Paleoseismic investigation of the northern San Gregorio fault, Half Moon Bay, California, Final Technical Report, U.S. Geological Survey National Earthquake Hazards Reduction Program, Award No. 04HQGR0045, 70 pp, <http://earthquake.usgs.gov/research/external/reports/04HQGR0045.pdf>
- Konigsmark, T., 1998, Angel Island—Metamorphism and Blue Schists, *in* Geologic Trips—San Francisco and the Bay Area: Gualala, California, GeoPress, p. 78–91.
- Kroeber, A. L., 1911, Shellmounds at San Francisco and San Mateo: Records of the Past (Records of the Past Exploration Society, Washington, D.C.), v. 10, p. 227–228.
- Labonte, J., 2013, San Francisco’s race against time: Should other US cities start running?: Journal American Water Works Association, v. 105, no. 11, p. 34–42.
- Lajoie, K.R., and Helley, E.J., 1975, Chapter III, differentiation of sedimentary deposits for purposes of seismic zonation, *in* Studies for seismic zonation of the San Francisco Bay region: Basis for reduction of earthquake hazards: U.S. Geological Survey Professional Paper 941-A, p. 39.
- Langenheim, V.E., Jachens, R.C., Wentworth, C.M., and McLaughlin, R.J., 2013, Previously unrecognized regional structure of the Coastal Belt of the Franciscan Complex, northern California, revealed by magnetic data: *Geosphere*, v. 9, p. 1,514-1,529.
- Lawson, A.C., 1895, Sketch of the geology of the San Francisco Peninsula, *in* Powell, J.W., Fifteenth annual report of the United States Geological Survey to the Secretary of the Interior, 1893-1894: U.S. Geological Survey Annual Report 15, p. 405-476
- Lawson, A.C., 1914, San Francisco folio, California, Tamalpais, San Francisco, Concord, San Mateo, and Hayward quadrangles: U.S. Geological Survey, Geologic Atlas of the United States Folio GF-193, scale 1:62,500.
- Lawson, A.C., Leuschner, A.O., Gilbert, G.K., Davidson, G., Reid, H. F., Burkhalter, C. Branner, J.C., Campbell, W.W., 1908, The California Earthquake of April 18, 1906: Report of the State Earthquake Investigation Commission, Carnegie Institution, Washington, DC.
- Lee, C.H., 1969, Case History 2, Treasure Island Fill, Geologic and Engineering Aspects of the San Francisco Bay Fill, California Division of Mines and Geology Special Report 97, Goldman, H.B., Editor, p. 69-72.
- Leo, G.W., 1967, The plutonic and metamorphic rocks of the Ben Lomond Mountain area, Santa Cruz County, California: California Division of Mines and Geology Special Report 91, p. 27-43.
- Leventhal, A., Field, L., Alvarez, H., and Cambra, R., 1994, The Ohlone Back From Extinction, *in* Bean, L.J., ed., The Ohlone Past and Present: Native Americans of the San Francisco Region: Ballena Press, Menlo Park, CA, p. 297-336.
- Lienkaemper, J.J., 1992, Map of recently active traces of the Hayward fault, Alameda and Contra Costa counties, California: U.S. Geological Survey Miscellaneous Field Studies Map MF-2196, scale 1:24,000.
- Lienkaemper, J.J., 2006, Digital database of recently active traces of the Hayward fault,

- California: U.S. Geological Survey DS-177, available at http://pubs.usgs.gov/ds/2006/177/index_viewers.html.
- Lienkaemper, J.J., Borchardt, G., 1996, Holocene slip rate of the Hayward fault at Union City, California: *Journal of Geophysical Research*, v. 101, p. 6,099–6,108.
- Lienkaemper, J.J., Galehouse, J.S., 1997, Revised long-term creep rates on the Hayward fault, Alameda and Contra Costa Counties: California, U.S. Geological Survey Open-File Report 97-690, 18 p.
- Lienkaemper, J.J., Galehouse, J.S., and Simpson, R.W., 2001, Long-term monitoring of creep rate along the Hayward fault and evidence for a lasting creep response to 1989 Loma Prieta earthquake: *Geophysical Research Letters*, v. 28, p. 2,265–2,268.
- Lienkaemper, J. J., F. S. McFarland, R. W. Simpson, R. G. Bilham, D. A. Ponce, J. J. Boatwright, and S. J. Caskey (2012), Long-term creep rates on the Hayward fault: Evidence for controls on the size and frequency of large earthquakes, *Bull. Seismol. Soc. Am.*, 102, doi:10.1785/0120110033.
- Lienkaemper, J.J., McFarland, F.S., Simpson, R.W., and Caskey, S.J., 2014, Using surface creep rate to infer fraction locked for sections of the San Andreas Fault System in Northern California from alignment array and GPS data: *Bulletin of the Seismological Society of America*, v. 104, no. 6, p. 3,094–3,114, <https://doi.org/10.1785/0120140117>.
- Lienkaemper, J.J., Schwartz, D.P., Kelson, K.I., Lettis, W.R., Simpson, G.D., Southon, J.R., Wanket, J.A., and Williams, P.L., 1999, Timing of paleoearthquakes on the northern Hayward fault – preliminary evidence in El Cerrito, California: U.S. Geological Survey Open-File Report 99-318, p. 34.
- Lienkaemper, J.J., and Williams, P.L., 2007, A 1650-year record of large earthquake on the southern Hayward fault: *Bulletin of the Seismological Society of America*, v. 97, no. 6, p. 1,803–1,819, DOI: 10.1785/0120060258
- Lienkaemper, J.J., Williams P.L., and Guilderson, T.P., 2010. Evidence for a twelfth large earthquake on the southern Hayward fault in the past 1900 years: *Bulletin of the Seismological Society of America*, v. 100, no. 5a, p. 2,024–2,034.
- Lienkaemper, J. J., F. S. McFarland, R. W. Simpson, R. G. Bilham, D. A. Ponce, J. J. Boatwright, and S. J. Caskey (2012), Long-term creep rates on the Hayward fault: Evidence for controls on the size and frequency of large earthquakes, *Bull. Seismol. Soc. Am.*, 102, doi:10.1785/0120110033.
- Lienkaemper, J.J., McFarland, F.S., Simpson, R.W., and Caskey, S.J., 2014, Using surface creep rate to infer fraction locked for sections of the San Andreas Fault System in Northern California from alignment array and GPS data: *Bulletin of the Seismological Society of America*, v. 104, no. 6, p. 3094–3114, <https://doi.org/10.1785/0120140117>.
- Linecki-Laporte, M., and Andersen, D.W., 1988, Possible new constraints on late Miocene depositional patterns in west-central California: *Geology*, v.16, no.3, p.216–220.
- Lomax, A., 2005, A reanalysis of the hypocentral location and related observations for the Great 1906 California Earthquake: *Bulletin of the Seismological Society of America*, v. 95, p. 861–877.
- Luhdorff & Scalmanini Consulting Engineers, Inc. (LSCE), 2010, Final task 8B, technical memorandum no. 1, hydrologic setting of the Westside Basin: Prepared for San Francisco Public Utilities Commission, May 2010.
- Maier, K.L., Gatti, E., Wan, E., Ponti, D. J., Tinsley, J.C., Starratt, S.W., Hillhouse, J., Pagenkopp, M., Olson, H.A., Burt, D., Rosa, C.M., Holzer, T.L., 2013, New identification and interpreted correlation, deposition, and significance of widespread Quaternary volcanic ash in the Sacramento-San Joaquin Delta, California [abs.]: *American Geophysical Union, Fall Meeting*, abstract #V13D-2637.
- Martini, J., 2016, West Battery and Fort Scott Endicott batteries construction, evolution, and modification, *Coast Defense Journal*, v. 30, no. 3.
- Matthews, G., 2012, *The Golden State in the Civil War: Thomas Starr King, the Republican Party,*

- and the Birth of Modern California: Cambridge University Press, Cambridge, MA, 272 p.
- Matthews, V., 1976, Correlation of Pinnacles and Neenach volcanic formations and their bearing on San Andreas Fault problems: American Association of Petroleum Geologists Bulletin, v. 60, p. 2,128-2,141.
- McDonald, S.D., Nichols, D.R., Wright, N.A., and Atwater, B., 1978, Map Showing Thickness of Young Bay Mud Southern San Francisco Bay, California, U.S. Geological Survey Miscellaneous Field Studies Map MF – 976, 1:125,000 scale.
- McFarland, F.S., Lienkaemper, J.J., and Caskey, S.J., 2016, Data from theodolite measurements of creep rates on San Francisco Bay Region faults, California (ver. 1.8, March 2016): U.S. Geological Survey Open-File Report 2009–1119, 21 p. and data files, <http://pubs.usgs.gov/of/2009/1119/>, <https://pubs.usgs.gov/of/2009/1119/>.
- McGuire, D.J., 1988, Depositional framework of the Upper Cretaceous-lower Tertiary Moreno Formation, central San Joaquin Basin, California, *in* Graham, S.A., and Olson, H.C., eds., Studies of the geology of the San Joaquin Basin: Los Angeles, Pacific Section, Society of Economic Paleontologists and Mineralogists, book 60, p. 173-188.
- McLaughlin, R.J., Ellen, S.D., Blake, M.C., Jr., Jayko, A.S., Irwin, W.P., Aalto, K.R., Carver, G.A., Clarke, S.H., Barnes, J.B., Cecil, J.D., and Cyr, K.A., 2000, Geology of the Cape Mendocino, Eureka, Garberville, and Southwestern Part of the Hayfork 30 x 60 Minute Quadrangles and Adjacent Offshore Area, Northern California, with Digital Database: U.S. Geological Survey Miscellaneous Field Studies Map MF-2336, scale 1:137,000.
- McLaughlin, R.J., Powell, C.L., McDougall-Reid, K., and Jachens, R.C., 2007, Cessation of Slip on the Pilarcitos Fault and Initiation of the San Francisco Peninsula Segment of the (Modern) San Andreas Fault, California [abs.]: American Geophysical Union, Fall Meeting, abstract #T43A-1089.
- McLaughlin, R. J., Sliter, W.V., Sorg, D. H., Russell, P.C., and Sarna- Wojcicki, A. M., 1996, Large-scale right-slip displacement on the East San Francisco Bay Region fault system: Implications for location of late Miocene to Pliocene Pacific plate boundary: Tectonics, v. 15, p. 1-18.
- Meyer, J., 2014, Holocene Stratigraphy and Landscape Evolution of Yerba Buena Cove, Site of the Transbay Man Skeleton, San Francisco. Far Western Anthropological Research Group Inc., Davis, California.
- Milliken, R., Shoup, L.H., and Ortiz, B.R., 2009, Ohlone/Costanoan Indians of the San Francisco Peninsula and their Neighbors, Yesterday and Today: Archaeological and Historical Consultants Oakland, California, Prepared for: National Park Service Golden Gate National Recreation Area, San Francisco, California in response to: Solicitation No. Q8158020405, 356 p.
- Moratto, M.J, 1984, California Archaeology: San Francisco Bay and Central Coast Regions, Academic Press, Inc., 1984, p. 266.
- Murchev, B.L., 1980, Significance of chert age determination in the Marin Headlands, California [abs.]: Geological Society of America Abstracts with Programs, v. 12, no. 3, p. 144.
- Murchev, B.L., 1984, Biostratigraphy and lithostratigraphy of chert in the Franciscan Complex, Marin Headlands, California, *in* Blake, M.C., Jr., ed., Franciscan Geology of Northern California: Pacific Section, Society of Economic Paleontologists and Mineralogists, v. 43, p. 51-70.
- Murchev, B.L., and Jones, D.L., 1984, Age and significance of chert in the Franciscan Complex, in the San Francisco Bay region, *in* Blake, M.C., Jr., ed., Franciscan Geology of Northern California: Pacific Section, Society of Economic Paleontologists and Mineralogists, v. 43, p. 23-30.
- Murray, R.W., Buchholtz Ten Brink, M.R., Gerlach, D.C., Price, R.G., III, and Jones, D.L., 1991, Rare earth, major, and trace elements in chert from the Franciscan Complex and Monterey Group, California; Assessing REE sources to fine-grained marine sediments: Geochimica et Cosmochimica Acta, v. 55, p. 1875-1895.
- Murray, R.W., Jones, D.L., and Buchholtz Ten Brink, M.R., 1992, Diagenetic formation of bedded

- chert; evidence from chemistry of the chert-shale couplet: *Geology*, v. 20, p. 271-274.
- Myrick, D.F., 1972, San Francisco's Telegraph Hill, Howell-North Books, Berkeley, CA., 220 pp.
- Naeser, C.W., and Ross, D.C., 1976, Fission-track ages of sphene and apatite of granitic rocks of Salinian block, Coast Ranges, California: *Journal of Research*, U.S. Geological Survey, v. 4, no. 4, p. 415-420.
- National Oceanic and Atmospheric Administration (NOAA), 2018, Climate at a Glance: U.S. Time Series, Precipitation, NOAA National Centers for Environmental information, U.S. Department of Commerce, January 2018, Available online at: <http://www.ncdc.noaa.gov/cag/>.
- National Park Service (NPS), 2015b, Presidio of San Francisco, California: Spanish Period: 1776 to 1822, Available online at: <https://www.nps.gov/prsf/learn/historyculture/spanish-period.htm>.
- National Park Service (NPS), 2018a, The Panama-Pacific International Exhibition, Available online at: <https://www.nps.gov/goga/learn/historyculture/ppie.htm>.
- National Park Service (NPS), 2018b, World War II in the San Francisco Bay Area. Available online at: <https://www.nps.gov/nr/travel/wwiibayarea/mobilization.htm>.
- National Research Council, 2012, Sea-Level Rise for the Coasts of California, Oregon, and Washington: Past, Present, and Future. Washington, DC: The National Academies Press.
- Naval Facilities Engineering Command (NAVFAC), 2018, Former Naval Station Treasure Island, NAVFAC: Naval Facilities Engineering Command, U.S. Navy, Available online at: https://www.bracpmo.navy.mil/brac_bases/california/former_ns_treasure_island/documents2.html.
- Nichols, D.R., and Wright, N.A., 1971, Preliminary map of historical margins of marshland, San Francisco Bay, California: U.S. Geological Survey Open-File Report, Basic Data Contribution 9, scale 1:125,000.
- Niemi, T.M. and Hall, N.T., 1992, Late Holocene slip rate and recurrence of great earthquakes on the San Andreas fault in northern California: *Geology*, v. 20, p. 195-198.
- Niemi, T.M., 2002, Paleoseismic work, Northern San Andreas fault: Northern San Francisco Bay region geologic mapping and earthquake hazards workshop, U.S. Geological Survey, Menlo Park, Ca, March 11.
- Nilsen, T.H., Wright, R.H., Vlastic, T.C., and Spangle, W.E., 1979, Relative slope stability and land-use planning in the San Francisco Bay region, California: U.S. Geological Survey Professional Paper 944, map scale 1:125,000.
- Northern California Earthquake Data Center (NCEDC), 2014, UC Berkeley Seismological Laboratory. Dataset. doi:10.7932/NCEDC.
- O'Rourke, T.D., Bonneau, A. L., Pease, J. W., Shi, P. and Wang, Y., 2006, Liquefaction and ground failures in San Francisco: *Earthquake Spectra*, v. 22, no. S2, p. 91-112, <https://doi.org/10.1193/1.2185686>.
- O'Shaughnessy, M.M., 1934, Hetch Hetchy: Its Origin and History. The Recorder Printing and Publishing Company.
- Oakeshott, G.(ed.), 1959, The San Francisco Earthquakes of March 1957, CDMG Special Report 57.
- Office of Community Investment and Infrastructure (OCII), 2018, Mission Bay, City and County of San Francisco: OCII, Available online at: <http://sfocii.org/mission-bay>.
- Ojakangas, R.W., 1968, Cretaceous sedimentation, Sacramento Valley, California: *Geological Society of America Bulletin*, v. 79, p. 973-1008.
- Olmsted, N., 1986, Vanished Waters, a History of San Francisco's Mission Bay, Mission Creek Conservancy 1986.
- Oppenheimer, D.H., Bakun, W.H., and Lindh, A.G., 1990, Slip partitioning of the Calaveras fault, California, and prospects for future earthquakes: *Journal of Geophysical Research*, v. 95, p. 8483-8498.
- Oppenheimer, D.H. and Lindh, A.G., 1992, The potential for earthquake rupture of the northern

- Calaveras fault, *in* Proceedings of the Second Conference on Earthquake Hazards in the Eastern San Francisco Bay Area, Borchardt, G., Hirschfeld, S.E., Lienkaemper, J.J., McClellan, P., Williams, P.L. and Wong, I.G. (eds.), California Division of Mines and Geology Special Publication 113, p. 233-240.
- Oppenheimer, D.H. and Macgregor-Scott, N., 1992, The seismotectonics of the eastern San Francisco Bay region, *in* Proceedings of the Second Conference on Earthquake Hazards in the Eastern San Francisco Bay Area, Borchardt, G., Hirschfeld, S.E., Lienkaemper, J.J., McClellan, P., Williams, P.L. and Wong, I.G. (eds.), California Division of Mines and Geology Special Publication 113, p. 11-16.
- Page, B.M., 1978, Franciscan mélanges compared with olistostromes of Taiwan and Italy: Tectonophysics, v. 47, p. 223-246.
- Page, B.M., 1982, Modes of Quaternary tectonic movement in the San Francisco Bay region, California, *in* Hart, E.W., ed., Proceedings, Conference on Earthquake Hazards in the Eastern San Francisco Bay Area: California Division of Mines and Geology Special Publication 62, p. 1-10.
- Pampeyan, E.H., 1993, Geologic map of the Palo Alto and part of the Redwood Point 1-1/2 degree quadrangles, San Mateo and Santa Clara Counties, California: U.S. Geological Survey Miscellaneous Investigations Series Map I-2371, 26 p., scale 1:24,000.
- Pampeyan, E.H., 1994, Geologic Map of the Montara Mountain and San Mateo 7-1/2' Quadrangles, San Mateo County, California: US Geological Survey, Map I-2390, scale 1:24,000.
- Parsons, C., 1878, The city of San Francisco. Birds eye view from the bay looking south-west, New York, Currier & Ives; B. McQuillan, agent for the Pacific Coast, San Francisco, 1878. Map. Retrieved from the Library of Congress, www.loc.gov/item/75693104/.
- Parulekar, N. and Kennedy, C., 2011, Study of existing groundwater supplies, opportunities and constraints analysis: Technical memorandum prepared for San Francisco Public Utilities Commission by RMC Water and Environment, June 8, 2011, 13 p., 10 figs.
- Pease, J.W., O'Rourke, T.D., 1998, Liquefaction hazards in the Mission District and South of Market area, San Francisco, *in* Holzer ed., The Loma Prieta, California, earthquake of October 17, 1989—Liquefaction, U.S. Geological Survey Professional Paper 1551-B, p. 25-60.
- Pease, J. W. and O'Rourke, T.D., 1997, Seismic Response of Liquefaction Sites, Journal of Geotechnical Engineering, ASCE, Vol. 123, No. 1, 37-45.
- Peck, J.H., Jr., 1960, Paleontology and correlation of the Ohlson Ranch Formation: University of California Publications in Geological Sciences, v. 36, no. 4, p. 233-241.
- Perkins, J.B., Chakos, A., Olson, R.A., Tobin, L.T., Turner, F., 2006, A retrospective on the 1906 earthquake's impact on Bay Area and California public policy: Earthquake Spectra, Vol. 22, no. S2, p. 237-259.
- Pezzetti, T., and Waer, M., 2000, Downtown basin water quality evaluation: Technical memorandum prepared for San Francisco Public Utilities Commission by CH2M HILL, April 17, 2000, 13 p., 10 figs.
- Phillips, S.P., Hamlin, S.N., and Yates, E.B., 1993, Geohydrology, water quality, and estimation of ground-water recharge in San Francisco, California 1987-92: U.S. Geological Survey Water-Resources Investigations Report 93-4019, 69 p., 3 plates. in pocket.
- Phipps, S.P., 1984, Ophiolitic olistostromes in the basal Great Valley sequence, Napa County, northern California Coast Ranges, *in* Raymond, L.A., ed., Mélanges—Their nature, origin, and significance: Geological Society of America Special Paper 198, p. 103-125.
- Pike, R, J., 1997, Index to detailed maps of landslides in the San Francisco Bay region, California: U.S. Geological Survey Open-File Report 97-745 D.
- Polenghi-Gross, I., Sabol, S.A., Ritchie, S.R., Norton, M.R., 2014, Water storage and gravity for urban sustainability and climate readiness. Journal

- American Water Works Association: December. /EXD-700-WtrQRpt-2016.pdf, January 14, 6 p.
- Pomerantz, J., 2015, Seep City Water Exploration Map: Published by Joel Pomerantz, San Francisco, California.
- Ponti, D.J., and Wells, R.E., 1991, Off-fault ground ruptures in the Santa Cruz Mountains: Ridge-top spreading versus tectonic extension during the 1989 Loma Prieta earthquake, *Bull. Seismol. Soc. Am.*, 81, 1480-1510.
- Powell, C.L., II, Allen, J.R., and Holland, P.J., 2004, Invertebrate paleontology of the Wilson Grove Formation (late Miocene to late Pliocene), Sonoma and Marin counties, California, with some observations on its stratigraphy, thickness, and structure: U.S. Geological Survey Open-File Report 2004-1017, 105 p., 2 plates, scale 1:53,360.
- Power, M.S., Egan, J.A., Shewbridge, S.E., deBecker, J., Faris, J.R., 1998, Analysis of Liquefaction-Induced Damage at Treasure Island, *in* The Loma Prieta, California, earthquake of 1989—Liquefaction, Holzer, T.L., ed., U.S. Geological Survey Professional Paper 1551-B.
- Prentice, C.S., and Ponti, D.J., 1996, Coseismic deformation of the Wrights tunnel during the 1906 San Francisco earthquake: A key to understanding 1906 fault slip and 1989 surface ruptures in the southern Santa Cruz Mountains, California, *Journ. Geophys. Res.*, v. 102, no. B1, 635-648.
- Prentice, C.S., and Schwartz, D.P., 1991, Re-evaluation of 1906 surface faulting, geomorphic expression, and seismic hazard along the San Andreas fault in the southern Santa Cruz Mountains; *Bulletin of the Seismological Society of America* (1991) 81 (5): 1424-1479.
- Presidio Trust, 2014. Mountain Lake Adaptive Management Plan. March 7, 2014, Available online at: http://www.planningediting.com/uploads/5/4/4/6/54463697/mtl_2014_amp.pdf.
- Presidio Trust, 2018a, 2016 Annual Water Quality Report, Presidio of San Francisco: Available online at <https://www.presidio.gov/presidio-trust/planning-internal/Shared%20Documents/Annual%20Reports>
- Presidio Trust, 2018b. Mountain Lake Overview. Available online at: <https://www.presidio.gov/places/mountain-lake>.
- Prohoroff, R., Wakabayashi, J., and Dumitru, T.A., 2012, Sandstone matrix olistostrome deposited on intra-subduction complex serpentinite, Franciscan Complex, western Marin County, California: *Tectonophysics*, v. 568-569, p. 296-305.
- Radbruch, D. H., 1957, Areal and engineering geology of the Oakland West quadrangle, California: U.S. Geological Survey Miscellaneous Geologic Investigations Map 1-239.
- Radbruch, D. H., 1967, Approximate location of fault traces and historic surface ruptures within the Hayward fault zone between San Pablo and Warm Springs, California: U.S. Geological Survey Miscellaneous Geologic Investigations. Map 1-522, scale 1:62,500.
- Ramirez-Herrera, T., Sowers, J.M., and Richard, C., 2007, Creek & Watershed Map of San Francisco: Oakland Museum of California, Oakland, CA, 1:25,800 scale.
- Ransome, F.L., 1895, On lawsonite, a new rock-forming mineral from the Tiburon Peninsula, Marin County: *University of California, Department of Geological Science Bulletin*, v. 1, p. 301-312.
- Raymond, 2017, What is Franciscan? Revisited, *International Geology Review*, Vol 59, Issue 5-6.
- Reeder-Myers, L., Erlandson, J., Muhs, D. R., Rick, T., 2015, Sea level, paleogeography, and archeology on California's Northern Channel Islands, *Quaternary Research* 83 (2015) 263–272, available at <http://digitalcommons.unl.edu/usgsstaffpub/938>.
- Reid, H.F., 1910, The mechanics of the earthquake, v. 2 of *The California Earthquake of April 18, 1906: Report of the State Earthquake Investigation Commission: Carnegie Institution of Washington Publication 87, C192 p.2 vols.*
- Reid, J.A., Reid, J.M., Jenkins, C.J., Zimmerman, M., Williams, S.J., and Field, M.E., 2006, *usSEABED—Pacific Coast (California, Oregon,*

- Washington) offshore surficial-sediment data release: U.S. Geological Survey Data Series 182, available at <http://pubs.usgs.gov/ds/2006/182/>
- Righter, R.W., 2006, *The Battle over Hetch Hetchy: America's Most Controversial Dam and the Birth of Modern Environmentalism*, Oxford University Press.
- Risk Management Solutions, 2015, *Property Value at Risk in San Francisco from Sea Level Rise*, RMS, 2015.
- Rodgers, J. D., and J. M. Halliday, Exploring the Calaveras-Las Trampas fault junction in the Danville-San Ramon area, *in* Proceedings of the Second Conference on Earthquake Hazards in the Eastern San Francisco Bay Area, Spec. Publ. Calif. Div. Mines Geol., 113, 261–270, 1992.
- Rogers, J.D., 2001a, Influence of geology on the design and construction of BART's Transbay tube, *in* Engineering Geology Practice in Northern California, edited by Horacio Ferriz and Robert Anderson, pp. 487-499.
- Rogers, J.D., 2001b, Influence of geology on BART's San Francisco Subways, *in* Engineering Geology Practice in Northern California, edited by Horacio Ferriz and Robert Anderson, pp. 501-517.
- Ross, D.C., 1970, Quartz gabbro and anorthositic gabbro; markers of offset along the San Andreas fault in the California Coast Ranges: Geological Society of America Bulletin, v. 81, no. 12, p. 3647–3661.
- Ryan, H.F., Parsons, T., and Sliter, R.W., 2008, Vertical tectonic deformation associated with the San Andreas fault zone offshore of San Francisco, California: Tectonophysics, v. 427, p. 209–223, doi:10.1016/j.tecto.2008.06.011.
- Safonov, A., 1962, The challenge of the Sacramento Valley, California, *in* Geologic guide to the gas and oil fields of northern California: California Division of Mines and Geology Bulletin, v. 181, p. 77-97.
- Saleeby, J., 2003, Segmentation of the Laramide slab—evidence from the southern Sierra Nevada region: Geological Society of America Bulletin, v. 115, p. 655-668.
- San Francisco Bay Area Planning and Urban Research Association (SPUR), 2011, *San Francisco Gets Serious About Earthquakes*, Available online at: <http://www.spur.org/news/2011-10-24/san-francisco-gets-serious-about-earthquakes>.
- San Francisco Bay Area Planning and Urban Research Association (SPUR), 2017, *Harnessing High-Speed Rail: How California and its cities can use rail to reshape their growth*.
- San Francisco Department of Building Inspection, 2018, *Mandatory Soft Story Program*, Available online at: <http://sfdbi.org/Softstory>.
- San Francisco Department of Public Works, 1972, *Wastewater Master Plan*, City and County of San Francisco: San Francisco Department of Public Works, 1972.
- San Francisco Fire Department, 2008, *Water Supplies Manual*, City and County of San Francisco: San Francisco Fire Department, 2008.
- San Francisco Municipal Transportation Agency, 2018, *Central Subway Project: San Francisco's T Third Line light rail extension to downtown*, Available online at: <https://www.sfmta.com/projects/central-subway-project>.
- San Francisco Planning Department, 2011, *Central Corridor Planning Project: Background Report*.
- San Francisco Planning Department, 2013, *San Francisco Groundwater Supply Project, Final Environmental Impact Report: Planning Department Case No. 2008.1122E, State Clearinghouse No. 2009122075*, December.
- San Francisco Public Utilities Commission (SFPUC), 1933, *Report of the San Francisco Public Utilities Commission, Fiscal Year 1931-1932 and Fiscal Year 1932-1933*: p. 28 – 59.
- San Francisco Public Utilities Commission (SFPUC), 1934, *Report of the San Francisco Public Utilities Commission, Fiscal Year 1933-1934*: p. 7, 19, 20, 42.
- San Francisco Public Utilities Commission (SFPUC), 1935, *Report of the San Francisco Public Utilities Commission, Fiscal Year 1934-1935*: p. 22 - 23.
- San Francisco Public Utilities Commission (SFPUC),

- 1936, Report of the San Francisco Public Utilities Commission, Fiscal Year 1935-1936: p. 12, 22.
- San Francisco Public Utilities Commission (SFPUC), 1997, San Francisco Groundwater Master Plan: May 1997, various pages.
- San Francisco Public Utilities Commission (SFPUC), 2005. A History of the Municipal Water Department & Hetch Hetchy System. San Francisco Water and Power: 2005 Edition. Available Online at: <https://sfwater.org/modules/showdocument.aspx?documentid=5224>.
- San Francisco Public Utilities Commission (SFPUC), 2010, San Francisco Sewer System Master Plan
- San Francisco Public Utilities Commission (SFPUC), 2016, Map of Auxiliary Water Supply System.
- San Francisco Public Utilities Commission (SFPUC), 2017. Water Resources Annual Report. Fiscal Year 2016-17.
- San Francisco Public Utilities Commission (SFPUC), 2018a. Lake Merced History, Available online at: <http://sfwater.org/index.aspx?page=861>.
- San Francisco Public Utilities Commission (SFPUC), 2018b, Water System Improvement Program Quarterly Report, 3rd Quarter, Fiscal Year 2017-2018.
- San Francisco Public Utilities Commission (SFPUC), 2018c, San Francisco Sewer System Master Plan Updates, Available online at: <http://www.sfwater.org/index.aspx?page=116>.
- San Francisco Public Utilities Commission (SFPUC), 2018d, Non-Potable Water Program Guidebook: A Guide for Implementing Onsite Non-potable Water Systems in San Francisco, SFPUC, 2018.
- San Francisco Public Utilities Commission (SFPUC), 2018e, Westside Enhanced Water Recycling Project, Available online at: <http://sfwater.org/index.aspx?page=144>.
- San Francisco Public Utilities Commission (SFPUC), 2018f, 2017 Annual Groundwater Monitoring Report, Westside Basin: May 2018, various pages.
- San Francisco Redevelopment Agency, 2018, Hunters Point Shipyard Redevelopment Plan.
- San Francisco Water Department, 1994, Data Book, Data concerning San Francisco Water Department Hetch Hetchy catchment, storage and treatment facilities: p. 21.
- San Francisco Water Power Sewer, 2016, North Westside Basin Groundwater Sustainability Plan, draft: February 2016.
- Sarna-Wojcicki, A.M., 1976, Correlation of Late Cenozoic tuffs in the central Coast Ranges of California by means of trace and minor-element chemistry: U.S. Geological Survey Professional Paper 972, 30 p.
- Sarna-Wojcicki, A.M., 1992, Long-term displacement rates on the San Andreas fault system in northern California from the 6-Ma Roblar tuff, *in* Borchardt, Glenn, and others, eds., Earthquake hazards in the eastern San Francisco Bay Area, Proceedings of the 2nd Conference on Earthquake Hazards in the eastern San Francisco Bay Area: California Division of Mines and Geology Special Publication 113, p. 29-30.
- Sarna-Wojcicki, A.M., Deino, A.L., Fleck, R.J., McLaughlin, R.J., Wagner, D., Wan, E., Wahl, D.B., Hillhouse, J.W., and Perkins, M., 2011, Age, composition, and areal distribution of the Pliocene Lawlor Tuff, and three younger Pliocene tuffs, California and Nevada: *Geosphere*, v. 7, p. 599-628.
- Sarna-Wojcicki, A.M., Meyer, C.E., Bowman, H.R., Hall, T.H., Russell, P.C., Woodward, M.J., Slate, J.L., 1985, Correlation of the Rockland ash bed, a 400,000-year-old stratigraphic marker in northern California and western Nevada, and implications for middle Pleistocene paleogeography of central California, *In* Quaternary Research, V. 23, No. 2, p. 236-257,
- Sarna-Wojcicki, A.M., Pringle, M.S., and Wijbrans, J., 2000, New ⁴⁰Ar/³⁹Ar age of the Bishop Tuff from multiple sites and sediment rate calibration for the Matuyama-Brunhes boundary: *Journal of Geophysical Research*, v. 105, no. B9, p. 21,431-21,433.
- Sawyer, T., 2015, Characterizing rates of contractional deformation on the Mt. Diablo thrust fault, eastern San Francisco Bay region, northern California: U.S. Geological Survey National

- Hazards Reduction Program Final Technical Report 02HQGR0014, 38 p.
- Schlocker, J., 1958, Geology of the San Francisco North quadrangle, California: U.S. Geological Survey Professional Paper 782, 109 p.
- Schlocker, J., 1974, Geology of the San Francisco North quadrangle, California: U.S. Geological Survey Professional Paper 782, 104 p., 3 plates, scale 1:24,000.
- Schlocker, J., Bonilla, M.G., and Imlay, R.W., 1954, Ammonite indicates Cretaceous age for part of Franciscan group in San Francisco Bay area, California: American Association of Petroleum Geologists Bulletin, v. 38, p. 2372-2381.
- Schlocker, J., Bonilla, M.G., and Radbruch, D.H., 1958, Geology of the San Francisco North quadrangle: U.S. Geological Survey Miscellaneous Geologic Investigations Map I-272, scale 1:24,000.
- Schmidt, D.A., Burgmann, R., Nadeau, R. M., and d'Alessio, M., 2005, Distribution of aseismic slip rate on the Hayward fault inferred from seismic and geodetic data, *J. Geophys. Res.* 110, no. B08406, doi:10.1029/2004jb003397.
- Schmidt, K.M., Ellen S.D., Haugerud, R.A., Peterson, D.M., Phelps, G.A., 1995, Breaks in pavement and pipes as indicators of range-front faulting resulting from the 1989 Loma Prieta Earthquake near the southwestern margin of the Santa Clara Valley, California: U.S. Geological Survey Open-File Report 95-820, 33 p.
- Schwartz, D.P., Lienkaemper, J.J., Hecker, S., Kelson, K.I., Fumal, T.E., Baldwin, J.N., Seitz, G.G., and Niemi, T.M., 2014, The earthquake cycle in the San Francisco Bay Region: AD 1600-2012, *Bull. Seism. Soc. Am.*, v. 104, pp. 1299-1328, doi: 10.1785/50120120322.
- Schwartz, D.P., Pantosti, D., Hecker, S., Okomura, K., Budding, K.E., and Powers, T., 1992, Late Holocene behavior and seismogenic potential of the Rodgers Creek fault zone, Sonoma County, California, *in* Proceedings of the Second Conference on Earthquake Hazards in the Eastern San Francisco Bay Area, Borchardt, G., Hirschfeld, S.E., Lienkaemper, J.J., McClellan, P., Williams, P.L. and Wong, I.G. (eds.), California Division of Mines and Geology Special Publication 113, p. 393-398.
- Sedgwick, A. E., 1931, Foundations of the Golden Gate Bridge, Golden Gate Bridge and Highway District, 14 pp.
- Seed, H.B., 1969, Seismic problems in the use of fills in San Francisco Bay; in Geologic and engineering aspects of San Francisco Bay fill: California Division of Mines and Geology Special Report 97.
- Seed, R.B., Riemer, M.F., Dickenson, S.E., 1991, Liquefaction of Soils in the 1989 Loma Prieta Earthquake, Proceedings of the Second International Conference on Recent Advances in Geotechnical Engineering and Soil Dynamics, March 11-15, St. Louis Missouri, Paper No. LP02.
- Segall, P., and Lisowski, M., 1990, Surface displacements in the 1906 San Francisco and 1989 Loma Prieta earthquakes: *Science*, v. 250, p. 1,241–1,244, 10.1126/science.250.4985.1241.
- Seiders, V.M., 1982, Geologic map of an area near York Mountain, San Luis Obispo County, California: U.S. Geological Survey Miscellaneous Investigations Series Map I-1369, scale 1:24,000.
- Sharman, G.R., Graham, S.A., Grove, M., and Hourigan, J.K., 2013, A reappraisal of the early slip history of the San Andreas fault, central California, USA: *Geology*, v. 41, p. 727-730.
- Shervais, J.W., 1989, Geochemistry of igneous rocks from Marin Headlands, *in* Wahrhaftig, C. and Sloan, D., eds., Geology of San Francisco and vicinity: 28th International Geological Congress Field Trip Guidebook T105, p. 40-41.
- Shervais, J.W., Choi, S.H., Sharp, W.D., Ross, J., Zoglman-Schuman, M., Mukasa, S.B., 2011, Serpentinite matrix mélange; implications of mixed provenance for mélange formation, *in* Wakabayashi, J., and Dilek, Y., eds., mélanges; Processes of formation and societal significance: Geological Society of America Special Paper 480, p. 1-30.
- Shervais, J.W., Kimbrough, D.L., Renne, P., Hanan, B.B., Murchey, B., Snow, C.A., Zoglman Schuman, M.M., and Beaman, J., 2004, Multi-

- Stage Origin of the Coast Range Ophiolite, California: Implications for the Life Cycle of Supra-Subduction Zone Ophiolites: *International Geology Review*, v. 46, 289-315.
- Shervais, J.W., Murchey, B.L., Kimbrough, D.L., Renne, P.R., and Hanan, B., 2005, Radioisotopic and biostratigraphic age relations in the Coast Range Ophiolite, northern California; implications for the tectonic evolution of the western Cordillera: *Geological Society of America Bulletin*, v. 117, p. 633-653.
- Shirzaei, M., and Burgmann, R., 2013, Time-dependent model of creep on the Hayward fault from joint inversion of 18 years of InSAR and surface creep data, *J. Geophys. Res.* 118, no. 4, 1733–1746, doi: 10.1002/jgrb.50149.
- Simkin, T., Tilling, R.I., Vogt, P.R., Kirby, S.H., Kimberly, P., and Stewart, D.B., 2006, This Dynamic Planet—World Map of Volcanoes, Earthquakes, Impact Craters, and Plate Tectonics: U.S. Geological Survey Geologic Investigations Series Map I-2800, scale 1:30,000,000.
- Simpson, G.D., Thompson, S.C., Noller, J.S. and Lettis, W.R., 1997, The northern San Gregorio fault zone: Evidence of the timing of late Holocene earthquakes near Seal Cove, California: *Bulletin of the Seismological Society of America*, v. 87, p. 1,158-1,170.
- Simpson, G.D., Baldwin, J.N., Kelson, K.I. and Lettis, W.R., 1999, Late Holocene slip rate and earthquake history for the northern Calaveras fault at Welch Creek, eastern San Francisco Bay Area, California: *Bulletin of the Seismological Society of America*, v. 89, p. 1,250-1,263.
- Simpson, G.D., Thompson, S.C., Noller, J.S. and Lettis, W.R., 1997, The northern San Gregorio fault zone: Evidence of the timing of late Holocene earthquakes near Seal Cove, California: *Bulletin of the Seismological Society of America*, v. 87, p. 1,158-1,170.
- Simpson, G. D., and K. L. Knudsen (2000). Paleoseismic investigation of the northern San Gregorio fault at the Pillar Point Marsh near Half Moon Bay, California, Final Technical Report submitted to U.S. Geological Survey Western Region, Bay Area Paleoseismological Experiment (BAPEX), Contract Number 98WRCN1012, CLIN0014, 34 pp.
- Simpson, J.W., 2005, *Dam!: Water, Power, Politics, and Preservation in Hetch Hetchy and Yosemite National Park*. Pantheon Books, New York, 2005.
- Sims, J.D., 1988, Geologic map of the San Andreas Fault Zone in the Cholame Valley and Cholame Hills quadrangles, San Luis Obispo and Monterey counties, California: U.S. Geological Survey Miscellaneous Field Studies Map MF-1995, scale 1:24,000.
- Sliter, R.W., Johnson, S.Y., Ross, S.L., and Chin, J.L., 2014, Seismic-reflection profiles, Offshore of Pacifica map area, California, sheet 8 in Cochran, S.A., and Edwards, B.D. (eds.), *California State Waters Map Series—Offshore of Pacifica, California: U.S. Geological Survey Open-File Report 2014-1260*, pamphlet 38 p., 10 sheets, scale 1:24,000, <http://dx.doi.org/10.3133/ofr20141260>.
- Sloan, D., 1992, The Yerba Buena mud: Record of the last-interglacial predecessor of San Francisco Bay, California. *Geological Society of America Bulletin*, v. 104, no. 6, p. 716–727.
- Sloan, D., 2006, *Geology of the San Francisco Bay Region: California*, University of California Press, 337 p.
- Smith, D., 2005, *San Francisco is Burning, the Untold Story of the 1906 Earthquake and Fires*: New York, Viking Penguin Group, 294p.
- Smith, D.D., 1960, *The geomorphology of the San Francisco Peninsula [Ph.D. thesis]*: Stanford University.
- Smith, J.R., 2005, *San Francisco's Lost Landmarks*, Word Dancer Press, Sanger, CA, 236 p.
- Snow, C.A., Wakabayashi, J., Ernst, W.G., and Wooden, J.L., 2010, Detrital zircon evidence for progressive underthrusting in Franciscan metagraywackes, west-central California: *Geological Society of America Bulletin*, v. 122, p. 282-291.
- Song, S.G., Beroza, G.C. and Segall, P., 2008, A unified source model for the 1906 San 1246 Francisco Earthquake, *Bull. Seism. Soc. Am.* 98 823-831.

- Sonoma State University Library, 2018, William A. Richardson, 1795-1856, available online at: <http://library.sonoma.edu/research/guides/regional/notablepeople/richardson>.
- Sowers, J.M., Givler, R.W., Ramirez-Herrera, M.T., Tillery, A., Richard, C., Pearce, S., Dulberg, R. and Holmberg, J.F., 2007, Creek & watershed map of the San Francisco peninsula: a digital database, version 1.0: William Lettis and Associates, Inc., Walnut Creek, CA, 1:24,000 scale.
- Spring Valley Water Company, 1926, San Francisco Water, 32 p.
- Spudich, P., 1996, Synopsis, *in* The Loma Prieta, California, earthquake of October 17, 1989—Main shock characteristics, Spudich, P., ed., U.S. Geological Survey Professional Paper 1550-A, p. A1–A9.
- Stanford University, 2006, Stanford University and the Centennial of the 1906 Earthquake, Evolution of Codes: Mitchell Earth Sciences, Available online at: <https://quake06.stanford.edu/centennial/tour/stop10.html>.
- Stanford, J.D., Hemingway, R., Rohling, E.J., Challenor, P.G., Medina-Elizalde, M., and Lester, A.J., 2011, Sea-level probability for the last deglaciation—A statistical analysis of far-field records: *Global and Planetary Change*, v. 79, p. 193–203, <https://doi.org/10.1016/j.gloplacha.2010.11.002>.
- Storlazzi, C.D., and Wingfield, D.K., 2005, Spatial and temporal variations in oceanographic and meteorologic forcing along the central California coast, 1980-2002: U.S. Geological Survey Scientific Investigations Report 2005-5085, 39 p.
- Sullivan, R., 2006, A walk along the old bay margins in downtown San Francisco: Retracing the events of the 1906 earthquake and fire, *in* Prentice, C.S., Scotchmoor, J. G., Moores, E.M., and Kirkland, J.P., eds., 1906 San Francisco, California Earthquake Centennial Field Guides; Geological Society of America Guide 7, p. 1-23.
- Surpless, K.D., 2015, Geochemistry of the Great Valley Group; an integrated provenance record: *International Geology Review*, v. 57, p. 747-766.
- Tetra Tech EM Inc., 2015, Draft Site Management Plan, Naval Station Treasure Island San Francisco, California.
- Tetreault, J.L., and Buitter, S.J.H., 2012, Geodynamic models of terrane accretion—Testing the fate of island arcs, oceanic plateaus, and continental fragments in subduction zones: *Journal of Geophysical Research*, v. 117, B08403.
- Thatcher, W., 1975, Strain accumulation and release mechanism of the 1906 San Francisco earthquake: *Journal of Geophysical Research*, v. 80, no. 35, p. 4862-4872.
- Thatcher, W., Marshall, G., and Lisowski, M., 1997, Resolution of fault slip along the 470-km-long rupture of the Great 1906 San Francisco Earthquake and its implications: *Journal of Geophysical Research*, v. 102, p. 5353–5367, doi: 10.1029/96JB03486.
- The Virtual Museum of the City of San Francisco, 2017a, San Francisco Gold Rush Chronology 1846-1849, Available online at: <http://www.sfmuseum.net/hist/chron1.html>.
- The Virtual Museum of the City of San Francisco, 2017b, San Francisco Gold Rush Chronology 1850-1851, Available online at: <http://www.sfmuseum.net/hist/chron2.html>.
- The Virtual Museum of the City of San Francisco, 2017c, San Francisco Gold Rush Chronology 1852-1854: <http://www.sfmuseum.net/hist/chron3.html>.
- Tinsley, J.C., III, Egan, J.A., Kayen, R.E., Bennett, M.J., Kropp, A., and Holzer, T.L., 1998, Appendix: Maps and descriptions of liquefaction and associated effects, *in* Holzer, T.L., ed., The Loma Prieta, California, earthquake of October 17, 1989—Liquefaction: U.S. Geological Survey Professional Paper 1551-B.
- Tobriner, S., 2006, Bracing for Disaster, Earthquake-Resistant Architecture and Engineering in San Francisco 1838-1933: The Bancroft Library, Univ. of California, Berkeley, Heyday Books, Berkeley, California, 330 p.
- Topozada, T.R., Real, C.R., Bezore, S.P., Parke, D.L., 1981, Preparation of isoseismal maps

- and summaries of reported effects for pre-1900 California earthquakes, U.S. Geological Survey Open-File Report 81-262.
- Topozada, T. R. and Parke, D. L., 1982. Area damaged by the 1868 Hayward earthquake and recurrence of damaging earthquakes near Hayward, *in* Hart, Earl W., Hirschfeld, Sue E., and Schulz, Sandra S., editors. Proceedings, Conference on Earthquake Hazards in the eastern San Francisco Bay area: California Division of Mines and Geology. Special Publication 62, p. 321-328.
- Trask, P.D., and Rolston, J.W., 1951, Engineering geology of San Francisco Bay, California. *Bulletin of the Geological Society of America*. 62: 1079-1110.
- Tuolumne County Historical Society, 2013, Timeline of History, Price, and Economics of U.S. Gold, Available online at: https://www.tchistory.org/tchistory/gold_timeline.htm.
- Ukar, E., Cloos, M., and Vasconcelos, P., 2012, First ^{40}Ar - ^{39}Ar ages from low-T mafic blueschist blocks in a Franciscan mélange near San Simeon—Implications for initiation of subduction: *The Journal of Geology*, v. 120, p. 543-556.
- United States Environmental Protection Agency, 2018, Cleanup Activities Treasure Island Naval Station-Hunters Point Annex, San Francisco, CA, Available online at: <https://cumulis.epa.gov/supercpad/SiteProfiles/index.cfm?fuseaction=second.cleanup&id=0902722>.
- United States Geological Survey (USGS), Earthquake Hazards Program. “Hayward Fault Scenario Earthquakes”, Available online at: <http://earthquake.usgs.gov/regional/nca/simulations/hayward/>.
- United States Geological Survey (USGS), 2018, Bay Area Quad Browser: USGS Earthquake Hazards Program, Available online at: <https://earthquake.usgs.gov/learn/topics/geologicmaps/quadrangles.php>, San Francisco North Quadrangle, January 15, 2018.
- U.S. Geological Survey, 1968, The geology of the San Francisco Bay area and its significance in land use planning: Berkeley, Calif., Association of Bay Area Governments, Bay Area Regional Planning Program, Regional Geology, supplemental Report IS-3, 47 p.
- U.S. Geological Survey (2018a). The Great 1906 San Francisco earthquake, U.S. Geological Survey website, accessed 3/2/18 at <https://earthquake.usgs.gov/earthquakes/events/1906calif/18april/>
- U.S. Geological Survey and California Geological Survey, 2010, Quaternary fault and fold database of the United States: U.S. Geological Survey database, accessed April 5, 2018, at <http://earthquake.usgs.gov/hazards/qafaults/>
- Waelbroeck, C., Labeyrie, L., Michel, E., Duplessy, J.C., McManus J.F., Lambeck, K., Balbon, E., and Labracherie, M., 2002, Sea-level and deep water temperature changes derived from benthic foraminifera isotopic records, *Quaternary Science Reviews* 21: 295–305.
- Wagner, D.L., and Bortugno, E.J., 1982, Geologic map of the Santa Rosa quadrangle, California: California Division of Mines and Geology Regional Geologic Map Series Map No. 2A, scale 1:250,000.
- Wagner, D.L., Saucedo, G.J., Clahan, K.B., Fleck, R.J., Langenheim, V.E., McLaughlin, R.J., Sarna-Wojcicki, A.M., Allen, J.R., and Deino, A.L., 2011, Geology, geochronology, and paleogeography of the southern Sonoma volcanic field and adjacent areas, northern San Francisco Bay region, California: *Geosphere*, v. 7, p. 658-683.
- Wahrhaftig, C., 1984a, A streetcar to subduction and other plate tectonic trips by public transport in San Francisco, revised edition: Washington, D.C., American Geophysical Union, 72 p.
- Wahrhaftig, C., 1984b, Structure of the Marin Headlands block, California; A progress report, *in* Blake, M.C., Jr., ed., Franciscan geology of Northern California: Pacific Section, Society of Economic Paleontologists and Mineralogists, v. 43, p. 31-50.
- Wahrhaftig, C., and Wakabayashi, J., 1989, Tectonostratigraphic terranes, *in* Wahrhaftig, C., and Sloan, D., eds., *Geology of San Francisco and vicinity: 28th International Geological Congress Field Trip Guidebook T105*, p. 6-8.

- Wakabayashi, J., 1992, Nappes, tectonics of oblique plate convergence, and metamorphic evolution related to 140 million years of continuous subduction, Franciscan Complex, California: *Jour. of Geology*, v. 100, p. 19-40.
- Wakabayashi, J., 2004, Contrasting settings of serpentinite bodies, San Francisco Bay area, California; Derivation from the subducting plate vs. mantle hanging wall?: *International Geology Review*, v. 46, p. 1103-1118.
- Wakabayashi, J., 2011, Mélanges of the Franciscan Complex, California; diverse structural settings, evidence for sedimentary mixing, and their connection to subduction processes, *in* Wakabayashi, J., and Dilek, Y., eds., Mélanges; processes of formation and societal significance: *Geological Society of America Special Paper 480*, p. 117–141.
- Wakabayashi, J., 2015, Anatomy of a subduction complex; architecture of the Franciscan Complex, California, at multiple length and time scales: *International Geology Review*, v. 57, p. 669-746.
- Wakabayashi, J., 2017, Structural context and variation of ocean plate stratigraphy, Franciscan Complex, California: insight into mélange origins and subduction-accretion processes, *Progress in Earth and Planetary Sciences*, vol. 4, no. 18.
- Wallace, R.E., 1990, The San Andreas Fault System, California: U.S. Geological Survey Professional Paper 1515, 283 p.
- Watt, J., Ponce, D., Parsons, T., and Hart, P., 2016, Missing link between the Hayward and Rodgers Creek faults. *Sci. Adv.* 2, e1601441
- Wentworth, C.M., 1997, General distribution of geologic materials in the San Francisco Bay region, California: a digital map database: U.S. Geological Survey Open-File Report 97-774, database resolution 1:125,000.
- Williams, T.A., and Graham, S.A., 2013, Controls on forearc basin architecture from seismic and sequence stratigraphy of the Upper Cretaceous Great Valley Group, central Sacramento Basin, California: *International Geology Review*, v. 55, p. 2030-2059.
- Woodbridge, S. B., and Woodbridge, J., 1982, Architecture; San Francisco the Guide: San Francisco, 101 Publications, 200 p.
- Woodring, W.P., Stewart, R., and Richards, R.W., 1940, Geology of the Kettleman Hills Oil Field, California: U.S. Geological Survey Professional Paper 195, 170 p.
- Working Group on Northern California Earthquake Potential (WGNCEP), 1996, Database of potential sources for earthquakes larger than magnitude 6 in northern California: U.S. Geological Survey Open-File Report 96-705, 53 p., [<http://quake.wr.usgs.gov:80/hazprep/NCEP/>]
- Working Group on California Earthquake Probabilities (WGCEP), 1999, Earthquake probabilities in the San Francisco Bay Region: 2000 to 2030, A summary of findings: U.S. Geological Survey Open-File Report 99-517, 34 p.
- Working Group for California Earthquake Probabilities (WGCEP), 2003, Earthquake probabilities in the San Francisco Bay area: 2002-2031: U.S. Geological Survey Open-File Report 03-214.
- Working Group for California Earthquake Probabilities (WGCEP), 2013, Uniform California Earthquake Rupture Forecast, Version 3 (UCERF3) – The time-independent model, U.S. Geological Survey Open-File Report 2013-1165.
- Wright, J.W., and Wyld, S.J., 2007, Alternative tectonic model for Late Jurassic through Early Cretaceous evolution of the Great Valley Group, California, *in* Cloos, M., Carlson, W.D., Gilbert, M.C., Liou, J.G., and Sorensen, S.S., eds., *Convergent Margin Terranes and Associated Regions—A Tribute to W.G. Ernst*: Geological Society of America Special Paper 419, p. 81–95.
- Wurm, T., 1990, Hetch Hetchy and Its Dam Railroad. Trans-Anglo Books, 1990.
- Yancey, T.E., 1978, Stratigraphy of the Plio-Pleistocene strata in the Twelvemile Creek area, San Francisco Peninsula, California: *Proceedings of the California Academy of Sciences*, fourth series, v. XLI, p. 357-370.
- Yang, H., and Johnson, K.A., 2011a, Geotechnical conditions and design considerations for Central Subway project in downtown San Francisco, proceedings of the Rapid Excavation and

Tunneling Conference, San Francisco, California, pp. 1252-1268.

- Yang, H., and Johnson, K.A., 2011b, Characterization of a weak rock for a subway tunnel project in San Francisco, proceedings of the 45th US Rock Mechanics/Geomechanics Symposium, San Francisco, CA, Paper ARMA 11-545, 9 pp.
- Youd, T.L., 1973, Liquefaction, flow and associated ground failure: U.S. Geological Survey Circular 688, 12 pp.
- Youd, T.L., and Hoose, S.N., 1978, Historical ground failures in Northern California triggered by earthquakes: U.S. Geological Survey Professional Paper 993.
- Youngman, M.R., 1989, K-Ar and ⁴⁰Ar/³⁹Ar geochronology, geochemistry, and structural reinterpretation of the southern Sonoma Volcanic field, Sonoma County, California [M.S. thesis]: Berkeley, University of California, 92 p., 1 plate.
- Yu, E., and Segall, P., 1996, Slip in the 1868 Hayward earthquake from the analysis of historical triangulation data, *J. Geophys. Res.*, 101(B7), 16,101–16,118, doi:10.1029/96JB00806.
- Zhang, E., Fuis, G.S., Catchings, R.D., Scheirer, D.S., Goldman, M., and Bauer, K., 2018, Reexamination of the subsurface fault structure in the vicinity of the 1989 moment-magnitude-6.9 Loma Prieta earthquake, central California, using steep-reflection, earthquake, and magnetic data: U.S. Geological Survey Open-File Report 2018–1093, 35 p., <https://doi.org/10.3133/ofr20181093>.
- Zoback, M.L., Olson, J.A., and Jachens, R.C., 1995, Seismicity and basement structure beneath south San Francisco Bay, California, *in* Sangines, E.M., Anderson, D.W., and Buising, A.V., eds., Recent geologic studies in the San Francisco Bay area: Society of Economic Paleontologists and Mineralogists, Pacific Section Special Publication 76, p. 31-46.

LIST OF MAP UNITS

SURFICIAL DEPOSITS

- Qaf Artificial fill
- Qmf Artificial fill over bay mud
- Qs Beach deposits
- Qd Dune sand
- Qsr Slope and ravine fill
- Qls Landslide deposits
- Qob Older beach deposits
- Qu Undifferentiated surficial deposits
- Qc Colma Formation

OVERLAP STRATA

- QTm Merced Formation

FRANCISCAN COMPLEX

Coastal Belt

- Tfs SAN BRUNO MOUNTAIN TERRANE Sandstone

Central Belt

- Kfbs BOLINAS RIDGE TERRANE Sandstone

- Kfbh Shale

- Kfas ALCATRAZ TERRANE Sandstone

- Kfah Shale

- Kfa Sandstone and shale

- Kfms MARIN HEADLANDS TERRANE Sandstone

- KJfmc Chert

- Jfmg Greenstone

- Kfaims ANGEL ISLAND TERRANE Metasandstone
 - fsr MÉLANGE Sheared sandstone and shale with small blocks of other rock
 - KJfh High-grade block
- FRANCISCAN OR COAST RANGE OPHIOLITE**
- sp HUNTERS POINT SERPENTINITE-MATRIX MÉLANGE Serpentinite with small blocks of other rock
 - sph Hard serpentinite
 - fsr-spm Intermixed serpentinite and sheared sandstone and shale
 - gb Gabbro
 - Kfss Franciscan(?) sandstone

MAP SYMBOLS

- Contact—Depositional or intrusive contact or large mélangé block edge; dashed where approximately located; dotted where concealed
- Fault—Dashed where approximately located; small dashed where inferred, dotted where concealed; dip value and direction
- Strike and dip of bedding
- Vertical bedding
- Strike and dip of foliation
- Strike and dip of joint
- Vertical joint

Plate 1. Geologic map of the City and County of San Francisco. Modified from Blake and others (2000); Bonilla (1998; 1971); and Schlocker (1974).

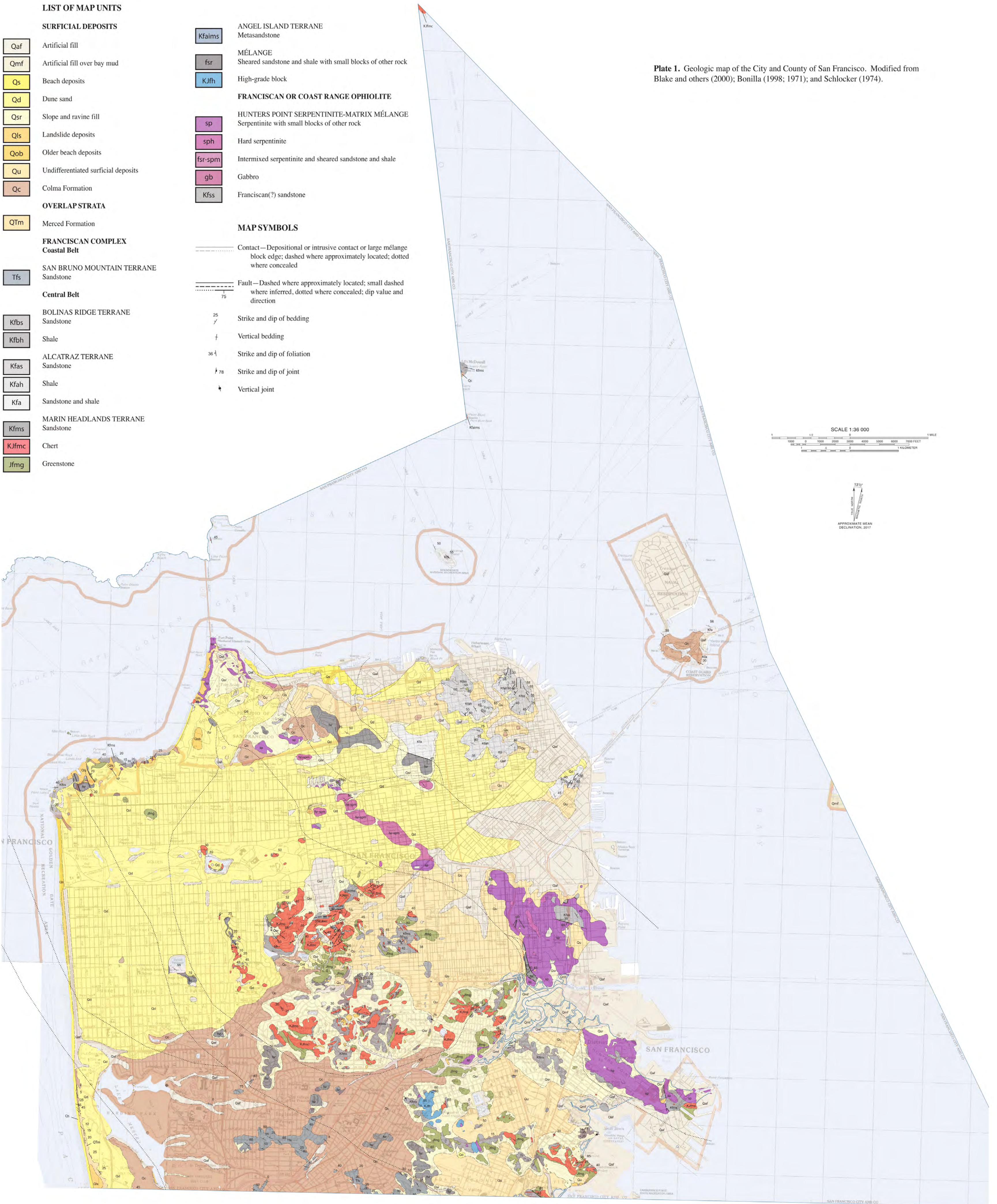
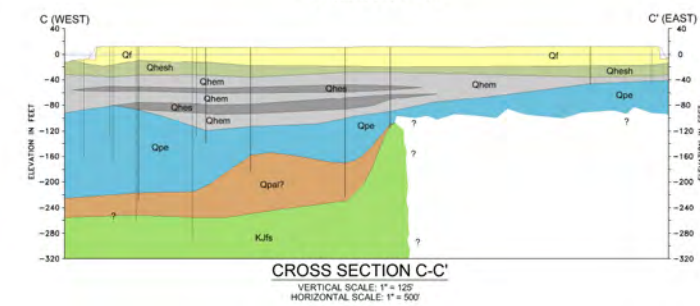
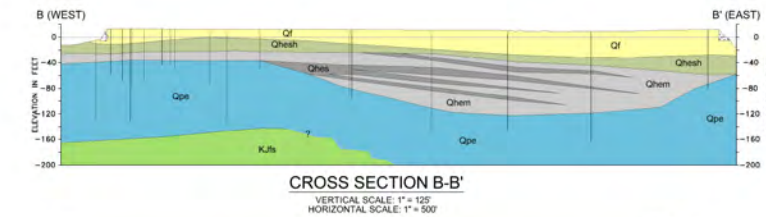
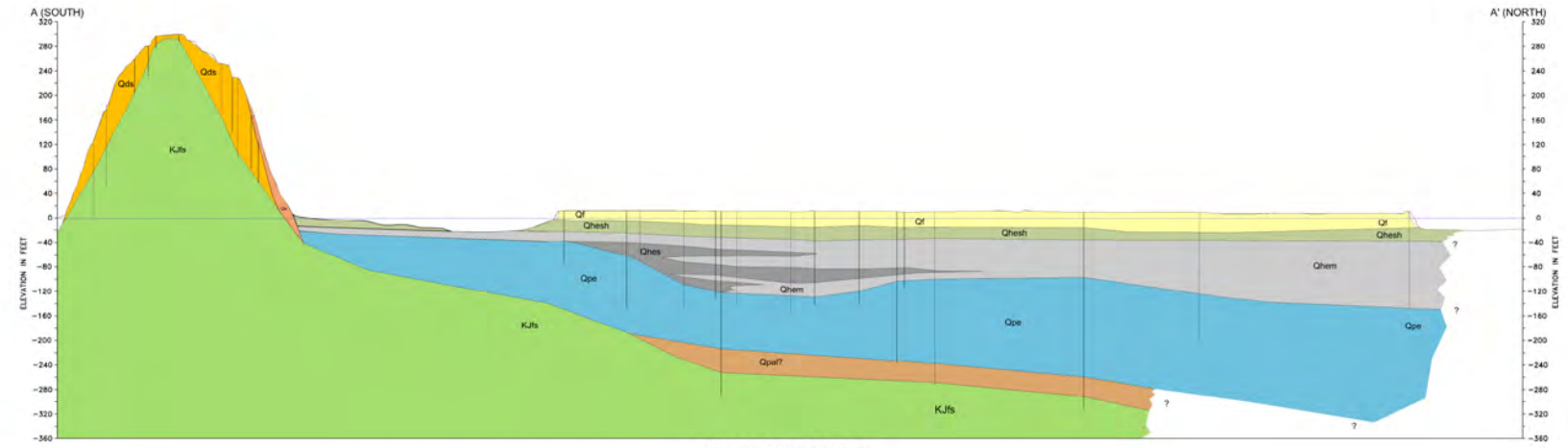
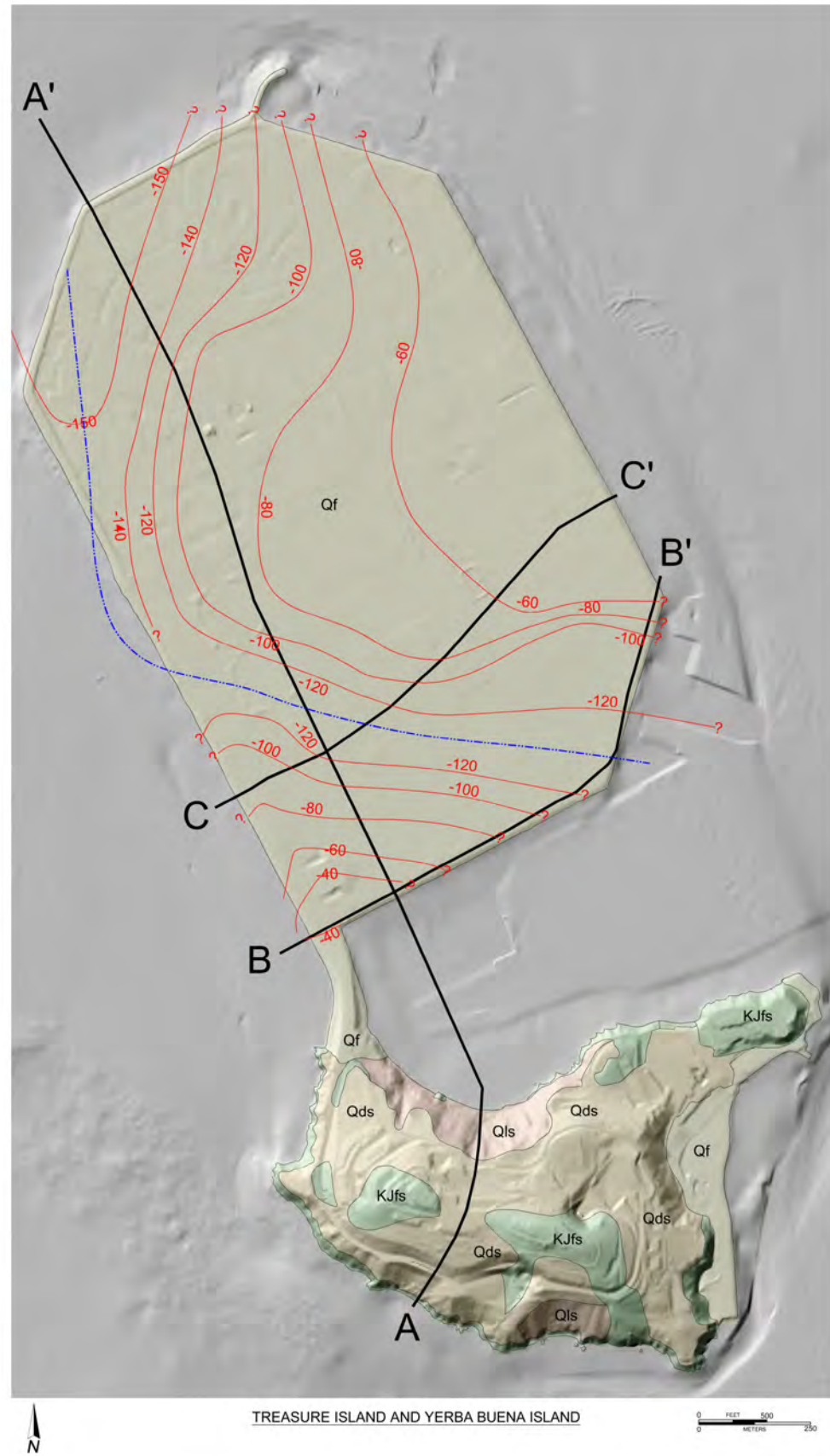


Plate 2. Treasure Island Geology and Stratigraphy.



- EXPLANATION**
- PROBABLE PALEO-CHANNEL
 - ELEVATION CONTOURS ON TOP OF OLDER BAY DEPOSITS*
 - Qf HYDRAULIC FILL
 - Qls LANDSLIDE
 - Qds EOLIAN SAND
 - Qsh SHOAL SAND
 - Qem HOLOCENE ESTUARINE CLAYS (BAY MUD)
 - Qsh HOLOCENE ESTUARINE SANDS
 - Qpe LATE PLEISTOCENE ESTUARINE DEPOSITS (OLD BAY DEPOSITS)
 - Qpa? LATE PLEISTOCENE ALLUVIUM
 - KJfs FRANCISCAN ASSEMBLAGE BEDROCK
 - LOCATIONS OF BORINGS DEPICTED ON CROSS SECTIONS

*VERTICAL DATUM NAVD88

